frontiers | Research Topics

Antimicrobial resistance in zoonotic bacteria

Edited by
Guyue Cheng, Liang-xing Fang, Xunde Li, Zuowei Wu and Jie Feng

Published in
Frontiers in Microbiology

ISSN 1664-8714
ISBN 978-2-8325-4413-6
DOI 10.3389/978-2-8325-4413-6

About Frontiers

Frontiers is more than just an open access publisher of scholarly articles: it is a pioneering approach to the world of academia, radically improving the way scholarly research is managed. The grand vision of Frontiers is a world where all people have an equal opportunity to seek, share and generate knowledge. Frontiers provides immediate and permanent online open access to all its publications, but this alone is not enough to realize our grand goals.

Frontiers journal series

The Frontiers journal series is a multi-tier and interdisciplinary set of open-access, online journals, promising a paradigm shift from the current review, selection and dissemination processes in academic publishing. All Frontiers journals are driven by researchers for researchers; therefore, they constitute a service to the scholarly community. At the same time, the *Frontiers journal series* operates on a revolutionary invention, the tiered publishing system, initially addressing specific communities of scholars, and gradually climbing up to broader public understanding, thus serving the interests of the lay society, too.

Dedication to quality

Each Frontiers article is a landmark of the highest quality, thanks to genuinely collaborative interactions between authors and review editors, who include some of the world's best academicians. Research must be certified by peers before entering a stream of knowledge that may eventually reach the public - and shape society; therefore, Frontiers only applies the most rigorous and unbiased reviews. Frontiers revolutionizes research publishing by freely delivering the most outstanding research, evaluated with no bias from both the academic and social point of view. By applying the most advanced information technologies, Frontiers is catapulting scholarly publishing into a new generation.

What are Frontiers Research Topics?

Frontiers Research Topics are very popular trademarks of the *Frontiers journals series*: they are collections of at least ten articles, all centered on a particular subject. With their unique mix of varied contributions from Original Research to Review Articles, Frontiers Research Topics unify the most influential researchers, the latest key findings and historical advances in a hot research area.

Find out more on how to host your own Frontiers Research Topic or contribute to one as an author by contacting the Frontiers editorial office: frontiersin.org/about/contact

Antimicrobial resistance in zoonotic bacteria

Topic editors

Guyue Cheng — Huazhong Agricultural University, China
Liang-xing Fang — South China Agricultural University, China
Xunde Li — University of California, Davis, United States
Zuowei Wu — Iowa State University, United States
Jie Feng — Lanzhou University Medical College, China

Citation

Cheng, G., Fang, L.-x., Li, X., Wu, Z., Feng, J., eds. (2024). *Antimicrobial resistance in zoonotic bacteria*. Lausanne: Frontiers Media SA. doi: 10.3389/978-2-8325-4413-6

Table of contents

frontiers | Frontiers in Microbiology

TYPE Editorial
PUBLISHED 23 January 2024
DOI 10.3389/fmicb.2024.1362380

OPEN ACCESS

EDITED AND REVIEWED BY
Rustam Aminov,
University of Aberdeen, United Kingdom

*CORRESPONDENCE
Guyue Cheng
✉ chengguyue@mail.hzau.edu.cn

RECEIVED 28 December 2023
ACCEPTED 09 January 2024
PUBLISHED 23 January 2024

CITATION
Cheng G, Fang L-x, Feng J, Li X and Wu Z (2024) Editorial: Antimicrobial resistance in zoonotic bacteria.
Front. Microbiol. 15:1362380.
doi: 10.3389/fmicb.2024.1362380

Editorial: Antimicrobial resistance in zoonotic bacteria

Guyue Cheng[1]*, Liang-xing Fang[2], Jie Feng[3], Xunde Li[4] and Zuowei Wu[5]

[1]College of Animal Sciences and Technology, College of Veterinary Medicine, Huazhong Agricultural University, Wuhan, Hubei, China, [2]College of Veterinary Medicine, South China Agricultural University, Guangzhou, Guangdong, China, [3]School of Basic Medical Sciences, Lanzhou University, Lanzhou, Gansu, China, [4]School of Veterinary Medicine, University of California, Davis, Davis, CA, United States, [5]College of Veterinary Medicine, Iowa State University, Ames, IA, United States

KEYWORDS

antimicrobial resistance (AMR), antimicrobial resistance (AMR) genes, zoonotic pathogens, intervention strategies, monitoring and surveillance

Editorial on the Research Topic
Antimicrobial resistance in zoonotic bacteria

Antimicrobial resistance (AMR) is a global issue caused by excessive use of antimicrobial agents in clinical, agricultural, and veterinary settings. This has led to the emergence of resistant microorganisms, threatening public health and food safety. The situation is complicated by a variety of mechanisms in resistance gene transfer and emerging evolution in the genetic makeup of resistant bacteria. Monitoring AMR in wild, companion and farm animals can help combat AMR and limit the spread of antimicrobial resistance genes (ARGs). While several studies have focused on common foodborne pathogens like *Salmonella* and *Campylobacter*, attention must also be given to the role of other zoonotic pathogens in spreading AMR. Effective intervention strategies must be developed to reduce the transmission of ARGs to foodborne and other pathogenic microorganisms.

An understanding of the genetic variation and the transmission mechanisms of important ARGs helps control the propagation of AMR. *Moraxella* spp. cause various diseases in humans and animals and are resistant to many antibiotics, including quinolone, ampicillin, tetracycline, penicillin, and, most importantly, colistin. Che et al. discovered two novel variants of colistin resistance *mcr-1* genes, *mcr-1.35* and *mcr-1.36*, present in *Moraxella* spp. from infected pigs in China. Using a functional cloning assay, they also showed that these genes could transfer resistance from *Moraxella* to *Escherichia coli* DH5α and JM109. In addition to the existence of the *mcr-1* gene, Karim et al. detected the colistin-resistance *mcr-5* gene in Enterobacteriaceae from chicken meat and poultry samples in Malaysia. The *mcr-1* was prevalent in *E. coli* from litter and cloacal swab samples, while *Salmonella* spp. from chicken meat was positive for the *mcr-5*. However, *Klebsiella pneumoniae* isolates were found negative for any *mcr* genes, suggesting further studies on *mcr-5* and its plasmids. The drug-resistance gene *cfr(C)* is known to confer resistance to several critically essential antimicrobials, like streptogramin A, lincosamide, and pleuromutilin, by inducing A2503 methylation in bacterial 23S rRNA. An et al. focused on elucidating the intricate cross-resistance mechanisms of *cfr(C)* in *Campylobacter coli* isolates of swine origin and from the nine *cfr(C)*-positive strains, they identified three

novel single nucleotide polymorphism (SNP) sites (674C > A, 19delA, and 890 T > C) for this gene. Five cassettes were present on the chromosome of these six SNP sites, and the remaining one was found on a plasmid-like element. The resistance cluster for aminoglycoside-streptothricin resistance cluster "*aphA3-sat4-aadE*" was associated with three of the six *cfr(C)* SNP variants, while one gene cassette having *pcp* gene (GC-1, GC-4, and GC-5) formed a novel circular intermediate "*pcp*-hp-*cfr(C)-aphA3*".

Cross-species transfer of AMR in zoonotic pathogens may cause severe public health risks. Guan et al. studied *Wohlfahrtiimonas chitiniclastica* and isolated a novel strain (BM-Y) harboring a bla_{VEB-1}-gene-carrying plasmid for the first time from a deceased zebra in China. The authors reported that the dissemination of bla_{VEB-1} harboring plasmid could enhance resistance, resulting in infections that are difficult to treat. After genomic sequencing, they found three novel insertion sequences (IS), namely IS*Woch1*, IS*Woch2*, and IS*Woch3*, among which IS*Woch1* carried the transcription site of bla_{VEB-1} and proved to be an essential promoter for this gene. Card et al. focused on the prevalence of multidrug-resistant (MDR) and clinically significant non-typhoidal *Salmonella* in cloacal samples from migratory birds in Bangladesh. They identified six different serovars of *Salmonella* and an overall prevalence of 13.5%. All strains (MDR) were among these six serovars except the *S.* Perth and *S.* Weltevreden. The authors found that the resistance phenotype was strongly correlated with resistance genes that mainly resided on the *Salmonella* Genomic Islands. Ciprofloxacin-resistant *Salmonella* was associated with mutations in *gyrB* and *parC* genes present on chromosomes, and the *S.* Kentucky belonged to ST198, which is present in both animals and humans, hence a severe public health risk. Abdelhamid and Yousef unveiled the genetic similarities between eggs and poultry-associated *Salmonella enterica* serovar Enteritidis (SE) and indicated that eggs-related SE strains could potentially cause human infections. Comparative genomic analysis of 1,002 SE genomes revealed that SE strains from eggs and poultry have similar genetic lineage but differ from beef-associated SE strains. The *aac(6')-Iaa* and *mdsAB* genes were found to be responsible for prevalent drug resistance, and genetic analyses showed a comparable or similar number of virulence factors in both humans and eggs-associated SE strains.

Zhang et al. suggested the reasonable use of antibiotics according to the drug-resistance genes in clinical settings for patient safety and antibiotic efficacy. They reported that most carbapenem-resistant *Pseudomonas aeruginosa* (CRPA) isolates originated from intensive care unit (ICU) wards and sputum samples. The serious concern was the high-level coexistence of various resistance genes (cephalosporin enzyme, aminoglycoside-modifying enzyme, extended-spectrum β-lactamase, and genes involved in biofilms, membrane channel proteins, I integrons, and efflux systems) and hypervirulence associated genes (*exoS, exoU, exoY,* and *exoT*) in CRPA. The European Union Reference Laboratory for Antimicrobial Resistance (EURL-AR) recommended two reliable methods to separate *E. coli* that produce AmpC, ESBL, and CP enzymes. Hendriksen et al. tested multiple surveillance protocols and found that the Buffered Peptone Water pre-enrichment method was the best, showing the highest sensitivity and specificity for testing minced meat and caecal content samples. Moreover, they described two protocols for isolating and monitoring ESBL- and AmpC-producing *E. coli* and carbapenemase-producing *E. coli* from meat and caecal samples.

Using diet as an intervention to combat AMR has attracted the attention of scientists due to the role of various diets and antibiotics in modulating the composition and diversity of gut and fecal microbiomes. Jinno et al. demonstrated an increase in the relative abundance of beneficial bacteria like Bifidobacteriaceae and Lactobacillaceae in the intestines of enterotoxigenic *E. coli*-infected weaned pigs after supplementation of *Bacillus subtilis* in their diet. Their results also showed that the intestinal microbiome is greatly influenced by diet and other factors, including stress, bacterial infection, and the age of pigs. Similarly, the indispensable role of alkaline arginine in combating the drug-resistant *Salmonella* was studied by Zhu et al. Arginine was found to be an effective adjuvant for aminoglycosides due to its bactericidal effects through increased proton motive force (PMF) and drug uptake by the bacterial cells. During their *in vitro* study, Yang et al. showed that L-leucine can be used as a potential fluoroquinolone adjuvant for fighting clinically resistant *Salmonella* spp. by enhancing the bactericidal effect of sarafloxacin, a unique fluoroquinolone used in veterinary practice. The underpinning mechanisms involved reprogramming resistant bacteria, enhancing metabolism, and increasing ATP, NADH, and reactive oxygen species (ROS) levels inside cells, ultimately promoting antibiotic efficacy.

We need more research on how AMR develops and spreads at the molecular level to understand the mechanisms of AMR and control AMR in zoonotic bacteria from farm and wild animals. We also need enhanced monitoring and improved strategies to fight against AMR and protect public health. This Research Topic presented papers that showed important information and new directions for AMR research.

Author contributions

GC: Writing – original draft. L-xF: Writing – review & editing. JF: Writing – review & editing. XL: Writing – review & editing. ZW: Writing – review & editing.

Funding

The author(s) declare that no financial support was received for the research, authorship, and/or publication of this article.

Conflict of interest

The authors declare that the research was conducted in the absence of any commercial or financial relationships that could be construed as a potential conflict of interest.

Publisher's note

frontiers | Frontiers in Microbiology

TYPE Original Research
PUBLISHED 23 December 2022
DOI 10.3389/fmicb.2022.1064328

OPEN ACCESS

EDITED BY
Chang-Wei Lei,
Sichuan University, China

REVIEWED BY
Kun Li,
Nanjing Agricultural University, China
Jinhu Huang,
Nanjing Agricultural University, China

*CORRESPONDENCE
Yanhong Liu
✉ yahliu@ucdavis.edu

SPECIALTY SECTION
This article was submitted to Antimicrobials, Resistance and Chemotherapy, a section of the journal Frontiers in Microbiology

RECEIVED 08 October 2022
ACCEPTED 08 December 2022
PUBLISHED 23 December 2022

CITATION
Jinno C, Li X and Liu Y (2022) Dietary supplementation of *Bacillus subtilis* or antibiotics modified intestinal microbiome of weaned pigs under enterotoxigenic *Escherichia coli* infection. *Front. Microbiol.* 13:1064328. doi: 10.3389/fmicb.2022.1064328

Dietary supplementation of *Bacillus subtilis* or antibiotics modified intestinal microbiome of weaned pigs under enterotoxigenic *Escherichia coli* infection

Cynthia Jinno[1], Xunde Li[2] and Yanhong Liu[1]*

[1]Department of Animal Science, University of California, Davis, Davis, CA, United States, [2]Department of Population Health and Reproduction, School of Veterinary Medicine, University of California, Davis, Davis, CA, United States

Our previous research reported that supplementation of *Bacillus subtilis* DSM 25841 promoted growth and disease resistance of weaned pigs under enterotoxigenic *Escherichia coli* (ETEC) challenge and its efficacy is comparable to carbadox. This follow-up study aimed to characterize the effects of ETEC infection, supplementing *B. subtilis* DSM 25841 or carbadox on intestinal microbiota of pigs. Forty-eight weaned pigs (6.17 ± 0.36 kg BW) were randomly allotted to one of four treatments: negative control (NC), positive control (PC), antibiotics (AGP, 50 mg/kg of carbadox), and direct fed microbials (DFM, 2.56×10^9 CFU/kg of *B. subtilis*). The experiment lasted 28 days with 7 days before and 21 days after first *E. coli* inoculation (day 0). Pigs in the PC, AGP, and DFM groups were orally inoculated with F18 ETEC for 3 consecutive days with 10^{10} CFU per dose per day. Fecal samples were collected on day −7, and day 7 and day 21 post inoculation, digesta samples were collected from jejunum, ileum, and distal colon on day 21 post inoculation to perform 16S rRNA sequencing. Sampling days and locations influenced ($p < 0.05$) Chao1 index and beta-diversity. Age increased ($p < 0.05$) the relative abundance of Firmicutes but decreased ($p < 0.05$) the relative abundance of Bacteroidetes in feces. ETEC infection increased ($p < 0.05$) the relative abundance of Proteobacteria in feces on day 7 post inoculation. AGP reduced ($p < 0.05$) relative abundance of Firmicutes and *Lactobacillaceae* in feces compared with PC and DFM. AGP reduced ($p < 0.05$) relative abundance of *Bifidobacteriaceae* in jejunum and ileum, while DFM reduced ($p < 0.05$) relative abundance of *Actinomycetaceae* in jejunum and *Lachnospiraceae* in ileum, compared with PC. Pigs fed with DFM had greater ($p < 0.05$) relative abundance of *Ruminococcaceae*, *Veillonellaceae*, *Bifidobacteriaceae* in jejunum, *Lactobacillaceae* in ileum and colon, and *Bifidobacteriaceae* in colon than pigs in AGP. Current results indicate that carbadox or *B. subtilis* had stronger influences on microbial diversity and composition in ileum than other intestinal segments and feces. Supplementation of *B. subtilis* could increase or maintain the relative abundance of beneficial bacteria in ileum compared with carbadox.

KEYWORDS

antibiotics, *Bacillus subtilis*, *Escherichia coli* challenge, microbiome, weaned pigs

Introduction

Transitioning from farrowing to nursery stage is known to aggravate the stress of pigs raised for pork production. Newly weaned pigs can experience extreme discomfort when separated from their sows, as they are accompanied by a sudden change in diet, environment, and social life conditions (Campbell et al., 2013). Prolonged exposure to stress has shown to adversely impact the health and performance of pigs, resulting in huge economical losses. Stress can also induce microbial imbalance in the gut and increase vulnerability to pathogens (Madison and Kiecolt-Glaser, 2019). Enterotoxigenic *Escherichia coli* (ETEC) is an intestinal pathogenic strain that is commonly known to induce secretory diarrhea and intestinal inflammation in pigs under post-weaning stress (Lallès et al., 2004; Fairbrother et al., 2006). In-feed antibiotics, commonly known as antibiotics growth promoters (AGP), were used to apply into nursery diet to alleviate post-weaning diarrhea and to promote growth in weaned pigs (USDA, 2007). On globally estimation, pigs on average consumed approximately 172 mg of antimicrobials per kilogram body weight globally, which was greater than the amounts that cattle and chicken consumed (Boeckel et al., 2015). The global antimicrobial consumption is estimated to increase by 67% between 2010 and 2030 (Boeckel et al., 2015). The extensive use of AGP, however, may increase the chance of dispersing antimicrobial residues and the development of antimicrobial resistance in bacteria (Menkem et al., 2019; Ma et al., 2021). In addition, AGP can modify the gut microbiota and essentially kill beneficial bacteria, thus, may increase the susceptibility to other infections in weaned pigs (Looft et al., 2014). The heightening concerns toward antibiotics and AGP uses have led to the prohibited use of AGP (FDA-2011-D-0889) in livestock for growth-promoting purposes (FDA, 2013). Thus, alternatives to in-feed antibiotics are to be sought immediately.

The importance of gut microbiome in human and animal health, particularly in gut health has been largely reviewed (Kamada et al., 2013; Fouhse et al., 2016; Ke et al., 2019). During weaning, pigs were reported to have temporary loss of microbial diversity in their intestinal tracts, including a decrease in *Lactobacillus* spp. and an increase in a family of pathogenic bacteria such as *Enterobacteriaceae* (Cao et al., 2016; Gresse et al., 2017; Tian et al., 2017). The disturbance of gut microbiome, in combination with immature intestinal immunity, can lead to the expansion of enteric pathogens, such as ETEC infection. Direct-fed microbials (DFM) have been applied to nursery diets to enhance intestinal health, disease resistance, and performance (Liao and Nyachoti, 2017). DFM are categorized into three main groups, including lactic acid-producing bacteria, yeast, and *Bacillus* spp. Compared with other categories, *Bacillus*-based DFMs are spore-forming and thermostable, thus, easy to handle for feed storage and processing. Dietary supplementation of *Bacillus subtilis* was reported to enhance growth performance and diarrhea in nursery pigs by modulating the intestinal immunity and microbiota (Hu et al., 2014; Luise et al., 2019). In our previous studies, we observed that supplementing *B. subtilis* DSM 25841 reduced diarrhea and enhanced growth performance by enhancing intestinal barrier function of weaned pigs experimentally infected with ETEC F18 (Kim et al., 2019; He et al., 2020). However, the impacts of this *Bacillus* strain on gut microbiota of weaned pigs under post-weaning diarrhea has yet to be addressed. Thus, the major objectives of the present study included: (1) to determine the impacts of ETEC infection on fecal and intestinal microbiome of weaned pigs; and (2) to investigate the effects of supplementing *B. subtilis* DSM 25841 on gut microbiome of ETEC infected pigs, in comparison to antibiotics, carbadox.

Materials and methods

Animals and study design

Animal procedures were reviewed and approved by the Institutional Animal Care and Use Committee (IACUC #19322) at the University of California, Davis (UC Davis). A total of 48 weaned pigs (21 day (d) old; 6.17 ± 0.36 kg) with equal number of barrows and gilts were obtained from the Swine Teaching and Research Center and the experiment was conducted at Cole facility at UC Davis. All pigs and their sows did not receive *E. coli* vaccines, antibiotic injections, or antibiotics in feed prior to the experiment. After weaning, pigs were individually housed (pen size: 0.61 m × 1.22 m) and assigned into one of 4 treatment groups using a randomized complete block design with sex normalized by body weight and litter as blocks and pig as experimental unit. Four treatments were: (1) negative control (NC): control diet and without *E. coli* challenge, (2) positive control (PC): control diet and with ETEC challenge, (3) AGP: inclusion of 50 mg/kg carbadox and with ETEC challenge, (4) DFM: inclusion of 500 mg/kg *B. subtilis* DSM 25841 (2.56×10^9 CFU/kg) and with ETEC challenge. There were 12 replicate pigs per treatment. The experiment lasted 28 days with first 2 weeks as phase 1 and last 2 weeks as phase 2. Therefore, 6 diets were prepared and all diets met the current estimates for nutrient requirements for nursery pigs (NRC, 2012; Table 1).

The experiment included a 7-day habituation period and 21 days after the first ETEC F18 inoculation (day 0). Pigs in the ETEC challenge groups received 3 oral doses of ETEC F18 at 10^{10} CFU per dose per day, while pigs in NC group were orally inoculated with 3 ml phosphate-buffered saline per day. The ETEC F18 were cultured in Dr. Xunde Li's lab at Western institute for Food Safety & Security at UC Davis. The bacterial strain was originally isolated from a field disease outbreak by the University of Illinois Veterinary Diagnostic Lab (isolate number: U.IL-VDL # 05–27,242) and the strain expresses heat-labile toxin, heat-stable toxin b, and Shiga-like toxins. Our previous published research confirmed the current ETEC challenge dosage induced mild diarrhea in weaned pigs (Liu et al., 2013; Kim et al., 2019). The detailed animal study procedures and data

TABLE 1 Ingredient compositions of experimental diets[1].

Ingredient, %	Control, phase I	Control, phase II
Corn	44.41	57.27
Dried whey	15.00	10.00
Soybean meal	18.00	22.00
Fish meal	10.00	7.00
Lactose	6.00	–
Soy protein concentrate	3.00	–
Soybean oil	2.00	2.00
Limestone	0.56	0.70
L-Lysine·HCl	0.21	0.23
DL-Methionine	0.08	0.05
L-Threonine	0.04	0.05
Salt	0.40	0.40
Vit-mineral, Sow 6[2]	0.30	0.30
Total	100.00	100.00
Calculated energy and nutrient		
Metabolizable energy, kcal/kg	3,463	3,429
Net energy, kcal/kg	2,601	2,575
Crude protein, %	22.27	20.80
Arg,[3] %	1.23	1.15
His,[3] %	0.49	0.47
Ile,[3] %	0.83	0.76
Leu,[3] %	1.62	1.55
Lys,[3] %	1.35	1.23
Met,[3] %	0.45	0.39
Thr,[3]%	0.79	0.73
Trp,[3] %	0.23	0.21
Val,[3] %	0.91	0.84
Met + Cys,[3] %	0.74	0.68
Phe + Tye,[3] %	1.45	1.38
Ca, %	0.80	0.70
Total P, %	0.68	0.59
Digestible P, %	0.47	0.37
Analyzed nutrient, as-is		
Dry matter, %	90.70	89.90
Crude protein, %	23.13	21.30
ADF, %	7.26	9.35
NDF, %	2.54	3.60
Ca, %	0.96	0.88
P, %	0.71	0.59

(Continued)

TABLE 1 (Continued)

[1]In each phase, two additional diets were formulated by adding probiotics or Carbadox to the control diet, respectively. The dose for probiotics was 500 mg/kg, which was equal to 2.56×10^9 CFU *Bacillus subtilis*/kg diet. The dose for carbadox was 50 mg/kg diet.

[2]Provided the following quantities of vitamins and micro minerals per kilogram of complete diet: Vitamin A as retinyl acetate, 11,136 IU; vitamin D3 as cholecalciferol, 2,208 IU; vitamin E as DL-alpha tocopheryl acetate, 66 IU; vitamin K as menadione dimethylprimidinol bisulfite, 1.42 mg; thiamin as thiamine mononitrate, 0.24 mg; riboflavin, 6.59 mg; pyridoxine as pyridoxine hydrochloride, 0.24 mg; vitamin B12, 0.03 mg; D-pantothenic acid as D-calcium pantothenate, 23.5 mg; niacin, 44.1 mg; folic acid, 1.59 mg; biotin, 0.44 mg; Cu, 20 mg as copper sulfate and copper chloride; Fe, 126 mg as ferrous sulfate; I, 1.26 mg as ethylenediamine dihydriodide; Mn, 60.2 mg as manganese sulfate; Se, 0.3 mg as sodium selenite and selenium yeast; and Zn, 125.1 mg as zinc sulfate.

[3]Amino acids were indicated as standardized ileal digestible AA.

for growth performance and diarrhea were reported in He et al. (2020).

Sample collection

Prior to weaning, tail samples were collected from all piglets to assess their susceptibility to ETEC F18 using the genotyping analysis described in Kreuzer et al. (2013). All pigs used in the present study were susceptible to ETEC F18. Fresh fecal samples were collected from 7 pigs per treatment at the beginning of the experiment (day −7), and from all pigs on day 0 before ETEC inoculation, and day 7 and day 21 post-inoculation (PI). Samples were immediately stored at −80°C until further analysis. At the termination of the experiment (day 21 PI), all pigs were euthanized. For euthanasia, pigs were anesthetized by intramuscularly injecting 1 ml mixture of telazol (100 mg) ketamine (50 mg), and xylazine (50 mg) prior to an intracardiac injection of 78 mg sodium pentobarbital (Vortech Pharmaceuticals, Ltd., Dearborn, MI) per 1 kg of body weight. Digesta was collected from the middle of jejunum (approximately equal length from pylorus to ileocecal junction), ileum (close to the ileocecal junction), and distal colon (prior to the rectum) and was immediately frozen into liquid nitrogen and stored at −80°C until further analysis. A total of 6 pigs were removed from the whole data set due to health issues after *E. coli* infection or as outliers, including 3 pigs from the PC group and 3 pigs from the AGP group (He et al., 2020).

Library preparation

Bacterial DNA was extracted from 154 fecal samples and 126 intestinal digesta using the Quick-DNA Fecal/Soil Microbe Kit (Zymo Research, Irvine, CA, United States) according to the manufacturer's instructions. DNA samples was amplified by PCR at the V4 region of the 16S rRNA gene using primers 515F (5′-XXXXXXXX**GT**GTGCCAGCMGCCGCGGTAA-3′), which included an 8-nt poly-X sequence indicating a barcode unique to each sample followed by an 2-nt Illumina adapter (bold), and

806R (5′-GGACTACHVGGGTWTCTAAT-3′) (Caporaso et al., 2012). Samples were prepared for PCR amplification in duplicates, and each PCR reaction was comprised of 2 µl template DNA, 9.5 µl nuclease free water, 12.5 µl GoTaq 2× Master Mix (Promega, Madison, WI, United States), 0.5 µl V4 reverse primer (10 µM), and 0.5 µl barcoded forward primer (10 µM). Amplification was performed in a thermocycler with the following setting: 94°C for 3 min for initializing denaturation; followed by 35 cycles of 94°C for 45 s, 50°C for 1 min, and 72°C for 1.5 min; and 72°C for 10 min for final elongation. Agarose gel electrophoresis was used to verify the amplicon size for each sample and band brightness was observed to subjectively quantify the amount of sample to be added when pooling DNA amplication products. Pooled sample was then purified using the QIAquick PCR Purification Kit (Qiagen, Hilden, Germany) and submitted to the UC Davis Genome Center DNA Technologies Core for 250 bp paired-end sequencing on the Illumina MiSeq platform (Illumina, Inc., San Diego, CA, United States).

Microbiota analysis

Raw fastq files were first demultiplexed and barcode sequences were removed using the software saber[1] and demultiplexed sequences were then imported into Quantitative Insights into Microbial Ecology 2 (QIIME2; version 2019.4; Bolyen et al., 2019, 2). Using the DADA2 plugin, primers and lower quality reads were removed and the paired end reads were denoised and merged (Callahan et al., 2016, p. 2). Chimeras were removed after merging and amplicon sequence variants (ASVs) were constructed as well. Representative sequences for each ASV were aligned using MAFFT and masked alignments were used to generate phylogenetic trees using FastTree2 (Price et al., 2010; Katoh and Standley, 2013). Python library scikit-learn was used to assign taxonomy based on representative sequences against Silva (version 138), which was pre-trained in QIIME2 and clipped to only the V4 hypervariable region and clustered at 99% sequence identity (Pedregosa et al., 2011; Quast et al., 2012; Bokulich et al., 2018).

Shannon and Chao1 indices were measured for alpha diversity by using the estimate_richness function in phyloseq (McMurdie and Holmes, 2013). To compare community composition among treatments and day or intestinal site, Bray-Curtis matrix was measured to calculate beta diversity. Relative abundance of each taxon in each sample was calculated by dividing the taxa count by total number of filtered reads within each sample.

Statistical analyzes

Files were exported from QIIME2 and imported into the R 4.1.0 for data visualization and statistical analysis (Team, 2021). All microbiota analyzes was performed using the phyloseq package and data were visualized using the ggplot2 package (Wickham, 2011). Normality and homoscedasticity were tested using the Shapiro Wilks test and Bartlett test, respectively. Linear mixed-effect model was fitted using the lme4 package with treatment and site or day and interaction as fixed effects while pig as random effect (Bates et al., 2014, p. 4). Significance of each term in the model was determined using the F-test as type 3 analysis of variance using the Anova function in the car package, followed by group comparison using the cld function in the emmeans package (Fox and Weisberg, 2018; Lenth, 2021). When normality or homoscedasticity was not observed, non-parametric test was performed using the Kruskal-Wallis sum-rank test using the agricolae package (de Mendiburu and de Mendiburu, 2019). Bray–Curtis dissimilarity was first tested for homoskedasticity using the betadisper function and the statistical significance was tested using PERMANOVA and the vegan package (Oksanen et al., 2013). Statistical significance was assessed at $\alpha = 0.05$ and statistical tendency at $\alpha = 0.10$, and p-values were adjusted for multiple comparisons using false discovery rate (FDR).

Results

Shifts in fecal microbiota with age

After quality filtering in QIIME2, a total of 3,908,518 filtered sequences were obtained from 273 samples. The median reads per sample was 14,338 and the total number of taxa discovered was 3,430. No significant difference in Shannon index was observed among treatments throughout the experiment (Figure 1A). Sampling days influenced ($p < 0.05$) Chao1 index and an increase ($p < 0.05$) in Chao1 index was observed in all treatments on day 0 than day −7 (Figure 1B). Feces collected from pigs in the PC and DFM groups had decreased ($p < 0.05$) Chao1 index on day 7 PI, compared with feces collected on day 0. The principal coordinate analysis (PCoA) plot visualized dissimilarities between samples employing Bray-Curtis distance matrix. The samples grouped according to sampling days, as indicated by the statistical difference using adonis2 ($R^2 = 0.20$; $p < 0.05$) (Figure 2A). No distinctive clusters were observed among treatments on day −7. However, a separated cluster among treatments was observed on day 0 ($R^2 = 0.15$; $p < 0.05$), day 7 PI ($R^2 = 0.10$; $p < 0.05$) and day 21 PI ($R^2 = 0.14$; $p < 0.05$; Figure 2B).

Relative abundances of various phyla and families are presented in Table 2. Firmicutes and Bacteroidetes were the two most abundant phyla in feces throughout the experiment, accounting for more than 75% in relative abundance per treatment group on each sampling day. No difference was observed in the relative abundance of top 6 phyla in feces among all treatments on day −7. The relative abundance of Firmicutes was increased ($p < 0.05$), while the relative abundance of Bacteroidetes was decreased ($p < 0.05$) in NC as the pig age was increased. No difference was observed in the relative abundance of Spirochaetes,

1 https://github.com/najoshi/sabre

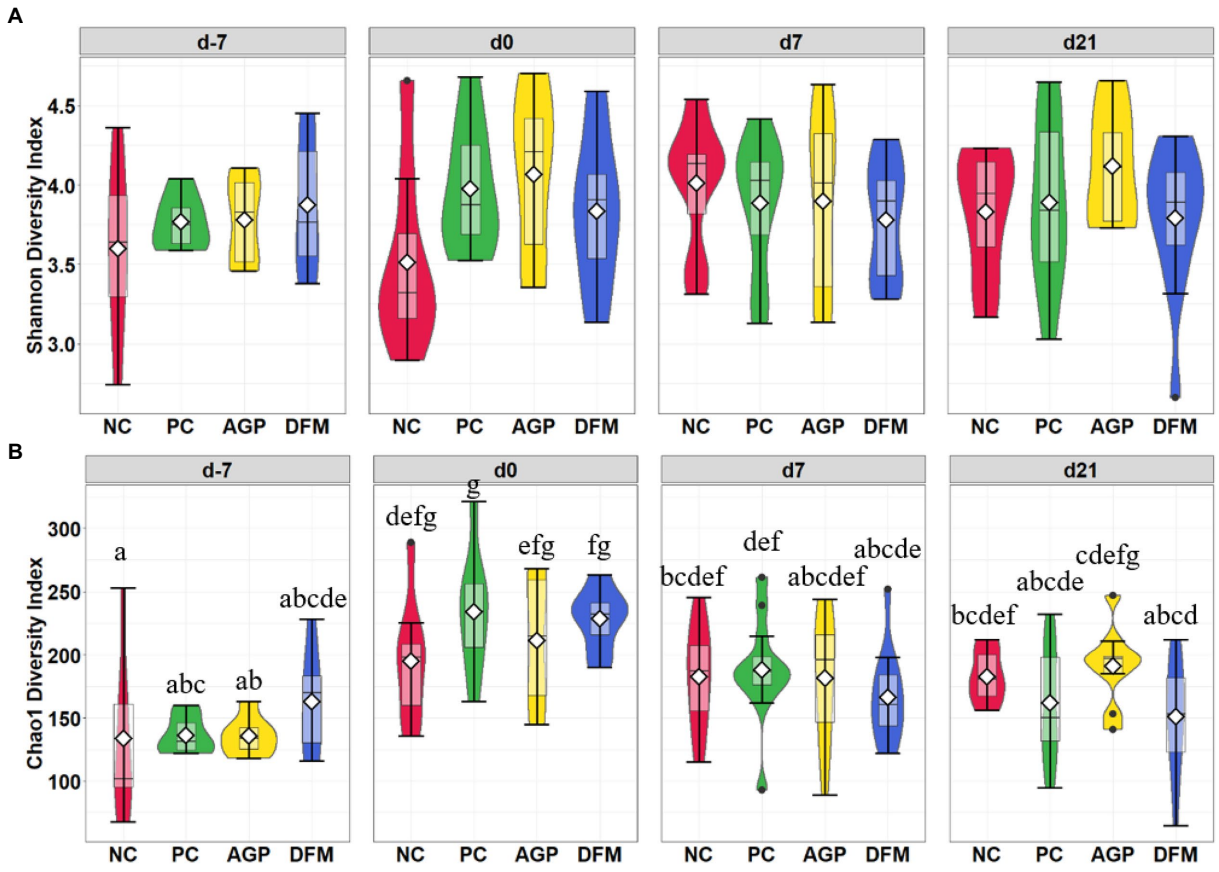

FIGURE 1
Alpha diversity as indicated by Shannon **(A)** and Chao1 **(B)** indices in feces collected from enterotoxigenic *Escherichia coli* challenged pigs fed diets supplemented with antibiotics (AGP) or *Bacillus subtilis* (DFM) at the beginning of the experiment, on day 0 before inoculation (day−7), on day 7 and 21 post-inoculation. No difference was observed in Shannon **(A)**. NC=negative control, PC=positive control, AGP=antibiotics, DFM=*B. subtilis*. Violin plots are colored by diet. Data are expressed as mean (diamond)±SEM. $^{a-g}$Means without a common superscript are different ($p<0.05$). Each mean represents 7 observations on day −7 and each mean represents 9–12 observations on day 0 and day 7 and 21 post-inoculation.

Actinobacteria, and Euryarchaeota among treatments and sampling days. On day 0 and day 7 PI, pigs in NC and DFM had greater ($p<0.05$) relative abundance of Firmicutes in feces than pigs in PC and AGP. At the concluding day of the experiment (day 21 PI), pigs in the AGP group had lower (77.22% vs. 82.36%, $p<0.05$) relative abundance of Firmicutes in feces than pigs in NC. No difference was observed in the relative abundance of Bacteroidetes between NC and PC on any sampling date. The relative abundance of Bacteroidetes was lower (10.03% vs. 18.31%, $p<0.05$) in feces of pigs fed with DFM than pigs supplemented with AGP on day 7 PI. Pigs in PC had greater ($p<0.05$) relative abundance of Proteobacteria in feces than pigs in NC on day 7 PI. No difference was observed in the relative abundance of Proteobacteria between AGP and DFM throughout the experiment.

Within Firmicutes phylum, the relative abundance of *Bacillaceae* was the greatest ($p<0.05$) in DFM among all treatment on day 0, 7, and 21 PI. The relative abundance of *Lactobacillaceae* in NC was increased ($p<0.05$) in feces on day 0 but decreased ($p<0.05$) on day 21 PI, compared with feces collected on day −7 (Table 2). In addition, pigs supplemented with AGP had reduced ($p<0.05$) relative abundance of *Lactobacillaceae* in feces on day 0 and day 21 PI. The relative abundance of *Lactobacillaceae* was lower ($p<0.05$) in feces of pigs fed with AGP than that in DFM (4.44% vs. 23.98%) on day 21 PI. Pigs in PC, AGP, and DFM had increased ($p<0.05$) relative abundance of *Lachnospiraceae* from day −7 to 0. *Bacteroidaceae* was the most abundant family in Bacteroidetes phylum on day −7, while *Prevotellaceae* was the most abundant one on day 0, 7, and day 21 PI (Table 2). Pigs in AGP had greater ($p<0.05$) relative abundance of *Bacteroidaceae* in feces than pigs in NC and DFM on day 7 and day 21 PI. Within Proteobacteria phylum, the relative abundance of *Enterobacteriaceae* was decreased ($p<0.05$) but the relative abundance of *Succinivibrionaceae* was increased ($p<0.05$), as pig age was increased (Table 2). Pigs in PC and AGP had greater ($p<0.05$) relative abundance of *Enterobacteriaceae* than NC on

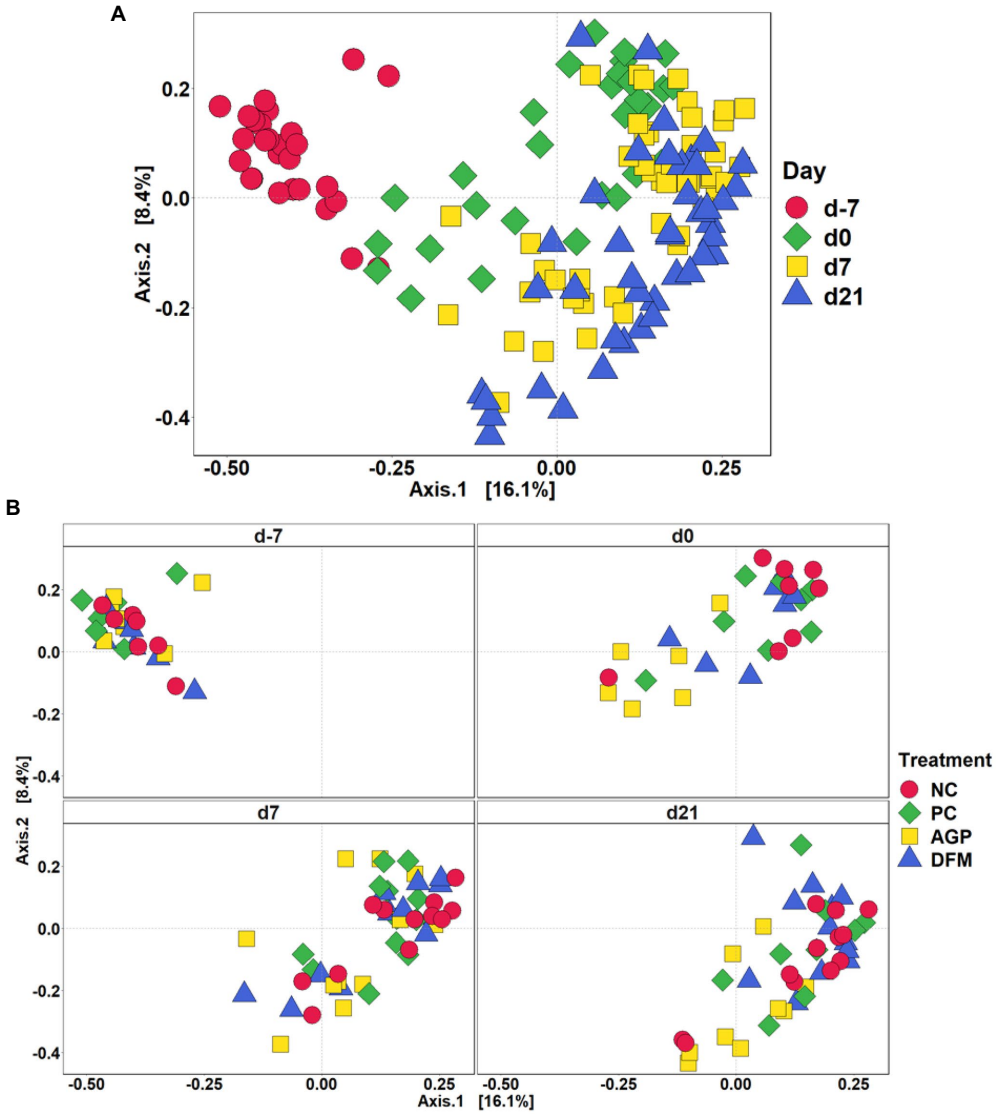

FIGURE 2
Beta diversity of fecal microbiota in enterotoxigenic *E. coli* F18 challenged pigs at the beginning of the experiment, on day 0 before inoculation, on day 7 and 21 post-inoculation by day **(A)** and treatment **(B)**. Data were analyzed by principal coordinate analysis (PCoA) based on the Bray–Curtis dissimilarity. NC=negative control, PC=positive control, AGP=antibiotics, DFM=*B. subtilis*. Each mean represents 7 observations on day −7 and each mean represents 9–12 observations on day 0 and day 7 and 21 post-inoculation.

day 7 PI. However, no difference was observed in the relative abundance of *Enterobacteriaceae* among other treatments on day 7 PI and other sampling dates. The relative abundance of *Succinivibrionaceae* was higher ($p < 0.05$) in PC and AGP than pigs in NC on day 21 PI.

The top 11 abundant genera in feces are presented in Figure 3. From day −7 to day 21 PI, all treatments had increased ($p < 0.05$) relative abundance of *Blautia* and reduced ($p < 0.05$) relative abundance of *Bacteroides* and *Escherichia-Shigella*. All treatments, except AGP, had reduced ($p < 0.05$) relative abundance of *Megasphaera* from day −7 to day 21 PI. The most abundant genus was *Lactobacillus*. In NC pigs, the relative abundance of *Lactobacillus* was increased ($p < 0.05$) from day −7 to 0, and then decreased ($p < 0.05$) by day 21 PI. Pigs in AGP had the lowest abundance ($p < 0.05$) of *Lactobacillus* on day 0 and pigs in DFM had the greatest abundance ($p < 0.05$) of *Lactobacillus* on day 21 PI among treatments. In addition, the relative abundance of *Lactobacillus* was greater in DFM (27.91% vs. 20.73%, $p < 0.05$) than in AGP on day 7 PI. The relative abundance of *Blautia* was greater ($p < 0.05$) in feces collected on day 0, 7 PI, and day 21 PI than in feces collected on day −7. The relative abundance of *Bacteroides* was greater ($p < 0.05$) in AGP than in PC on day 0 and was greater ($p < 0.05$) in AGP than in DFM on day 7 and day 21 PI.

TABLE 2 Relative abundance (%) of Firmicutes, Bacteroidetes, and Proteobacteria and their top families in feces of enterotoxigenic *Escherichia coli* challenged pigs fed diets supplemented with antibiotics (AGP) or *Bacillus subtilis* (DFM).

	Day 7				Day 0				Day 7 post-inoculation				Day 21 post-inoculation			
	Negative control	Positive control	AGP	DFM	Negative control	Positive control	AGP	DFM	Negative control	Positive control	AGP	DFM	Negative control	Positive control	AGP	DFM
Firmicutes	55.00^{g}	54.71^{g}	61.76^{fg}	56.61^{g}	77.84^{abcd}	72.20^{bcdef}	64.34^{fg}	75.93^{abcde}	79.17^{abc}	71.11^{def}	65.40^{efg}	80.11^{ab}	82.36^{a}	76.09^{abcd}	71.99^{cdef}	77.22^{abcd}
Bacillaceae	0.00^{bc}	0.00^{bc}	0.00^{bc}	0.00^{bc}	0.00^{bc}	0.00^{bc}	0.00^{bc}	0.03^{a}	0.00^{bc}	0.00^{bc}	0.00^{bc}	0.01^{c}	0.00^{bc}	0.00^{bc}	0.00^{c}	0.05^{ab}
Christensenellaceae	0.38^{b}	1.53^{ab}	2.15^{ab}	4.18^{a}	1.27^{ab}	1.73^{ab}	3.09^{ab}	1.72^{ab}	1.23^{ab}	0.90^{ab}	1.14^{ab}	2.28^{ab}	0.71^{b}	0.95^{ab}	0.76^{ab}	0.48^{b}
Clostridiaceae1	2.53^{abc}	3.68^{ab}	4.01^{ab}	6.74^{a}	0.24^{c}	0.49^{bc}	2.73^{abc}	1.04^{abc}	1.69^{bc}	1.14^{bc}	4.29^{ab}	3.55^{abc}	6.73^{ab}	1.93^{abc}	12.47^{ab}	2.22^{bc}
Lachnospiraceae	16.59^{bcde}	10.26^{de}	11.94^{cde}	6.58^{e}	17.98^{bcd}	26.26^{ab}	26.87^{ab}	23.64^{ab}	27.21^{a}	23.07^{ab}	20.04^{abcd}	23.88^{ab}	21.83^{ab}	21.32^{abc}	18.69^{bcd}	20.06^{abc}
Lactobacillaceae	11.55^{cde}	16.92^{bcde}	21.54^{bcd}	15.93^{bcde}	39.56^{a}	24.55^{abc}	6.42^{de}	27.09^{abc}	23.10^{abc}	28.21^{ab}	20.73^{bc}	27.91^{ab}	14.63^{cde}	14.24^{cde}	4.44^{e}	23.98^{bc}
Peptostreptococcaceae	1.46^{abcd}	2.29^{ab}	0.93^{abcd}	1.92^{ab}	0.16^{e}	0.12^{e}	0.14^{e}	0.38^{de}	0.65^{bcd}	0.53^{cde}	3.33^{abc}	1.69^{abc}	3.81^{a}	1.10^{abcd}	6.91^{a}	1.21^{bcd}
Ruminococcaceae	14.27	12.96	12.58	10.48	11.23	12.55	17.97	13.88	18.63	10.89	11.30	12.94	15.07	16.62	15.29	14.57
Streptococcaceae	0.64^{bc}	1.11^{ab}	0.39^{bcd}	0.61^{bcd}	0.05^{d}	0.08^{cd}	0.02^{d}	0.2^{cd}	0.18^{cd}	1.05^{bcd}	0.38^{bcd}	2.97^{bcd}	10.44^{a}	6.27^{ab}	0.10^{cd}	1.90^{b}
Veillonellaceae	2.32^{def}	0.67^{f}	1.22^{ef}	1.21^{ef}	4.08^{cdef}	3.41^{bcd}	2.64^{def}	3.46^{bcde}	3.77^{bcd}	2.38^{def}	1.87^{def}	2.56^{def}	6.69^{abc}	10.93^{a}	9.11^{bcd}	9.99^{ab}
Bacteroidetes	29.43^{ab}	31.97^{a}	21.97^{abc}	20.62^{abcd}	11.12^{cde}	14.20^{cde}	17.96^{abcd}	16.04^{bcde}	12.27^{cde}	12.65^{cde}	18.31^{abc}	10.03^{e}	9.70^{e}	10.25^{de}	15.85^{bcde}	13.73^{cde}
Bacteroidaceae	18.07^{a}	15.14^{ab}	8.57^{ab}	6.87^{abc}	0.65^{cde}	0.51^{ef}	1.00^{bcd}	0.68^{cde}	0.11^{fgh}	0.85^{de}	2.2^{cd}	0.28^{efg}	0.01^{h}	0.22^{gh}	0.16^{efg}	0.01^{h}
Muribaculaceae	0.50	1.83	0.79	0.79	2.13	3.75	4.20	3.63	2.50	1.83	2.36	1.24	2.40	1.64	3.05	2.52
Prevotellaceae	6.19	5.87	4.91	5.34	6.38	6.99	8.07	8.32	7.87	8.02	11.54	7.36	6.54	7.62	10.00	10.15
Rikenellaceae	3.51^{ab}	5.88^{a}	5.36^{ab}	5.39^{ab}	1.12^{bcde}	2.08^{abc}	3.92^{ab}	2.80^{abc}	1.31^{bcde}	1.49^{bcde}	1.63^{bcde}	0.87^{de}	0.61^{e}	0.65^{e}	2.27^{abcd}	0.97^{cde}
Tannerellaceae	0.41^{ab}	1.88^{a}	1.36^{a}	1.17^{ab}	0.32^{ab}	0.31^{bcd}	0.26^{bcd}	0.47^{ab}	0.13^{cde}	0.03^{e}	0.12^{bcde}	0.11^{bcd}	0.04^{de}	0.05^{de}	0.22^{bc}	0.03^{de}
Proteobacteria	8.21^{abc}	6.72^{ab}	3.78^{abc}	5.92^{ab}	1.52^{abc}	1.86^{abc}	2.82^{abc}	2.72^{abc}	1.18^{c}	7.38^{a}	8.88^{abc}	2.45^{abc}	2.25^{bc}	6.60^{ab}	5.26^{abc}	2.46^{bc}
Desulfovibrionaceae	0.60^{ab}	1.14^{a}	1.46^{a}	1.09^{ab}	0.34^{abcd}	0.32^{bcde}	0.33^{bcde}	0.38^{abc}	0.17^{def}	0.30^{bcde}	0.24^{cdef}	0.22^{def}	0.16^{ef}	0.14^{ef}	0.16^{def}	0.13^{f}
Enterobacteriaceae	6.07^{bcd}	4.23^{abc}	1.97^{abc}	3.60^{ab}	0.49^{de}	0.79^{cd}	0.60^{bcd}	1.75^{abc}	0.69^{cd}	6.49^{a}	8.35^{ab}	1.94^{abc}	0.10^{de}	0.03^{e}	0.01^{e}	0.01^{e}
Pasteurellaceae	0.22^{ab}	1.27^{abcd}	0.09^{abc}	0.19^{a}	0^{d}	0^{d}	0^{cd}	0^{cd}	0^{cd}	0.01^{bcd}	0^{d}	0^{cd}	0^{cd}	0.01^{bcd}	0^{d}	0^{d}
Succinivibrionaceae	0.58^{ef}	0^{f}	0.01^{f}	0.87^{ef}	0.65^{cde}	0.52^{bcd}	1.76^{cde}	0.54^{bcde}	0.28^{def}	0.50^{cde}	0.17^{def}	0.20^{def}	1.56^{cde}	6.12^{a}	5.07^{ab}	2.30^{abc}

[a–g]Means without a common superscript are different ($p < 0.05$). Each mean represents 7 observations on day −7 and each mean represents 9–12 observations on day 0 and day 7 and 21 post-inoculation.

10.3389/fmicb.2022.1064328

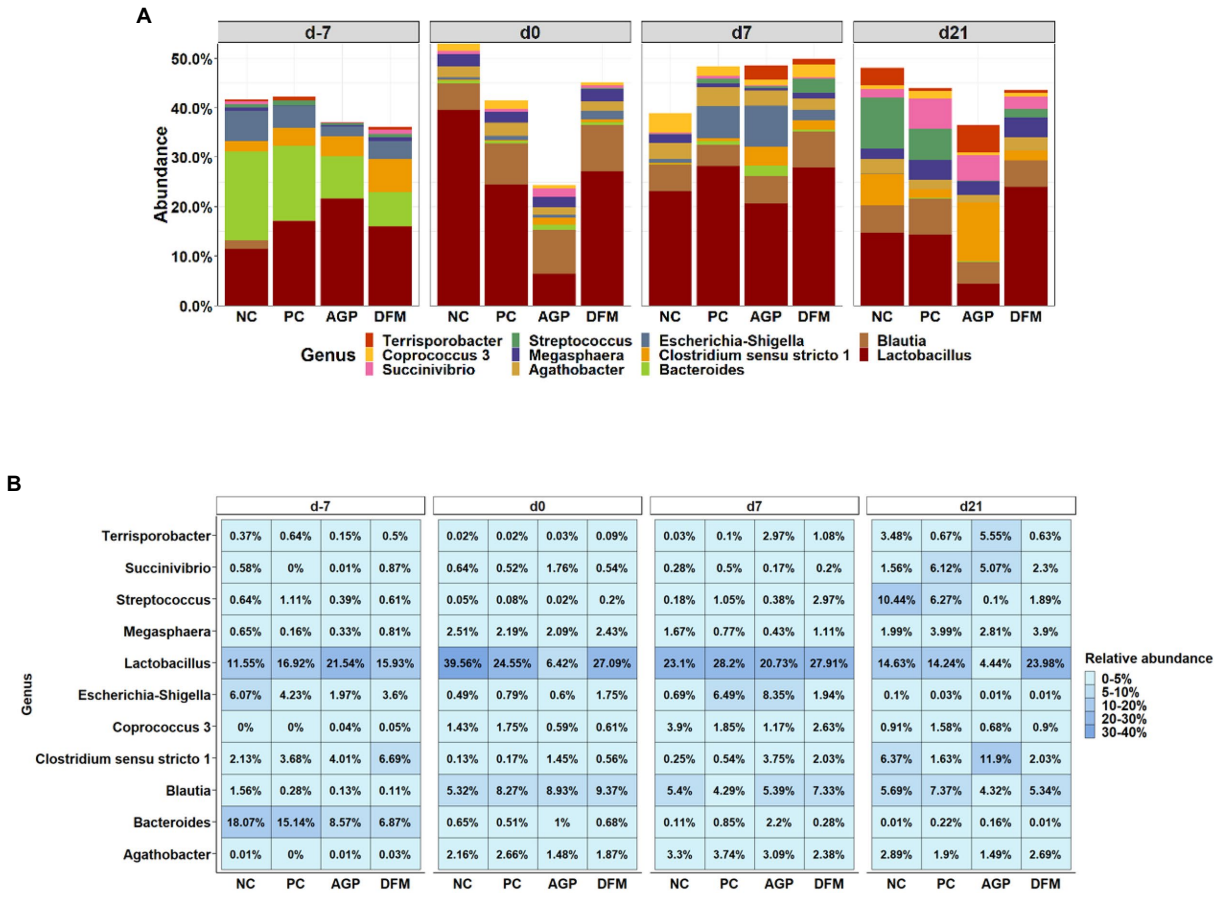

FIGURE 3
Relative abundance of genus that were most abundant in fecal microbiota of piglets visualized in bar plot **(A)** and heatmap **(B)**. Each mean represents 7 observations on day –7 and each mean represents 9–12 observations on day 0 and day 7 and 21 post-inoculation.

Shifts in gut microbiota within different intestinal sites

The microbial composition in the digesta of jejunum, ileum, and colon was also investigated at the conclusion of this experiment (day 21 PI). Significant interaction between treatment and intestinal site was observed ($p < 0.001$) in both Shannon and Chao1 diversities (Figure 4). Shannon and Chao1 indices in colon digesta were greater ($p < 0.05$) than in jejunal and ileal digesta. No difference was observed in Shannon and Chao1 indices between NC and PC in any of intestinal sites. Pigs supplemented with AGP had greater ($p < 0.05$) Shannon index than other treatments in the ileum (Figure 4A) and had greater ($p < 0.05$) Chao1 index in the jejunum than NC (Figure 4B). Supplementation of DFM reduced ($p < 0.05$) Chao 1 index in ileal digesta when compared with NC.

The adonis2 test demonstrated significance in treatment ($R^2 = 0.10$, $p < 0.05$), intestinal site ($R^2 = 0.18$, $p < 0.05$), and treatment and intestinal site interaction ($R^2 = 0.05$, $p < 0.05$). In Figure 5A, all colon samples were clustered together and were separated from jejunal and ileal samples, whereas clusters for ileum and jejunum were indistinguishable from each other. No clear separation was observed among treatments in jejunum, while the AGP cluster was distinct from DFM cluster in ileum (Figure 5B). Within colon samples, AGP cluster partially overlapped with DFM cluster, while NC and PC clusters were overlapping with each other.

The relative abundance of phyla, families, and genera are presented in Table 3. Firmicutes, Bacteroidetes, Actinobacteria, and Proteobacteria were the top four abundant phyla in the intestinal tract of weaned pigs. Firmicutes was the most abundant phylum in jejunum, ileum, and colon in all pigs. Unlike fecal samples, Bacteroidetes was second most abundant phylum in colon, Actinobacteria was the second most abundant phylum in jejunum, and Proteobacteria was the second most abundant phylum in ileum. No difference was observed in the relative abundance of phyla between NC and PC in all intestinal sites. The relative abundance of Bacteroidetes in ileal digesta was greater ($p < 0.05$) in AGP than DFM. The relative abundance of Actinobacteria in ileal digesta was greater ($p < 0.05$) in PC than AGP. Pigs in AGP had the greatest ($p < 0.05$) relative abundance of Proteobacteria in jejunal digesta among all treatments and had greater ($p < 0.05$) relative abundance of Proteobacteria in ileal digesta than pigs in DFM (4.12% vs. 0.22%).

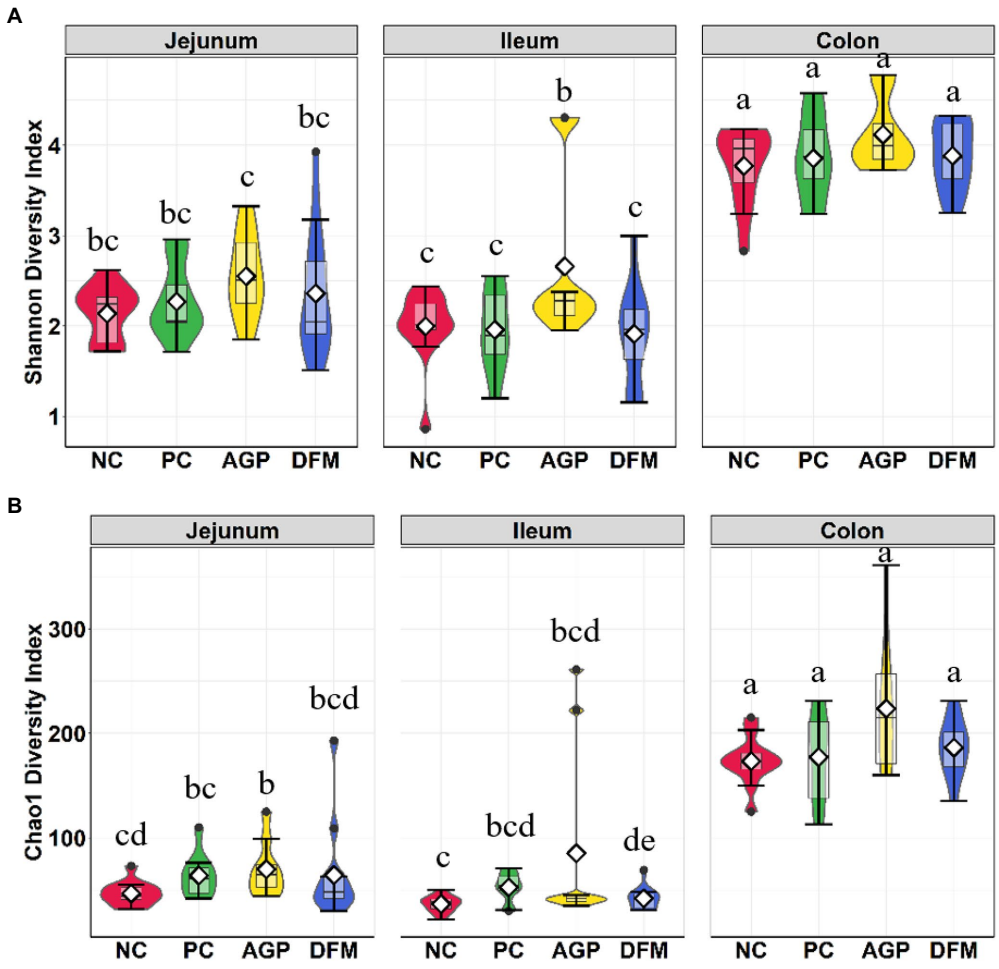

FIGURE 4
Alpha diversity as indicated by Shannon **(A)** and Chao1 **(B)** indices in intestinal digesta collected from weaned pigs challenged with enterotoxigenic *E. coli*. Pigs were supplemented with antibiotics (AGP) or *B. subtilis* (DFM). NC=negative control, PC=positive control. Violin plots are colored by diet. Data are expressed as mean (diamond)±SEM. [a-g]Means without a common superscript are different ($p < 0.05$). Each mean represents 9–12 observations.

Under family level, jejunal digesta contained highest ($p < 0.05$) relative abundance of *Lactobacillaceae*, *Actinomycetaceae*, and *Micrococcaceae* among three intestinal sites. Ileal digesta had more ($p < 0.05$) relative abundance of *Clostridiaceae1* and *Enterobacteriaceae* than jejunal and colon digesta. Colon digesta contained more ($p < 0.05$) *Lachnospiraceae*, *Ruminococcaceae*, *Veillonellaceae*, *Coriobacteriaceae*, *Succinivibrionaceae*, and top 4 families under Bacteroidetes than jejunal and ileal digesta. The relative abundance of *Lactobacillaceae* was greater ($p < 0.05$) in DFM than NC and AGP in ileal digesta and was greater ($p < 0.05$) in DFM than AGP in colon digesta. ETEC F18 challenge increased ($p < 0.05$) the relative abundance of *Actinomycetaceae* and *Micrococcaceae* in jejunal and ileal digesta, *Lachnospiraceae* in ileal digesta and *Succinivibrionaceae* in colon digesta, but reduced ($p < 0.05$) *Streptococcaceae* in colon digesta. Compared with PC, supplementation of AGP enhanced ($p < 0.05$) the relative abundance of *Peptostreptococcaceae* and *Pasteurellaceae* in jejunal digesta, *Muribacelaceae* in ileal digesta, and *Bacteroidaceae* and *Rikenellaceae* in colon digesta. In addition, inclusion of AGP reduced ($p < 0.05$) the relative abundance of *Veillonellaceae*, *Actinomycetaceae*, *Atopobiaceae*, *Bifidobacteriaceae*, *Eggerthellaceae* in jejunal digesta, *Lachnospiraceae*, *Actinomycetaceae*, *Bifidobacteriaceae* in ileal digesta, and *Veillonellaceae* and *Coriobacteriaceae* in colon digesta. In comparison to PC, supplementation of DFM reduced ($p < 0.05$) the relative abundance of *Actinomycetaceae* in jejunal digesta and *Lachnospiraceae* in ileal digesta. Pigs fed with DFM had greater ($p < 0.05$) the relative abundance of *Ruminococcaceae*, *Veillonellaceae*, *Bifidobacteriaceae* in jejunal digesta, *Lactobacillaceae* in both ileum and colon, and *Bifidobacteriaceae* in colon when compared with pigs in AGP. However, pigs fed with DFM had reduced ($p < 0.05$) the relative abundance of *Pasteurellaceae* in jejunum, *Ruminococcaceae*, *Rikenellaceae*, *Pasteurellaceae*, *Succinivibrionaceae* in ileum, and *Bacteroidaceae* in colon, compared with pigs fed with AGP. In all intestinal

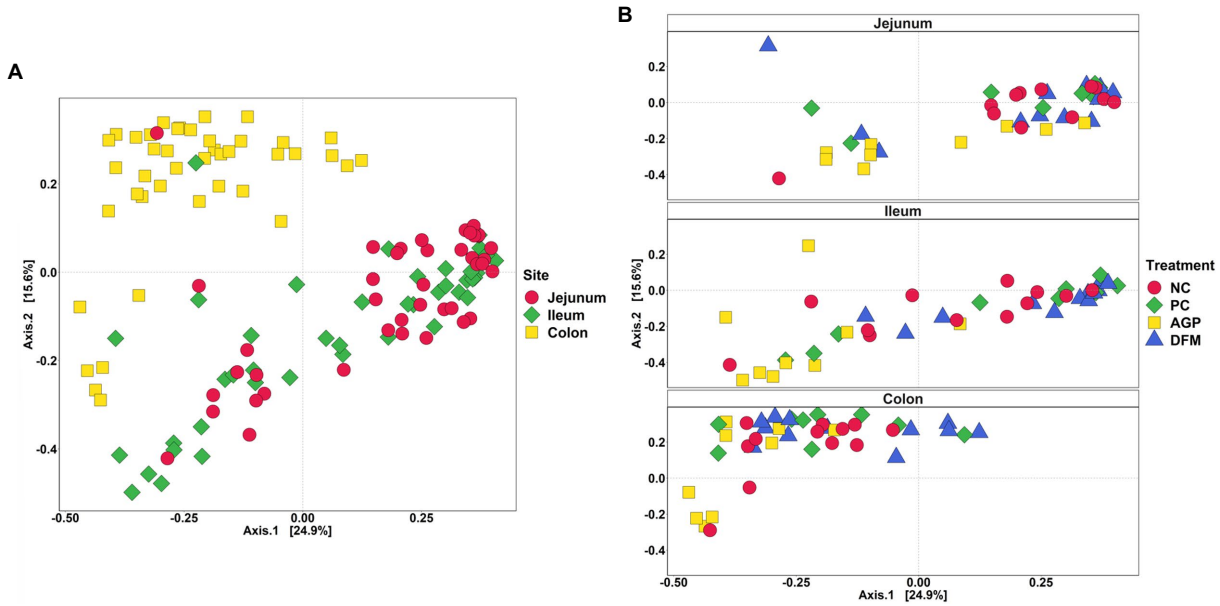

FIGURE 5
Beta diversity of intestinal digesta microbiota in pigs challenged with enterotoxigenic *E. coli* by intestinal site **(A)** and treatment **(B)**. Data were analyzed by principal coordinate analysis (PCoA) based on Bray–Curtis dissimilarity. NC=negative control, PC=positive control, AGP=antibiotics, DFM=*B. subtilis*. Each mean represents 9–12 observations.

sites, pigs in DFM had the highest ($p < 0.05$) relative abundance of *Bacillaceae* among all treatments.

The relative abundances of top abundant genera are presented in Figure 6. Relative abundance of *Lactobacillus* was greater ($p < 0.05$) but the relative abundance of *Clostridium sensu stricto 1* was less ($p < 0.05$) in ileal and colon digesta of pigs fed with DFM than in AGP. ETEC infection reduced the relative abundance of *Streptococcus* in ileum and colon, however, pigs supplemented with AGP had more ($p < 0.05$) *Streptococcus* in jejunum but lower ($p < 0.05$) *Streptococcus* in ileum and colon when compared with NC.

Discussion

Our previous studies reported that dietary supplementation of *B. subtilis* DSM 25841 promoted growth performance, reduced diarrhea, and enhanced intestinal immunity in weaned piglets under ETEC challenge (Kim et al., 2019; He et al., 2020). However, the potential mechanisms of the beneficial effects of *B. subtilis* on swine health and the impacts of this *B. subtilis* strain on intestinal microbiota remain unclear. In the present study, we characterized the impacts of ETEC F18 infection, *B. subtilis* DSM 25841, and carbadox on the dynamics of microbial composition in feces during the weaning transition period. The microbiota composition in different segments of the intestine were also investigated as ETEC F18 mainly target the small intestine of weaned pigs. Identifying shifts in microbial communities in the intestines could facilitate the development of nutritional interventions to control post-weaning diarrhea when the use of AGP is restricted, and to understand the impacts of currently available DFM on swine health.

Fecal microbiota

Temporal analysis in fecal microbiota was performed using fecal samples collected throughout the experiment. Richness in microbial population was measured in Chao1 and richness and evenness were measured in Shannon index (Shannon, 1948; Chao, 1984, p. 1). Lack of significant treatment effect was observed in the Shannon diversity metric in fecal samples of pigs throughout the experiment. Microbial richness was increased during the habituation period (from day −7 to day 0) but decreased from day 0 to day 7 PI in feces collected from pigs in the positive control, which indicate that ETEC F18 challenge reduced microbial richness in feces. Beta diversity measures the variability in microbial community composition among samples. Samples collected at the beginning of the experiment (day −7) separately clustered from samples collected from other time points, suggesting weaning significantly shifted microbial community composition. Distinctive clusters were also observed between samples on day 0 and day 7 PI. However, feces collected from positive control were not fully separated from samples collected from negative control, which suggests the impacts of ETEC F18 on fecal microbial community composition might be limited. Results of alpha and beta diversities also suggest that dietary supplementation of

TABLE 3 Relative abundance (%) of Firmicutes, Bacteroidetes, Actinobacteria, and Proteobacteria and their top families in intestinal digesta of enterotoxigenic *E. coli* challenged pigs fed diets supplemented with antibiotics (AGP) or *B. subtilis* (DFM).

	Jejunal digesta				Ileal digesta				Colon digesta			
	Negative control	Positive control	AGP	DFM	Negative control	Positive control	AGP	DFM	Negative control	Positive control	AGP	DFM
Firmicutes	93.20^{ab}	84.11^{bcde}	89.51^{abc}	91.85^{abc}	93.28^{a}	92.77^{abc}	86.08^{abcd}	95.67^{a}	85.64^{cde}	80.75^{de}	74.89^{e}	81.23^{de}
Bacillaceae	0.03^{cde}	0.07^{cd}	0.27^{b}	0.64^{a}	0.00^{e}	0.06^{cde}	0.02^{cde}	0.18^{ab}	0.00^{e}	0.00^{e}	0.00^{de}	0.02^{c}
Clostridiaceae1	2.89^{bc}	1.78^{c}	4.91^{bc}	3.59^{bc}	11.89^{a}	11.96^{ab}	22.22^{a}	2.88^{abc}	7.22^{ab}	1.46^{bc}	13.56^{ab}	2.35^{bc}
Lachnospiraceae	0.46^{bc}	1.52^{b}	0.43^{bc}	2.55^{bc}	0.13^{d}	0.42^{bc}	2.04^{cd}	0.09^{d}	23.19^{a}	23.15^{a}	21.93^{a}	24.36^{a}
Lactobacillaceae	76.09^{a}	60.26^{ab}	59.44^{ab}	70.54^{a}	47.48^{b}	56.22^{ab}	22.98^{c}	77.12^{a}	15.09^{cd}	14.42^{cd}	4.11^{d}	21.20^{c}
Peptostreptococcaceae	3.82^{bc}	0.06^{c}	3.50^{ab}	2.14^{bc}	9.59^{a}	5.24^{ab}	15.18^{a}	3.82^{ab}	3.96^{a}	0.86^{ab}	7.48^{a}	1.42^{ab}
Ruminococcaceae	0.06^{cde}	0.44^{bc}	0.13^{b}	1.55^{cde}	0.01^{de}	0.04^{cde}	2.59^{bcd}	0.01^{e}	15.52^{a}	18.15^{a}	15.24^{a}	15.75^{a}
Streptococcaceae	4.93^{abc}	9.61^{ab}	18.40^{a}	5.69^{abc}	19.42^{a}	12.98^{abc}	11.01^{abc}	8.94^{abc}	10.78^{a}	6.60^{bcd}	0.09^{d}	3.21^{cd}
Veillonellaceae	4.40^{cd}	6.30^{abcd}	0.09^{g}	3.85^{cde}	1.38^{efg}	1.98^{def}	1.21^{fg}	0.93^{fg}	6.63^{abc}	12.32^{a}	8.09^{bcd}	9.81^{ab}
Bacteroidetes	0.03^{bc}	0.02^{bc}	0.01^{bc}	1.08^{bc}	0^{bc}	0.03^{bc}	4.16^{b}	0^{c}	7.25^{a}	7.35^{a}	12.41^{a}	9.96^{a}
Bacteroidaceae	0^{b}	0^{b}	0^{b}	0^{b}	0^{b}	0^{b}	0.06^{b}	0^{b}	0.01^{b}	0.11^{b}	0.16^{a}	0.01^{b}
Muribaculaceae	0^{c}	0.01^{c}	0.01^{c}	0.11^{bc}	0^{c}	0^{c}	0.49^{b}	0^{c}	2.22^{a}	1.74^{a}	1.94^{a}	2.09^{a}
Prevotellaceae	0.03^{bc}	0.01^{b}	0^{c}	0.94^{bc}	0^{c}	0.03^{bc}	2.98^{b}	0^{bc}	4.64^{a}	5.09^{a}	8.93^{a}	7.23^{a}
Rikenellaceae	0^{d}	0^{cd}	0^{d}	0.03^{cd}	0^{d}	0.01^{cd}	0.54^{c}	0^{d}	0.28^{ab}	0.35^{b}	1.17^{a}	0.57^{ab}
Actinobacteria	4.76^{a}	9.43^{a}	1.79^{abc}	4.37^{a}	2.93^{abc}	4.38^{ab}	0.36^{c}	3.35^{abc}	2.26^{abc}	2.99^{abc}	0.5^{bc}	2.48^{ab}
Actinomycetaceae	0.01^{bc}	0.14^{a}	0.07^{b}	0.05^{b}	0^{c}	0.06^{b}	0^{c}	0.01^{bc}	0^{c}	0^{c}	0^{c}	0^{c}
Atopobiaceae	0.43^{ab}	0.54^{a}	0^{b}	0.32^{ab}	0.13^{ab}	0.17^{ab}	0.07^{ab}	0.09^{ab}	0.36^{ab}	1.45^{ab}	0.28^{ab}	1.01^{ab}
Bifidobacteriaceae	4.22^{a}	8.21^{a}	0.04^{b}	3.81^{a}	2.76^{a}	3.94^{a}	0.11^{b}	3.20^{a}	1.67^{a}	1.10^{ab}	0.01^{b}	1.22^{a}
Coriobacteriaceae	0^{c}	0^{c}	0^{c}	0.02^{c}	0^{c}	0^{c}	0.05^{c}	0^{c}	0.21^{ab}	0.38^{a}	0.20^{b}	0.22^{ab}
Eggerthellaceae	0.06^{ab}	0.21^{a}	0^{b}	0.05^{ab}	0.03^{ab}	0.05^{ab}	0^{b}	0.02^{ab}	0.02^{ab}	0.05^{ab}	0.01^{ab}	0.03^{ab}
Micrococcaceae	0.04^{c}	0.32^{ab}	1.51^{a}	0.11^{bc}	0.01^{d}	0.15^{bc}	0.12^{bc}	0.03^{c}	0^{d}	0^{d}	0^{d}	0^{d}
Proteobacteria	1.89^{b}	0.4^{b}	4.12^{a}	0.22^{b}	3.77^{ab}	2.21^{ab}	7.61^{a}	0.92^{b}	1.69^{ab}	4.84^{a}	4.6^{a}	2.08^{a}
Burkholderiaceae	0^{a}	0^{a}	0.04^{a}	0^{a}	0^{a}	0^{a}	0.41^{a}	0^{a}	0^{a}	0.01^{a}	0^{a}	0^{a}
Desulfovibrionaceae	0^{b}	0^{b}	0^{b}	0.01^{b}	0^{b}	0^{b}	0.04^{b}	0^{b}	0.07^{a}	0.1^{a}	0.14^{a}	0.11^{a}
Enterobacteriaceae	0.17^{c}	0.02^{abc}	0.04^{abc}	0.01^{c}	3.56^{a}	0.64^{ab}	0.71^{bc}	0.04^{bc}	0.07^{abc}	0.01^{c}	0.01^{c}	0.01^{c}
Pasteurellaceae	1.7^{bc}	0.29^{bcd}	3.75^{a}	0.02^{bcd}	0.21^{bcd}	1.54^{ab}	4.85^{a}	0.87^{bc}	0^{cd}	0.01^{bcd}	0^{cd}	0^{d}
Succinivibrionaceae	0^{d}	0.01^{cd}	0.09^{bc}	0.15^{cd}	0^{d}	0^{cd}	1.5^{bc}	0^{d}	1.41^{b}	4.71^{a}	4.45^{a}	1.94^{a}

$^{a-g}$Means without a common superscript are different ($p < 0.05$). Each mean represents 7 observations on day −7 and each mean represents 9–12 observations on day 0 and day 7 and 21 post-inoculation.

10.3389/fmicb.2022.1064328

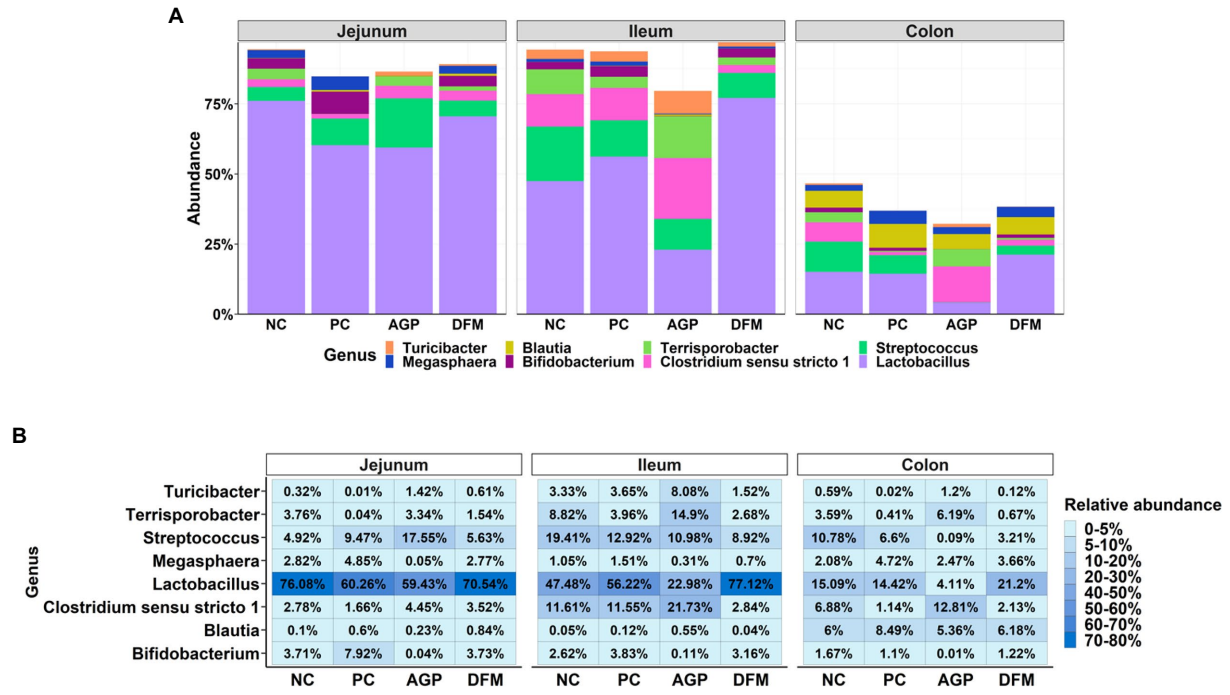

FIGURE 6
Relative abundance of top 8 genus in intestinal microbiota of piglets visualized in bar plot **(A)** and heatmap **(B)**. Each mean represents 9–12 observations.

antibiotics or *B. subtilis* have limited impacts on the microbial diversity in fecal samples.

In consistent with other published research (Frese et al., 2015; Li et al., 2020), Firmicutes and Bacteroidetes were the top two most abundant phyla in fecal samples of weaned pigs. As the age of pigs was increased, the relative abundance of Firmicutes were increased but the relative abundance of Bacteroidetes were decreased (Mach et al., 2015; Chen et al., 2017), indicating that the fecal microbiota has greatly shifted during post-weaning period. The likely reason was the sudden change in diet from sow milk to solid and plant-based ingredients and the changes in environment after weaning. Weaning and dietary change shift the swine core gut microbiome, including *Clostridiaceae1*, *Peptostreptococcaceae*, *Streptococcaceae*, *Bacteroidaceae*, *Enterobacteriaceae*, and *Lactobacillaceae* in feces (Mach et al., 2015; Chen et al., 2017; Luise et al., 2021). The increased *Lactobacillaceae* is highly correlated with enriched plant-derived mono- and di-saccharides (Frese et al., 2015). At the end of this experiment, most of pigs were recovered from weaning stress and ETEC infection as indicated by the absence of ETEC F18 in feces and normal diarrhea scores (He et al., 2020). The relative abundance of the core gut microbiota listed above was reversed in feces, suggesting that the impacts of weaning stress on gut microbiota are significant but temporary. When pigs adapt to their new diets and environment, diet becomes the main driver of regulating gut microbial composition.

Post-weaning ETEC infection can reduce pig appetite, disrupt intestinal barrier, and induce intestinal inflammation, all of which may contribute to the imbalance of the microbiota (Pollock et al., 2019). ETEC is categorized under the family of *Enterobacteriaceae*, which is likely the reason for the increased relative abundance of Proteobacteria and *Enterobacteriaceae* was observed in the current study. Similar results were also reported in mice inoculated with ETEC (Wang et al., 2018). Growing evidence suggests that an increased abundance of Proteobacteria might be associated with dysbiosis (Shin et al., 2015). ETEC infected pigs in the present study were fully recovered on day 21 PI, as reported no diarrhea was observed and no β-hemolytic coliforms were present in feces (He et al., 2020). Thus, the impacts of ETEC infection on fecal microbiome were also gradually reduced on day 21 PI.

The use of carbadox in feed also induced changes in the fecal microbiota. Carbadox is an oxidative DNA-damaging agent that mainly target gram-positive bacteria (Breijyeh et al., 2020). During habituation period, supplementation of carbadox reduced relative abundance of Firmicutes and *Lactobacillaceae* in feces. Although ETEC infection temporarily increased the relative abundance of *Lactobacillaceae* in feces of pigs in the antibiotics group, the abundance of *Lactobacillaceae* was sharply reduced when pigs were recovered from ETEC infection. The relative abundance of Bacteroidetes was also numerically higher in carbadox group than pigs in control. These observations indicate the impacts of in-feed antibiotics on gut microbiome were immediate (Lourenco et al., 2021). The reduced *Lactobacillaceae* in feces is consistent with previous research (Gao et al., 2018), suggesting that supplementation of carbadox modified the intestinal environment

which may be not supportive to maintain the growth of some favorable bacteria in the intestines.

Compared with carbadox, the influences of *B. subtilis* on fecal microbiome of weaned pigs were limited throughout the experiment. The relative abundance of *Bacillaceae* was the greatest in feces fed with *B. subtilis* among all treatments on day 0 before ETEC infection and day 21 PI, which is likely due to *B. subtilis* is categorized under the family *Bacillaceae*. Supplementation of *B. subtilis* significantly enhanced the relative abundance of Firmicutes, but numerically reduced Proteobacteria and *Enterobacteriaceae* in feces at the peak of ETEC infection. This observation is also consistent with the published fecal culture results, in which pigs fed with *B. subtilis* had lower percentage of β-hemolytic coliforms in feces on day 7 PI (He et al., 2020). Our previous research revealed that both carbadox and *B. subtilis* supplementation were effective in enhancing growth performance and reducing diarrhea of weaned pigs challenged with ETEC F18 (He et al., 2020). However, results in fecal microbiome suggest that the impacts of dietary supplementation of *B. subtilis* and antibiotics on fecal microbiome were different in weaned pigs. The major highlights are the modulation of Firmicutes phylum. Overall, pigs fed with *B. subtilis* contained relative higher *Lactobacillaceae* but lower *Bacteroidaceae* than pigs fed with antibiotics throughout the experiment, although ETEC infection temporarily reduced this difference on day 7 PI. Although carbadox mainly targets gram-positive bacteria, it can also disturb bacterial DNA synthesis and induce the breakdown of chromosome in many gram-negative bacteria, including ETEC (Suter et al., 1978; Cheng et al., 2015). However, *B. subtilis* as a probiotic strain must colonize into the intestines of pigs in order to perform beneficial effects on gut ecosystem. Thus, it is not supersizing to observe the different impacts of these two supplements on fecal microbiome due to their different modes of action.

Intestinal microbiota

In the current study, the intestinal microbiota changes were also analyzed in intestinal content collected at the end of experiment when pigs were fully recovered from ETEC infection. Similar to the results shown in Crespo-Piazuelo et al. (2018), Shannon and Chao1 index values in distal colon were higher than in jejunum and ileum. Consistently, beta diversity results showed clear separation between colon content vs. jejunal and ileal digesta, indicating the spatial heterogeneity of bacteria colonization across different intestinal sites (Mu et al., 2017). Supplementation of carbadox or *B. subtilis* had stronger influences on microbial diversity and composition in the ileum than in the jejunum and distal colon.

Ileal and jejunal digesta had greater relative abundance of Firmicutes and lowest relative abundance of Bacteroidetes than colon content, suggesting the luminal environment remarkably modulates digesta microbiome (Gao et al., 2018; Pollock et al., 2019). The relatively acidic environment and high oxygen level prevent the colonization of anaerobes in the small intestine (Donaldson et al., 2016). In addition, the small intestinal digesta contains more simple carbohydrates that could be utilized by the host and the microbiota, while the large intestine lumen comprises more complex carbohydrates for microbial fermentation (Zoetendal et al., 2012). The enriched *Lachnospiraceae*, *Ruminococcaceae*, and *Prevotellaceae* enable the large intestine's capacity to degrade complex carbohydrates (Duncan et al., 2007; Arumugam et al., 2011; Zhang et al., 2018). The ileum is a major intestinal site where ETEC colonizes, which is probably the major reason that more abundant *Enterobacteriaceae* were observed in ileal digesta than jejunum and colon (Nagy et al., 1992). However, there were limited changes in the microbial composition in different intestinal segments when comparing positive control vs. negative control pigs on day 21 PI, which was likely due to the recovery of weaned pigs from ETEC F18 infection (He et al., 2020). The relative abundance of *Micrococcaceae* was proliferated in jejunal and ileal digesta of pigs infected with ETEC. *Micrococcaceae* are relatively abundant in newborn pigs, but are gradually reduced during pre-weaning period (Pena Cortes et al., 2018). The increased abundance of *Micrococcaceae* were also observed in diarrheal fecal samples in a human study (De et al., 2020). However, the reason for this change is not clear and needs to be further investigated.

In comparison to the positive control, carbadox supplementation had more influences on the intestinal microbiota than *B. subtilis*. In addition, carbadox supplementation altered jejunal and ileal microbiota more than colon microbiota in weaned pigs, which is in close agreement with a previous study using a mixed antibiotics supplementation (Mu et al., 2017). This observation also indicates that antibiotics treatment may mainly target the microbiota in the small intestine. At the taxonomic level, pigs fed with carbadox had greater relative abundance of gram-negative bacteria, including *Succinivibrionaceae* and *Pasteurellaceae* in jejunum and *Muribaculaceae* in ileum, but lower relative abundance of *Lactobacillaceae* and *Bifidobacteriaceae* in ileum. This observation suggest that gram-negative bacteria may be more tolerant to carbadox due to their complicated outer membrane structure, containing lipopolysaccharides and peptidoglycans that can reduce the chance of carbadox penetrating into the bacterial membranes (Breijyeh et al., 2020). Gram-negative bacteria are more resistant to commonly used antibiotics by developing antibiotics resisting enzymes and undergoing mutations to increase resistance against antibiotics (Miller, 2016; Sumi et al., 2019). Therefore, the accumulation of gram-negative bacteria in the small intestine when carbadox is applied may increase the risk of developing antimicrobial resistance. However, in the production side, supplementation of carbadox was reported to effectively enhance growth performance and reduce intestinal inflammation of weaned pigs (Roof and Mahan, 1982; Stahly et al., 1997; He et al., 2020). The potential reason might include that carbadox can increase the population of short-chain fatty acid producing microbiota (i.e., *Ruminococcaceae*) in the small intestine, which may benefit to intestinal health and energy utilization in pigs (Bedford and Gong, 2018).

Pigs supplemented with *B. subtilis* had increased the relative abundance of gram-positive bacteria than pigs supplemented with carbadox, including *Lactobacillaceae, Bacillaceae*, and *Bifidobacteriaceae* in ileal digesta. The increased abundance of *Bacillaceae* was likely due to the colonization of *B. subtilis* in the intestinal tract (Pollock et al., 2019), which needs to be further confirmed in the future study. The more enriched *Lactobacillaceae* and *Bifidobacteriaceae* suggest that supplementing *B. subtilis* may help to maintain the desirable bacteria in the small intestine of weaned pigs, which may contribute to the concomitant decrease in enteric bacterial infection. Previous research also reported that *B. subtilis* supplementation can also decrease luminal pH and oxidation potential of the gut matrix, which may provide a favorable condition for *Lactobacillaceae* to thrive but inhibit the growth of the pathogenic bacteria (Yang et al., 2015). Therefore, results from the current study indicate that the modulation of gut microbiome by *B. subtilis* supplementation also contributes to the reduced diarrhea and enhanced intestinal health of ETEC infected pigs (He et al., 2020).

Conclusion

Our previous study reported that supplementation of *B. subtilis* DSM 25841 improved growth performance and disease resistance of weaned pigs under ETEC challenge (He et al., 2020). The current study characterized the microbial diversity and composition of fecal samples and intestinal contents collected from He et al. (2020). The present results indicate that weaning stress, age of pigs, ETEC infection, and dietary supplements all contributed to the fecal and intestinal microbiome changes in weaned pigs. Supplementation of carbadox and *B. subtilis* differently modified fecal and intestinal microbiota. Pigs supplemented with *B. subtilis* had higher abundance of *Bacillaceae* than pigs supplemented with carbadox in fecal and intestinal content. Supplementation of carbadox increased the relative abundance of gram-negative bacteria including Bacteroidetes and Proteobacteria which may impose risk of increasing antibiotics resistance. Supplementation of *B. subtilis* was associated with an increase or maintenance of the relative abundance of beneficial bacteria including *Lactobacillaceae* and *Bifidobacteriaceae* in the ileum and colon. Future research is needed to quantify *B. subtilis* colonization in the gastrointestinal tract and to investigate the interactions of *B. subtilis* with other bacteria, especially ETEC. In addition, the limits of 16S rRNA sequencing has been recognized, thus, the analysis of gut bacterial biomass and the functional genomes from the gut microbiota should be considered in the future research as well.

Data availability statement

The datasets presented in this study can be found in online repositories. The names of the repository/repositories and accession number(s) can be found at: https://www.ncbi.nlm.nih.gov/, PRJNA885119.

Ethics statement

Animal procedures were reviewed and approved by the Institutional Animal Care and Use Committee (IACUC #19322) at the University of California, Davis (UC Davis).

Author contributions

YL and XL designed and supervised the entire experiment. CJ performed all gut microbiome analysis, including sample analysis and data analysis. CJ wrote the manuscript. YL and XL revised and approved the final version. All authors contributed to the article and approved the submitted version.

Acknowledgments

The authors would like to thank the National Pork Board (#18-081) for financial support of this research.

Conflict of interest

The authors declare that the research was conducted in the absence of any commercial or financial relationships that could be construed as a potential conflict of interest.

Publisher's note

All claims expressed in this article are solely those of the authors and do not necessarily represent those of their affiliated organizations, or those of the publisher, the editors and the reviewers. Any product that may be evaluated in this article, or claim that may be made by its manufacturer, is not guaranteed or endorsed by the publisher.

References

Arumugam, M., Raes, J., Pelletier, E., Le Paslier, D., Yamada, T., Mende, D. R., et al. (2011). Enterotypes of the human gut microbiome. *Nature* 473, 174–180. doi: 10.1038/nature09944

Bates, D., Mächler, M., Bolker, B., and Walker, S. (2014). Fitting linear mixed-effects models using lme4. *arXiv preprint arXiv:1406.5823v1* 67:48. doi: 10.48550/arXiv.1406.5823

Bedford, A., and Gong, J. (2018). Implications of butyrate and its derivatives for gut health and animal production. *Anim. Nutr.* 4, 151–159. doi: 10.1016/j.aninu.2017.08.010

Boeckel, T. P. V., Brower, C., Gilbert, M., Grenfell, B. T., Levin, S. A., Robinson, T. P., et al. (2015). Global trends in antimicrobial use in food animals. *PNAS* 112, 5649–5654. doi: 10.1073/pnas.1503141112

Bokulich, N. A., Kaehler, B. D., Rideout, J. R., Dillon, M., Bolyen, E., Knight, R., et al. (2018). Optimizing taxonomic classification of marker-gene amplicon sequences with QIIME 2's q2-feature-classifier plugin. *Microbiome* 6:90. doi: 10.1186/s40168-018-0470-z

Bolyen, E., Rideout, J. R., Dillon, M. R., Bokulich, N. A., Abnet, C. C., Al-Ghalith, G. A., et al. (2019). Reproducible, interactive, scalable and extensible microbiome data science using QIIME 2. *Nat. Biotechnol.* 37, 852–857. doi: 10.1038/s41587-019-0209-9

Breijyeh, Z., Jubeh, B., and Karaman, R. (2020). Resistance of gram-negative bacteria to current antibacterial agents and approaches to resolve it. *Molecules* 25:1340. doi: 10.3390/molecules25061340

Callahan, B. J., McMurdie, P. J., Rosen, M. J., Han, A. W., Johnson, A. J. A., and Holmes, S. P. (2016). DADA2: high resolution sample inference from Illumina amplicon data. *Nat. Methods* 13, 581–583. doi: 10.1038/nmeth.3869

Campbell, J. M., Crenshaw, J. D., and Polo, J. (2013). The biological stress of early weaned piglets. *J. Anim. Sci. Biotechnol.* 4:19. doi: 10.1186/2049-1891-4-19

Cao, K. F., Zhang, H. H., Han, H. H., Song, Y., Bai, X. L., and Sun, H. (2016). Effect of dietary protein sources on the small intestine microbiome of weaned piglets based on high-throughput sequencing. *Lett. Appl. Microbiol.* 62, 392–398. doi: 10.1111/lam.12559

Caporaso, J. G., Lauber, C. L., Walters, W. A., Berg-Lyons, D., Huntley, J., Fierer, N., et al. (2012). Ultra-high-throughput microbial community analysis on the Illumina HiSeq and MiSeq platforms. *ISME J.* 6, 1621–1624. doi: 10.1038/ismej.2012.8

Chao, A. (1984). Nonparametric estimation of the number of classes in a population. *Scand. J. Stat.* 11, 265–270.

Chen, L., Xu, Y., Chen, X., Fang, C., Zhao, L., and Chen, F. (2017). The maturing development of gut microbiota in commercial piglets during the weaning transition. *Front. Microbiol.* 8:1688. doi: 10.3389/fmicb.2017.01688

Cheng, G., Li, B., Wang, C., Zhang, H., Liang, G., Weng, Z., et al. (2015). Systematic and molecular basis of the antibacterial action of quinoxaline 1,4-di-N-oxides against *Escherichia coli*. *PLoS One* 10:e0136450. doi: 10.1371/journal.pone.0136450

Crespo-Piazuelo, D., Estellé, J., Revilla, M., Criado-Mesas, L., Ramayo-Caldas, Y., Óvilo, C., et al. (2018). Characterization of bacterial microbiota compositions along the intestinal tract in pigs and their interactions and functions. *Sci. Rep.* 8:12727. doi: 10.1038/s41598-018-30932-6

de Mendiburu, F., and de Mendiburu, M. F. (2019). Package "Agricolae". *R Package, Version*, 1–2.

De, R., Mukhopadhyay, A. K., and Dutta, S. (2020). Metagenomic analysis of gut microbiome and resistome of diarrheal fecal samples from Kolkata, India, reveals the core and variable microbiota including signatures of microbial dark matter. *Gut. Pathog.* 12:32. doi: 10.1186/s13099-020-00371-8

Donaldson, G. P., Lee, S. M., and Mazmanian, S. K. (2016). Gut biogeography of the bacterial microbiota. *Nat. Rev. Microbiol.* 14, 20–32. doi: 10.1038/nrmicro3552

Duncan, S. H., Louis, P., and Flint, H. J. (2007). Cultivable bacterial diversity from the human colon. *Lett. Appl. Microbiol.* 44, 343–350. doi: 10.1111/j.1472-765X.2007.02129.x

Fairbrother, J., Gyles, C., Straw, B., Zimmerman, J., D'Allaire, S. and Taylor, D. (2006). Diseases of swine.

FDA (2013). *Guidance for Industry# 213, New Animal Drugs and New Animal Drug Combination Products Administered in or on Medicated Feed or Drinking Water of Food-producing Animals: Recommendations for Drug Sponsors for Voluntarily Aligning Product use Conditions with GFI# 209*. Center for Veterinary Medicine, Rockville, MD.

Fouhse, J. M., Zijlstra, R. T., and Willing, B. P. (2016). The role of gut microbiota in the health and disease of pigs. *Anim. Fron.* 6, 30–36. doi: 10.2527/af.2016-0031

Fox, J., and Weisberg, S. (2018). *An R Companion to Applied Regression*. Thousand Oaks: Sage Publications.

Frese, S. A., Parker, K., Calvert, C. C., and Mills, D. A. (2015). Diet shapes the gut microbiome of pigs during nursing and weaning. *Microbiome.* 3, 28–37. doi: 10.1186/s40168-015-0091-8

Gao, J., Xu, K., Liu, H., Liu, G., Bai, M., Peng, C., et al. (2018). Impact of the gut microbiota on intestinal immunity mediated by tryptophan metabolism. *Front. Cell Infect. Microbiol.* 8:13. doi: 10.3389/fcimb.2018.00013

Gresse, R., Chaucheyras-Durand, F., Fleury, M. A., Van de Wiele, T., Forano, E., and Blanquet-Diot, S. (2017). Gut microbiota dysbiosis in postweaning piglets: understanding the keys to health. *Trends Microbiol.* 25, 851–873. doi: 10.1016/j.tim.2017.05.004

He, Y., Kim, K., Kovanda, L., Jinno, C., Song, M., Chase, J., et al. (2020). *Bacillus subtilis*: a potential growth promoter in weaned pigs in comparison to carbadox. *Anim. Sci. J.* 98:skaa290. doi: 10.1093/jas/skaa290

Hu, Y., Dun, Y., Li, S., Zhao, S., Peng, N., and Liang, Y. (2014). Effects of *Bacillus subtilis* KN-42 on growth performance, diarrhea and faecal bacterial flora of weaned piglets. *Asian Australas. J. Anim. Sci.* 27, 1131–1140. doi: 10.5713/ajas.2013.13737

Kamada, N., Seo, S. U., Chen, G. Y., and Núñez, G. (2013). Role of the gut microbiota in immunity and inflammatory disease. *Nat. Rev. Immunol.* 13, 321–335. doi: 10.1038/nri3430

Katoh, K., and Standley, D. M. (2013). MAFFT multiple sequence alignment software version 7: improvements in performance and usability. *Mol. Bio. Evol.* 30, 772–780. doi: 10.1093/molbev/mst010

Ke, S., Fang, S., He, M., Huang, X., Yang, H., Yang, B., et al. (2019). Age-based dynamic changes of phylogenetic composition and interaction networks of health pig gut microbiome feeding in a uniformed condition. *BMC. Vet. Res.* 15, 1–13.

Kim, K., He, Y., Xiong, X., Ehrlich, A., Li, X., Raybould, H., et al. (2019). Dietary supplementation of *Bacillus subtilis* influenced intestinal health of weaned pigs experimentally infected with a pathogenic *E. coli*. *J. Anim. Sci. Biotechnol* 10, 1–12. doi: 10.1186/s40104-019-0364-3

Kreuzer, S., Reissmann, M., and Brockmann, G. A. (2013). New fast and cost-effective gene test to get the ETEC F18 receptor status in pigs. *Vet. Microbiol.* 163, 392–394. doi: 10.1016/j.vetmic.2012.12.040

Lallès, J.-P., Boudry, G., Favier, C., Floc'h, N. L., Luron, I., Montagne, L., et al. (2004). Gut function and dysfunction in young pigs: physiology. *Anim. Res.* 53, 301–316. doi: 10.1051/animres:2004018

Lenth, R. V. (2021). Emmeans: Estimated Marginal Means, Aka Least-squares Means. *R Package Version*, 1.6. 1.

Li, N., Zuo, B., Huang, S., Zeng, B., Han, D., Li, T., et al. (2020). Spatial heterogeneity of bacterial colonization across different gut segments following inter-species microbiota transplantation. *Microbiome.* 8, 161–174. doi: 10.1186/s40168-020-00917-7

Liao, S. F., and Nyachoti, M. (2017). Using probiotics to improve swine gut health and nutrient utilization. *Anim. Nutr.* 3, 331–343. doi: 10.1016/j.aninu.2017.06.007

Liu, Y., Song, M., Che, T. M., Almeida, J. A. S., Lee, J. J., Bravo, D., et al. (2013). Dietary plant extracts alleviate diarrhea and alter immune responses of weaned pigs experimentally infected with a pathogenic *Escherichia coli*. *J. Anim. Sci.* 91, 5294–5306. doi: 10.2527/jas.2012-6194

Looft, T., Allen, H. K., Casey, T. A., Alt, D. P., and Stanton, T. B. (2014). Carbadox has both temporary and lasting effects on the swine gut microbiota. *Front. Microbiol.* 5:276. doi: 10.3389/fmicb.2014.00276

Lourenco, J. M., Hampton, R. S., Johnson, H. M., Callaway, T. R., Rothrock, M. J., and Azain, M. J. (2021). The effects of feeding antibiotic on the intestinal microbiota of weanling pigs. *Front. Vet. Sci.* 8:131. doi: 10.3389/fvets.2021.601394

Luise, D., Bertocchi, M., Motta, V., Salvarani, C., Bosi, P., Luppi, A., et al. (2019). *Bacillus* sp. probiotic supplementation diminish the *Escherichia coli* F4ac infection in susceptible weaned pigs by influencing the intestinal immune response, intestinal microbiota, and blood metabolomics. *J. Anim. Sci. Biotechnol.* 10, 74–89. doi: 10.1186/s40104-019-0380-3

Luise, D., Sciellour, M. L., Buchet, A., Resmond, R., Clement, C., Rossignol, M.-N., et al. (2021). The fecal microbiota of piglets during weaning transition and its association with piglet growth across various farm environments. *PLoS One* 16:e0250655. doi: 10.1371/journal.pone.0250655

Ma, F., Xu, S., Tang, Z., Li, Z., and Zhang, L. (2021). Use of antimicrobials in food animals and impact of transmission of antimicrobial resistance on humans. *Biosaf. Health* 3, 32–38. doi: 10.1016/j.bsheal.2020.09.004

Mach, N., Berri, M., Estellé, J., Levenez, F., Lemonnier, G., Denis, C., et al. (2015). Early-life establishment of the swine gut microbiome and impact on host phenotypes. *Environ. Microbiol. Rep.* 7, 554–569. doi: 10.1111/1758-2229.12285

Madison, A., and Kiecolt-Glaser, J. K. (2019). Stress, depression, diet, and the gut microbiota: human–bacteria interactions at the core of psychoneuroimmunology and nutrition. *Curr. Opin. Behav. Sci.* 28, 105–110. doi: 10.1016/j.cobeha.2019.01.011

McMurdie, P. J., and Holmes, S. (2013). Phyloseq: an R package for reproducible interactive analysis and graphics of microbiome census data. *PLoS One* 8:e61217. doi: 10.1371/journal.pone.0061217

Menkem, Z. E., Ngangom, B. L., Tamunjoh, S. S. A., and Boyom, F. F. (2019). Antibiotic residues in food animals: public health concern. *Acta Ecol. Sin.* 39, 411–415. doi: 10.1016/j.chnaes.2018.10.004

Miller, S. I. (2016). Antibiotic resistance and regulation of the gram-negative bacterial outer membrane barrier by host innate immune molecules. *MBio* 7:e01541. doi: 10.1128/mBio.01541-16

Mu, C., Yang, Y., Su, Y., Zoetendal, E. G., and Zhu, W. (2017). Differences in microbiota membership along the gastrointestinal tract of piglets and their differential alterations following an early-life antibiotic intervention. *Front. Microbiol.* 8:797. doi: 10.3389/fmicb.2017.00797

Nagy, B., Arp, L. H., Moon, H. W., and Casey, T. A. (1992). Colonization of the small intestine of weaned pigs by enterotoxigenic *Escherichia coli* that lack known colonization factors. *Vet. Pathol.* 29, 239–246. doi: 10.1177/030098589202900308

NRC (2012). *Nutrient Requirements of Swine*. *11*. Washington, DC: The National Academies Press.

Oksanen, J., Blanchet, F. G., Kindt, R., Legendre, P., Minchin, P. R., O'hara, R. B., et al. (2013). Package 'Vegan'. Community Ecology Package, *R Package Version*, 2.

Pedregosa, F., Varoquaux, G., Gramfort, A., Michel, V., Thirion, B., Grisel, O., et al. (2011). Scikit-learn: machine learning in python. *J. Mach. Learn. Res.* 12, 2825–2830.

Pena Cortes, L. C., LeVeque, R. M., Funk, J. A., Marsh, T. L., and Mulks, M. H. (2018). Development of the tonsil microbiome in pigs and effects of stress on the microbiome. *Front. Vet. Sci* 5:220. doi: 10.3389/fvets.2018.00220

Pollock, J., Hutchings, M. R., Hutchings, K. E. K., Gally, D. L., and Houdijk, J. G. M. (2019). Changes in the ileal, but not fecal, microbiome in response to increased dietary protein level and enterotoxigenic *Escherichia coli* exposure in pigs. *Appl. Environ. Microbiol.* 85, e01252–e01219. doi: 10.1128/AEM.01252-19

Price, M. N., Dehal, P. S., and Arkin, A. P. (2010). FastTree 2 – approximately maximum-likelihood trees for large alignments. *PLoS One* 5:e9490. doi: 10.1371/journal.pone.0009490

Quast, C., Pruesse, E., Yilmaz, P., Gerken, J., Schweer, T., Yarza, P., et al. (2012). The SILVA ribosomal RNA gene database project: improved data processing and web-based tools. *Nucleic Acids Res.* 41, D590–D596. doi: 10.1093/nar/gks1219

Roof, M. D., and Mahan, D. C. (1982). Effect of carbadox and various dietary copper levels for weanling swine. *J. Anim. Sci.* 55, 1109–1117. doi: 10.2527/jas1982.5551109x

Shannon, C. E. (1948). A mathematical theory of communication. *Bell Syst. Tech. J.* 27, 379–423. doi: 10.1002/j.1538-7305.1948.tb01338.x

Shin, N.-R., Whon, T. W., and Bae, J.-W. (2015). Proteobacteria: microbial signature of dysbiosis in gut microbiota. *Trends Biotechnol.* 33, 496–503. doi: 10.1016/j.tibtech.2015.06.011

Stahly, T. S., Williams, N. H., and Swenson, S. G. (1997). Growth Response to Carbadox in Pigs with a High or Low Genetic Capacity for Lean Tissue Growth. *Animal Industry Report, Swine Research Report, 1996*. Ames, IA: Iowa State University Digital Press, pp. 1–5.

Sumi, C. D., Heffernan, A. J., Lipman, J., Roberts, J. A., and Sime, F. B. (2019). What antibiotic exposures are required to suppress the emergence of resistance for gram-negative bacteria? A systematic review. *Clin. Pharmacokinet.* 58, 1407–1443. doi: 10.1007/s40262-019-00791-z

Suter, W., Rosselet, A., and Knüsel, F. (1978). Mode of action of quindoxin and substituted quinoxaline-di-N-oxides on *Escherichia coli*. *Antimicrob. Agents Chemother.* 13, 770–783. doi: 10.1128/AAC.13.5.770

Team, R. C. (2021). *R: A Language and Environment for Statistical Computing*. Vienna, Austria: R Foundation for Statistical Computing.

Tian, L., Bruggeman, G., van den Berg, M., Borewicz, K., Scheurink, A. J. W., Bruininx, E., et al. (2017). Effects of pectin on fermentation characteristics, carbohydrate utilization, and microbial community composition in the gastrointestinal tract of weaning pigs. *Mol. Nutr. Food Res.* 61. doi: 10.1002/mnfr.201600186

USDA. (2007). Swine 2006, Part II: Reference of Swine Health and Health Management Practices in the United States, 2006 USDA:APHIS:VS, CEAH. Fort Collins, CO., Program No. N479.1207.

Wang, T., Teng, K., Liu, G., Liu, Y., Zhang, J., Zhang, X., et al. (2018). *Lactobacillus reuteri* HCM2 protects mice against enterotoxigenic *Escherichia coli* through modulation of gut microbiota. *Sci. Rep.* 8:17485. doi: 10.1038/s41598-018-35702-y

Wickham, H. (2011). ggplot2. *Wiley Interdiscip. Rev.* 3, 180–185. doi: 10.1002/wics.147

Yang, J. J., Niu, C. C., and Guo, X. H. (2015). Mixed culture models for predicting intestinal microbial interactions between *Escherichia coli* and lactobacillus in the presence of probiotic *Bacillus subtilis*. *Benef. Microbes* 6, 871–877. doi: 10.3920/BM2015.0033

Zhang, L., Wu, W., Lee, Y.-K., Xie, J., and Zhang, H. (2018). Spatial heterogeneity and co-occurrence of mucosal and luminal microbiome across swine intestinal tract. *Front. Microbiol.* 9:48. doi: 10.3389/fmicb.2018.00048

Zoetendal, E. G., Raes, J., van den Bogert, B., Arumugam, M., Booijink, C. C., Troost, F. J., et al. (2012). The human small intestinal microbiota is driven by rapid uptake and conversion of simple carbohydrates. *ISME J.* 6, 1415–1426. doi: 10.1038/ismej.2011.212

frontiers | Frontiers in Microbiology

TYPE Original Research
PUBLISHED 12 May 2023
DOI 10.3389/fmicb.2023.1186841

OPEN ACCESS

EDITED BY
Jie Feng,
Lanzhou University Medical College, China

REVIEWED BY
Bijit Bhowmik,
Croda Inc, United States
Volker Behrends,
University of Roehampton London,
United Kingdom

*CORRESPONDENCE
Binghu Fang
✉ fangbh@scau.edu.cn

RECEIVED 15 March 2023
ACCEPTED 21 April 2023
PUBLISHED 12 May 2023

CITATION
Yang H, Zhou Y, Luo Q, Zhu C and Fang B (2023) L-leucine increases the sensitivity of drug-resistant *Salmonella* to sarafloxacin by stimulating central carbon metabolism and increasing intracellular reactive oxygen species level.
Front. Microbiol. 14:1186841.
doi: 10.3389/fmicb.2023.1186841

L-leucine increases the sensitivity of drug-resistant *Salmonella* to sarafloxacin by stimulating central carbon metabolism and increasing intracellular reactive oxygen species level

Heng Yang[1,2], Yanhong Zhou[1,2], Qiong Luo[1,2], Chunyang Zhu[1,2] and Binghu Fang[1,2]*

[1]Guangdong Provincial Key Laboratory of Veterinary Pharmaceutics Development and Safety Evaluation, South China Agricultural University, Guangzhou, China, [2]National Risk Assessment Laboratory for Antimicrobial Resistance of Animal Original Bacteria, South China Agricultural University, Guangzhou, China

Introduction: The overuse of antibiotics has made public health and safety face a serious cisis. It is urgent to develop new clinical treatment methods to combat drug resistant bacteria to alleviate the health crisis. The efficiency of antibiotics is closely related to the metabolic state of bacteria. However, studies on fluoroquinolone resistant *Salmonella* are relatively rare.

Methods: CICC21484 were passaged in medium with and without sarafloxacin and obtain sarafloxacin- susceptible *Salmonella Typhimurium* (SAR-S) and sarafloxacin resistant *Salmonella Typhimurium* (SAR-R), respectively. Non-targeted metabolomics was used to analyze the metabolic difference between SAR-S and SAR-R. Then we verified that exogenous L-leucine promoted the killing effect of sarafloxacin in vitro, and measured the intracellular ATP, NADH and reactive oxygen species levels of bacteria. Gene expression was determined using Real Time quantitative PCR.

Results: We confirmed that exogenous L-leucine increased the killing effect of sarafloxacin on SAR-R and other clinically resistant *Salmonella* serotypes. Exogenous L-leucine stimulated the metabolic state of bacteria, especially the TCA cycle, which increased the working efficiency of the electron transfer chain and increased the intracellular NADH, ATP concentration, and reactive oxygen species level. Our results suggest that when the metabolism of drug-resistant bacteria is reprogrammed, the bactericidal effect of antibiotics improves.

Discussion: This study further enhances research in the anti-drug resistance field at the metabolic level and provides theoretical support for solving the current problem of sarafloxacin drug resistance, a unique fluoroquinolone drug for animals and indicating the potential of L-leucine as a new antibiotic adjuvant.

KEYWORDS

L-leucine, sarafloxacin, *salmonella*, metabolism, reactive oxygen species

1. Introduction

Salmonella is a zoonotic pathogen that can cross-spread among humans, animals, and the environment. It has important biological significance in gastrointestinal diseases (Ao et al., 2015; Gut et al., 2018). There are more than 900,000 cases of *Salmonella* infection worldwide each year, with 15,500 deaths, which has caused a massive burden on public health and safety (Majowicz

et al., 2010; Feasey et al., 2012; Kirk et al., 2015). After infection, the main symptoms are vomiting, fever, and diarrhea. Infection in infants with low immunity and the elderly may further lead to more severe bacteremia and endanger life safety, and a few may even experience meningitis (Yang et al., 2012). Livestock and poultry infected with *Salmonella* will spread the pathogen to humans through food, environmental pollution, or other ways. *Salmonella* in animals can also reduce the rate of weight gain, resulting in reduced production performance and increased feed conversion rate, causing economic losses (Farzan and Friendship, 2010). At present, more than 2,500 *Salmonella* serotypes that have been identified (Hendriksen et al., 2011), of which *Salmonella Typhimurium* is one of the typical representatives and the primary serotype in the detection of non-human *Salmonella* (Galanis et al., 2006). In Thailand and Vietnam, the detection rate of *Salmonella Typhimurium* is 34 and 37.5%, respectively, the most prevalent serotype (Phu Huong Lan et al., 2016; Sinwat et al., 2016). In sub-Saharan Africa, Typhimurium accounts for two-thirds of all serotypes (Reddy et al., 2010). In China, the prevalence of *Salmonella Typhimurium* has also attracted people's attention to pig breeding (Tian et al., 2021).

Sarafloxacin is the third generation of fluoroquinolones. The most common preparation is sarafloxacin hydrochloride, which can kill both Gram-negative and Gram-positive bacteria (Hooper, 1998; Oliphant and Green, 2002). After entering the cell, sarafloxacin can combine with DNA cyclooxygenase and topoisomerase IV to form a "drug-enzyme-DNA" ternary complex, thus preventing bacterial DNA replication and killing bacteria (Correia et al., 2017). In 1995, the U.S. Food and Drug Administration approved sarafloxacin as a special quinolone antibiotic for animals, which has a good curative effect on clinical respiratory tract infections, urinary system infections, skin tissue infections, and intra-abdominal infections (Kim and Hooper, 2014). Unfortunately, the overuse of antibiotics during bacterial infection in aquaculture, directly or indirectly, has led to the emergence and prevalence of drug-resistant *Salmonella*. The detection rate of fluoroquinolone-resistant *Salmonella* has also gradually increased (Fang, 2015). In 2019, drug-resistant *Salmonella* serotype Typhi was defined as a serious threat (CDC, 2019). The common resistance mechanism of fluoroquinolones includes: (i) the target mutation of DNA gyrase and topoisomerase IV, which leads to a decreased affinity between drugs and enzymes (Aldred et al., 2014); (ii) the modification of cell membrane protein and drug efflux pumps OqxAB, QepA, and AcrAB-TolC, which reduces intracellular drug concentrations (Redgrave et al., 2014); and (iii) plasmid-mediated acquired drug resistance (*qnrA*, *qnrB*, *qnrS*, *qnrC*, and *qnrD*; Aldred et al., 2014). However, with the development and application of metabolomics, researchers can directly observe the metabolic state changes of cells caused by various mechanisms (Schrimpe-Rutledge et al., 2016), and the analysis of drug resistance from a metabolic perspective has gradually become a research hotspot.

The effect of antibiotics on bacteria is closely related to metabolic status (Stokes et al., 2019; Lopatkin et al., 2021). The metabolomic results of cefoperazone/sulbactam-resistant *Pseudomonas aeruginosa* have shown the inhibition of the central carbon and riboflavin metabolism, while the related glucose metabolism and the electric transport chain also decreased (Chen et al., 2022). The decompressed central carbon and energy metabolism led to levofloxacin resistance in *Vibrio algenolyticus*, and the biosynthesis of fatty acids was also affected (Cheng et al., 2018). These studies have proved that biochemical metabolism plays a key role in the drug-resistant characteristics of bacteria. Consistently reprogramming metabolism by exogenous addition of certain substances can also reverse the drug-resistant characteristics of bacteria. Exogenous D-ribose activates glycolysis, the pentose phosphate pathway, and the TCA cycle, and increases NADH production and proton motive force (PMF) and, thus, increases drug uptake and promotes the killing effect of gentamicin against drug-resistant *Salmonella*. Exogenous citrulline similarly promotes the germicidal effect of apramycin (Yong et al., 2021; Zhou et al., 2022). The abundance of glutamine in the metabolomics results decreased. After supplementation, exogenous glutamine promotes the killing effect of β-lactams, aminoglycosides, quinolones and tetracyclines on pathogenic *E. coli* in the urinary tract through various metabolic pathways, and delay the development of ampicillin resistance (Zhao et al., 2021).

One of the common characteristics of bactericidal antibiotics is that reactive oxygen species (ROS) will be produced after targeting bacteria (Kohanski et al., 2007). ROS is an inevitable by-product of cellular aerobic respiration. These molecules are produced due to excessive activation of the electron transfer chain and leakage of electrons to the oxygen molecule to generate superoxide (O_2^-) ($O_2 + e^- = O_2^-$). Superoxide dismutases can catalyze superoxide generation to hydrogen peroxide and oxygen ($2H^+ + 2O_2^- = O_2 + H_2O_2$). Superoxide can destroy the iron–sulfur cluster in protein, thus producing unstable ferrous ions (Fe^{2+}). One of the products of the reaction of Fe^{2+} and hydrogen peroxide is the lethal hydroxyl radical ($Fe^{2+}\ H_2O_2 = Fe^{3+} + OH^- + HO^*$). Hydroxyl radicals can destroy cell DNA, lipids, and proteins, resulting in death (Belenky et al., 2015). At the same time, it will also destroy the iron sulfide cluster protein, regenerate free iron ions, and generate more hydroxyl radicals through the Fenton reaction to accelerate bacterial death (Van Acker and Coenye, 2017). Some studies have confirmed that the overactivated electron transfer chain is related to central carbon metabolism, as the production of NADH mainly comes from the TCA cycle (Kohanski et al., 2007). Exogenous thymine can up regulate the bacterial metabolic state, activate the TCA cycle, accelerate respiration, promote the production of ATP and ROS, and promote the killing effect of ciprofloxacin on some Gram-negative bacteria (Liu et al., 2021). The addition of exogenous serine has been shown to promote the TCA cycle of *E. coli*, increase the production of NADH and the ratio of NAD^+/NADH, activate the electron transfer chain, and increase the production of endogenous ROS, making the killing effect of ofloxacin or moxifloxacin on *E.coli* stronger (Duan et al., 2016). Alanine can also promote kanamycin killing of antibiotic resistant bacteria by promoting ROS production (Ye et al., 2018). Therefore, linking the metabolic state of bacteria to the production of ROS and the increase of intracellular ROS levels after the drug has targeted drug-resistant bacteria by stimulating metabolism has great research potential.

In this study, non-targeted metabolomics was used to analyze the metabolic characteristics of SAR-R and SAR-S. We found that carbon metabolism and other related pathways, such as the TCA cycle, decreased in SAR-R. The addition of exogenous L-leucine promoted the killing effect of sarafloxacin against multidrug-resistant *Salmonella*. The specific mechanism included activating the TCA cycle and the electron transfer chain, thus cooperating with antibiotics to produce more ROS, which accelerated the death of bacteria. Our results provide theoretical support for alleviating the clinical drug resistance of fluoroquinolones, especially the special animal drug sarafloxacin.

2. Materials and methods

2.1. Chemicals

Sarafloxacin hydrochloride was purchased from the China Institute of Veterinary Drug Control (Beijing, China). L-leucine and thiourea were purchased from Shanghai Macklin Biochemical Technology Co., Ltd. (Shanghai, China). Mueller Hinton (MH) broth, tryptic soy agar (TSA), Luria-Bertani (LB) broth, MacConkey agar, and MH agar were purchased from Guangdong Huankai Microbial Sci & Tech Co., Ltd. (Guangdong, China). M9 Minimal medium was purchased from Shanghai ELITE Biotech Co., Ltd. (Shanghai, China). Methanol and acetonitrile (high-performance liquid chromatography grade) were purchased from Thermo Fisher Scientific (Waltham, MA, United States).

2.2. Bacterial strains

Standard strains of *E. coli* (ATCC25922) were purchased from the American Type Culture Collection (Manassas, VA, United States). Standard strains of *Salmonella Typhimurium* (CICC21484) were purchased from the China Center of Industrial Culture Collection (Beijing, China). Clinically resistant *Salmonella* strains (Typhimurium B2, Derby A2, London E1) were donated by the Guangdong Dahuanong Animal Health Products Co., Ltd. (Guangdong, China). Cells were cultured in LB medium at 37°C shaking at 200 rpm unless specified otherwise.

2.3. Minimum inhibitory concentration and induction of bacterial antibiotic resistance

The MICs of sarafloxacin against different *Salmonella* strains were determined using the microdilution method (Wiegand et al., 2008). All MICs were tested in duplicate at least twice. The increasing concentration method was used to induce drug-resistant strains. *Salmonella* strain CICC21484 was inoculated into the LB medium, and sarafloxacin was added at half of the MIC concentration. The MIC of the bacteria was rechecked every 3 days. Then, a new half MIC concentration was added to the medium until the MIC reached the breakpoint, and we obtained SAR-R. Concurrently *Salmonella Typhimurium* was obtained without adding drugs but undergoing the same continuous reproductive process as SAR-S.

2.4. Non-targeted metabolomic determination and analysis

SAR-S and SAR-R were used for metabolomic determination. Two strains were cultured in LB medium until the exponential stage. The bacterial suspension (10 mL) was then centrifuged at 4°C and 12,000 g for 10 min, and the precipitate was washed twice with PBS. The two collected bacterial strains quickly quenched in liquid nitrogen to stop their metabolism. Then, precooled methanol/acetonitrile/water solution (2:2:1, v/v) was added, mixed by vortexing, and subjected to low-temperature ultrasound for 30 min. The sample rested at 20°C for 10 min, followed by centrifugation at 14000 g and 4°C for 20 min. The supernatant was collected for vacuum drying, and 100 μL acetonitrile aqueous solution (acetonitrile: water = 1:1, v/v) was added for mass spectrometry and to redissolve the pellet. The contents were centrifuged at 4°C for 15 min, and the supernatant was collected for further analysis. The samples were separated by an Agilent 1,290 Infinity LC ultrahigh performance liquid chromatography (UHPLC) HILIC column. Specifications were: column temperature 25°C; flow rate 0.5 mL/min; injection volume 2 μL; mobile phase composition A: water +25 mM ammonium acetate +25 mM ammonia water; B: acetonitrile. The gradient elution procedure was as follows: 0–0.5 min, 95% B; 0.5–7 min, B changed linearly from 95 to 65%; 7–8 min, B changed linearly from 65 to 40%; 8–9 min, B was maintained at 40%; 9–9.1 min, B changed linearly from 40 to 95%; 9.1–12 min, B was maintained at 95%. The sample was placed in the 4°C automatic sampler during the analysis process. In order to avoid the impact caused by the fluctuation of the instrument detection signal, continuous analysis of samples was performed in random order. Quality control (QC) samples were inserted into the sample queue to monitor and evaluate the stability of the system and the reliability of the experimental data. The Electron Spray Ionization source conditions after HILIC chromatographic separation were as follows: ion source gas 1 (gas 1): 60; ion source gas 2 (gas 2): 60; curtain gas (CUR): 30; source temperature: 600°C, ionSapary voltage floating ±5,500 V (positive and negative modes); TOF MS scan m/z range: 60–1,000 Da; product ion scan m/z range: 25–1,000 Da; TOF MS scan accumulation time: 0.20 s/spectra; and product ion scan accumulation time: 0.05 s/spectra. The secondary mass spectrometry was obtained by information-dependent acquisition (IDA) and high sensitivity mode with a clustering potential of ±60 V (positive and negative modes) and collision energy at 35 ± 15 eV. The IDA settings were as follows: exclude isotopes within 4 Da; and candidate ions to monitor per cycle: 10.

The XCMS software was used for peak alignment, retention time correction, and peak area extraction. For the data extracted with the software, we first identified the metabolite structure, pretreated the data, and then evaluated the quality of the experimental data and analysis. All metabolites identified (metabolites identified by combining positive and negative ions) were then classified and counted according to chemical taxonomy attribution information. The data were analyzed using principal component analysis (PCA), partial least squares discriminant analysis (PLS-DA), orthogonal partial least squares discriminant analysis (OPLS-DA), multivariate analysis, and the Student's *t*-test to study the intra- and inter-group differences between samples and to identify the different metabolites. The variable importance for the projection (VIP) obtained from the OPLS-DA model was used to measure the influence intensity and interpretation ability of each metabolite's expression pattern on the classification and discrimination of each sample group in order to mine the different metabolic molecules with biological significance. We used OPLS-DA VIP > 1 and p value <0.05 as the screening criteria for significantly different metabolites for subsequent pathway analysis. The MetaboAnalyst and Heatmapper online website (https://www.metaboanalyst.ca/MetaboAnalyst/ and http://www.heatmapper.ca/) online tools were used for hierarchical clustering of differential metabolites.

2.5. Antibiotic survival assay

To assess the effect of L-leucine on the bactericidal activity of sarafloxacin against SAR-R and the other three clinical strains, The

cells were first cultured in LB to reach the exponential phase, centrifuged at 12,000 g for 5 min, and washed twice with sterile PBS buffer. Cells were then resuspended to M9 at an initial concentration of 1×10^6 colony-forming units (CFU)/mL. Experimental strains were treated with sarafloxacin (1-fold MIC: 16 μg/mL for SAR-R, 4 μg/mL for Typhimurium B2, 8 μg/mL for Derby A2, and 2 μg/mL for London E1), and with or without L-leucine (20 mM or other concentrations) for 8 h in M9 Minimal medium. In the ROS quenching experiment, 60 mM thiourea was added to the medium and incubated for 2 h at 37°C. After incubation, 100 μL of the sample was used in a dilution series, and 20 μL of each dilution was spread onto TSA agar plates. CFUs were counted after overnight (16 h) incubation. Percentage survival was determined by the ratio of CFU obtained from the test and control samples.

2.6. NADH measurements

The NADH measurement assay was performed as described previously (Yong et al., 2021). NADH production was determined using an NAD^+/NADH Assay Kit (BioAssay Systems, Hayward, CA, United States). In brief, after culturing bacteria and L-leucine in M9 Minimal medium for 4 h, 1 mL of culture was centrifuged for 5 min at 13,000 g. The supernatant was discarded, and the pellet was washed and precipitated with PBS 3 times. Approximately 100 μL of NADH extraction buffer was added to the washed bacterial pellet and incubated at 60°C for 5 min. Then, 20 μL of the assay buffer and 100 μL of NAD extraction buffer were added. After centrifugation, the concentration of NADH was measured with a multi-function e-microplate reader.

2.7. ATP measurements

The ATP concentration was determined using an ATP Assay Kit (Beyotime, China). In brief, after co-culturing bacteria (1×10^6 CFU/mL) and L-leucine for 4 h, 1 mL of the bacterial solution was centrifuged at 4°C and 12,000 g for 5 min. The supernatant was discarded, and the bacterial pellet was washed twice and resuspended in PBS. Because ATP is relatively stable at low temperatures, the following operations were performed in an ice bath. Approximately 200 μL of the cracking solution was added to the bacterial suspension and incubated for 15 min, with shaking during the incubation period to crack fully. The sample was then centrifuged at 4°C and 12,000 g for 5 min, and the supernatant was collected for subsequent detection. A luminometer was used to detect the ATP concentration.

2.8. ROS measurements

The ROS Assay Kit was used to measure the intracellular ROS level (Beyotime, China). In brief, 1 mL of bacterial solution in the exponential phase cells was loaded with a 10 μL fluorescent probe DCFH-DA. Samples were incubated in the dark for 20 min with gentle shaking to ensure loading efficiency. After incubation, the samples were centrifuged at 4°C and 12,000 g for 5 min. The supernatant was discarded, and the pellet was washed twice with PBS to ensure the probe was cleared. The washed bacteria were resuspended in M9 Minimal medium, the initial concentration was adjusted to 1×10^6 CFU/mL, and cultured in sarafloxacin with or without L-leucine. The ROS level was measured at 488 nm excitation wavelength and 525 nm emission wavelength at 2 h. The ROS relative level is expressed by the ratio of the experimental group sample to the control sample.

2.9. Real time quantitative PCR

After co-culturing the bacteria and L-leucine for 6 h, 5 mL of the bacterial solution was collected by centrifugation and precipitated for subsequent experiments. The RNAiso Plus Kit (Takara Japan) was used to extract the total RNA according to the manufacturer's instructions. The Hifair® II 1st Strand cDNA Synthesis Kit (Yeasen, Shanghai, China) and 2000 ng total RNA were used for RT-qPCR according to the manufacturer's instructions. The RT-qPCR reaction setup included 5 μL SYBR Green Master Mix (Yeasen, Shanghai, China), forward primer (2 μM), reverse primer (2 μM), and 2 μL cDNA added to RNase-free water to a total volume of 10 μL. The reaction tube was briefly centrifuged to ensure all the reaction liquid was collected at the bottom. The cycle parameters were as follows: initial denaturation at 95°C for 5 min; and 40 cycles of denaturation at 95°C for 10 s, and annealing and extension at 60°C for 30 s. The heating rate was 0.05°C/s for 60–95°C, in which a melting curve was obtained. The 16S rRNA gene was used as an internal reference. The experiment was performed with 3 biological replicates. The specific primers are listed in the Supplementary material (Supplementary Table 1).

3. Results

3.1. Induction and growth characteristics of drug-resistant *Salmonella*

After standard strains of *Salmonella Typhimurium* (CICC21484) were continuously sub-cultured *in vitro* with half the MIC concentration of sarafloxacin, we obtained drug-resistant strain SAR-R. The MIC measurement for strain SAR-R was 16 μg/mL, indicating that the resistant bacteria were successfully induced. The MIC test results of the three clinically isolated *Salmonella* strains with different serotypes of drug resistance are shown in Table 1.

3.2. Metabolomic analysis

We used UHPLC-Q-TOF MS to perform non-targeted metabolomic analysis of SAR-S, SAR-R, and 6 biological repeats in each group to observe the metabolic changes caused by drug resistance. A total of 453 metabolites were identified, including carbohydrates, amino acids, lipids, nucleotides, etc. (Supplementary Table 2). In order to show the metabolic differences more clearly, Principal component analysis (PCA) was used to score the two strains. The results showed that the repeated experimental samples in each group had good aggregation, and the two groups were separated by the main component, indicating that the metabolic components of the two sample groups were significantly different. QC samples were also closely clustered

TABLE 1 MIC value of different antimicrobials against *Salmonella* (μg/mL).

	SAR-S	SAR-R	Typhimurium B2	Derby A2	London E1
Sarafloxacin	0.03	16	4	8	2
Ciprofloxacin	0.015	4	2	1	1
Enrofloxacin	0.03	8	8	4	4
Danooxacin	0.03	4	4	4	2
Gentamicin	0.25	0.25	64	16	64
Apramycin	2	2	128	128	64
Tobramycin	0.25	0.25	64	32	32
Ampicillin	2	2	128	256	64
Tetracycline	1	1	64	32	64

(Figures 1A,B). To obtain more reliable and significantly different metabolites, we adopted OPLS-DA analysis, with VIP score > 1 and p value <0.05 as the screening criteria for significantly different metabolites. A total of 62 metabolites were selected for subsequent bioinformatics analysis (Supplementary Table 3), where the first four metabolites with the highest content were amino acids and peptides (38%), fatty acids and conjugates (10%), pyrimidines (9%), and TCA acids (7%; Figure 1C). To demonstrate the different metabolites more clearly, the hierarchical clustering of differential metabolites is plotted (Figure 1D). When we further analyzed these differential metabolites, it was found that there were some metabolites with reduced abundance, such as acetyl coenzyme A, succinate, citrate, L-glutamate, nicotinamide adenine dinucleotide, adenosine 5 '- diphosphate, hypoxantine, adenosine monophosphate, thymine, uridine 5' - monophosphate, which belong to the following metabolic pathways: TCA cycle, glycolysis/gluconogenesis, alanine, aspartate and glutamate metabolism, oxidative phosphorylation, purine/pyrimidine metabolism. Therefore, we speculate that these metabolic pathways are affected during the evolution of cell resistance and should be responsible for the development of drug resistance. Among these, the TCA cycle is crucial to the biochemical metabolic system as the central link of bacterial metabolism. It can receive pyruvate produced by the glycolysis pathway to promote the absorption and metabolism of carbohydrates and the production of ATP. Furthermore, the intermediate products NADH and FADH are also important components of oxidative physiology and provide raw materials for the synthesis of alanine, aspartate, and glutamate (pyruvate, oxaloacetate, and 2-oxoglutarate) to ensure the raw materials (amino acid) for protein synthesis are sufficient. Aspartate and glutamine provide synthetic raw materials for nucleotides, and oxidative phosphorylation provides energy; however, these are all based on the normal operation of the TCA cycle. Therefore, we speculate that the weakening of the TCA cycle affects other biochemical metabolic processes, which delay the global metabolism of drug-resistant bacteria. The bacteria enter hibernation, thus resisting the pressure of antibiotics and producing a drug-resistant phenotype.

3.3. L-leucine specifically increased the susceptibility of drug-resistant *Salmonella* to sarafloxacin

The metabolic state of bacteria is crucial to the killing effect of antibiotics (Stokes et al., 2019). Many studies have shown that exogenous amino acids such as alanine, citrulline, and serine can modify the inhibited metabolic state, thereby promoting the killing effect of antibiotics on drug-resistant bacteria (Duan et al., 2016; Ye et al., 2018; Yong et al., 2021). Therefore, we speculate that a certain amino acid will modify the metabolic state of drug-resistant *Salmonella*, thereby synergizing the bactericidal effect of sarafloxacin. Then, we conducted a screening test on 20 protein amino acids. Among them, L-leucine proved to have the efficacy of synergizing with sarafloxacin in killing drug-resistant *Salmonella*. Furthermore, SAR-R, Typhimurium B2, Derby A2, and London E1 were incubated with sarafloxacin in M9 media with or without L-leucine for 8 h. The results showed that from the killing curve at each time point, the percent survival rate of the combination group (L-leucine plus sarafloxacin) was significantly lower than that of the sarafloxacin monotherapy group (Figure 2A). However, each strain's most significant synergy time differed, which may be due to the different absorption and utilization efficiency of L-leucine. At a similar antibiotic concentration (1MIC), L-leucine with different concentrations (0, 5, 10, and 20 mM) showed dose-dependent manner synergistic effects (Figure 2B). Interestingly, when we increased the dose of L-leucine to 40 mM, the potential of L-leucine on sarafloxacin did not increase further, which may be due to the limited utilization of L-leucine by bacteria. Nevertheless, L-leucine, as an amino acid, can provide nutrients for the growth of bacteria, which may promote growth in a nutrient-poor medium and indirectly synergize the killing effect of bactericidal antibiotics. Therefore, to eliminate the role of L-leucine as a nutrient, we used glucose (the representative of nutrients) in combination with sarafloxacin to observe whether the same synergistic effect exists. The results indicate that the addition of glucose promoted the growth of bacteria but did not promote the bactericidal effect of sarafloxacin (Figures 2C,D). These results show that L-leucine specifically promoted the killing effect of sarafloxacin in drug-resistant *Salmonella*.

3.4. L-leucine increased intracellular NADH concentration

We speculated that exogenous L-leucine affects the TCA cycle and can stimulate drug-resistant bacteria since all carbon and nitrogen sources are ultimately metabolized in the TCA cycle. As a key intermediate, the increase in NADH concentration can indicate, to some extent, the activation of the TCA cycle. Therefore, we added

10.3389/fmicb.2023.1186841

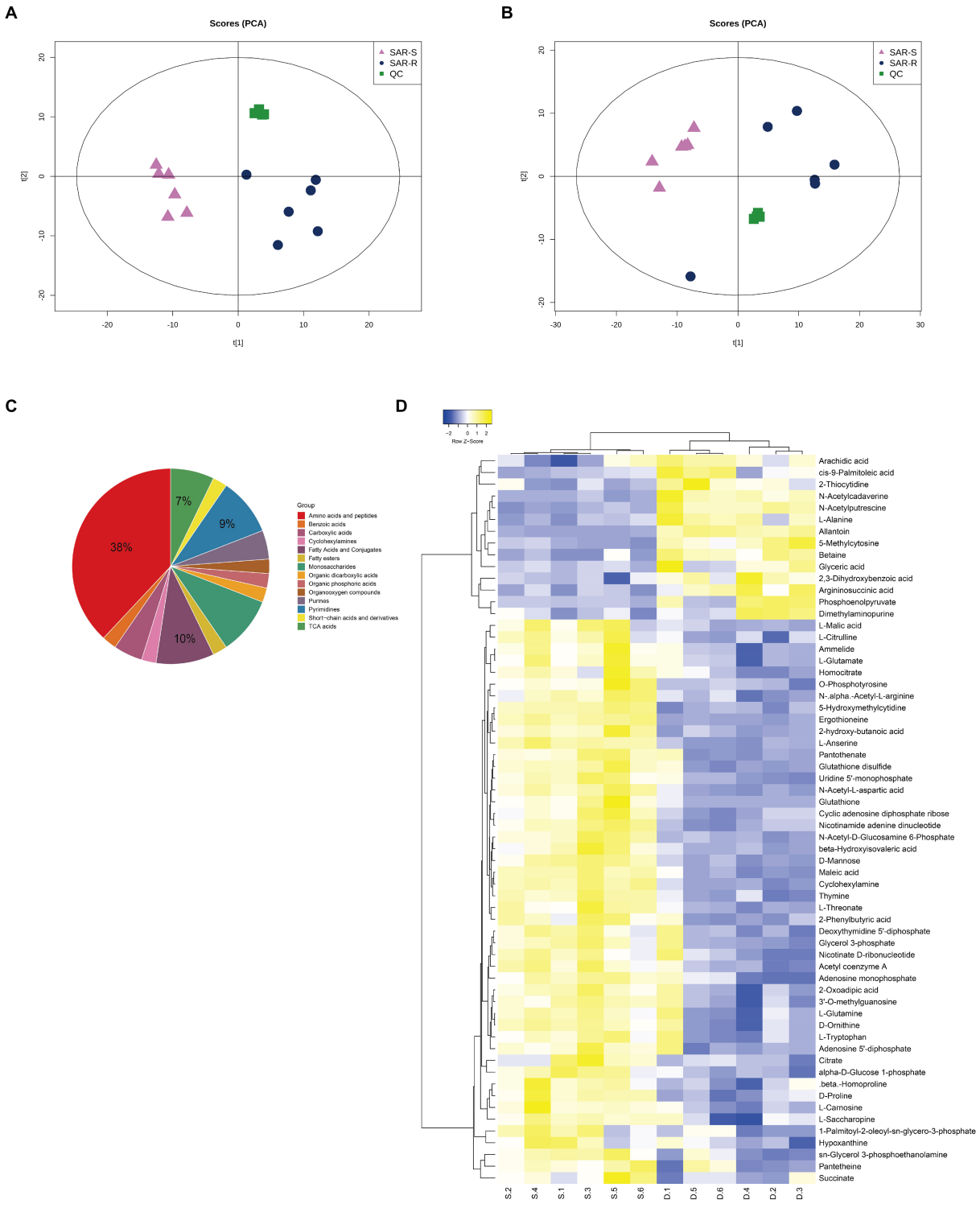

FIGURE 1
Analysis of metabolic profile. **(A)** PCA score of SAR-R and SAR-S in positive mode. **(B)** PCA score of SAR-R and SAR-S in negative mode. **(C)** Classification pie chart of all differential metabolites. **(D)** Cluster analysis of different metabolites. "D" represents sarafloxacin -induced resistant *Salmonella*, "S" represents sarafloxacin -sensitive *Salmonella*.

L-leucine into the culture medium and measured the intracellular NADH concentration of bacteria after 4 h of cultivation. As shown in Figure 3, the NADH concentration of all drug-resistant bacteria increased after adding L-leucine compared with the control group. This indicates that L-leucine entered the TCA cycle and increased the NADH level.

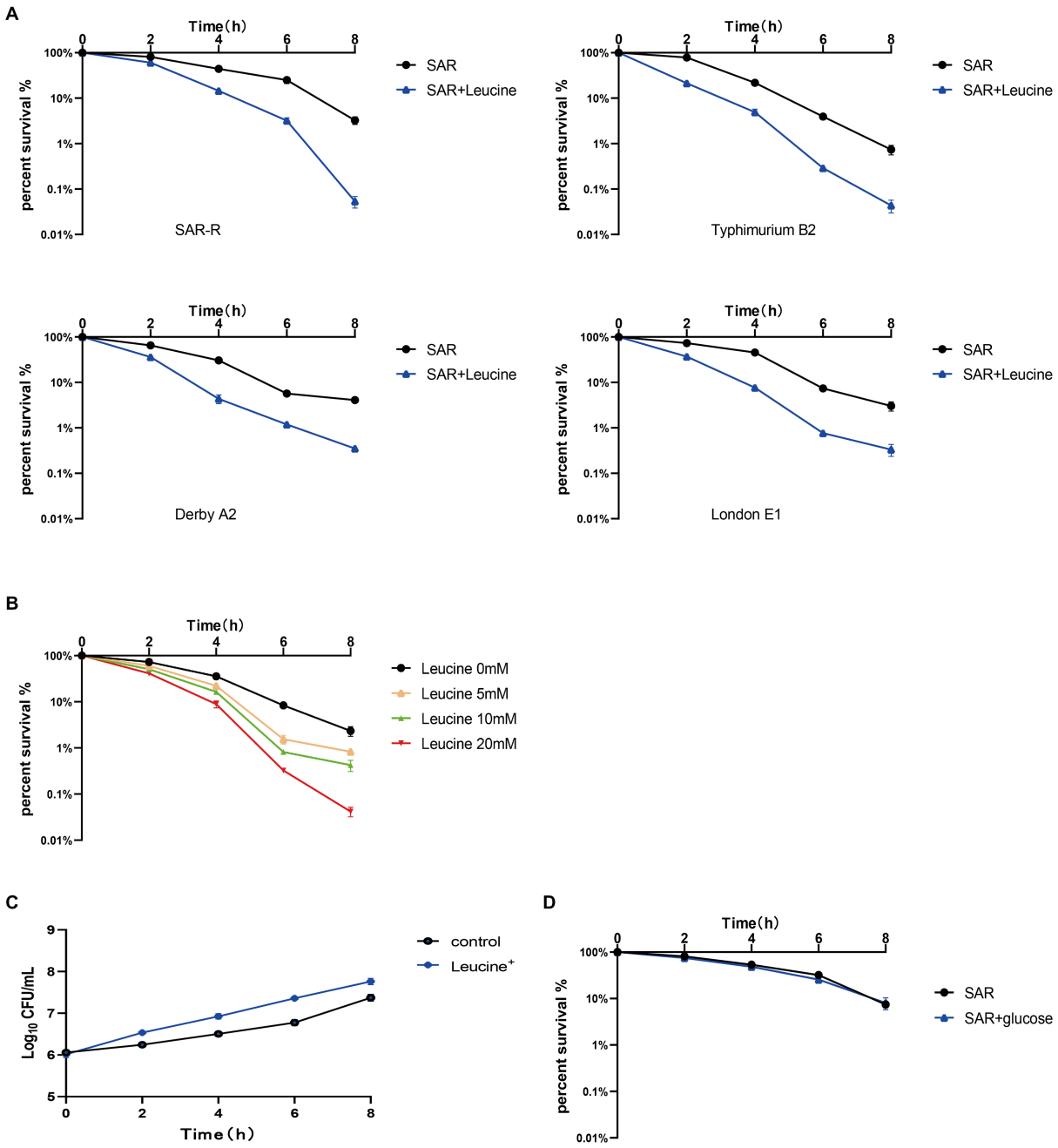

FIGURE 2
Killing curve of SAR-R and clinical drug-resistant *Salmonella*. **(A)** Percent survival curve of sarafloxacin (1MIC) and L-leucine (20mM) action on four drug-resistant bacteria in M9 Minimal medium. **(B)** Percent survival curve of different concentrations of L-leucine (0, 5, 10, 20mM) combined with sarafloxacin (1MIC) on SAR-R in M9 Minimal medium. **(C)** Growth promotion curve of glucose (40mM) on SAR-R in M9 Minimal medium. **(D)** Percent survival curve of sarafloxacin (1MIC) and glucose (40mM) action on SAR-R in M9 Minimal medium. Results are displayed as the mean±SEM and three biological repeats are carried out.

3.5. L-leucine enhanced intracellular ATP concentration and activated the oxidative phosphorylation pathway

The electron transport chain is an important pathway for cells to generate energy. When the electron transfer chain pumps electrons across the membrane to form a potential difference, ATP is synthesized by ATP synthase to fuel life activities. As the substrate of the electron transfer chain, NADH is also affected by L-leucine, which may increase the intracellular ATP concentration. Therefore, we added L-leucine into the culture medium and measured the intracellular ATP concentration at 4 h. As shown in Figure 4A, the intracellular ATP concentration increased significantly after adding L-leucine compared with the control group. This shows that the increased

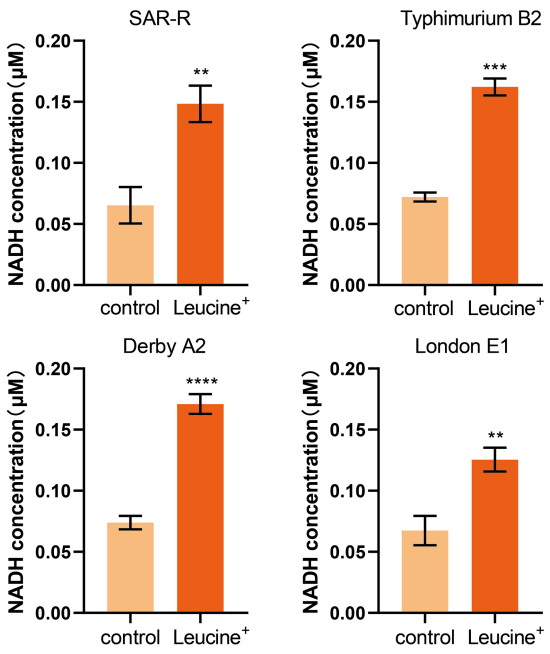

FIGURE 3
L-leucine increases the intracellular NADH concentration of SAR-R and clinical drug-resistant *Salmonella* in the presence 20mML-leucine. Results are displayed as the mean±SEM and three biological repeats are carried out. Significant differences are identified (**p<0.01), determined by unpaired t-test.

abundance of NADH entered the electron transfer chain and produced ATP, which improved the metabolic activity of the drug-resistant bacteria. To further verify the influence of the electron transfer chain, RT-qPCR was used to determine the expression level of key genes. As shown in Figure 4B, the expression of key genes *nuoI*, *ndh*, *cyoB*, *atpC*, *atpD*, *atpG*, and *atpH* all increased after L-leucine addition. These results showed that after L-leucine treatment, the oxidative phosphorylation pathway was activated, and the intracellular ATP concentration increased, indicating that the energy metabolism of drug-resistant bacteria was reprogrammed.

3.6. L-leucine stimulates the TCA cycle

To confirm that the increased NADH and ATP levels were related to the TCA cycle, we measured the gene expression of key enzymes in the TCA cycle, pyruvate dehydrogenase (*aceE*, *aceF*), citrate synthase (*gltA*), isocitrate dehydrogenase (*icdA*), 2-oxoglutarate dehydrogenase E1 component (*sucA*), succinyl-CoA synthetase (*sucC*), dihydrolipoyl dehydrogenase (*lpdA*), succinate dehydrogenase (*sdhA*, *sdhC*), fumarate reductase (*frdA*, *frdB*, *frdC*), fumarate hydratase (*fumA*, *fumC*), and malate dehydrogenase (*mdh*). The expression level of these 15 genes is shown in Figure 5. After co-culturing bacteria with L-leucine for 6 h, the expression level of most genes increased significantly, suggesting that exogenous L-leucine promoted the function of the TCA cycle and that the increased NADH and ATP concentration was attributed to the activation of this cycle.

3.7. L-leucine increase the ROS level upon treatment with sarafloxacin

Three types of bactericidal antibiotics, β-lactamides, aminoglycosides, and fluoroquinolones, promote the production of harmful hydroxyl radicals in bacterial cells destroying DNA, lipids, and proteins in cells, thus causing cell death (Kohanski et al., 2007). Quinolones combine with DNA gyrase and DNA topoisomerase IV to form a ternary complex during DNA replication. When DNA is degraded, superoxide is first generated, then peroxide through a disproportionation reaction, and finally, harmful hydroxy radicals through the Fenton reaction. Some studies have shown that electrons leak during the transmission of the respiratory chain and form superoxide (Kohanski et al., 2007). In this study, the activation of NADH and the electron transfer chain was confirmed. In order to explore whether L-leucine enhanced the killing effect of sarafloxacin by increasing endogenous ROS, we used a DCFH-DA fluorescence probe to detect ROS levels with or without L-leucine (Figure 6A). Compared with the sarafloxacin group alone, the ROS levels significantly increased. Consistently, when thiourea, a ROS eliminator, was added to the combined treatment group, the content of ROS content decreased significantly (Figure 7A). the enhanced bactericidal effect of L-leucine disappeared (Figure 7B). These results suggest that ROS plays an important role in the process of collaborative killing.

4. Discussion

Due to the overuse of clinical antibiotics, the prevalence of multidrug-resistant bacteria poses a huge threat to public health safety. Combining adjuvants and antibiotics may be safer and more effective than developing new antibiotics (Pieren and Tigges, 2012; Worthington and Melander, 2013). In this study, we first used half of the MIC concentration to obtained SAR-R and SAR-S. UHPLC-Q-TOF MS was used for the non-targeted metabolomic detection of SAR-S and SAR-R. The results showed significant metabolic differences caused by drug resistance. A total of 62 different metabolites were identified in the positive and negative ion modes. Then we found that some differential metabolites with reduced abundance were involved in the central carbon metabolism related metabolic pathway led by TCA. However, the abundance of phosphoenolpyruvate involved in the glycolysis process showed an increase, which may be due to the disorder of central carbon metabolism leading to the accumulation of intermediate products, further inhibiting the normal operation of the TCA cycle.

Various of studies have demonstrate improved killing by antibiotics following the reprogramming of deranged metabolism. Multiple amino acids have been confirmed to potentially modify metabolisms, such as, serine, citrulline, and alanine (Duan et al., 2016; Ye et al., 2018; Yong et al., 2021). We also tested a variety of amino acids in our experiments, but these above were not effectively repeated, which may be due to differences in experimental drugs, different experimental strains. In this study, we have measured the combined bactericidal efficacy of all 20 protein amino acids with sarafloxacin, including the above amino acids that have been proven to have synergistic effects. However, in all experiments, only the synergistic effect of L-leucine was confirmed. This may be due to the different

10.3389/fmicb.2023.1186841

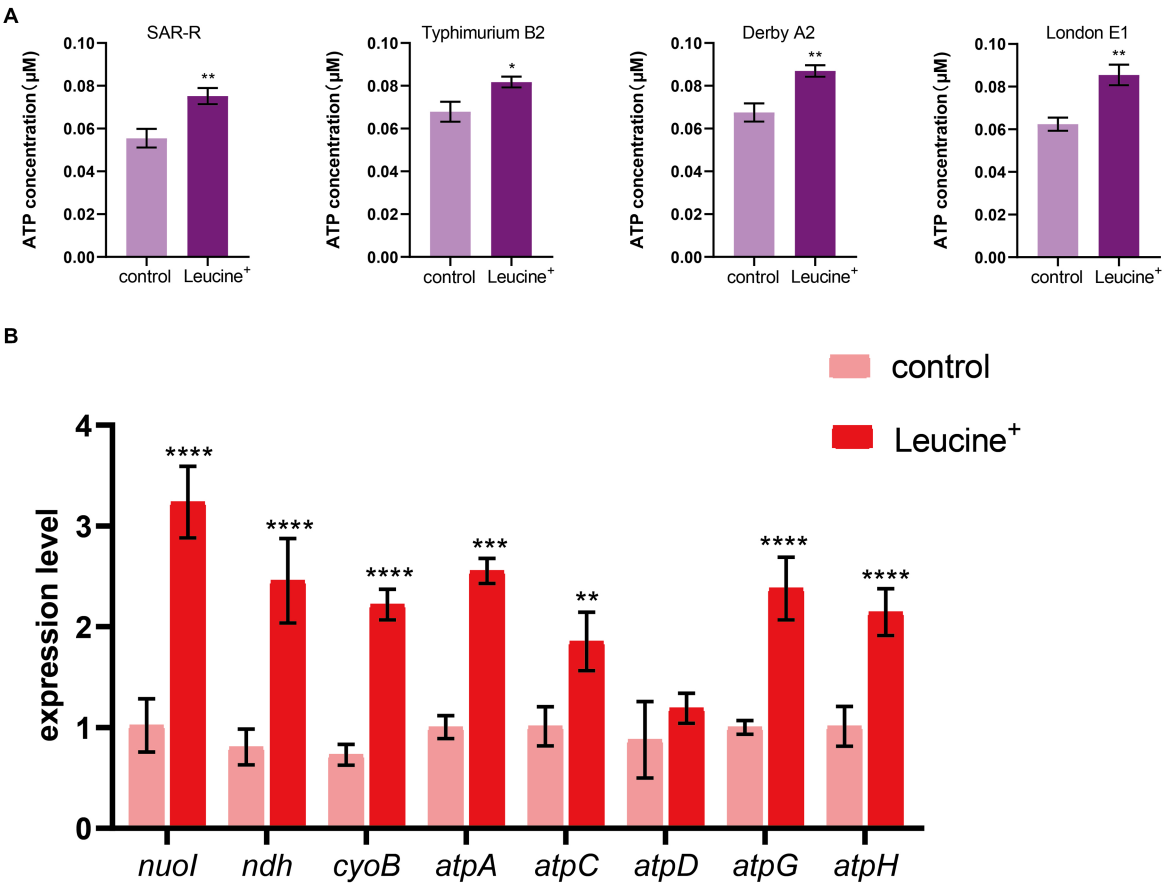

FIGURE 4
L-leucine activates electron transfer chain. **(A)** L-leucine increases the intracellular ATP concentration of SAR-R and clinical drug-resistant *Salmonella* in the presence 20mML-leucine. **(B)** RT-qPCR of key gene expression of electron transfer chain in SAR-R in the presence of 20mML-leucine. *nuoI*, NADH dehydrogenase I chain I; *ndh*, NADH:quinone reductase; *cyoB*, cytochrome o ubiquinol oxidase subunit I; *atpA*, *atpD*, *atpG*, *atpH* and *atpC*, membrane-bound ATP synthase, F1 sector, alpha-subunit, beta-subunit, gamma-subunit, delta-subunit, and epsilon-subunit. Results are displayed as the mean±SEM and three biological repeats are carried out. Significant differences are identified (*p<0.05, **p<0.01, ***p<0.001, ****p<0.0001), determined by unpaired *t*-test.

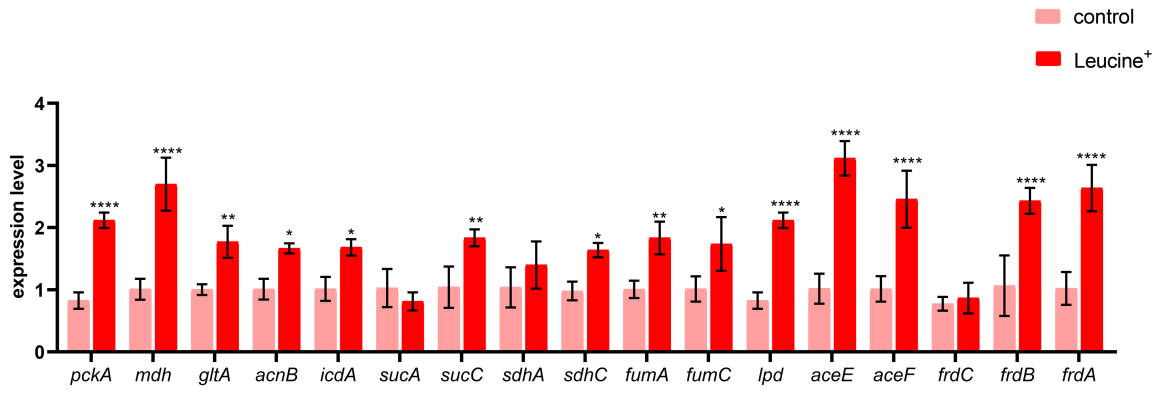

FIGURE 5
L-leucine activates TCA cycle. RT-qPCR of key gene expression of TCA cycle in SAR-R in the presence of 20mML-leucine. *pckA*, phosphoenolpyruvate carboxykinase; *mdh*, malate dehydrogenase; *gltA*, citrate synthase; *acnB*, aconitate hydratase 2; *icdA*, isocitrate dehydrogenase; *sucA*, 2-oxoglutarate dehydrogenase E1 component; *sucC*, succinyl-CoA synthetase beta subunit; *sdhA*, succinate dehydrogenase; *sdhC*, succinate dehydrogenase; *fumA*, fumarate hydratase, class I; *fumC*, fumarate hydratase, class II; lpd, dihydrolipoyl dehydrogenase; *aceE*, pyruvate dehydrogenase E1 component; *aceF*, pyruvate dehydrogenase E2 component; *frdC*, fumarate reductase subunitC; *frdB*, fumarate reductase iron–sulfur subunit; *frdA*, fumarate reductase flavoprotein subunit. Results are displayed as the mean±SEM and three biological repeats are carried out. Significant differences are identified (*p<0.05,**p<0.01, ***p<0.001,****p<0.0001).

absorption and utilization effects of various amino acids by different bacteria. We speculate that different drugs act differently on various bacteria, although most bacteria adjust their metabolic situation to lower their metabolism to evade the killing effect of antibiotics. However these alterations are special and we can only summarize several features in common, such as the attenuation of the central carbon metabolism. Specific alterations were unique in each sample. It is also interesting to note that several studies have demonstrated that sugars (glucose, fructose, D-ribose) can function as an antibiotic adjuvant (Peng et al., 2015; Su et al., 2015; Zhou et al., 2022), However, in this experiment glucose only promoted bacterial growth, and deficiency did not play a role in promoting killing, supporting the view that "every metabolic change that develops as a result of drug resistance is unique." In summary, L-leucine was specifically selected during our experiments and targeted in our study targeted in our study.

Furthermore, we found that L-leucine promoted the killing effect of sarafloxacin against SAR-R and other clinically resistant *Salmonella Typhimurium* B2, Derby A2, and London E1 with different serotypes. However, each bacterium's most effective synergistic killing time differed, which may be due to the different biochemical characteristics of each strain and the difference in the absorption rate and utilization efficiency of L-leucine. In order to exclude the role of L-leucine as a nutrient, we also used glucose as a control. The results were similar to those we predicted. Glucose did not show a synergistic effect, which also signifies the special role of L-leucine. We performed the same experiment on other fluoroquinolones (such as danooxacin). Interestingly, the results showed that only some strains had a synergistic killing effect, which may be attributed to the specific synergistic effect caused by different drug structures or the resistance of different strains to various fluoroquinolones, which needs further study.

In order to explore the specific mechanism of L-leucine in the cell, we measured the NADH and ATP concentrations and ROS levels of bacteria after cultivation with L-leucine. Overall, NADH, ATP, and ROS levels increased with L-leucine. To further confirm these results, we used RT-qPCR to determine the expression of each gene in the TCA cycle and electron transfer chain. The results showed that the expression level of most genes increased. Therefore, we concluded that exogenous L-leucine activated the TCA cycle after entering the cell membrane; thus, the abundance of NADH, the intermediate product of the TCA cycle, increased. When NADH entered the electron transfer chain as a substrate, it accelerated the electron transfer, increasing the ATP concentration from the product and correcting the inhibited carbon metabolism. Simultaneously, the function of the electron transfer chain accelerated, increasing the leakage of electrons, and the oxygen molecules received electrons and produced more ROS through the Fenton reaction, which promoted the death of bacteria (Figure 6). This was also confirmed by the ROS elimination agent, thiourea. When exogenous thiourea was added to the culture medium, the intracellular ROS level decreased rapidly, and the synergistic effect of L-leucine disappeared.

In addition to interacting with the target, bactericidal antibiotics will cause bacteria to produce ROS and destroy the cell structure (Kohanski et al., 2007). Many studies have also begun to look for antibiotic adjuvants at the metabolic level. Fructose, D-ribose, serine, alanine, thymine, citrulline, and glutamine as metabolites have been proven to reprogram the metabolic state of bacteria to improve the bactericidal effect of various antibiotics

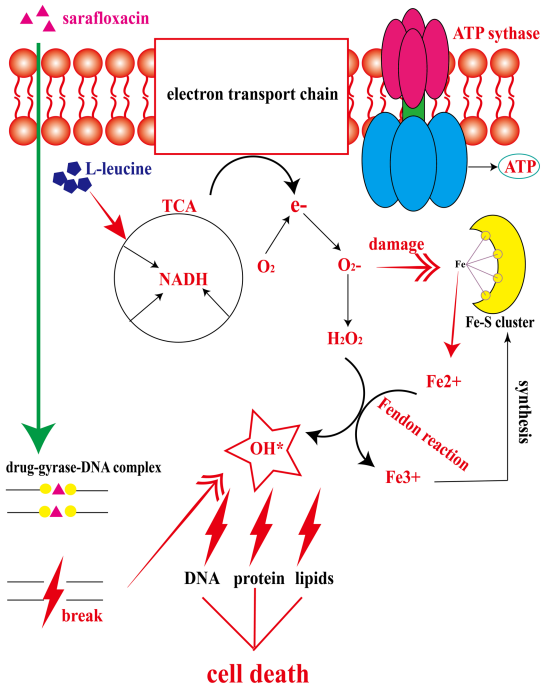

FIGURE 6
The mechanism of L-leucine promoting the killing effect of sarafloxacin on drug-resistant *Salmonella*. After L-leucine enters the cell, it stimulates TCA cycle and increases NADH content. NADH enters the electron transfer chain to accelerate electron transfer and ATP synthesis. The excessively activated electron transfer chain leads to electron leakage, and O_2 receives e- to become superoxide, which then generates hydrogen peroxide under the catalysis of superoxide dismutases. Meanwhile, superoxide dismutases can disrupt the Fe-S cluster and produce free Fe^{2+}. $Fe^{2+}$and hydrogen peroxide produce a Fenton reaction, generating deadly hydroxyl radical to kill cells, while the oxidation product Fe^{3+}continues to synthesize Fe-S cluster.

(Duan et al., 2016; Ye et al., 2018; Liu et al., 2021; Yong et al., 2021; Zhao et al., 2021; Zhou et al., 2022). However, most of these studies are aimed at aminoglycoside drugs, such as citrulline, glutamine and apramycin, D-ribose and gentamicin, alanine and kanamycin. This is due to the unique absorption mechanism of aminoglycoside drugs which is related to PMF. The generation of PMF is also associated with the electron transfer chain, as it is responsible for generating the potential difference in cell membranes. Ultimately, they are closely related to the TCA cycle because the substrate NADH of the electron transfer chain comes from the reaction catalyzed by isocitrate dehydrogenase and malate dehydrogenase in the TCA cycle. Fluoroquinolones are widely used in clinical antibacterial treatment, but the current drug resistance caused by overuse and misuse also encourages us to speed up the search for antibiotic adjuvants. Animals, especially edible livestock and poultry, are closely related to humans, and even some drug-resistant plasmids can be transmitted to humans to cause health and safety crises (Katale et al., 2020). As a special fluoroquinolone drug for animals, sarafloxacin is significant in finding an antibiotic adjuvant to relieve the pressure of clinical drug resistance, whether for aquaculture or public health safety.

In summary, non-targeted metabolomics was performed to determine the differential metabolites caused by drug resistance, and

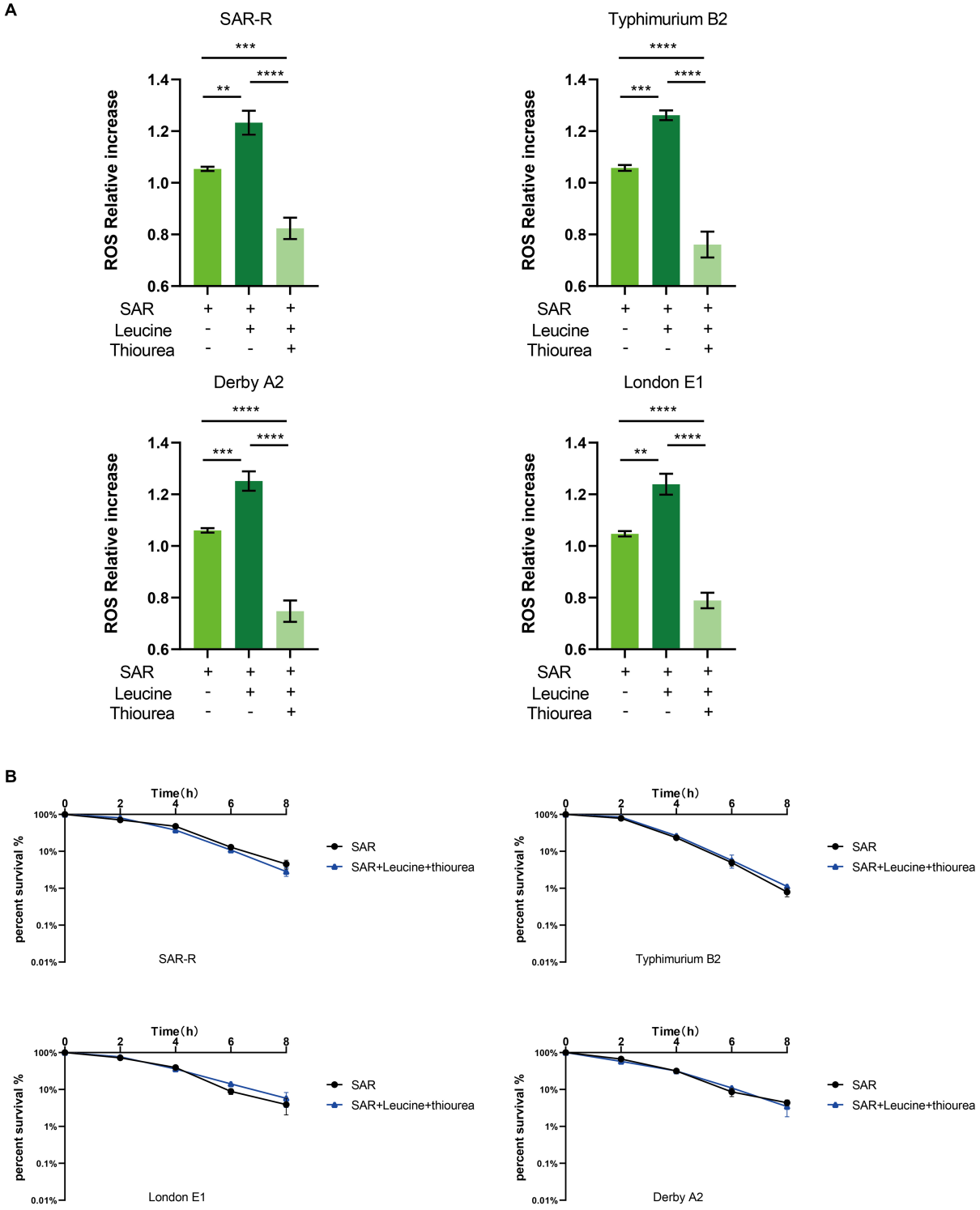

FIGURE 7
Intracellular ROS level of SAR-R and clinical drug-resistant *Salmonella*. **(A)** Combination of L-leucine and sarafloxacin enhanced ROS production. **(B)** Percent survival curve of 1 MIC and 20mML-leucine and 60mM thiourea action on SAR-R and clinical drug-resistant *Salmonella* in M9 Minimal medium. Results are displayed as the mean±SEM and three biological repeats are carried out. Significant differences are identified (***p*<0.01, *****p*<0.0001), determined by unpaired *t*-test.

we further speculate that central carbon metabolism plays a crucial role in the evolution of drug resistance. It was also proved that L-leucine could increase the intracellular NADH and ATP concentration and ROS level of bacteria. This makes L-leucine specific in promoting the killing effect of sarafloxacin against drug-resistant *Salmonella*. Our results provide a theoretical basis for alleviating

clinical drug resistance. It also provides evidence that L-leucine can be used as a potential adjuvant to enhance the efficacy of fluoroquinolones.

Data availability statement

The datasets presented in this study can be found in online repositories. The names of the repository/repositories and accession number(s) can be found at: https://www.ebi.ac.uk/metabolights/; MTBLS7711, MTBLS7713.

Author contributions

HY carried out the main experiments and data analysis and wrote the manuscript. YZ participated in the *in vitro* validation tests. QL and CZ participated in the isolation and identification of clinical drug-resistant bacteria. BF conceived and designed the experiments. All authors contributed to the article and approved the submitted version.

Funding

This work was funded by the Local Innovative and Research Teams Project of Guangdong Pearl River Talents Program (No. 2019BT02N054).

Acknowledgments

The authors thank the native English-speaking scientists of Charlesworth Data Services (Beijing) Co., Ltd. (Beijing, China) for editing the manuscript.

Conflict of interest

The authors declare that the research was conducted in the absence of any commercial or financial relationships that could be construed as a potential conflict of interest.

Publisher's note

Supplementary material

The Supplementary material for this article can be found online at: https://www.frontiersin.org/articles/10.3389/fmicb.2023.1186841/full#supplementary-material

References

Aldred, K. J., Kerns, R. J., and Osheroff, N. (2014). Mechanism of quinolone action and resistance. *Biochemistry* 53, 1565–1574. doi: 10.1021/bi5000564

Ao, T. T., Feasey, N. A., Gordon, M. A., Keddy, K. H., Angulo, F. J., and Crump, J. A. (2015). Global burden of invasive nontyphoidal Salmonella disease. *Emerg. Infect. Dis.* 21, 941–949. doi: 10.3201/eid2106.140999

Belenky, P., Ye, J. D., Porter, C. B., Cohen, N. R., Lobritz, M. A., Ferrante, T., et al. (2015). Bactericidal antibiotics induce toxic metabolic perturbations that Lead to cellular damage. *Cell Rep.* 13, 968–980. doi: 10.1016/j.celrep.2015.09.059

CDC (2019). Antibiotic resistance threats in the United States [online]. Available at: https://www.cdc.gov/drugresistance/pdf/threats-report/2019-ar-threats-report-508.pdf (Accessed July 8, 2022).

Chen, Y. T., Yang, K. X., Dai, Z. Y., Yi, H., Peng, X. X., Li, H., et al. (2022). Repressed central carbon metabolism and its effect on related metabolic pathways in Cefoperazone/Sulbactam-resistant *Pseudomonas aeruginosa*. *Front. Microbiol.* 13:847634. doi: 10.3389/fmicb.2022.847634

Cheng, Z. X., Yang, M. J., Peng, B., Peng, X. X., Lin, X. M., and Li, H. (2018). The depressed central carbon and energy metabolisms is associated to the acquisition of levofloxacin resistance in *Vibrio alginolyticus*. *J. Proteome* 181, 83–91. doi: 10.1016/j.jprot.2018.04.002

Correia, S., Poeta, P., Hebraud, M., Capelo, J. L., and Igrejas, G. (2017). Mechanisms of quinolone action and resistance: where do we stand? *J. Med. Microbiol.* 66, 551–559. doi: 10.1099/jmm.0.000475

Duan, X., Huang, X., Wang, X., Yan, S., Guo, S., et al. (2016). L-serine potentiates fluoroquinolone activity against *Escherichia coli* by enhancing endogenous reactive oxygen species production. *J. Antimicrob. Chemother.* 71, 2192–2199. doi: 10.1093/jac/dkw114

Fang, F. C. (2015). Fluoroquinolone resistance in Salmonella and the utility of Pefloxacin disk diffusion [corrected]. *J. Clin. Microbiol.* 53, 3401–3404. doi: 10.1128/JCM.02270-15

Farzan, A., and Friendship, R. M. (2010). A clinical field trial to evaluate the efficacy of vaccination in controlling Salmonella infection and the association of Salmonella-shedding and weight gain in pigs. *Can. J. Vet. Res.* 74, 258–263.

Feasey, N. A., Dougan, G., Kingsley, R. A., Heyderman, R. S., and Gordon, M. A. (2012). Invasive non-typhoidal salmonella disease: an emerging and neglected tropical disease in Africa. *Lancet* 379, 2489–2499. doi: 10.1016/S0140-6736(11)61752-2

Galanis, E., Wong, D. M., Patrick, M. E., Binsztein, N., Cieslik, A., Chalermchaikit, T., et al. (2006). Web-based surveillance and global Salmonella distribution, 2000-2002. *Emerg. Infect. Dis.* 12, 381–388. doi: 10.3201/eid1205.050854

Gut, A. M., Vasiljevic, T., Yeager, T., and Donkor, O. N. (2018). Salmonella infection - prevention and treatment by antibiotics and probiotic yeasts: a review. *Microbiology (Reading)* 164, 1327–1344. doi: 10.1099/mic.0.000709

Hendriksen, R. S., Vieira, A. R., Karlsmose, S., Lo Fo Wong, D. M. A., Jensen, A. B., Wegener, H. C., et al. (2011). Global monitoring of Salmonella serovar distribution from the World Health Organization global foodborne infections network country data Bank: results of quality assured laboratories from 2001 to 2007. *Foodborne Pathog. Dis.* 8, 887–900. doi: 10.1089/fpd.2010.0787

Hooper, D. C. (1998). Clinical applications of quinolones. *Biochim. Biophys. Acta* 1400, 45–61. doi: 10.1016/s0167-4781(98)00127-4

Katale, B. Z., Misinzo, G., Mshana, S. E., Chiyangi, H., Campino, S., Clark, T. G., et al. (2020). Genetic diversity and risk factors for the transmission of antimicrobial resistance across human, animals and environmental compartments in East Africa: a review. *Antimicrob. Resist. Infect. Control* 9:127. doi: 10.1186/s13756-020-00786-7

Kim, E. S., and Hooper, D. C. (2014). Clinical importance and epidemiology of quinolone resistance. *Infect. Chemother.* 46, 226–238. doi: 10.3947/ic.2014.46.4.226

Kirk, M. D., Pires, S. M., Black, R. E., Caipo, M., Crump, J. A., Devleesschauwer, B., et al. (2015). World Health Organization estimates of the global and regional disease burden of 22 foodborne bacterial, Protozoal, and viral diseases, 2010: a data synthesis. *PLoS Med.* 12:e1001921. doi: 10.1371/journal.pmed.1001921

Kohanski, M. A., Dwyer, D. J., Hayete, B., Lawrence, C. A., and Collins, J. J. (2007). A common mechanism of cellular death induced by bactericidal antibiotics. *Cells* 130, 797–810. doi: 10.1016/j.cell.2007.06.049

Liu, Y., Yang, K., Jia, Y., Shi, J., Tong, Z., and Wang, Z. (2021). Thymine sensitizes gram-negative pathogens to antibiotic killing. *Front. Microbiol.* 12:622798. doi: 10.3389/fmicb.2021.622798

Lopatkin, A. J., Bening, S. C., Manson, A. L., Stokes, J. M., Kohanski, M. A., Badran, A. H., et al. (2021). Clinically relevant mutations in core metabolic genes confer antibiotic resistance. *Science* 371:eaba0862. doi: 10.1126/science.aba0862

Majowicz, S. E., Musto, J., Scallan, E., Angulo, F. J., Kirk, M., O'Brien, S. J., et al. (2010). The global burden of nontyphoidal Salmonella gastroenteritis. *Clin. Infect. Dis.* 50, 882–889. doi: 10.1086/650733

Oliphant, C. M., and Green, G. M. (2002). Quinolones: a comprehensive review. *Am. Fam. Physician* 65, 455–464.

Peng, B., Su, Y. B., Li, H., Han, Y., Guo, C., Tian, Y. M., et al. (2015). Exogenous alanine and/or glucose plus kanamycin kills antibiotic-resistant bacteria. *Cell Metab.* 21, 249–262. doi: 10.1016/j.cmet.2015.01.008

Phu Huong Lan, N., le Thi Phuong, T., Nguyen Huu, H., Thuy, L., Mather, A. E., Park, S. E., et al. (2016). Invasive non-typhoidal Salmonella infections in Asia: clinical observations, disease outcome and dominant Serovars from an infectious disease Hospital in Vietnam. *PLoS Negl. Trop. Dis.* 10:e0004857. doi: 10.1371/journal.pntd.0004857

Pieren, M., and Tigges, M. (2012). Adjuvant strategies for potentiation of antibiotics to overcome antimicrobial resistance. *Curr. Opin. Pharmacol.* 12, 551–555. doi: 10.1016/j.coph.2012.07.005

Reddy, E. A., Shaw, A. V., and Crump, J. A. (2010). Community-acquired bloodstream infections in Africa: a systematic review and meta-analysis. *Lancet Infect. Dis.* 10, 417–432. doi: 10.1016/S1473-3099(10)70072-4

Redgrave, L. S., Sutton, S. B., Webber, M. A., and Piddock, L. J. (2014). Fluoroquinolone resistance: mechanisms, impact on bacteria, and role in evolutionary success. *Trends Microbiol.* 22, 438–445. doi: 10.1016/j.tim.2014.04.007

Schrimpe-Rutledge, A. C., Codreanu, S. G., Sherrod, S. D., and McLean, J. A. (2016). Untargeted metabolomics strategies-challenges and emerging directions. *J. Am. Soc. Mass Spectrom.* 27, 1897–1905. doi: 10.1007/s13361-016-1469-y

Sinwat, N., Angkittitrakul, S., Coulson, K. F., Pilapil, F., Meunsene, D., and Chuanchuen, R. (2016). High prevalence and molecular characteristics of multidrug-resistant Salmonella in pigs, pork and humans in Thailand and Laos provinces. *J. Med. Microbiol.* 65, 1182–1193. doi: 10.1099/jmm.0.000339

Stokes, J. M., Lopatkin, A. J., Lobritz, M. A., and Collins, J. J. (2019). Bacterial metabolism and antibiotic efficacy. *Cell Metab.* 30, 251–259. doi: 10.1016/j.cmet.2019.06.009

Su, Y. B., Peng, B., Han, Y., Li, H., and Peng, X. X. (2015). Fructose restores susceptibility of multidrug-resistant *Edwardsiella tarda* to kanamycin. *J. Proteome Res.* 14, 1612–1620. doi: 10.1021/pr501285f

Tian, Y., Gu, D., Wang, F., Liu, B., Li, J., Kang, X., et al. (2021). Prevalence and characteristics of Salmonella spp. from a pig farm in Shanghai, China. *Foodborne Pathog. Dis.* 18, 477–488. doi: 10.1089/fpd.2021.0018

Van Acker, H., and Coenye, T. (2017). The role of reactive oxygen species in antibiotic-mediated killing of Bacteria. *Trends Microbiol.* 25, 456–466. doi: 10.1016/j.tim.2016.12.008

Wiegand, I., Hilpert, K., and Hancock, R. E. (2008). Agar and broth dilution methods to determine the minimal inhibitory concentration (MIC) of antimicrobial substances. *Nat. Protoc.* 3, 163–175. doi: 10.1038/nprot.2007.521

Worthington, R. J., and Melander, C. (2013). Combination approaches to combat multidrug-resistant bacteria. *Trends Biotechnol.* 31, 177–184. doi: 10.1016/j.tibtech.2012.12.006

Yang, C. C., Chuang, F. R., Wu, C. H., Chen, J. B., Lee, C. H., and Lee, C. T. (2012). Refractory *Salmonella enterica* serotype choleraesuis-related renal cyst infection in a patient with autosomal dominant polycystic kidney disease undergoing hemodialysis treated successfully with intracystic ciprofloxacin infusion. *Med. Princ. Pract.* 21, 576–578. doi: 10.1159/000339199

Ye, J. Z., Su, Y. B., Lin, X. M., Lai, S. S., Li, W. X., Ali, F., et al. (2018). Alanine enhances aminoglycosides-induced ROS production as revealed by proteomic analysis. *Front. Microbiol.* 9:29. doi: 10.3389/fmicb.2018.00029

Yong, Y., Zhou, Y., Liu, K., Liu, G., Wu, L., and Fang, B. (2021). Exogenous Citrulline and glutamine contribute to reverse the resistance of Salmonella to Apramycin. *Front. Microbiol.* 12:759170. doi: 10.3389/fmicb.2021.759170

Zhao, X. L., Chen, Z. G., Yang, T. C., Jiang, M., Wang, J., Cheng, Z. X., et al. (2021). Glutamine promotes antibiotic uptake to kill multidrug-resistant uropathogenic bacteria. *Sci. Transl. Med.* 13:eabj0716. doi: 10.1126/scitranslmed.abj0716

Zhou, Y., Yong, Y., Zhu, C., Yang, H., and Fang, B. (2022). Exogenous D-ribose promotes gentamicin treatment of several drug-resistant Salmonella. *Front. Microbiol.* 13:1053330. doi: 10.3389/fmicb.2022.1053330

frontiers | Frontiers in Microbiology

TYPE Original Research
PUBLISHED 15 May 2023
DOI 10.3389/fmicb.2023.1162657

OPEN ACCESS

EDITED BY
Xunde Li,
University of California,
Davis, United States

REVIEWED BY
Pankaj Dhaka,
Guru Angad Dev Veterinary and Animal Sciences University, India
Veronica Cibin,
Experimental Zooprophylactic Institute of the Venezie (IZSVe), Italy

*CORRESPONDENCE
Roderick M. Card
✉ Roderick.Card@apha.gov.uk
Mohammed Abdus Samad
✉ msamad@blri.gov.bd

RECEIVED 09 February 2023
ACCEPTED 31 March 2023
PUBLISHED 15 May 2023

CITATION
Card RM, Chisnall T, Begum R, Sarker MS, Hossain MS, Sagor MS, Mahmud MA, Uddin ASMA, Karim MR, Lindahl JF and Samad MA (2023) Multidrug-resistant non-typhoidal *Salmonella* of public health significance recovered from migratory birds in Bangladesh.
Front. Microbiol. 14:1162657.
doi: 10.3389/fmicb.2023.1162657

Multidrug-resistant non-typhoidal *Salmonella* of public health significance recovered from migratory birds in Bangladesh

Roderick M. Card[1]*, Thomas Chisnall[1], Ruhena Begum[2], Md Samun Sarker[2], Muhammad Sazzad Hossain[2], Md Shahjalal Sagor[2], Mohammad Asheak Mahmud[2], A. S. M. Ashab Uddin[2], Md Rezaul Karim[2], Johanna F. Lindahl[3] and Mohammed Abdus Samad[2]*

[1]Animal and Plant Health Agency, New Haw, Addlestone, United Kingdom, [2]Antimicrobial Resistance Action Center (ARAC), Animal Health Research Division, Bangladesh Livestock Research Institute, Savar, Bangladesh, [3]Department of Clinical Sciences, Swedish University of Agricultural Sciences, Uppsala, Sweden

Non-typhoidal *Salmonella* provides an exemplar for the One Health approach as it encompasses public and animal health, food safety, and environmental considerations. The contribution of environmental aspects is currently less well-defined. The purpose of this study was to determine the carriage occurrence of non-typhoidal *Salmonella* in migratory birds in Bangladesh and assess the potential significance to public and animal health. Cloacal swabs (N=453) were collected in the years 2018–2020 from Tanguar and Hakaluki Haors, important wetland ecosystems in Northeastern Bangladesh. The prevalence of *Salmonella* was 13.5% (61 positive swabs). Classical serotyping identified six serovars: *Salmonella enterica* subsp. *enterica* serovars Perth, Kentucky, Albany, Infantis, Weltevreden, and Brancaster. Resistance towards 14 antimicrobials was assessed by broth microdilution minimum inhibitory concentration determination and the antimicrobial resistance (AMR) genotype established by whole-genome sequencing. *S.* Perth and *S.* Weltevreden isolates were susceptible and harbored no acquired AMR genes. Isolates from the remaining serovars were multidrug resistant, commonly possessing resistance to tetracycline, ampicillin, chloramphenicol, sulfamethoxazole, trimethoprim, and ciprofloxacin. *Salmonella* resistant to ciprofloxacin meets WHO criteria for priority pathogens. There was excellent concordance between resistance phenotype and the presence of corresponding AMR genes, many of which reside on *Salmonella* Genomic Islands. High-level ciprofloxacin resistance correlated with the presence of mutations in the chromosomal *gyrB* and/or *parC* genes. The *S.* Kentucky isolates were ST198, a widely distributed multidrug-resistant lineage reported in humans and animals, and constituting an ongoing risk to public health worldwide. We have demonstrated that multidrug-resistant non-typhoidal *Salmonella* of public health significance can be recovered from migratory birds. A potential for risk can manifest through direct interaction, transmission to food-producing livestock on farms, and dissemination via the long range migratory movements of birds. Risks can be mitigated by measures including continued surveillance and implementation of good farm biosecurity practices.

KEYWORDS

***Salmonella*, migratory birds, multidrug resistance, antimicrobial resistance, Bangladesh**

Introduction

Salmonella enterica is a zoonotic pathogen of significant public and animal health concern worldwide (Majowicz et al., 2010). The species is highly diverse, having over 2,600 serovars (Grimont and Weill, 2007), which have been divided into typhoidal and non-typhoidal *Salmonella* (NTS) serovars. Non-typhoidal *Salmonella* (NTS) can cause gastroenteritis that is generally self-limiting in humans, but can lead to an invasive infection that presents a greater risk to health and may require antimicrobial treatment (Acheson and Hohmann, 2001). The number of foodborne illnesses and deaths caused by NTS globally in 2010 has been estimated at over 78 million and >59,000, respectively, (Havelaar et al., 2015). The prevalence of NTS serovars differs, but in any given country, most human isolates (>90%) will be from about 30 serovars (Grimont and Weill, 2007). Poultry and poultry products are a common source of human infection by NTS, and important *Salmonella enterica* subsp. *enterica* serovars include *S.* Typhimurium, *S.* Enteritidis, *S.* Kentucky, and *S.* Infantis, among others (Koutsoumanis et al., 2019).

Antimicrobial resistance (AMR) in *Salmonella* is of considerable concern as it limits therapeutic options and increases the risk of treatment failure. Furthermore, multidrug resistance (resistance to ≥3 antimicrobial classes) has been associated with more serious disease in people (Parisi et al., 2018). Traditional first-line antibiotics include ampicillin, chloramphenicol, and trimethoprim/sulfamethoxazole (Crump et al., 2015). The high prevalence of resistance in *Salmonella* to these antimicrobials has led to increased use of critically important antimicrobials such as ciprofloxacin (fluoroquinolone), ceftriaxone (third-generation cephalosporin), and alternatively azithromycin (macrolide; Crump et al., 2015). *Salmonella* with resistance to fluoroquinolones, carbapenems, or third generation cephalosporins have been listed as high-priority pathogens by the World Health Organization (Tacconelli et al., 2018).

Salmonella has been found in resident and migratory free-living birds in many countries (Tizard, 2004; Beleza et al., 2020). Wild birds can act as vectors that introduce pathogens including *Salmonella* onto farms, necessitating the need for appropriate biosecurity (De Lucia et al., 2018; Koutsoumanis et al., 2019). The role of resident and migratory birds as a reservoir and disseminator of *Salmonella* (Tizard, 2004; De Lucia et al., 2018; Beleza et al., 2020; Lin et al., 2020), AMR (Lin et al., 2020; Islam et al., 2021, 2022), and viruses (Gilbert et al., 2010; Bi et al., 2015) is widely recognized. The aggregation of large mixed species groups of wild birds can facilitate the spread of *Salmonella*, AMR, and other pathogens. The long-range migratory movements of birds frequently span countries and continents, providing significant potential for the dispersal to other areas of *Salmonella* and AMR harbored therein.

Bangladesh lies in the path of two migratory flyways, the East Asian–Australasian Flyway and the Central Asian Flyway. Birds migrate between breeding grounds in Northern regions and their overwintering quarters in the South. Migratory birds either overwinter in Bangladesh or pass through as part of their annual migration. Haors, diverse wetland ecosystems in Northeastern Bangladesh, provide important habitats for resident and migratory birds. Two important Haors are Tanguar Haor and Hakaluki Haor located in the sub-districts of Tahirpur and Fenchuganj under the districts of Sunamganj and Sylhet, respectively. Tanguar Haor is a wetland of international importance listed as a Ramsar site Under the Convention on Wetlands[1] and was declared an Ecologically Critical Area in 1999 by the Bangladesh government. Tanguar Haor provides a habitat for 98 migratory bird species and up to ~40,000 migratory waterfowl converge on the area in the northern winter months.[2] The Haor also supports the livelihoods of many people, potentially bringing them into contact with wildlife, and is an important inland fisheries system with rich breeding grounds for freshwater fish. Studies of rivers and surface water in Bangladesh have shown the presence of *Salmonella* (Faridullah et al., 2022; Yasmin et al., 2023).

The occurrence of *Salmonella* in poultry and poultry products in Bangladesh has been well documented and includes serovars of public health significance, such as *S.* Typhimurium, *S.* Enteritidis, and *S.* Kentucky (Barua et al., 2012, 2013; Makendi et al., 2016). The poultry-adapted serovars *S.* Gallinarum and *S.* Gallinarum biovar Pullorum, which cause fowl typhoid and Pullorum disease, respectively, have also been reported in Bangladesh (Parvej et al., 2016). *Salmonella* has also been detected in shrimp and on shrimp farms in Bangladesh (Hossain et al., 2013; Faridullah et al., 2016). Furthermore, *Salmonella* has been described in migratory (Islam et al., 2021) and resident (Faruq et al., 2016) wild birds in Bangladesh. Both studies reported multidrug-resistant *Salmonella*, but neither described the serovar or the AMR genotype. Determination of serovar, occurrence of AMR, and genotype can allow the assessment of the significance of isolates to public and animal health. The importance of a One Health approach to tackling AMR and food-borne zoonoses such as *Salmonella* in a manner that encompasses wildlife has been highlighted in a systematic review from the Bangladesh perspective (Khan et al., 2020).

The prevalence and diversity in migratory birds of *Salmonella* and its AMR in Bangladesh remain poorly defined. To address this evidence gap, we undertook a study to assess the occurrence of *Salmonella* and AMR in migratory wild birds at Haors in Bangladesh over 3 years. To help assess potential for risk to livestock and people, we determined the serovar and antimicrobial susceptibilities of isolates obtained and used whole-genome sequencing (WGS) to define resistance gene carriage.

Materials and methods

Study design and location

During three consecutive years from 2018 to 2020, cloacal samples of different migratory birds were collected from Tanguar Haor and Hakaluki Haor in Bangladesh (Figure 1). Hakaluki and Tanguar Haors are in Northeastern Bangladesh and were chosen as the study sites as every year these wetlands intake thousands of migratory birds (Hassan et al., 2020). The birds were captured alive by expert trappers using the nets during the winter period of Bangladesh (November–December and January–February). No anesthesia, euthanasia, or animal sacrifice was conducted in this study, and precautionary measures were taken to avoid any potential harm to the birds. Out of 453 samples, 109 were collected in 2018, 133 in 2019, and 211 in 2020. Most samples (419)

1 http://www.ramsar.org/about-the-ramsar-convention

2 https://rsis.ramsar.org/ris/1031

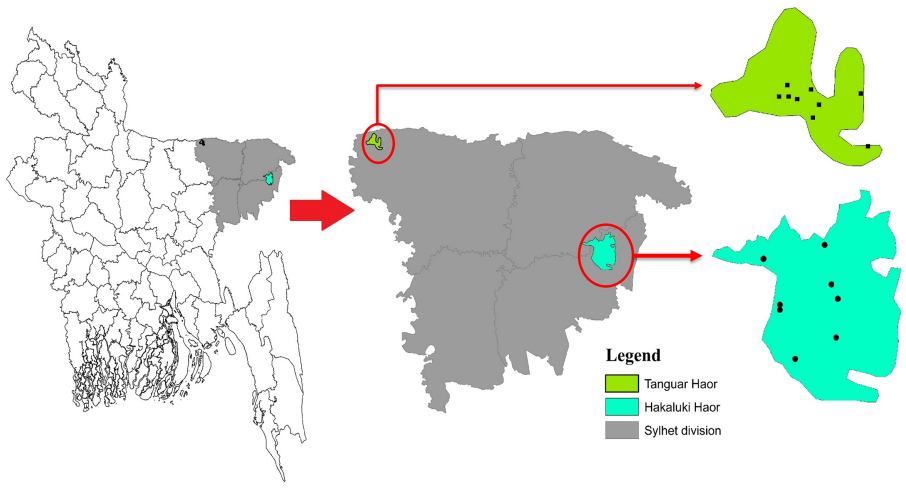

FIGURE 1
Sampling area of Tanguar Haor and Hakaluki Haor in Bangladesh.

were collected from Tanguar Haor during three consecutive years, and 34 samples were collected from Hakaluki Haor in 2018. The number of migratory birds sampled varied depending on availability and capability to capture by expert trappers in different years and locations. During 2018, there was access to both Tanguar Haor and Hakaluki Haor, but from 2019 onwards, access to Hakaluki Haor was restricted by the local authority for conservation purposes. The samples were collected from 10 species of migratory birds, those locally called Thila (*Mareca strepera*), Peri (*Aythya ferina*), Lenja Has (*Bucephala clangula*), Bali Has (*Branta canadensis*), Oikko (*Unknown*), Kalo Kura/Ramer Kura (*Fulica atra*), Boral (*Aythya nyroca*), Moulovi (*Netta rufina*), Matarangi (*Mareca penelope*), Oda (*Unknown*), and Khaium (*Unknown*). The details of the sampling pattern are shown in Table 1.

Ethical approval

The ethical approval was received from the Ethical Committee of the Animal Health Research Division at the Bangladesh Livestock Research Institute, Dhaka, Bangladesh (ARAC: 10/1/2018:01).

Isolation and identification of *Salmonella* species

Isolation and identification of *Salmonella* were carried out according to the ISO guidelines as follows: cloacal swabs were pre-enriched in buffered peptone water (BPW; Oxoid, UK) with a dilution rate of 1:10 then incubated aerobically at 37°C for 18–24 h. After enrichment, 0.1 ml of sample was then inoculated at three different locations on Modified Semisolid Rappaport Vassiliadis (MSRV; Oxoid, UK) agar medium and incubated at 41.5°C for 20–24 h. Furthermore, MSRV was plated onto xylose lysine deoxycholate (XLD; Oxoid, UK) and MacConkey agar plate and incubated overnight at 37°C (ISO, 6579: 2002; Foley et al., 2008). Characteristic black-centered colonies with reddish zones on the XLD and non-lactose-fermenting colonies on the MacConkey were selected and sub-cultured on nutrient agar medium and performed biochemical testing [triple sugar iron (TSI), motile indole urea (MIU)], catalase, and oxidase. Final confirmation was performed with a Vitek-2 compact analyzer (bioMérieux, Marcyl'Étoile, France), followed by the polymerase chain reaction. The antigenic formula of each strain was determined using standardized methods (Shipp and Rowe, 1980), and serovar was assigned according to the White–Kauffmann–Le Minor scheme (Grimont and Weill, 2007). The proportion of positive samples by year and serovar (see results) and the 95% confidence interval of the proportions were calculated with GraphPad[3] using the modified Wald method for confidence intervals.

Antimicrobial susceptibility testing

Antimicrobial susceptibility testing was performed by broth microdilution minimum inhibitory concentration (MIC) determination using commercial plates (Sensititre™ EU Surveillance Salmonella/*Escherichia coli* EUVSEC plate, Thermo Fisher Scientific, Basingstoke, UK), according to the manufacturer's instructions. Briefly, a suspension of each isolate was prepared to a density of 0.5 McFarland in 5 ml of demineralized water and 10 µl transferred to 11 ml of Mueller Hinton broth to obtain a target inoculum density of between 1×10^5 and 1×10^6 CFU/ml. Fifty microlitres were dispensed into each well of the microtitre plate and incubated at 35–37°C for 18 to 24 h. Fourteen antimicrobials were tested in this manner (sulfamethoxazole, trimethoprim, ciprofloxacin, tetracycline, tigecycline, azithromycin, nalidixic acid, ampicillin, cefotaxime, ceftazidime, meropenem, chloramphenicol, colistin, and gentamicin), and the MICs were recorded as the lowest concentration preventing visible growth. *Escherichia coli* NCTC 12241 (ATCC 25922) was used as the control strain. Susceptibility was assessed using epidemiological cutoff (ECOFF) values (EUCAST, 2020), except for azithromycin,

3 https://www.graphpad.com/quickcalcs/confInterval1/

TABLE 1 Geographic and demographic information of samples.

Year	Haor	Samples per species of migratory birds										Total samples
		Mareca strepera	*Aythya ferina*	*Bucephala clangula*	*Branta canadensis*	Oikko *(Unknown)**	*Fulica atra*	*Aythya nyroca*	*Netta rufina*	*Mareca penelope*	Oda *(Unknown)**	Khaium *(Unknown)**	
2018	Tanguar	15	9	10	0	3	15	7	3	3	8	2	75
	Hakaluki	6	8	6	0	0	5	0	0	0	9	0	34
2019	Tanguar	11	13	14	3	4	38	24	17	7	2	0	133
2020	Tanguar	22	32	34	0	3	47	50	0	3	9	11	211

Bird species with an asterisk (*) were identified by the local Bangladeshi common name only.

colistin, and tigecycline for which the human clinical breakpoints proposed by EFSA were employed (ECDC, 2016; as ECOFF values were not available). Isolates with non-wild type susceptibilities have been termed "microbiologically resistant," although it is recognized this is not necessarily synonymous with clinical resistance. Isolates were defined as multidrug resistant when non-wild type for three or more classes of antimicrobial (Schwarz et al., 2010).

Whole-genome sequencing

Deoxyribonucleic acid (DNA) extracts were prepared from overnight Mueller Hinton broth cultures and extracted with the MagMAX™ CORE extraction kit (Thermo Fisher Scientific, Basingstoke, UK) using the semi-automated KingFisher Flex system (Thermo Fisher Scientific, Basingstoke, UK) according to the manufacturer's instructions. Extracted DNA was processed for whole-genome sequencing using the Illumina HiSeq platform. The resulting raw sequences were analyzed using the Nullarbor 2 pipeline,[4] using as reference the published genome *S.* Kentucky strain 201001922 [accession number CP028357; (Hawkey et al., 2019)], Spades for genome assembly [version 3.14.1; (Bankevich et al., 2012)], and Prokka for annotation [version 1.14.6; (Seemann, 2014)]. The presence of genes and point mutations conferring AMR was assessed using AMRFinderPlus (Feldgarden et al., 2019). The sequence type (ST) was determined with MLST (version 2.19.0; https://github.com/tseemann/mlst) using the PubMLST database (Jolley et al., 2018). Virulence gene presence was assessed using Abricate[5] and the virulence factor database (Chen et al., 2016) in Nullarbor. The presence of heavy metal resistance genes was assessed using AMRFinderPlus.

The relatedness of the *S.* Perth isolates (see results) was assessed using Snippy (version 4.6.0) and SNPdist (version 0.8.2), with the reference genome *S.* Perth strain FDA363901 (Accession GCA_006407535.1) obtained from a Bangladesh Pabda fish. Two additional *S.* Perth isolates from Bangladesh Pabda fish and three human isolates from the UK were included in this comparison (Supplementary Table S2). These isolates represented all publicly available *S.* Perth genomes in EnteroBase (accessed 21 June 2022; Zhou et al., 2020). The relatedness of the *S.* Kentucky isolates (see results) was assessed in the same manner, using *S.* Kentucky strain 201001922 as a reference genome (accession number GCA_003030965.1). This analysis included the two published genomes from Bangladesh isolates (poultry strain K_50, accession number SRS3092506, and a human strain deposited in EnteroBase as SAL_LB9505AA) and 115 additional isolates from Asia and the Middle East (Supplementary Table S3), to enable an assessment of relatedness towards *S.* Kentucky from Bangladesh and other countries. Phylogenetic trees were produced using the core genome single-nucleotide polymorphism (SNP) alignments using default settings, and maximum-likelihood trees were bootstrapped 200 times using RAxML-NG (version 1.1.0; Kozlov et al., 2019). Trees were viewed and annotated in Interactive Tree Of Life (version 6.6; Letunic and Bork, 2016).

4 https://github.com/tseemann/nullarbor

5 https://github.com/tseemann/abricate

The whole-genome sequences were deposited in the National Center for Biotechnology Information (NCBI) National Library of Medicine under BioProject accession number PRJNA933150.

Results

Prevalence of *Salmonella* in migratory birds

To assess the carriage of *Salmonella* in migratory birds, 453 cloacal samples were analyzed and 61 cloacal samples were found to be positive for *Salmonella* species, giving an overall prevalence of 13.5% (Table 2). The prevalence was 33.02, 14.28, and 2.84% in the years 2018, 2019, and 2020, respectively. In 2018, sampling was undertaken at Tanguar and Hakaluki Haors, and *Salmonella* prevalence was 41% (31/75) and 16% (5/34), respectively.

Six *Salmonella* serovars were identified in the 61 isolates (Table 3; Supplementary Table S1). The most common was *S.* Perth, which comprised 62% (38/61) of all isolates and was detected in each of the three study years. *S.* Infantis was the only other serovar detected in more than 1 year, in 2018 and 2020, with an overall prevalence of 7% (4/61). The remaining four serovars were detected in 1 year only, including 12 *S.* Kentucky in 2018 (Table 3). In 2018, three serovars were detected at both Haors: *S.* Perth, *S.* Kentucky, and *S.* Albany (Supplementary Table S1).

Eight species of migratory birds were positive for *Salmonella*, with the majority (49/61; 80%) from four migratory species that overwinter in Bangladesh: *Aythya farina* ($n = 10$), *A. nyroca* ($n = 12$), *Fulica atra* ($n = 12$), and *Mareca strepera* ($n = 15$; Supplementary Table S1). There was no apparent association between bird species and the presence of *Salmonella*. Low numbers of birds were affected by some serovars, and the most prevalent serovar affected the highest number of different bird species. *S.* Perth was isolated from eight bird species, *S.* Kentucky from four bird species, *S.* Infantis was isolated from three species, and *S.* Albany was isolated from two species (Supplementary Table S1). Three positive samples were obtained from birds for which only the common name was known.

Antimicrobial resistance and carriage of AMR genes

Antimicrobial resistance was assessed using phenotypic (broth microdilution) and genotypic (WGS) approaches, and there was excellent correspondence between resistances and the presence of AMR determinants (Supplementary Table S1). No isolates were resistant to azithromycin, colistin, cefotaxime, ceftazidime, or meropenem. Indeed, the *S.* Perth ($n = 38$) and *S.* Weltevreden ($n = 1$) isolates were fully susceptible to all 14 antimicrobials tested. No AMR genes were detected in *S.* Weltevreden, whereas the *S.* Perth isolates harbored the chromosomally encoded fosfomycin resistance gene *fosA7.7* (susceptibility towards this antimicrobial was not tested). The five *S.* Albany isolates harbored the SGI-1 associated genes $bla_{\text{CARB-2}}$, *floR*, *sul1*, *tet*(G), and *dfrA1*, and were correspondingly resistant to ampicillin, phenicols, sulfamethoxazole, tetracycline, and trimethoprim. Additionally, Albany isolates were resistant to the quinolone antimicrobials ciprofloxacin and nalidixic acid, and carried a mutation in the *gyrA* gene giving the D87N substitution in the amino acid sequence associated with quinolone resistance. The *S.* Brancaster isolate was also multidrug resistant, with non-wild type susceptibilities for ampicillin ($bla_{\text{TEM-176}}$), phenicols (*floR*), ciprofloxacin (*qnrS*), tetracycline (*tet*(A)), and trimethoprim (*dfrA14*); it also harbored the resistance gene *aph*(3′)-*Ia* (susceptibility towards this antimicrobial was not tested). The *S.* Kentucky isolates harbored $bla_{\text{TEM-1}}$, *aac*(3)-*Id*, *sul1*, and *tet*(A) and were resistant to ampicillin, gentamicin, sulfamethoxazole, and tetracycline. They were also resistant to ciprofloxacin and nalidixic acid and harbored mutations *gyrA* (S83F), *gyrA* (D87Y), and *parC* (S80I) associated with resistance to quinolones. Additionally, the streptomycin resistance gene *aadA7* was in all isolates and the kanamycin resistance gene *aph*(3′)-*Ia* was present in two isolates (susceptibility towards these two antimicrobials was not tested). All four *S.* Infantis isolates were resistant to sulfamethoxazole (*sul1*), trimethoprim (*dfrA14*), ciprofloxacin, and nalidixic acid (*gyrA* (D87Y)). Three *S.* Infantis isolates, all from 2020, were additionally resistant to ampicillin ($bla_{\text{TEM-1}}$), chloramphenicol (*cmlA5*), gentamicin [*ant*(2″)-*Ia*], and tetracycline [*tet*(A)].

TABLE 2 Prevalence of *Salmonella* by year.

Year	2018	2019	2020	Total
Field samples tested	109	133	211	453
Positive samples	36	19	6	61
Prevalence	33.0%	14.3%	2.8%	13.5%
Confidence interval (95% CI)	25.0–42.3%	9.3–21.3	1.2–6.2%	10.6–16.9%

Sequence type

Isolate serovar was closely associated with sequence type (ST): *S.* Albany (ST292), *S.* Brancaster (ST2133), *S.* Infantis (ST32), *S.* Kentucky (ST198), *S.* Perth (ST2245), and *S.* Weltevreden (ST365; Supplementary Table S1).

Given the high prevalence of *S.* Perth, its persistence across 3 years, detection at two Haors, and conserved ST, we further examined the genomic diversity of these isolates by comparison to a reference genome. The phylogenetic tree demonstrates that all *S.* Perth were closely related, except one isolate from a human in the UK (Figure 2). Indeed, in the core genome spanning 4,706,256 bp, only 2,282 were variable single-nucleotide polymorphisms (SNPs). The migratory bird isolates had a 0–7 SNPs difference from each other, compared to 15–19 SNPs difference with the reference isolate, which was obtained from a Bangladesh fish (Supplementary Table S2). There was also high sequence identity with a second isolate from a Bangladesh fish (12–18 SNPs difference) and with two UK human isolates (21–26 SNPs difference); there was considerably greater SNPs difference in comparison to the third UK human isolate (2,188–2,275 SNPs; Supplementary Table S2).

Another of the serovars further examined was *S.* Kentucky, which was identified from isolates from 2018 and detected in two Haors. We compared the genomic diversity of these isolates to the reference genome *S.* Kentucky strain 201001922 (accession number CP028357.1), alongside 117 *S.* Kentucky strains isolated from across

10.3389/fmicb.2023.1162657

TABLE 3 Distribution of different *Salmonella* serovars by year.

Serovar	2018	2019	2020	Total	Overall prevalence	Confidence interval (95% CI)
Perth	18	19	1	38	62.3%	49.7–73.4%
Kentucky	12	0	0	12	19.7%	11.5–31.5%
Albany	5	0	0	5	8.2%	3.8–18.2%
Infantis	1	0	3	4	6.6%	2.1–16.1%
Weltevreden	0	0	1	1	1.6%	<0.1–9.6%
Brancaster	0	0	1	1	1.6%	<0.1–9.6%

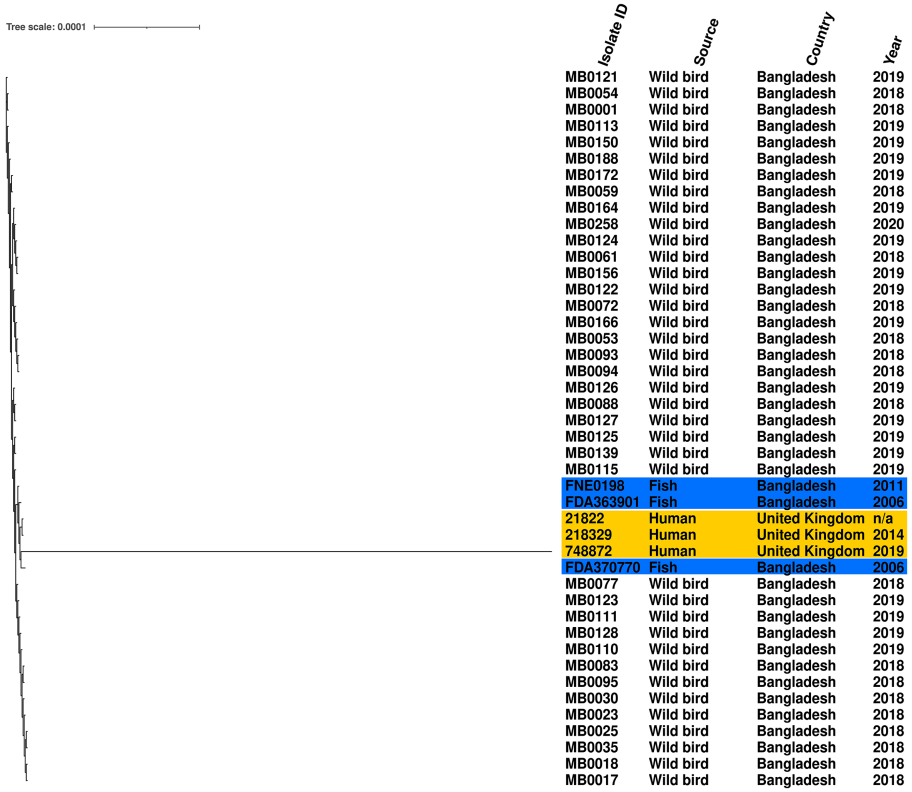

FIGURE 2
Maximum-likelihood phylogenetic tree generated from core genome single-nucleotide polymorphisms of *S.* Perth isolates. Blue highlight indicates published genomes from Bangladesh fish, and yellow highlight indicates published genomes from UK humans. Country, source, and year are given for each isolate. Reference was *S.* Perth strain FDA363901.

Asia. The migratory bird isolates clustered in a single sub-clade, which included isolates from humans (India and South Korea), poultry (India), or environmental samples (China; Figure 3). The two previously published *S.* Kentucky genomes from Bangladesh did not reside in this sub-clade (Figure 3). The core genome spanned 4,858,671 bp of which 292 were SNPs (Supplementary Table S3). The migratory bird isolates from this study had 4–46 SNPs difference from each other, compared to 222–262 SNPs difference with the reference isolate. The migratory bird isolates from this study had 125–169 SNPs differences from the two *S.* Kentucky strains previously isolated from Bangladesh, one from poultry and one from a human isolate (Supplementary Table S3).

Virulence and heavy metal tolerance genes

A total of 115 virulence factors were identified in the 61 *Salmonella* isolates (Supplementary Table S4), and the majority were shared by most serovars, including fimbriae (*fim* genes), adhesins (*misL*), invasins (*invA*), effectors (*avrA*), secretion systems (*prgJ*), and a macrophage inducible gene (*mig-14*). We also investigated the presence of heavy metal resistance genes (Supplementary Table S4). Heavy metal resistance genes from the *pco* (copper) and *sil* (copper/silver) operons were present in the *S.* Brancaster isolate. The *S.* Kentucky and Infantis isolates carried genes from the *mer* (mercury) operon; Infantis isolates additionally harbored *arsR* (arsenic resistance).

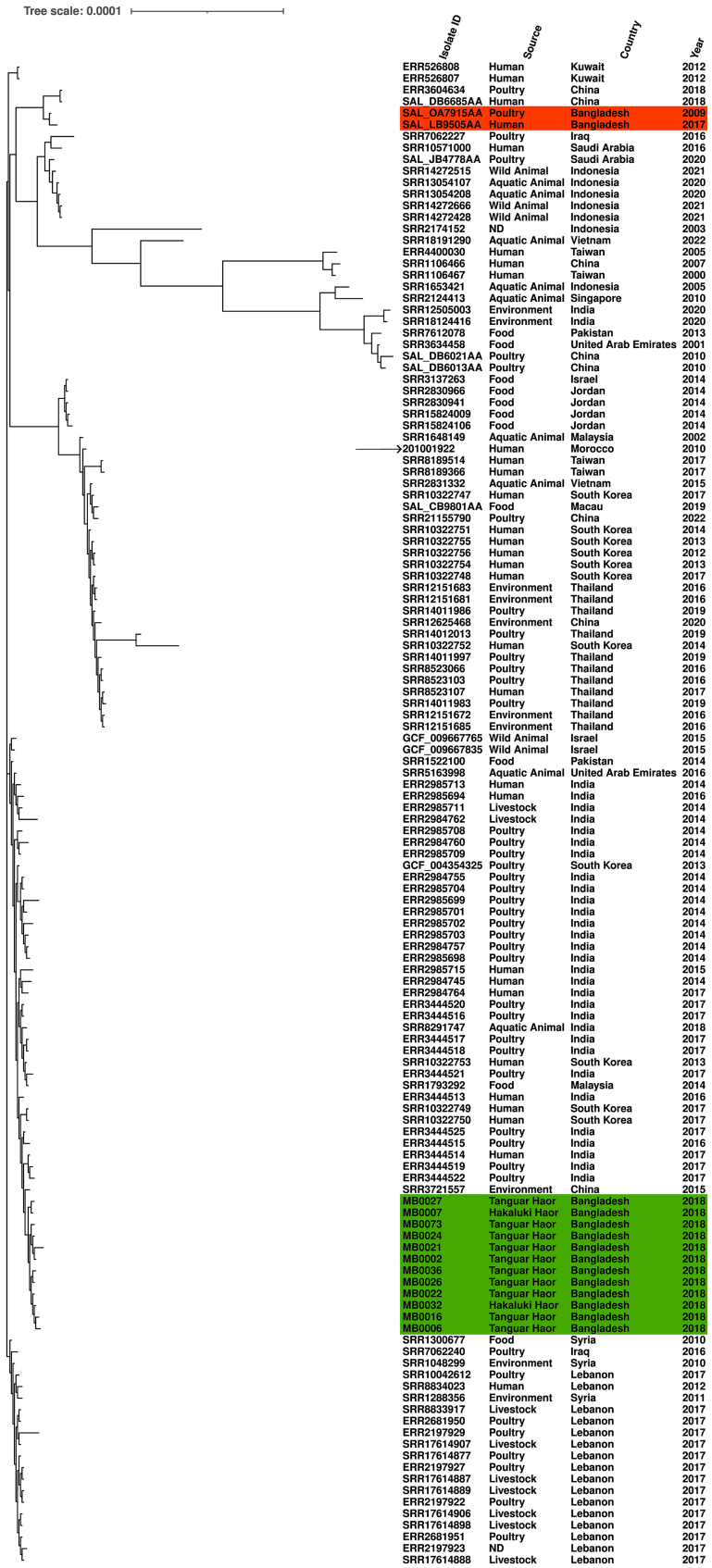

FIGURE 3
Maximum-likelihood phylogenetic tree generated from core genome single-nucleotide polymorphisms of *S.* Kentucky isolates. Migratory bird isolates indicate in green and previously published genomes from Bangladesh are shown in orange. Country, source, and year are given for each isolate. Reference was *S.* Kentucky strain 201001922 (indicated by arrow).

Discussion

In this study, the overall prevalence of *Salmonella* in migratory birds in Bangladesh was 13.5%. This is similar to the prevalence of 21.2% reported in Bangladesh by a previous study (Saiful Islam et al., 2021); however, this earlier study was limited by a low sample size ($n = 66$) and tested freshly deposited fecal material without correlation to bird species. Another study of Bangladesh wild birds reported a *Salmonella* prevalence of 65% in *Corvus splendens* (house crow) and 67% in *Gracupica contra* (Asian pied starling), although neither bird is migratory (Faruq et al., 2016). We observed a reduction in *Salmonella* prevalence between 2018 and 2020, from 33.0 to 2.8%, despite increased sampling efforts over this period. This may reflect fluctuations in prevalence and changes in the *Salmonella* population resident in migratory birds over time. Changes in *Salmonella* prevalence over time in wild bird populations are currently poorly defined. Studies in other countries have sampled across multiple years but reported *Salmonella* prevalence in the aggregate, such as South Korea (0.93%), Singapore (0.99%), Uganda (4.3%), and Poland (6.4%; Krawiec et al., 2015; Afema and Sischo, 2016; Aung et al., 2019; Wei et al., 2020).

We identified six different *Salmonella* serovars in the birds, of which *S.* Albany, *S.* Kentucky, and *S.* Infantis have been described in wild birds previously (Beleza et al., 2020). Unexpectantly, the most common serovar was *S.* Perth. This serovar has been rarely reported, with only six genomes available in EnteroBase (accessed 21 June 2022; Zhou et al., 2020), including three UK human isolates and three isolates from Bangladesh freshwater fish. The high sequence identity observed within our wild bird isolates (0–7 SNPs in the core genome) meets the proposed relatedness threshold criteria (Schurch et al., 2018) to indicate that these isolates are likely to be representatives of a single clone, which had therefore been isolated from multiple birds in different years and at different Haors. Indeed, this was the only serovar detected every year, and may indicate a potential for a persistent environmental presence by this clone. The isolates also had high sequence identity to two *S.* Perth isolates from Bangladesh fish and two UK human isolates; however, the number of SNPs difference marginally exceeded the relatedness threshold to be classified as a clone. Nevertheless, the potential for an association of this rare serovar between migratory birds and freshwater fish in Bangladesh is noteworthy. Indeed, many of the bird species from which *S.* Perth was isolated are omnivorous and include small fish in their diet (Birdlife, 2023). Furthermore, *Salmonella* have been detected in rivers and surface water in Bangladesh, although serovars were not reported (Faridullah et al., 2022; Yasmin et al., 2023). This may suggest an ecological aspect in which fish and piscivorous birds share the same *Salmonella*; however, investigation of fish and other environmental reservoirs such as water and soil was beyond the scope of this study. This possibility of an ecological aspect may warrant further investigation in future as it could indicate a source and potential route for the infection of humans through the consumption of food. Importantly, the *S.* Perth isolates from wild birds harbored no acquired AMR genes.

In contrast, 12 *S.* Kentucky isolates were multidrug-resistant and harbored genes conferring resistance to antimicrobials, disinfectants, and heavy metals; these genes have previously been reported to reside on SGI-1 in this serovar (Hawkey et al., 2019). All isolates were ST198, a globally distributed multidrug-resistant lineage reported in humans and animals, constituting an ongoing risk to public health worldwide (Hawkey et al., 2019; Mahindroo et al., 2019; Lei et al., 2020). We believe this is the first report of the *S.* Kentucky ST198 lineage in migratory birds, although (Afema and Sischo, 2016) described multidrug-resistant *S.* Kentucky isolates from wild birds in Uganda but did not report the ST. The isolates were not closely related to the two published Bangladesh genomes from humans and poultry but did reside in a sub-clade that included isolates from China, India, and South Korea. Migratory bird isolates MB0002 and MB0024 met the proposed relatedness threshold criteria of <=5 SNPs in the core genome to be considered clones; both samples were collected at Tanguar Haor, MB0002 in January 2018 and MB0024 in December 2018. Poultry and poultry products are considered a major route for infection of people by this lineage, and *S.* Kentucky has been reported in poultry in Bangladesh (Barua et al., 2012, 2013; Hawkey et al., 2019). ST198 has also been reported in poultry from India (Mahindroo et al., 2019) and China (Lei et al., 2020), both countries on migratory flyways which pass through Bangladesh.

We detected *S.* Infantis ST32 in 2018 and 2020 and noted different resistance phenotypes and AMR gene carriage between the 2 years. *S.* Infantis is of global public health importance as it frequently causes foodborne illness in people and is a commonly isolated serovar from poultry (Koutsoumanis et al., 2019). Importantly, these isolates did not carry the extended-spectrum β-lactamase gene $bla_{\text{CTX-M-65}}$, associated with pESI-like plasmids (Alba et al., 2020), which has been detected in *S.* Infantis in many countries, including in wild owls from Chile (Fuentes-Castillo et al., 2019).

S. Albany has been emerging as a commonly isolated multidrug-resistant serovar from poultry, slaughterhouses, and human cases in several Asian countries (Hong et al., 2021; Wei et al., 2021). Here we describe multidrug-resistant *S.* Albany in Bangladesh migratory birds, harboring the same resistance phenotype and AMR determinants as reported in these countries, including the SGI-F associated genes $bla_{\text{CARB-2}}$, *floR*, *sul1*, *tet*(G), and *dfrA1*. The emergence of *S.* Albany in poultry in South Korea has been hypothesized to have resulted from international travel or imported meat (Wei et al., 2021), but migratory birds may have a role in the dissemination of this serovar to poultry and between countries as Bangladesh and South Korea both lie on the East Asian–Australasian Flyway.

Similarly, *S.* Weltevreden has emerged as an important foodborne pathogen causing gastroenteritis, particularly in South-East Asian countries, and has been found in Bangladesh poultry (Barua et al., 2013; Makendi et al., 2016). Antimicrobial susceptibility and the carriage of AMR genes are generally rare in this serovar (Aarestrup et al., 2003), and the single isolate we obtained from migratory birds harbored no AMR genes and was fully susceptible to the 14 antimicrobials tested.

A single *S.* Brancaster isolate was obtained from migratory birds. This serovar has been associated with human infection in Nigeria (Ifeanyi et al., 2014) and Senegal (Cardinale et al., 2005), and detected in poultry meat in Singapore, Malaysia, and Taiwan (Chin et al., 2017; Zwe et al., 2020; Chang et al., 2022). Multidrug resistance is common and associated with a core set of AMR genes, which were present in the wild bird isolates, comprising *floR* (phenicol), *qnrS* (quinolone),

bla$_{TEM-176}$ (ampicillin), *tet*(A; tetracycline), *dfrA14* (trimethoprim), and *aph*(*3′*)-*Ia* (aminoglycosides; Chin et al., 2017, Zwe et al., 2020).

Noteworthily, we did not detect *S.* Typhimurium or *S.* Enteritidis, major serovars associated with human infection. *S.* Gallinarum and *S.* Gallinarum biovar Pullorum, which cause fowl typhoid and Pullorum disease were outside the scope of this study and not detected, as MRSV is unsuitable for the detection of non-motile *Salmonella* bacteria (Poppe et al., 2004). These serovars have been described in Bangladesh poultry (Barua et al., 2013; Parvej et al., 2016; Siddiky et al., 2021) and wild birds in other countries (Beleza et al., 2020).

In conclusion, we have shown that a diversity of *Salmonella* serovars can be recovered from migratory birds in Bangladesh that can pose a threat to public health. *Salmonella* was detected every year for 3 years in a proportion of migratory birds. Many serovars were resistant to ampicillin, chloramphenicol, and trimethoprim/sulfamethoxazole and were multidrug resistant, which has been associated with more serious diseases in people (Parisi et al., 2018). Four of six serovars were resistant to the fluoroquinolone ciprofloxacin, meeting WHO criteria for classification as a priority pathogen (Tacconelli et al., 2018). However, all isolates in this study were susceptible to the critically important antimicrobials azithromycin, cefotaxime, ceftazidime, and meropenem (Anonymous, 2019). Exposure to *Salmonella* via wild birds can present a route to human infection, which may be an important consideration for those living and working in the Haors. Infected wild birds can present a risk of *Salmonella* infection to food-producing animals through interaction with the livestock and farm premises. Similarly, interaction with livestock and farm premises provides opportunities for exposure of wild birds to *Salmonella*. Inadequate farm biosecurity and inappropriate antimicrobial use, as has been reported for poultry farms in Bangladesh (Imam et al., 2021; Siddiky et al., 2022), heightens the risk of multidrug-resistant *Salmonella* becoming introduced and established on farms. A further concern is that the long migratory routes of the birds present a risk for the dissemination of *Salmonella* between countries, as has been observed for highly pathogenic avian influenza (Gilbert et al., 2010; Bi et al., 2015). Migratory birds could, therefore, play a role in the spreading of *Salmonella* serovars that subsequently emerge at high prevalence in livestock. The risk wild birds can present to livestock and people, therefore, requires ongoing assessment and further definition, such as greater insight into the persistence of *Salmonella* infection in wild birds and the routes by which they are exposed. The implementation of good farm biosecurity will help reduce this risk by minimizing opportunities for contact between wild birds and livestock such as poultry.

Data availability statement

The whole-genome sequences were deposited in the National Center for Biotechnology Information (NCBI) National Library of Medicine under BioProject accession number PRJNA933150.

Ethics statement

The animal study was reviewed and approved by Ethical Committee of the Animal Health Research Division at the Bangladesh Livestock Research Institute, Dhaka, Bangladesh (ARAC: 10/1/2018:01).

Author contributions

MAS, RB, RC, and JFL: conceptualization. TC, RB, MSSarker, MSH, MSSagor, MAM, ASMAU, and MRK: methodology and investigation. MAS and RC: supervision. TC, MSSarker, RC, JFL, and MAS: data curation and formal analysis. MAS and RC: resources. RC, MAS, and TC: writing-original draft preparation. MAS, RB, RC, JFL, TC, MSSarker, MSH, MAM, ASMAU, and MRK: writing–review and editing. All authors contributed to the article and approved the submitted version.

Funding

The study was conducted with the financial assistance of the Ministry of Fisheries and Livestock, Bangladesh and US CDC (Grant Number: 5 NU2GGH002077). RC and TC were supported by the UK FAO Reference Centre for Antimicrobial Resistance (which receives funding from the Department for Environment, Food & Rural Affairs and UK aid funding from the Department of Health and Social Care's Fleming Fund).

Acknowledgments

The authors are grateful to the members of the IUCN, Bangladesh for their kind help during field sampling. The authors are grateful to Chris Teale for the critical reading of the manuscript.

Conflict of interest

The authors declare that the research was conducted in the absence of any commercial or financial relationships that could be construed as a potential conflict of interest.

Publisher's note

Supplementary material

The Supplementary material for this article can be found online at: https://www.frontiersin.org/articles/10.3389/fmicb.2023.1162657/full#supplementary-material

References

Aarestrup, F. M., Lertworapreecha, M., Evans, M. C., Bangtrakulnonth, A., Chalermchaikit, T., Hendriksen, R. S., et al. (2003). Antimicrobial susceptibility and occurrence of resistance genes among salmonella Enterica Serovar Weltevreden from different countries. *J. Antimicrob. Chemother.* 52, 715–718. doi: 10.1093/jac/dkg426

Acheson, D., and Hohmann, E. L. (2001). Nontyphoidal Salmonellosis. *Clin. Infect. Dis.* 32, 263–269. doi: 10.1086/318457

Afema, J. A., and Sischo, W. M. (2016). Salmonella in wild birds utilizing protected and human impacted habitats, Uganda. *EcoHealth* 13, 558–569. doi: 10.1007/s10393-016-1149-1

Alba, P., Leekitcharoenphon, P., Carfora, V., Amoruso, R., Cordaro, G., di Matteo, P., et al. (2020). Molecular epidemiology of salmonella Infantis in Europe: insights into the success of the bacterial host and its parasitic Pesi-like Megaplasmid. *Microb. Genom.* 6:e000365. doi: 10.1099/mgen.0.000365

Anonymous, (2019). Critically important antimicrobials for human medicine, 6th revision. Licence: Cc By-Nc-Sa 3.0 Igo. World Health Organization.

Aung, K. T., Chen, H. J., Chau, M. L., Yap, G., Lim, X. F., Humaidi, M., et al. (2019). Salmonella in retail food and wild birds in Singapore—prevalence, antimicrobial resistance, and sequence types. *Int. J. Environ. Res. Public Health* 16:4235. doi: 10.3390/ijerph16214235

Bankevich, A., Nurk, S., Antipov, D., Gurevich, A. A., Dvorkin, M., Kulikov, A. S., et al. (2012). Spades: a new genome assembly algorithm and its applications to single-cell sequencing. *J. Comput. Biol.* 19, 455–477. doi: 10.1089/cmb.2012.0021

Barua, H., Biswas, P. K., Olsen, K. E., and Christensen, J. P. (2012). Prevalence and characterization of motile salmonella in commercial layer poultry farms in Bangladesh. *PLoS One* 7:E35914. doi: 10.1371/journal.pone.0035914

Barua, H., Biswas, P. K., Olsen, K. E., Shil, S. K., and Christensen, J. P. (2013). Molecular characterization of motile Serovars of salmonella Enterica from breeder and commercial broiler poultry farms in Bangladesh. *PLoS One* 8:E57811. doi: 10.1371/journal.pone.0057811

Beleza, A. J. F., Maciel, W. C., Lopes, E. S., De Albuquerque, A. H., Carreira, A. S., Nogueira, C. H. G., et al. (2020). Evidence of the role of free-living birds as disseminators of salmonella Spp. *Arq. Inst. Biol.* 87, 1–14. doi: 10.1590/1808-1657000462019

Bi, Y., Zhang, Z., Liu, W., Yin, Y., Hong, J., Li, X., et al. (2015). Highly pathogenic avian influenza a(H5n1) virus struck migratory birds in China in 2015. *Sci. Rep.* 5:12986. doi: 10.1038/srep12986

Birdlife, I. (2023). *Iucn red list for birds*. [online]. Available from: Http://Www.Birdlife.Org/ (Accessed, 03/02/2023).

Cardinale, E., Perrier Gros-Claude, J. D., Rivoal, K., Rose, V., Tall, F., Mead, G. C., et al. (2005). Epidemiological analysis of salmonella Enterica Ssp. Enterica Serovars Hadar, Brancaster and Enteritidis from humans and broiler chickens in Senegal using pulsed-field gel electrophoresis and antibiotic susceptibility. *J. Appl. Microbiol.* 99, 968–977. doi: 10.1111/j.1365-2672.2005.02618.x

Chang, Y. J., Chen, C. L., Yang, H. P., and Chiu, C. H. (2022). Prevalence, serotypes, and antimicrobial resistance patterns of non-typhoid salmonella in food in northern Taiwan. *Pathogens* 11:705. doi: 10.3390/pathogens11060705

Chen, L., Zheng, D., Liu, B., Yang, J., and Jin, Q. (2016). VFDB 2016: hierarchical and refined dataset for big data analysis—10 years on. *Nucleic Acids Res.* 44, D694–D697. doi: 10.1093/nar/gkv1239

Chin, P. S., Yu, C. Y., Ang, G. Y., Yin, W. F., and Chan, K. G. (2017). Draft genome sequence of multidrug-resistant salmonella Enterica Serovar Brancaster strain Ps01 isolated from chicken meat, Malaysia. *J. Glob. Antimicrob. Resist.* 9, 41–42. doi: 10.1016/j.jgar.2016.12.017

Crump, J. A., Sjolund-Karlsson, M., Gordon, M. A., and Parry, C. M. (2015). Epidemiology, clinical presentation, laboratory diagnosis, antimicrobial resistance, and antimicrobial management of invasive salmonella infections. *Clin. Microbiol. Rev.* 28, 901–937. doi: 10.1128/CMR.00002-15

De Lucia, A., Rabie, A., Smith, R. P., Davies, R., Ostanello, F., Ajayi, D., et al. (2018). Role of wild birds and environmental contamination in the epidemiology of salmonella infection in an outdoor pig farm. *Vet. Microbiol.* 227, 148–154. doi: 10.1016/j.vetmic.2018.11.003

ECDC (2016). Eu protocol for harmonised monitoring of antimicrobial resistance in human salmonella and campylobacter isolates. European Centre For Disease Prevention And Control.

Eucast. (2020). Data from the Eucast mic distribution website, last Accessed 14/09/2020. Available from: http://www.eucast.org [Online]. European Committee On Antimicrobial Susceptibility Testing.

Faridullah, M., Rani, B., Islam, M. R., and Rana, M. M. (2022). Salmonella and Escherichia Coli contamination in wild catfish and Rivers at northern part of Bangladesh. *Asian J. Med. Biol. Res.* 8, 9–15. doi: 10.3329/ajmbr.v8i1.58930

Faridullah, M., Roy, V. C., and Lithi, U. J. (2016). Prevalence of salmonella and Escherichia Coli contamination in shrimp (Penaeus Monodon) farms, depots and processing plants in different areas of Bangladesh. *Asian J. Med. Biol. Res.* 2, 171–176. doi: 10.3329/ajmbr.v2i2.29007

Faruq, A. A., Hassan, M. M., Uddin, M. M., Rahman, M. L., Rakib, T. M., Alam, M., et al. (2016). Prevalence and multidrug resistance pattern of salmonella isolated from resident wild birds of Bangladesh. *Int. J. One Health* 2, 35–41. doi: 10.14202/IJOH.2016.35-41

Feldgarden, M., Brover, V., Haft, D. H., Prasad, A. B., Slotta, D. J., Tolstoy, I., et al. (2019). Validating the Amrfinder tool and resistance gene database by using antimicrobial resistance genotype-phenotype correlations in a collection of isolates. *Antimicrob. Agents Chemother.* 63:e00483–19. doi: 10.1128/AAC.00483-19

Foley, S. L., Lynne, A. M., and Nayak, R. (2008). Salmonella challenges: Prevalence in swine and poultry and potential pathogenicity of such isolates. *J. Anim. Sci.* 86, 149–162. doi: 10.2527/jas.2007-0464

Fuentes-Castillo, D., Farfán-López, M., Esposito, F., Moura, Q., Fernandes, M. R., Lopes, R., et al. (2019). Wild owls colonized by international clones of extended-Spectrum B-lactamase (Ctx-M)-producing Escherichia Coli and salmonella Infantis in the southern cone of America. *Sci. Total Environ.* 674, 554–562. doi: 10.1016/j.scitotenv.2019.04.149

Gilbert, M., Newman, S. H., Takekawa, J. Y., Loth, L., Biradar, C., Prosser, D. J., et al. (2010). Flying over an infected landscape: distribution of highly pathogenic avian influenza H5n1 risk in South Asia and satellite tracking of wild waterfowl. *EcoHealth* 7, 448–458. doi: 10.1007/s10393-010-0672-8

Grimont, P. A. D., and Weill, F.-X. (2007). *Antigenic Formulae of the Salmonella Serovars. 9th Ed*. Institut Pasteur, Paris, France: Who Collaborating Centre For Reference And Research On Salmonella.

Hassan, M. M., Islam, A., Hasan, R. B., Rahman, M. K., Webby, R. J., Hoque, M. A., et al. (2020). Prevalence and distribution of avian influenza viruses in domestic ducks at the waterfowl-chicken Interface in wetlands. *Pathogens* 9:953. doi: 10.3390/pathogens9110953

Havelaar, A. H., Kirk, M. D., Torgerson, P. R., Gibb, H. J., Hald, T., Lake, R. J., et al. (2015). World Health Organization global estimates and regional comparisons of the burden of foodborne disease in 2010. *PLoS Med.* 12:E1001923. doi: 10.1371/journal.pmed.1001923

Hawkey, J., Le Hello, S., Doublet, B., Granier, S. A., Hendriksen, R. S., Fricke, W. F., et al. (2019). Global Phylogenomics of multidrug-resistant salmonella Enterica serotype Kentucky St198. *Microb. Genom.* 5:e000269. doi: 10.1099%2Fmgen.0.000269

Hong, Y.-P., Chen, Y.-T., Wang, Y.-W., Chen, B.-H., Teng, R.-H., Chen, Y.-S., et al. (2021). Integrative and conjugative element-mediated azithromycin resistance in multidrug-resistant salmonella Enterica Serovar Albany. *Antimicrob. Agents Chemother.* 65, E02634–E02620.

Hossain, M. S., Khaleque, H. N., Mazumder, F., and Mahbub, K. R. (2013). Prevalence of multidrug resistant salmonella in shrimp of Dhaka City. *Microbiol. J.* 3, 21–28. doi: 10.3923/mj.2013.21.28

Ifeanyi, C. I., Bassey, B. E., Ikeneche, N. F., and Al-Gallas, N. (2014). Molecular characterization and antibiotic resistance of salmonella in children with acute gastroenteritis in Abuja, Nigeria. *J. Infect. Dev. Ctries.* 8, 712–719. doi: 10.3855/jidc.4185

Imam, T., Gibson, J. S., Gupta, S. D., Hoque, M. A., Fournié, G., and Henning, J. (2021). Association between farm biosecurity practices and antimicrobial usage on commercial chicken farms in Chattogram, Bangladesh. *Preven. Vet. Med.* 196:105500. doi: 10.1016/j.prevetmed.2021.105500

Islam, M. S., Nayeem, M. M. H., Sobur, M. A., Ievy, S., Islam, M. A., Rahman, S., et al. (2021). Virulence determinants and multidrug resistance of Escherichia Coli isolated from migratory birds. *Antibiotics*:10:190. doi: 10.3390/antibiotics10020190

Islam, M. S., Sobur, M. A., Rahman, S., Ballah, F. M., Ievy, S., Siddique, M. P., et al. (2022). Detection of Blatem, Blactx-M, Blacmy, and Blashv genes among extended-Spectrum Beta-lactamase-producing Escherichia Coli isolated from migratory birds travelling to Bangladesh. *Microb. Ecol.* 83, 942–950. doi: 10.1007/s00248-021-01803-x

Jolley, K. A., Bray, J. E., and Maiden, M. C. J. (2018). Open-access bacterial population genomics: BIGSdb software, the PubMLST.Org website and their applications. *Wellcome Open Res.* 3:124. doi: 10.12688/wellcomeopenres.14826.1

Khan, S. A., Imtiaz, M. A., Sayeed, M. A., Shaikat, A. H., and Hassan, M. M. (2020). Antimicrobial resistance pattern in domestic animal - wildlife - environmental niche via the food chain to humans with a Bangladesh perspective; a systematic review. *Vet. Res.* 16:302. doi: 10.1186/s12917-020-02519-9

Koutsoumanis, K., Allende, A., Alvarez-Ordonez, A., Bolton, D., Bover-Cid, S., Chemaly, M., et al. (2019). Salmonella control in poultry flocks and its public health impact. *EFSA J.* 17:e05596. doi: 10.2903/j.efsa.2019.5596

Kozlov, A. M., Darriba, D., Flouri, T., Morel, B., and Stamatakis, A. (2019). Raxml-Ng: a fast, scalable and user-friendly tool for maximum likelihood phylogenetic inference. *Bioinformatics* 35, 4453–4455. doi: 10.1093/bioinformatics/btz305

Krawiec, M., Kuczkowski, M., Kruszewicz, A. G., and Wieliczko, A. (2015). Prevalence and genetic characteristics of salmonella in free-living birds in Poland. *BMC Vet. Res.* 11:15. doi: 10.1186/s12917-015-0332-x

Lei, C.-W., Zhang, Y., Wang, X.-C., Gao, Y.-F., and Wang, H.-N. (2020). Draft genome sequence of a multidrug-resistant salmonella Enterica serotype Kentucky St198 with chromosomal integration of Blactx-M-14b isolated from a poultry slaughterhouse in China. *J. Glob. Antimicrob. Resist.* 20, 145–146. doi: 10.1016/j.jgar.2019.12.006

Letunic, I., and Bork, P. (2016). Interactive tree of life (Itol) V3: an online tool for the display and annotation of phylogenetic and other trees. *Nucleic Acids Res.* 44, W242–W245. doi: 10.1093/nar/gkw290

Lin, Y., Dong, X., Sun, R., Wu, J., Tian, L., Rao, D., et al. (2020). Migratory birds-one major source of environmental antibiotic resistance around Qinghai Lake, China. *Sci. Total Environ.* 739:139758. doi: 10.1016/j.scitotenv.2020.139758

Mahindroo, J., Thanh, D. P., Nguyen, T. N. T., Mohan, B., Thakur, S., Baker, S., et al. (2019). Endemic fluoroquinolone-resistant Salmonellaenterica Serovar Kentucky St198 in northern India. *Microb. Genom.* 5:e000275. doi: 10.1099/mgen.0.000275

Majowicz, S. E., Musto, J., Scallan, E., Angulo, F. J., Kirk, M., O'Brien, S. J., et al. (2010). The global burden of Nontyphoidal salmonella gastroenteritis. *Clin. Infect. Dis.* 50, 882–889. doi: 10.1086/650733

Makendi, C., Page, A. J., Wren, B. W., le Thi Phuong, T., Clare, S., Hale, C., et al. (2016). A phylogenetic and phenotypic analysis of salmonella Enterica Serovar Weltevreden, an emerging agent of diarrheal disease in tropical regions. *PLoS Negl. Trop. Dis.* 10:E0004446. doi: 10.1371/journal.pntd.0004446

Parisi, A., Crump, J. A., Glass, K., Howden, B. P., Furuya-Kanamori, L., Vilkins, S., et al. (2018). Health outcomes from multidrug-resistant salmonella infections in high-income countries: a systematic review and meta-analysis. *Foodborne Pathog. Dis.* 15, 428–436. doi: 10.1089/fpd.2017.2403

Parvej, M. S., Nazir, K. H., Rahman, M. B., Jahan, M., Khan, M. F., and Rahman, M. (2016). Prevalence and characterization of multi-drug resistant salmonella Enterica Serovar Gallinarum Biovar Pullorum and Gallinarum from chicken. *Vet World* 9, 65–70. doi: 10.14202/vetworld.2016.65-70

Poppe, C., Mann, E., Shaw, S., Warburton, D., and Sewell, A. (2004). Procedure for the isolation of salmonella species by the modified semisolid Rappaport Vassiliadis (Msrv) method. Health Canada, Health Products Food Branch, Ottawa, ON, Canada.

Saiful Islam, M., Paul, A., Talukder, M., Roy, K., Abdus Sobur, M., Ievy, S., et al. (2021). Migratory birds travelling to Bangladesh are potential carriers of multi-drug resistant enterococcus Spp., salmonella Spp., and vibrio Spp. *Saudi J. Biol. Sci.* 28, 5963–5970. doi: 10.1016/j.sjbs.2021.06.053

Schurch, A. C., Arredondo-Alonso, S., Willems, R. J. L., and Goering, R. V. (2018). Whole genome sequencing options for bacterial strain typing and epidemiologic analysis based on single nucleotide polymorphism versus gene-by-gene-based approaches. *Clin. Microbiol. Infect.* 24, 350–354. doi: 10.1016/j.cmi.2017.12.016

Schwarz, S., Silley, P., Simjee, S., Woodford, N., Van Duijkeren, E., Johnson, A. P., et al. (2010). Assessing the antimicrobial susceptibility of bacteria obtained from animals. *Vet. Microbiol.* 141, 1–4. doi: 10.1016/j.vetmic.2009.12.013

Seemann, T. (2014). Prokka: rapid prokaryotic genome annotation. *Bioinformatics* 30, 2068–2069. doi: 10.1093/bioinformatics/btu153

Shipp, C. R., and Rowe, B. (1980). A mechanised microtechnique for salmonella serotyping. *J. Clin. Pathol.* 33, 595–597. doi: 10.1136/jcp.33.6.595

Siddiky, N. A., Sarker, M. S., Khan, M. S. R., Begum, R., Kabir, M. E., Karim, M. R., et al. (2021). Virulence and antimicrobial resistance profiles of salmonella enterica Serovars isolated from chicken at wet Markets in Dhaka, Bangladesh. *Microorganisms* 9:952. doi: 10.3390/microorganisms9050952

Siddiky, N. A., Sarker, S., Khan, S. R., Rahman, T., Kafi, A., and Samad, M. A. (2022). Virulence and antimicrobial resistance profile of non-typhoidal salmonella enterica serovars recovered from poultry processing environments at wet markets in Dhaka, Bangladesh. *PLoS One* 17:E0254465. doi: 10.1371/journal.pone.0254465

Tacconelli, E., Carrara, E., Savoldi, A., Harbarth, S., Mendelson, M., Monnet, D. L., et al. (2018). Discovery, research, and development of new antibiotics: the who priority list of antibiotic-resistant bacteria and tuberculosis. *Lancet Infect. Dis.* 18, 318–327. doi: 10.1016/s1473-3099(17)30753-3

Tizard, I. (2004). Salmonellosis in wild birds. *Sem. Avian Exotic Pet Med.* 13, 50–66. doi: 10.1053/j.saep.2004.01.008

Wei, B., Shang, K., Cha, S.-Y., Zhang, J.-F., Jang, H.-K., and Kang, M. (2021). Clonal dissemination of salmonella Enterica Serovar Albany with concurrent resistance to ampicillin, chloramphenicol, streptomycin, Sulfisoxazole, tetracycline, and Nalidixic acid in broiler chicken in Korea. *Poult. Sci.* 100:101141. doi: 10.1016/j.psj.2021.101141

Wei, B., Shang, K., Cha, S.-Y., Zhang, J.-F., Kang, M., and Jang, H.-K. (2020). Prevalence and potential risk of salmonella Enterica in migratory birds from South Korea. *Vet. Microbiol.* 249:108829. doi: 10.1016/j.vetmic.2020.108829

Yasmin, F., Hossain, T., Shahrukh, S., Hossain, M. E., and Sultana, G. N. N. (2023). Evaluation of seasonal changes in physicochemical and bacteriological parameters of Gomti River in Bangladesh. *Environ. Sust. Indicators* 17:100224. doi: 10.1016/j.indic.2023.100224

Zhou, Z., Alikhan, N. F., Mohamed, K., Fan, Y.the Agama Study Group, and Achtman, M. (2020). The Enterobase User's guide, with case studies on salmonella transmissions, Yersinia Pestis phylogeny, and Escherichia Core genomic diversity. *Genome Res.* 30, 138–152. doi: 10.1101/gr.251678.119

Zwe, Y. H., Chin, S. F., Kohli, G. S., Aung, K. T., Yang, L., and Yuk, H. G. (2020). Whole genome sequencing (Wgs) fails to detect antimicrobial resistance (Amr) from Heteroresistant subpopulation of salmonella Enterica. *Food Microbiol.* 91:103530. doi: 10.1016/j.fm.2020.103530

frontiers | Frontiers in Microbiology

TYPE Original Research
PUBLISHED 16 May 2023
DOI 10.3389/fmicb.2023.1153740

OPEN ACCESS

EDITED BY
Liang-xing Fang,
South China Agricultural University, China

REVIEWED BY
Jiyun Li,
Hunan Agricultural University, China
Tao He,
Jiangsu Academy of Agricultural Sciences, China
Jing Wang,
Yangzhou University, China

*CORRESPONDENCE
Lunjiang Zhou
✉ lunjiang@163.com

†These authors share first authorship

RECEIVED 30 January 2023
ACCEPTED 18 April 2023
PUBLISHED 16 May 2023

CITATION
Che Y, Wu R, Li H, Wang L, Wu X, Chen Q, Chen R and Zhou L (2023) Characterization of two novel colistin resistance gene *mcr-1* variants originated from *Moraxella* spp. *Front. Microbiol.* 14:1153740. doi: 10.3389/fmicb.2023.1153740

Characterization of two novel colistin resistance gene *mcr-1* variants originated from *Moraxella* spp.

Yongliang Che[1,2†], Renjie Wu[1,2†], Hongjie Li[1], Longbai Wang[1,2], Xuemin Wu[1,2], Qiuyong Chen[1,2], Rujing Chen[1,2] and Lunjiang Zhou[1,2*]

[1]Institute of Animal Husbandry and Veterinary Medicine, Fujian Academy of Agricultural Sciences, Fuzhou, China, [2]Fujian Animal Diseases Control Technology Development Center, Fuzhou, China

This study aimed to characterize two novel *mcr-1* variants, *mcr-1.35* and *mcr-1.36*, which originated from *Moraxella* spp. that were isolated from diseased pigs in China. The *Moraxella* spp. carrying novel *mcr-1* variants were subjected to whole-genome sequencing (WGS) and phylogenetic analysis based on the 16S rRNA gene. The *mcr-1* variants *mcr-1.35* and *mcr-1.36* were characterized using phylogenetic analysis, a comparison of genetic environments, and protein structure prediction. The WGS indicated that two novel *mcr-1* variants were located in the chromosomes of three *Moraxella* spp. with a genetic environment of *mcr-1-pap2*. In addition to the novel colistin resistance genes *mcr-1.35* and *mcr-1.36*, the three *Moraxella* spp. contained other antimicrobial resistance genes, including *aac(3)-IId*, *tet*(O), *sul2*, *floR*, and bla_{ROB-3}. A functional cloning assay indicated that either the *mcr-1.35* or *mcr-1.36* gene could confer resistance to colistin in *Escherichia coli* DH5α and JM109. The nucleotide sequences of *mcr-1.35* and *mcr-1.36* presented 95.33 and 95.33% identities, respectively, to *mcr-1.1*. The phylogenetic analysis showed that *mcr-1.35* and *mcr-1.36* were derived from *Moraxella* spp. that belonged to subclades that were different from those of the *mcr-1* variants (*mcr-1.1* to *mcr-1.34* except *mcr-1.10*) originating from Enterobacteriaceae. The deduced amino acid sequences of MCR-1.35 (MCR-1.36) showed 96.67% (96.49%), 82.59% (82.04%), 84.07% (83.52%), 55.52% (55.17%), 59.75% (59.57%), and 61.88% (61.69%) identity to MCR-1.10, MCR-2.2, MCR-6.1, MCR-LIN, MCR-OSL, and MCR-POR, respectively, that originated from *Moraxella* sp. Notably, protein structure alignment showed only a few changes in amino acid residues between MCR-1.1 and MCR-1.35, as well as between MCR-1.1 and MCR-1.36. In conclusion, this study identified *Moraxella* spp. carrying two novel *mcr-1* variants, *mcr-1.35* and *mcr-1.36*, conferring resistance to colistin, which were isolated from pig farms in China. In addition, *mcr*-like variants were observed to be located in the chromosomes of some species of *Moraxella* isolated from pig samples.

KEYWORDS

pig, *Moraxella*, *mcr-1* variant, colistin, resistance, *mcr-1.35*, *mcr-1.36*

Introduction

The overuse and misuse of antibiotics have resulted in the emergence of multidrug-resistant bacteria that pose a serious threat to people worldwide (Boucher et al., 2009; Nordmann and Poirel, 2016; Pham Thanh et al., 2016). Colistin is one of the last-line treatment options against infection by multidrug-resistant and carbapenem-resistant Gram-negative bacteria (Liu et al., 2016). However, the emergence of mobile colistin-resistant *mcr-1* genes threatens the clinical efficacy of colistin. Epidemiological studies have found the *mcr*-like genes in *Enterobacteriaceae*, *Moraxellaceae*, *Vibrionaceae*, and *Pseudomonadaceae* (Ling et al., 2017; Caselli et al., 2018; Ling et al., 2020). To date, variants from *mcr-1.1* to *mcr-1.34* and from *mcr-2* to *mcr-10* have been discovered in over 40 countries across five continents (Wang et al., 2018; Ling et al., 2020; Wang et al., 2020). With the exception of *mcr-1.10*, which was found in *Moraxella* spp., variants from *mcr-1.1* to *mcr-1.34* have been identified in various Enterobacteriaceae of different origins (AbuOun et al., 2017; Ling et al., 2020; Wang et al., 2020). Other *mcr* genes, including *mcr-5*, *mcr-8*, *mcr-9*, and *mcr-10*, have also been described in Enterobacteriaceae. Moreover, *mcr-3* and *mcr-7* were reported in *Aeromonas* spp. (Ling et al., 2020), and *mcr-4* was found in *Pseudomonas* spp. (Ling et al., 2020). Additionally, a genetic and bioinformatics analysis suggested that *Moraxella* spp. could be considered a potential source of MCR-1/2-like determinants (Kieffer et al., 2017). Moreover, several variants of the *mcr*-like genes, including *mcr-1.10*, *mcr-2.2*, and *mcr-6.1*, were first found in *Moraxella* sp. (AbuOun et al., 2017).

In addition to colistin resistance genes, *Moraxella* spp. are also known to contain ampicillin, penicillin, quinolone, macrolide, and tetracycline resistance genes, among others (Flamm et al., 2012; AbuOun et al., 2017; Krol-Turminska et al., 2020; Raveendran et al., 2020; Zhang et al., 2022). Bacteria of the genus *Moraxella* are aerobic, rod-shaped, opportunistic Gram-negative pathogens (Vela et al., 2010; Embers et al., 2011). The genus contains 18 species, including pathogens that cause infection in humans and animals (Woodbury et al., 2009; Kubota et al., 2012). For instance, *Moraxella lacunata* can cause infections in the eye and the upper respiratory tract (Woodbury et al., 2009; Mehmeti et al., 2021), while *Moraxella osloensis* and *Moraxella catarrhalis*, which are usually isolated from the human respiratory tract, can cause meningitis and pneumonia (Murphy and Parameswaran, 2009; Lee et al., 2017). Overall, *Moraxella* spp. pose a serious threat to human and animal health.

In the present study, we characterized two novel *mcr-1* variants, *mcr-1.35* and *mcr-1.36*, which originated from *Moraxella* spp. isolated from pigs with respiratory tract disease in swine farms in China.

Materials and methods

Isolation, purification, and identification of *Moraxella* sp.

A total of 312 nasal swabs were collected from pigs with a respiratory disease from 15 swine farms in Fujian Province, China (Supplementary Table S1). Subsequently, the samples were transferred into tryptic soy broth (TSB) (OXOID Ltd., UK). These TSB samples were then vortexed and plated onto tryptic soy agar (TSA) (OXOID Ltd., UK) supplemented with 5% defibrillated sheep blood (Zhengzhou Jiulong Biotechnology Co., Ltd., China) and 5% bovine serum (Zhejiang Tianhang Biotechnology Co., Ltd., China). A single colony was purified, after which PCR was performed to identify the 16S rRNA gene homology of the isolates using the primers 27F/1492R (Supplementary Table S2). Subsequently, the isolates identified as *Moraxella* spp. were further studied.

PCR screening of *mcr-1* in *Moraxella* spp. and antimicrobial susceptibility testing of *mcr-1*-positive *Moraxella* sp. isolates

PCR was performed to detect the presence of *mcr-1* in *Moraxella* sp. isolates using the primer mcr-1-F/R (Supplementary Table S2). The minimum inhibitory concentrations (MICs) of *mcr-1*-positive *Moraxella* sp. against 12 antibiotics were determined using the microbroth dilution method according to the Clinical and Laboratory Standards Institute (Wayne, 2020). The *Escherichia coli* ATCC 25922 strain was used for quality control.

Phylogenetic analysis of amino acid sequences of the mcr-like variants and the 16S rRNA gene sequences from *Moraxella* spp.

The phylogenetic analysis of the deduced amino acid sequences of the *mcr*-like variants and the 16S rRNA gene from *Moraxella* spp. was performed using MEGA 11.0 software (Tamura et al., 2021). The *mcr*-like variants included *mcr-1.35*, *mcr-1.36*, *mcr-1.10*, *mcr-2.2*, and *mcr-6.1* polymyxin resistance genes identified in *Moraxella* spp. and those identified in *M. osloensis*, *Moraxella lincolnii*, *and Moraxella porci* (mcr_{OSL}, $mcr_{LIN,}$ and mcr_{POR}, respectively) (Kieffer et al., 2017). In addition to the 16S rRNA genes of *mcr-1*-positive *Moraxella* spp. isolated in this study, other 16S rRNA genes from different *Moraxella* species were obtained from the NCBI database.

Phylogenetic analysis of all *mcr-1* gene variants

The phylogenetic analysis of the complete sequences of *mcr-1.35* and *mcr-1.36* found in *Moraxella* spp., as well as the complete sequences of *mcr-1.1* to *mcr-1.34* registered in GenBank, were performed using MEGA 11.0 software (Supplementary Table S3; Tamura et al., 2021).

Whole-genome sequencing analysis

The DNA of three *Moraxella* spp. was extracted using a bacterial DNA extraction kit (OMEGA, USA). The whole genomes of these *Moraxella* sp. were sequenced using the Illumina Hiseq and Oxford Nanopore MinIon platforms, and complete sequences were obtained by hybrid assembly using Unicycler version 0.5.0 (Wick et al., 2017). Functional element prediction was conducted using Prokka (Seemann, 2014). The sequences were annotated by comparing the

predicted gene sequences with functional databases such as RefSeq (O'Leary et al., 2016) and CARD (Alcock et al., 2020) with BLAST+. The genetic context of *mcr-1* was analyzed using Easyfig (Sullivan et al., 2011).

Functional cloning of novel *mcr-1* variants

A 1,623-bp DNA fragment of *mcr-1.35* and *mcr-1.36* was amplified from *Moraxella* spp. FZFQ2102, FZLJ2107, and FZLJ2109 using the primer mcr1L-F/R (Supplementary Table S2) and then cloned into pUC19 to obtain pUC19-*mcr-1.35* and pUC19-*mcr-1.36*. The vector was transformed into *E. coli* DH5α and *E. coli* JM109. The MICs of polymyxin B against DH5α and JM109 harboring pUC19-*mcr-1.35*, pUC19-*mcr-1.36*, and pUC19 were determined by the microbroth dilution method.

Protein structure analysis of MCR-1 variants from *Moraxella* sp.

The structure of lipooligosaccharide phosphoethanolamine transferase A (*EptA*) (PDB accession number 5FGN) was obtained from the Protein Data Bank.[1] The structures of MCR-1 variants were generated according to their amino acid sequences using the comparative protein-modeling SWISS-MODEL server (Waterhouse et al., 2018). These structures were then analyzed and visualized using PyMOL software.

Nucleotide sequence accession numbers

The complete nucleotide sequences of *Moraxella* spp. FZFQ2102, FZLJ2107, and FZLJ2109 were deposited in GenBank under the accession numbers CP099960, CP101111, and CP101112, respectively.

Results

Identification of *mcr-1*-positive *Moraxella* sp.

In total, 58 isolates that belonged to *Moraxellae* were isolated and identified from the 312 samples obtained from 15 swine farms in Fujian Province, China (Supplementary Table S1). Of these 58 isolates, three were identified as positive for *mcr-1* and were named FZFQ2102, FZLJ2107, and FZLJ2109, respectively (Table 1).

Due to FZFQ2102, FZLJ2107, and FZLJ2109 being identified as *Moraxella* sp. by PCR, the phylogenetic analysis was performed using the 16S rRNA genes of the *Moraxella* sp. obtained in this study and those in the NCBI database. According to 16S rRNA sequence identity, the phylogenetic tree of *Moraxella* sp. was divided into four groups: M1, M2, M3, and M4. The *Moraxella* sp. FZFQ2102 shared a close phylogenetic relationship with *Moraxella nonliquefaciens* and *Moraxella nasovis*. Moreover, the *Moraxella* spp. FZLJ2107 and FZLJ2109 shared a close phylogenetic relationship with *M. porci* and *Moraxella pluranimalium* (Figure 1).

Two novel colistin resistance gene *mcr-1* variants in *Moraxella* sp.

Between 2015 and 2022, an increasing number of *mcr*-like variants were found in *Moraxella* sp. (AbuOun et al., 2017; Kieffer et al., 2017). The three *mcr-1*-positive *Moraxella* sp. isolated in this study demonstrated multidrug resistance, including resistance to polymyxin B (MIC = 8 μg/mL) (Table 1). Sequence analysis indicated that the three *Moraxella* sp. carried two *mcr-1* variants. BLASTn results showed that the nucleotide sequence homology of the two *mcr-1* variants with *mcr-1* was 95.33% (Table 2). Furthermore, the phylogenetic analysis suggested that the nucleotide sequence identities of the two *mcr-1* variants from *Moraxella* sp. FZFQ2102, FZLJ2107, and FZLJ2109 were distinct from those of *mcr-1.1–mcr-1.34* (Figure 2). Therefore, the two novel *mcr-1* variants were named *mcr-1.35* and *mcr-1.36*.

Characterization of the three *mcr-1*-positive *Moraxella* sp.

Whole-genome sequencing (WGS) suggested that the three *Moraxella* sp., FZFQ2102, FZLJ2107, and FZLJ2109, have 2,336,058-bp, 2,422,986-bp, and 2,424,775-bp chromosomes, respectively, and no plasmids (Table 1). WGS also showed that the three *Moraxella* sp. possessed multiple drug-resistance genes. The *Moraxella* sp. FZFQ2102 contained the colistin resistance gene *mcr-1.35*; the aminoglycoside resistance genes *aac(3)-IId*, *aac(3)-IV*, *aph(2″)-If*, *aph(3′)-Ia*, *aph(3″)-Ib*, and *aph(6)-Id*; the macrolide resistance gene *erm*T; the tetracycline resistance genes *tet*(H) and *tet*(O); the sulfonamide resistance gene *sul2*; the phenicol resistance gene *floR*; and the β-lactamase resistance genes bla_{ROB-3} and bla_{ROB-9}. Moreover, the *Moraxella* sp. FZLJ2107 and FZLJ2109 contained the colistin resistance gene *mcr-1.36*; the aminoglycoside resistance genes *aadA8b*, *aph(2″)-If*, *aph(3′)-Ia*, *aph(3″)-Ib*, and *aph(6)-Id*; the tetracycline resistance genes *tet*(H) and *tet*(O); the sulfonamide resistance gene *sul2*; the phenicol resistance gene *floR*; and the β-lactamase resistance genes bla_{ROB-9} and $bla_{CARB-50}$ (Table 1).

The analysis of the context of the *mcr-1* variants suggested that their flanking regions were highly similar among the *Moraxella* sp. The *mcr* genes in the *Moraxella* sp. were downstream of a site-specific recombinase gene (*ssr*) and upstream of the *pap-2* gene. However, the genetic environment of *mcr-1* variants in other *mcr-1*-carrying bacteria differed from that of the *Moraxella* sp. Interestingly, *mcr-1* variants had a common genetic unit: *mcr-1-pap2* (Figure 3).

Functional confirmation of *mcr-1.35* and *mcr-1.36*

BLASTn analysis confirmed that two 1,623-bp open reading frames (ORFs) encoded the putative phosphoethanolamine

1 http://www.rcsb.org/pdb/

TABLE 1 Characterization of the *mcr-1*-carrying *Moraxella* spp. FZFQ2102, FZLJ2107, and FZLJ2109.

Isolates	MICs of polymyxin B (μg/mL)	Other resistance phenotypes	Chromosome size (bp)	Resistance genes	*mcr-1* genetic environment
FZFQ2102	8	CHL, FFC, GEN DOX, CTX, CIP, SMZ, AZM, PEN	2,336,058	*aac(3)-IId*, *aac(3)-IV*, *aph(2″)-If*, *aph(3′)-Ia*, *aph(3″)-Ib*, *aph(6)-Id*, *erm*(T), *floR*,***mcr-1.35***, bla_{ROB-3}, bla_{ROB-9}, *sul2*, *tet*(H), *tet*(O)	*mcr-1-pap-2*
FZLJ2107	8	CHL, FFC, GEN, DOX, CTX, CIP, SMZ, PEN	2,422,986	*aadA8b*, *aph(2″)-If*, *aph(3′)-Ia*, *aph(3″)-Ib*, *aph(6)-Id*, $bla_{CARB-50}$, *floR*,***mcr-1.36***, bla_{ROB-9}, *sul2*, *tet*(H), *tet*(O)	*mcr-1-pap-2*
FZLJ2109	8	CHL, FFC, GEN DOX, CTX, CIP, SMZ, PEN	2,424,775	*aadA8b*, *aph(2″)-If*, *aph(3′)-Ia*, *aph(3″)-Ib*, *aph(6)-Id*, $bla_{CARB-50}$, *floR*,***mcr-1.36***, bla_{ROB-9}, *sul2*, *tet*(H), *tet*(O)	*mcr-1-pap-2*

CHL, chloramphenicol; FFC, florfenicol; GEN, gentamicin; DOX, doxycycline; SMZ, sulfamethoxazole; CTX, cefotaxime; CIP, ciprofloxacin; AZM, azithromycin; PEN, penicillin. Bold respresents the colistin resistance gene.

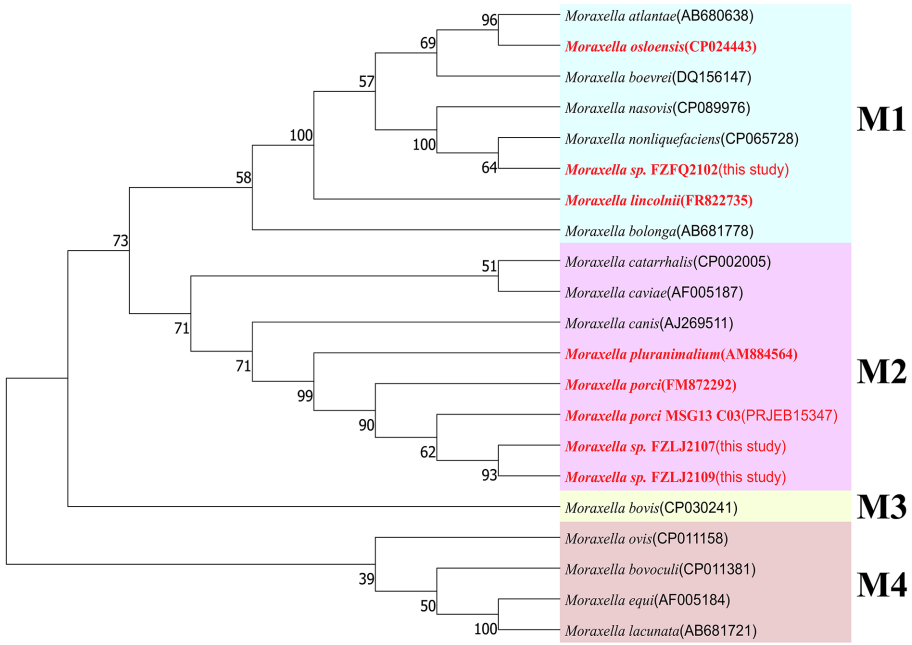

FIGURE 1
Phylogenetic tree of different *Moraxella* species based on 16S rRNA. The 16S rRNA genes of the three *mcr-1*-positive *Moraxella* spp. isolated in this study were compared with those of *Moraxella* spp. from the NCBI database. The neighbor-joining phylogeny was constructed using MEGA 11.0 with the 16S rRNA gene sequence of *Moraxella* spp. with the *mcr* gene (in red) and without the *mcr* gene (in black). Branch labels correspond to bootstrap support percentages out of 1,000 replicates. The tree is divided into four groups: M1 (light blue area), M2 (pink area), M3 (light yellow area), and M4 (light orange area).

transferase, which showed high nucleotide sequence identity to the original *mcr-1.1* gene. The amino acid sequences of MCR-1.35 and MCR-1.36 showed 97.23 and 96.67% identity, respectively, to that of MCR-1.1 (Table 2). To confirm the function of the putative phosphoethanolamine transferase, the recombinant vectors pUC19-*mcr-1.35* and pUC19-*mcr-1.36* were constructed and subsequently transformed into *E. coli* DH5α and JM109. Compared with *E. coli* DH5α and JM109 carrying pUC19 alone, the expression of these ORFs in *E. coli* DH5α and JM109 led to 4-fold increases in the MIC of polymyxin B, which further identified the function of the *mcr-1.35* and *mcr-1.36* genes (Table 3).

Analysis of *mcr*-like variants from *Moraxella* sp.

BLASTn results showed that *mcr-1.35* and *mcr-1.36* exhibited more than 95% nucleotide sequence identity to *mcr-1.10*, indicating a close phylogenetic relationship. *Mcr-1.35* and *mcr-1.36* also exhibited 78.62 and 78.13% nucleotide sequence identity to *mcr-2.2* and 80.18 and 79.69% nucleotide sequence identity to *mcr-6.1*, respectively. Furthermore, *mcr-1.35* (*mcr-1.36*) showed 57.88% (58.11%), 62.68% (62.74%), and 63.14% (63.50%) nucleotide sequence identity to the mcr_{LIN}, mcr_{OSL}, and mcr_{POR} genes found in *M. osloensis*, *M. porci*, and *M. lincolnii*, respectively. Additionally,

TABLE 2 Pairwise comparisons of *mcr-1.1* and *mcr*-like variants in *Moraxella* sp. based on nucleotide and amino acid sequence identity (%).

	mcr-1.1	*mcr-1.10*	*mcr-1.35*	*mcr-1.36*	*mcr-2.2*	*mcr-6.1*	mcr_{LIN}	mcr_{OSL}	mcr_{POR}
mcr-1.1	100	97.60	95.33	95.33	77.49	78.07	57.65	62.32	63.88
mcr-1.10	98.71	100	95.02	95.20	77.06	77.33	57.99	61.91	63.57
mcr-1.35	97.23	96.67	100	98.27	78.62	80.18	57.88	62.68	63.14
mcr-1.36	96.67	96.49	99.44	100	78.13	79.69	58.11	62.74	63.50
mcr-2.2	81.52	81.15	82.59	82.04	100	85.16	59.81	63.97	64.31
mcr-6.1	82.44	81.89	84.07	83.52	87.73	100	58.28	63.00	63.18
mcr_{LIN}	55.34	55.34	55.52	55.17	55.61	55.96	100	59.64	60.11
mcr_{OSL}	59.04	59.57	59.75	59.57	60.21	61.46	54.97	100	60.76
mcr_{POR}	62.13	61.76	61.88	61.69	61.44	62.66	54.30	59.33	100

Green and blue shading represent comparisons of nucleotide and amino acid sequence identity, respectively.

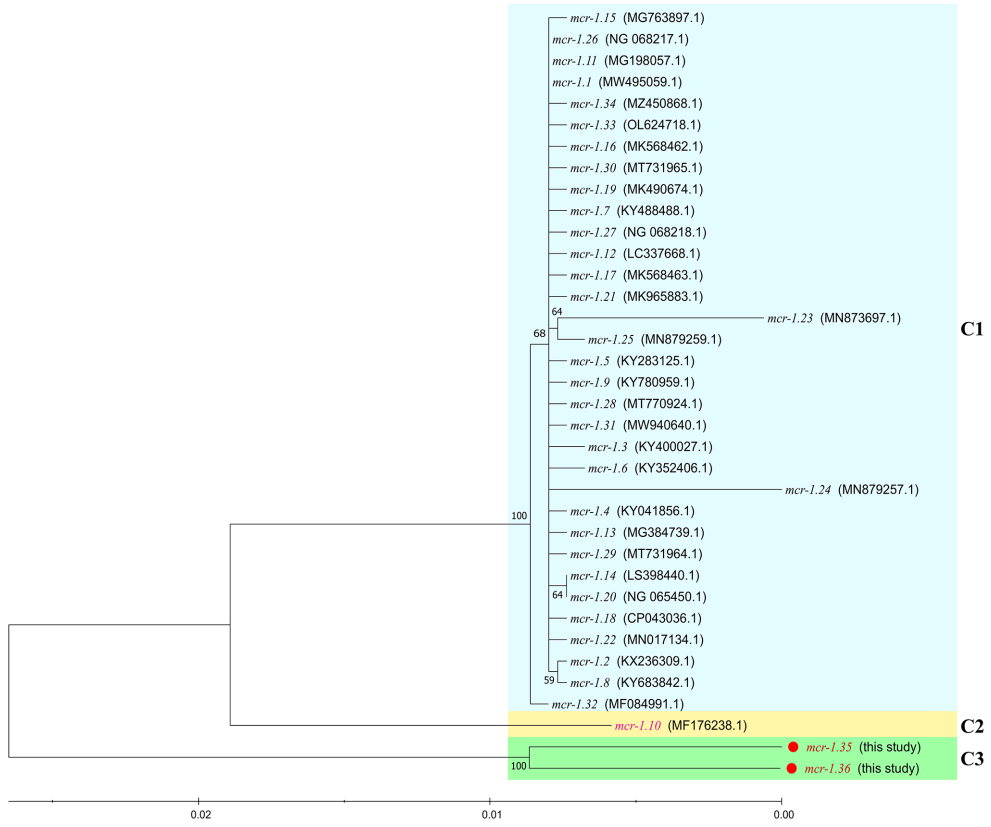

FIGURE 2
Comparison between *mcr-1.35* and *mcr-1.36* and all previously described *mcr-1* subtypes, based on nucleotide sequences. The neighbor-joining phylogeny was constructed using MEGA 11.0 with the nucleotide sequences of the novel colistin-resistance genes *mcr-1.35* and *mcr-1.36* (in red) and all previously described the *mcr-1* gene subtypes (*mcr-1.1* to *mcr-1.34* [in black and pink]). Branch labels correspond to bootstrap support percentages out of 1,000 replicates. The tree is divided into three groups: C1, which contains the *mcr-1* gene subtypes from other bacterial species (light blue area), C2, which contains the *mcr-1.10* gene from *Moraxella* spp. (light yellow area), and C3, which contains the *mcr-1.35* and *mcr-1.36* genes from *Moraxella* spp. (green area).

mcr-1.35 exhibited 98.27% nucleotide sequence identity to *mcr-1.36* in this study (Table 2).

Compared with other phosphoethanolamine transferases in *Moraxella* sp., MCR-1.35, and MCR-1.36 aligned closely with an MCR-1.10 found in *M. porci* isolated from a pig in Great Britain (> 96%). MCR-1.35 and MCR-1.36 also exhibited 82.59 and 82.04% amino acid identity to MCR-2.2 and 84.07 and 83.52% amino acid identity to MCR-6.1, found in *Moraxella pluranimalium* isolated from pigs in Europe, respectively. In addition, MCR-1.35 (MCR-1.36) showed 55.52% (55.17%), 59.75% (59.57%), and 61.88% (61.69%) amino acid sequence identity to the MCR-OSL, MCR-POR, and MCR-LIN proteins found in *M. osloensis*, *M. porci*, and *M. lincolnii*, respectively (Table 2; Figure 4).

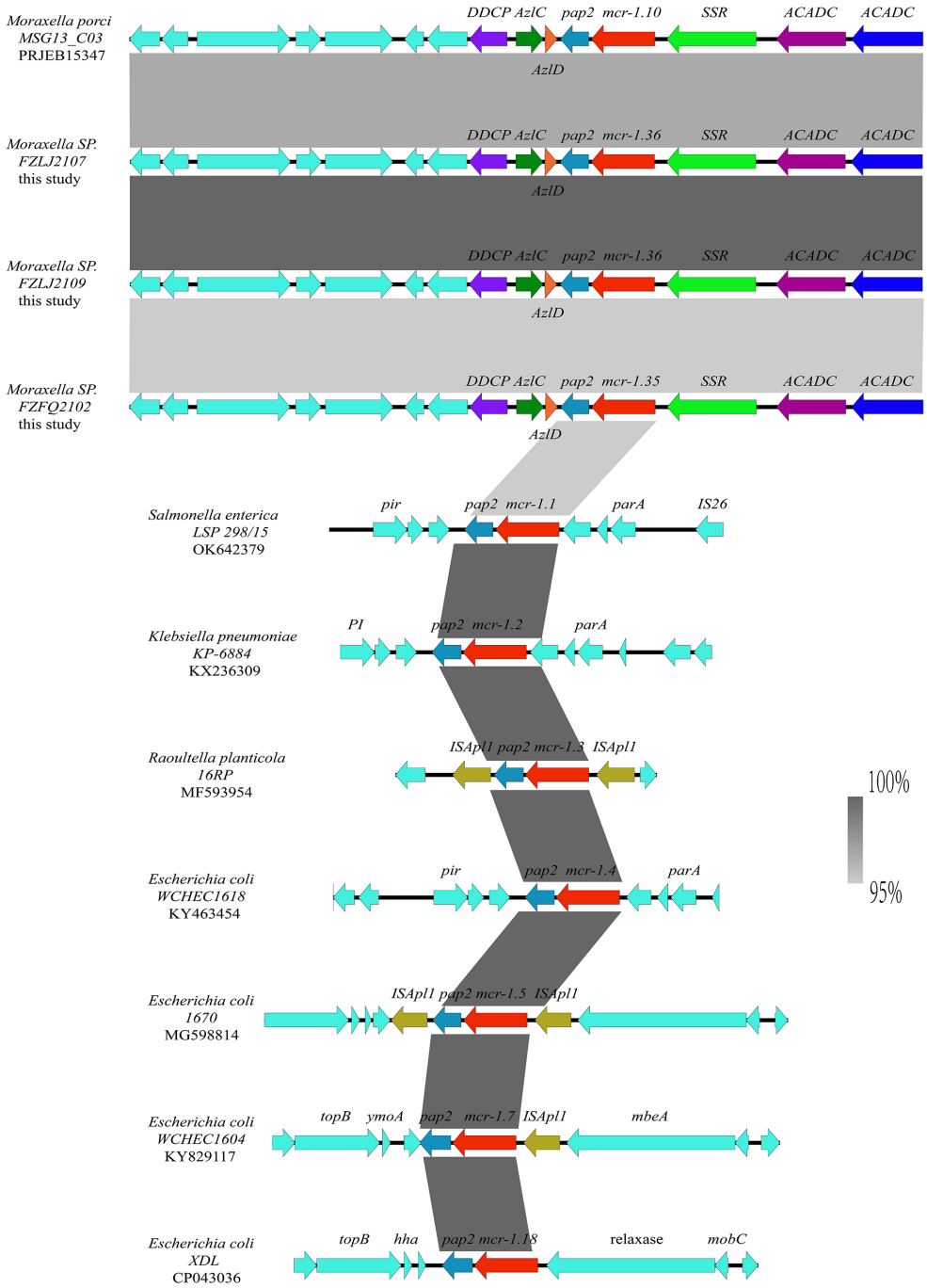

FIGURE 3
Comparison between the genetic context of the *mcr-1* subtypes from *Moraxella* spp. and those from other bacterial species. The extents and directions of genes are shown by arrows labeled with gene names, with the *mcr-1* subtypes represented by red arrows and the *pap2* gene represented by a light blue arrow. Other flanking genes have been annotated. The shadow parallelograms between each sequence denote sequence identity.

Structure prediction and amino acid sequence analysis of MCR-1 variants from *Moraxella* sp.

MCR-1 variants from *Moraxella* sp. were aligned using BioEdit (Figure 5A). When aligned with MCR-1.1, MCR-1.10 presented six amino acid mutations at residues R11C, A23S, M155V, M234T, A354T, and A443T. Four residues, S^{23}, V^{155}, T^{354}, and T^{443}, were located in the α-helix of the secondary structure, while residues C^{11} and T^{234} were located in the random coil. However, compared with those of MCR-1.1, the amino acid sequences of MCR-1.35 exhibited changes at residues Q^{277}, T^{354}, T^{381}, A^{491}, S^{498}, N^{499}, N^{500}, S^{501}, S^{502}, 503 deletion, F^{503}, T^{506}, S^{508}, and A^{511}. Three residues, T^{354}, T^{506}, and S^{508}, were located in the α-helix on the secondary structure, while all other residues were located in the random coil. In addition, amino acid sequences of MCR-1.36 presented changes at residues S^{23}, Q^{277},

T^{354}, T^{381}, M^{451}, A^{491}, S^{498}, N^{499}, N^{500}, S^{501}, S^{502}, 503 deletion, F^{503}, T^{506}, S^{508}, and A^{511}. In addition, the four residues S^{23}, T^{354}, T^{506}, and S^{508} were located in the α-helix on the secondary structure, with all other residues located in the random coil (Figures 5C, D). Notably, protein structure alignment revealed only a few differences between MCR-1.1 and MCR-1.10, MCR-1.1 and MCR-1.35, and MCR-1.1 and MCR-1.36 (Figure 5D).

Discussion

Moraxella spp. have been identified as potential sources of MCR-like polymyxin resistance determinants (Kieffer et al., 2017; Poirel et al., 2017). One study identified the *mcr*-like genes, including *mcr-1.10* (*M. porci*), *mcr-2.2* (*M. pluranimalium*), and *mcr-6.1* (*M. pluranimalium*), in *Moraxella* spp. isolated from the cecal contents of healthy pigs on farms in Great Britain (AbuOun et al., 2017). Furthermore, the proteins MCR-POR (*M. porci*), MCR-OSL (*M. osloensis*), and MCR-LIN (*M. lincolnii*) in *Moraxella* spp. shared high amino acid identities with MCR-1/2-like (Kieffer et al., 2017). In the present study, the novel *mcr-1* variants *mcr-1.35* and *mcr-1.36* were identified in *Moraxella* spp. recovered from the nasal swabs of pigs with respiratory diseases in farms in China. Notably, the emergence of different *mcr*-like variants in various *Moraxella* spp. indicates that the *mcr*-like variants were stored in the chromosomes of some *Moraxella* species.

TABLE 3 MICs of polymyxin B for the constructed strains.

Species	MICs (μg/mL)
	Polymyxin B
E. coli DH5α + pUC19-*mcr-1.35*	2
E. coli DH5α + pUC19-*mcr-1.36*	2
E. coli DH5α + pUC19	0.5
E. coli JM109 + pUC19-*mcr-1.35*	2
E. coli JM109 + pUC19-*mcr-1.36*	2
E. coli JM109 + pUC19	0.5
E. coli 25,922	0.25

Three *Moraxella* spp. containing novel *mcr-1* variants showed resistance to polymyxin (Table 1). Additionally, the MIC of colistin for *Moraxella* spp. containing *mcr-1.10*, *mcr-2.2*, and *mcr-6.1* ranged from 1 to 2 μg/mL (AbuOun et al., 2017), while the MIC of colistin for EptA-containing *Moraxella* spp. ranged from 2 to 64 μg/mL (AbuOun et al., 2017; Kieffer et al., 2017). Moreover, *mcr-1.35*, *mcr-1.36*, *mcr-2.2*, mcr_{osl}, mcr_{lin}, and mcr_{por} conferred resistance to polymyxin in *E. coli* (Kieffer et al., 2017; Poirel et al., 2017). In addition to colistin resistance genes (*mcr-1.10*, *mcr-1.35*, *mcr-1.36*, *mcr-2.2*, and *mcr-6.1*), *Moraxella* spp. also carried genes for β-lactam resistance (bla_{BRO-1} and bla_{BRO-2}) aminoglycoside resistance (*aac(3)-IId*, *aac(3)-IV*, *aph(2″)-If*, *aph(3′)-Ia*, *aph(3″)-Ib*, and *aph(6)-Id*); tetracycline resistance [*tet*(B), *tet*(D), *tet*(L), and *tet*(O)]; chloramphenicol resistance (*floR*), sulfonamide resistance (*sul2*), and macrolide resistance (*erm*T) (Flamm et al., 2012; AbuOun et al., 2017; Krol-Turminska et al., 2020; Raveendran et al., 2020; Zhang et al., 2022). In recent studies, *Moraxella* spp. from human samples have proven to be mainly resistant to β-lactam, tetracycline, and macrolide (Flamm et al., 2012; Krol-Turminska et al., 2020; Raveendran et al., 2020; Zhang et al., 2022). The three *Moraxella* spp. from animal samples collected in this study showed multidrug resistance, indicating that *Moraxella* spp. pose potential threats to human and animal health.

The phylogenetic analysis showed that the *mcr-1* variants (*mcr-1.10*, *mcr-1.35*, and *mcr-1.36*) that originated from *Moraxella* spp. belonged to subclades (C2 and C3 group) distinct from that of the

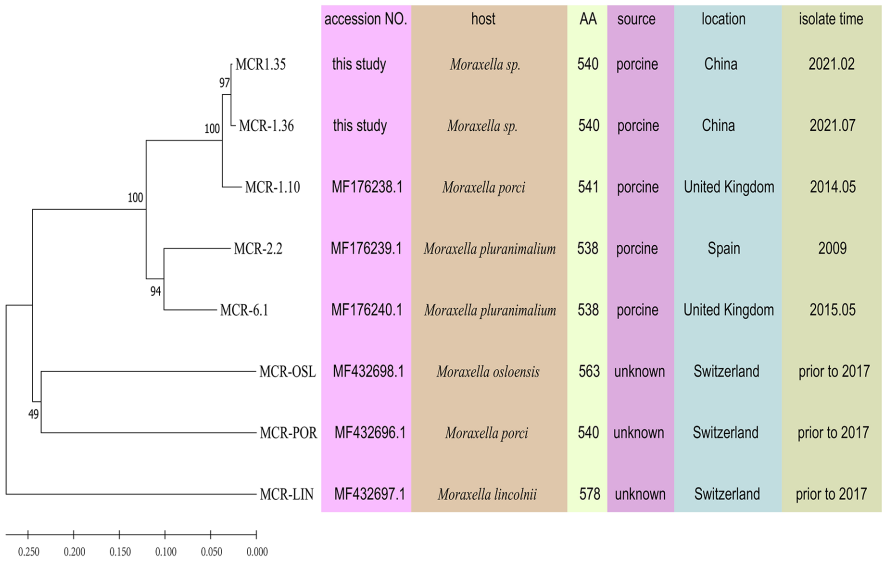

FIGURE 4
Phylogeny of MCR-like variants from *Moraxella* spp. determined based on amino acid sequences using MEGA 11.0. MCR-OSL, MCR-POR, and MCR-LIN are polymyxin resistance determinants that were identified in *M. osloensis*, *M. porci* and *M. lincolnii*, respectively. Some parameters relevant to the MCR proteins are presented, including bacterial host, the number of amino acids, isolate source, isolate location, and isolate time.

10.3389/fmicb.2023.1153740

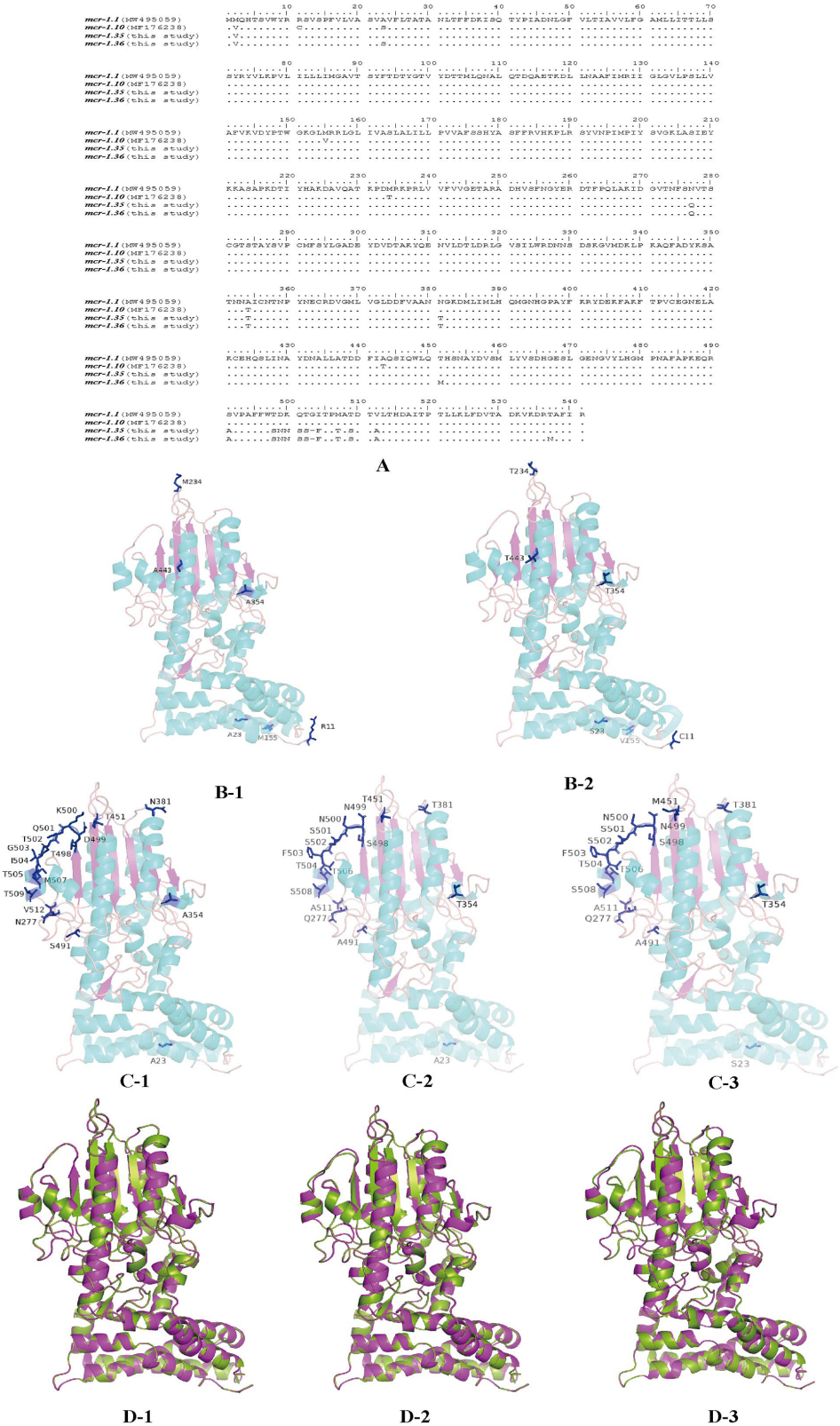

FIGURE 5
Structures of MCR-1 variants (MCR-1.1, MCR-1.10, MCR-1.35, and MCR-1.36) **(A)** Amino acid sequences of MCR-1.10, MCR-1.35, and MCR-1.36 compared with MCR-1.1. Amino acid residues are depicted in black, and the same amino acids are represented by dots in the alignment. **(B)** Structural models comparison of the MCR-1.1 protein (B-1) and MCR-1.10 (B-2) from *Moraxella* spp. based on lipooligosaccharide phosphoethanolamine transferase EptA. **(C)** Structural models comparison of the MCR-1.1 protein (C-1), and MCR-1.35 (C-2), MCR-1.36 (C-3) from Moraxella spp. based on lipooligosaccharide phosphoethanolamine transferase EptA. Models were constructed using the SWISS-MODEL server, and structures were viewed and edited using PyMOL2.5.4. Mutated amino acids are shown in the structural model. **(D)** Comparison between the structure of MCR-1.1 (in green) and that of MCR-1.10 (D-1), MCR-1.35 (D-2) and MCR-1.36 (D-3) (in pink).

mcr-1 variants originating from *Enterobacteriaceae* (C1 group) (Figure 2). The phylogenetic relationships between *mcr-1.35*, *mcr-1.36*, and *mcr-1.1* differed, but the products of these genes are known to be responsible for polymyxin resistance (Liu et al., 2016). The comparisons of the nucleotide sequences showed that the context of the *mcr-1* variants was similar among *Moraxella* spp. but differed from the genetic environment of the *mcr-1* variants in other bacteria. These results indicate that *mcr-1-pap2* acts as the genetic unit of the *mcr-1* variants in *Moraxella* spp. (AbuOun et al., 2017; Poirel et al., 2017).

Compared with that of MCR-1.1, the amino acid sequences of MCR-1.35 and MCR-1.36 exhibited mutations located at the α-helix and random coil on the secondary structure. Previous research has suggested that the eight active sites (E246, T285, K333, H395, D465, H466, E468, and H478) located on the β-sheet of the protein's secondary structure are essential for the activity of MCR-1 (Hu et al., 2016; Ma et al., 2016; Stojanoski et al., 2016; Hinchliffe et al., 2017). Notably, these β-sheet mutations were highly conserved in MCR-1.35 and MCR-1.36 ORFs (Carroll et al., 2019; Wang et al., 2020), indicating that the mutations of MCR-1.35 and MCR-1.36 have no influence on their polymyxin resistance activity. Furthermore, protein structure alignment indicated that the structures of MCR-1.35, MCR-1.36, and MCR-1.1 did not differ significantly.

In conclusion, this study identified the *Moraxella* spp. carrying two novel *mcr-1* variants, *mcr-1.35* and *mcr-1.36*, conferring resistance to colistin, which were isolated from pig farms in China. *Moraxella* spp. were considered potential sources of MCR-like determinants, and the *mcr*-like variants were observed to be located in the chromosomes of some *Moraxella* species isolated from pig samples. Therefore, further research on the *mcr*-like genes in *Moraxella* spp. may help us understand the evolution and spread of the *mcr*-like genes.

Data availability statement

The datasets presented in this study can be found in online repositories. The names of the repository/repositories and accession number(s) can be found in the article/Supplementary material.

Author contributions

LZ and YC designed the experiments. YC, RW, and HL performed the experiments. LW and XW prepared the tables and figures. YC, RW, QC, and RC prepared the manuscript. All authors read and approved the final version of the manuscript.

Funding

This study was supported by the National Nature Science Foundation of China (No. 31872502), basic scientific research projects of provincial public welfare scientific research institutions (Fujian Province), China (No. 2022R10260013), and the key project of the Fujian "5511" Collaborative Innovation Project, China (No. XTCXGC2021008).

Conflict of interest

The authors declare that the research was conducted in the absence of any commercial or financial relationships that could be construed as a potential conflict of interest.

Publisher's note

All claims expressed in this article are solely those of the authors and do not necessarily represent those of their affiliated organizations, or those of the publisher, the editors and the reviewers. Any product that may be evaluated in this article, or claim that may be made by its manufacturer, is not guaranteed or endorsed by the publisher.

Supplementary material

The Supplementary material for this article can be found online at: https://www.frontiersin.org/articles/10.3389/fmicb.2023.1153740/full#supplementary-material

References

AbuOun, M., Stubberfield, E. J., Duggett, N. A., Kirchner, M., Dormer, L., Nunez-Garcia, J., et al. (2017). Mcr-1 and mcr-2 variant genes identified in *Moraxella* species isolated from pigs in Great Britain from 2014 to 2015. *J. Antimicrob. Chemother.* 72, 2745–2749. doi: 10.1093/jac/dkx286

Alcock, B. P., Raphenya, A. R., Lau, T. T. Y., Tsang, K. K., Bouchard, M., Edalamand, A., et al. (2020). CARD 2020: antibiotic resistome surveillance with the comprehensive antibiotic resistance database. *Nucleic Acids Res.* 48, D517–D525. doi: 10.1093/nar/gkz935

Boucher, H. W., Talbot, G. H., Bradley, J. S., Edwards, J. E., Gilbert, D., Rice, L. B., et al. (2009). Bad bugs, no drugs: no ESKAPE! An update from the Infectious Diseases Society of America. *Clin. Infect. Dis.* 48, 1–12. doi: 10.1086/595011

Carroll, L. M., Gaballa, A., Guldimann, C., Sullivan, G., Henderson, L. O., and Wiedmann, M. (2019). Identification of novel mobilized Colistin resistance gene mcr-9 in a multidrug-resistant, Colistin-susceptible *Salmonella enterica* serotype Typhimurium isolate. *MBio* 10:e00853–19. doi: 10.1128/mBio.00853-19

Caselli, E., D'Accolti, M., Soffritti, I., Piffanelli, M., and Mazzacane, S. (2018). Spread of mcr-1-driven Colistin resistance on hospital surfaces, Italy. *Emerg. Infect. Dis.* 24, 1752–1753. doi: 10.3201/eid2409.171386

Embers, M. E., Doyle, L. A., Whitehouse, C. A., Selby, E. B., Chappell, M., and Philipp, M. T. (2011). Characterization of a *Moraxella* species that causes epistaxis in macaques. *Vet. Microbiol.* 147, 367–375. doi: 10.1016/j.vetmic.2010.06.029

Flamm, R. K., Sader, H. S., Farrell, D. J., and Jones, R. N. (2012). Macrolide and tetracycline resistance among *Moraxella catarrhalis* isolates from 2009 to 2011. *Diagn. Microbiol. Infect. Dis.* 74, 198–200. doi: 10.1016/j.diagmicrobio.2012.06.007

Hinchliffe, P., Yang, Q. E., Portal, E., Young, T., Li, H., Tooke, C. L., et al. (2017). Insights into the mechanistic basis of plasmid-mediated Colistin resistance from crystal structures of the catalytic domain of MCR-1. *Sci. Rep.* 7:39392. doi: 10.1038/srep39392

Hu, M., Guo, J., Cheng, Q., Yang, Z., Chan, E. W. C., Chen, S., et al. (2016). Crystal structure of *Escherichia coli* originated MCR-1, a phosphoethanolamine transferase for Colistin resistance. *Sci. Rep.* 6:38793. doi: 10.1038/srep38793

Kieffer, N., Nordmann, P., and Poirel, L. (2017). *Moraxella* species as potential sources of MCR-like Polymyxin resistance determinants. *Antimicrob. Agents Chemother.* 61:e00129–17. doi: 10.1128/AAC.00129-17

Krol-Turminska, K., Olender, A., and Bogut, A. (2020). Tetracycline resistance in *Moraxella catarrhalis* clinical strains isolated in Poland. *New Microbiol.* 43, 103–106.

Kubota, H., Mitani, A., Niwano, Y., Takeuchi, K., Tanaka, A., Yamaguchi, N., et al. (2012). *Moraxella* species are primarily responsible for generating malodor in laundry. *Appl. Environ. Microbiol.* 78, 3317–3324. doi: 10.1128/AEM.07816-11

Lee, W. S., Hsueh, P. R., Yu, F. L., Chen, F. L., Hsieh, T. C., and Ou, T. Y. (2017). *Moraxella osloensis* bacteremia complicating with severe pneumonia in a patient with lung cancer. *J. Microbiol. Immunol. Infect.* 50, 395–396. doi: 10.1016/j.jmii.2015.03.005

Ling, Z., Yin, W., Li, H., Zhang, Q., Wang, X., Wang, Z., et al. (2017). Chromosome-mediated mcr-3 variants in *Aeromonas veronii* from chicken meat. *Antimicrob. Agents Chemother.* 61:e01272–17. doi: 10.1128/AAC.01272-17

Ling, Z., Yin, W., Shen, Z., Wang, Y., Shen, J., and Walsh, T. R. (2020). Epidemiology of mobile colistin resistance genes mcr-1 to mcr-9. *J. Antimicrob. Chemother.* 75, 3087–3095. doi: 10.1093/jac/dkaa205

Liu, Y. Y., Wang, Y., Walsh, T. R., Yi, L. X., Zhang, R., Spencer, J., et al. (2016). Emergence of plasmid-mediated colistin resistance mechanism MCR-1 in animals and human beings in China: a microbiological and molecular biological study. *Lancet Infect. Dis.* 16, 161–168. doi: 10.1016/S1473-3099(15)00424-7

Ma, G., Zhu, Y., Yu, Z., Ahmad, A., and Zhang, H. (2016). High resolution crystal structure of the catalytic domain of MCR-1. *Sci. Rep.* 6:39540. doi: 10.1038/srep39540

Mehmeti, F., Cochard, B., Cuerel, C., De Coulon, G., Dayer, R., Steiger, C., et al. (2021). *Moraxella lacunata* subacute osteomyelitis in a child. *J. Pediatric. Infect. Dis. Soc.* 10, 161–163. doi: 10.1093/jpids/piz089

Murphy, T. F., and Parameswaran, G. I. (2009). *Moraxella catarrhalis*, a human respiratory tract pathogen. *Clin. Infect. Dis.* 49, 124–131. doi: 10.1086/599375

Nordmann, P., and Poirel, L. (2016). Plasmid-mediated colistin resistance: an additional antibiotic resistance menace. *Clin. Microbiol. Infect.* 22, 398–400. doi: 10.1016/j.cmi.2016.03.009

O'Leary, N. A., Wright, M. W., Brister, J. R., Ciufo, S., Haddad, D., McVeigh, R., et al. (2016). Reference sequence (RefSeq) database at NCBI: current status, taxonnomic expansion, and functional annotation. *Nucleic Acids Res.* 44, D733–D745. doi: 10.1093/nar/gkv1189

Pham Thanh, D., Thanh Tuyen, H., Nguyen Thi Nguyen, T., Chung The, H., Wick, R. R., Thwaites, G. E., et al. (2016). Inducible colistin resistance via a disrupted plasmid-borne mcr-1 gene in a 2008 Vietnamese *Shigella sonnei* isolate. *J. Antimicrob. Chemother.* 71, 2314–2317. doi: 10.1093/jac/dkw173

Poirel, L., Kieffer, N., Fernandez-Garayzabal, J. F., Vela, A. I., Larpin, Y., and Nordmann, P. (2017). MCR-2-mediated plasmid-borne polymyxin resistance most likely originates from *Moraxella pluranimalium*. *J. Antimicrob. Chemother.* 72, 2947–2949. doi: 10.1093/jac/dkx225

Raveendran, S., Kumar, G., Sivanandan, R. N., and Dias, M. (2020). *Moraxella catarrhalis*: a cause of concern with emerging resistance and presence of BRO Beta-lactamase gene-report from a tertiary care hospital in South India. *Int. J. Microbiol.* 2020:7316257. doi: 10.1155/2020/7316257

Seemann, T. (2014). Prokka: rapid prokaryotic genome annotation. *Bioinformatics* 30, 2068–2069. doi: 10.1093/bioinformatics/btu153

Stojanoski, V., Sankaran, B., Prasad, B. V., Poirel, L., Nordmann, P., and Palzkill, T. (2016). Structure of the catalytic domain of the colistin resistance enzyme MCR-1. *BMC Biol.* 14:81. doi: 10.1186/s12915-016-0303-0

Sullivan, M. J., Petty, N. K., and Beatson, S. A. (2011). Easyfig: a genome comparison visualizer. *Bioinformatics* 27, 1009–1010. doi: 10.1093/bioinformatics/btr039

Tamura, K., Stecher, G., and Kumar, S. (2021). MEGA11: molecular evolutionary genetics analysis version 11. *Mol. Biol. Evol.* 38, 3022–3027. doi: 10.1093/molbev/msab120

Vela, A. I., Sanchez-Porro, C., Aragon, V., Olvera, A., Dominguez, L., Ventosa, A., et al. (2010). *Moraxella porci* sp. nov., isolated from pigs. *Int. J. Syst. Evol. Microbiol.* 60, 2446–2450. doi: 10.1099/ijs.0.016626-0

Wang, C., Feng, Y., Liu, L., Wei, L., Kang, M., and Zong, Z. (2020). Identification of novel mobile colistin resistance gene mcr-10. *Emerg. Microbes. Infect.* 9, 508–516. doi: 10.1080/22221751.2020.1732231

Wang, X., Wang, Y., Zhou, Y., Li, J., Yin, W., Wang, S., et al. (2018). Emergence of a novel mobile colistin resistance gene, mcr-8, in NDM-producing *Klebsiella pneumoniae*. *Emerg. Microbes Infec.* 7:122. doi: 10.1038/s41426-018-0124-z

Waterhouse, A., Bertoni, M., Bienert, S., Studer, G., Tauriello, G., Gumienny, R., et al. (2018). SWISS-MODEL: homology modelling of protein structures and complexes. *Nucleic Acids Res.* 46, W296–W303. doi: 10.1093/nar/gky427

Wayne, P. A. (2020) in *Performance standards for antimicrobial disk and dilution susceptibility tests for Bacteria isolated from animals*. ed. Clinical and laboratory standards institute (CLSI). *5th* ed (Pittsburgh: CLSI Supplement VET01S; Clinical and Laboratory Standards Institute)

Wick, R. R., Judd, L. M., Gorrie, C. L., and Holt, K. E. (2017). Unicycler: resolving bacterial genome assemblies from short and long sequencing reads. *PLoS Comput. Biol.* 13:e1005595. doi: 10.1371/journal.pcbi.1005595

Woodbury, A., Jorgensen, J., Owens, A., and Henao-Martinez, A. (2009). *Moraxella lacunata* septic arthritis in a patient with lupus nephritis. *J. Clin. Microbiol.* 47, 3787–3788. doi: 10.1128/JCM.01403-09

Zhang, Z., Yang, Z., Xiang, X., Liao, P., and Niu, C. (2022). Mutation of TonB-dependent receptor encoding gene MCR_0492 potentially associates with macrolides resistance in *Moraxella catarrhalis* isolates. *Infect. Drug. Resist.* 15, 2419–2426. doi: 10.2147/IDR.S364397

frontiers | Frontiers in Microbiology

TYPE Original Research
PUBLISHED 03 August 2023
DOI 10.3389/fmicb.2023.1208314

OPEN ACCESS

EDITED BY
Zuowei Wu,
Iowa State University, United States

REVIEWED BY
Nikolaos Strepis,
Erasmus Medical Center, Netherlands
Hazem Ramadan,
Mansoura University, Egypt

*CORRESPONDENCE
Zunita Zakaria
✉ zunita@upm.edu.my

RECEIVED 18 April 2023
ACCEPTED 12 July 2023
PUBLISHED 03 August 2023

CITATION
Karim MR, Zakaria Z, Hassan L, Faiz NM and Ahmad NI (2023) The occurrence and molecular detection of *mcr-1* and *mcr-5* genes in *Enterobacteriaceae* isolated from poultry and poultry meats in Malaysia. *Front. Microbiol.* 14:1208314. doi: 10.3389/fmicb.2023.1208314

The occurrence and molecular detection of *mcr-1* and *mcr-5* genes in *Enterobacteriaceae* isolated from poultry and poultry meats in Malaysia

Md Rezaul Karim[1,2], Zunita Zakaria[1,3]*, Latiffah Hassan[4], Nik Mohd Faiz[5] and Nur Indah Ahmad[1]

[1]Department of Veterinary Pathology & Microbiology, Faculty of Veterinary Medicine, Universiti Putra Malaysia, UPM, Serdang, Selangor, Malaysia, [2]Bangladesh Livestock Research Institute, Dhaka, Bangladesh, [3]Institute of Bioscience, Universiti Putra Malaysia, UPM, Serdang, Selangor, Malaysia, [4]Department of Veterinary Laboratory Diagnostics, Faculty of Veterinary Medicine, Universiti Putra Malaysia, UPM, Serdang, Selangor, Malaysia, [5]Department of Veterinary Clinical Studies, Faculty of Veterinary Medicine, Universiti Putra Malaysia, UPM, Serdang, Selangor, Malaysia

The advent of antimicrobials-resistant (AMR), including colistin-resistant bacteria, poses a significant challenge to animal and human health, food safety, socio-economic growth, and the global environment. This study aimed to ascertain the colistin resistance prevalence and molecular mechanisms of colistin resistance in *Enterobacteriaceae*. The colistin resistance was determined using broth microdilution assay, PCR; and Sanger sequencing of *mcr* genes responsible for colistin resistance in *Enterobacteriaceae* ($n = 627$), including *Escherichia coli* (436), *Salmonella* spp. ($n = 140$), and *Klebsiella pneumoniae* ($n = 51$), obtained from chicken and chicken meats. Out of 627 *Enterobacteriaceae*, 8.6% of isolates exhibited colistin resistance phenotypically. Among these colistin resistant isolates, 9.3% ($n = 37$) were isolated from chicken meat, 7.2% ($n = 11$) from the cloacal swab of chicken and 7.9% ($n = 6$) from the litter samples. Overall, 12.96% of colistin-resistant isolates were positive with *mcr* genes, in which *mcr-1* and *mcr-5* genes were determined in 11.11% and 1.85% of colistin-resistant isolates, respectively. The *E. coli* isolates obtained from chicken meats, cloacal swabs and litter samples were found positive for *mcr-1*, and *Salmonella* spp. originated from the chicken meat sample was observed with *mcr-5*, whereas no *mcr* genes were observed in *K. pneumoniae* strains isolated from any of the collected samples. The other colistin resistance genes, including *mcr-2, mcr-3, mcr-4, mcr-6, mcr-7, mcr-8, mcr-9,* and *mcr-10* were not detected in the studied samples. The *mcr-1* and *mcr-5* genes were sequenced and found to be 100% identical to the *mcr-1* and *mcr-5* gene sequences available in the NCBI database. This is the first report of colistin resistance *mcr-5* gene in Malaysia which could portend the emergence of *mcr-5* harboring bacterial strains for infection. Further studies are needed to characterize the *mr-5* harbouring bacteria for the determination of plasmid associated with *mcr-5* gene.

KEYWORDS

***Enterobacteriaceae*, MCR, colistin resistance, poultry, Malaysia**

Introduction

Antimicrobial agents are essential medicines in animals and humans to curb infections. Owing to the overuse and abuse of antimicrobial agents, the globe is being faced with the rapid proliferation of resistant microbes. Currently, the advent of antimicrobial-resistant (AMR) bacteria poses a significant challenge to animal and human health, food safety, socio-economic growth, and the global environment (Theuretzbacher, 2017). The proliferation of Gram-negative bacterial strains which are resistant to multiple drugs, and the absence of new drugs to combat such microbes, reintroduced colistin as a last-line therapy (Ezadi et al., 2019).

The resistance to colistin is a crucial problem to be tackled today. Numerous studies have demonstrated that this colistin resistance was present in various bacterial strains around the world. The plasmid-mediated *mcr* genes are accountable for exceptional colistin resistance, as it is a conduit that spreads via horizontal transmission from one bacterial strain to another and through food chain or direct contact to humans, animals, and the environments (Gharaibeh and Shatnawi, 2019). Before 2015, all documented colistin-resistance was chromosomally regulated, involving modification of a two-component regulatory structure, phoPQ and pmrAB with the negative regulator, *mgrB* gene alteration (Cannatelli et al., 2013; Liu et al., 2016). In 2016, the *Escherichia coli* strains isolated from humans, retail chicken meat and pork, and *Klebsiella pneumoniae* strains isolated from humans were reported with the plasmid-encoded *mcr-1* gene in China (Liu et al., 2016). The plasmid-mediated new *mcr* genes have rapidly emerged. The therapeutic effectiveness of colistin has been compromised by the advent of the plasmid-encoded *mcr* genes, including *mcr-1* to *mcr-10,* which were reported during the last four years (Ling et al., 2020). The *E. coli* isolates recovered from chicken liver, and chicken feed in the trough (Yu et al., 2016), and poultry meat in Malaysia were found positive for *mcr-1* gene (Aklilu and Raman, 2020).

Poultry meat is an important source of protein for humans, it could also be a significant conduit for spreading multidrug-resistant bacterial species from food-producing animals to humans. Previous study has shown that retail chicken meat plays a role in disseminating multiple antibiotic-resistant strains among humans and their environment, posing a severe threat to environmental health and food safety (Aidara-Kane et al., 2013). The colistin resistance-producing gene, *mcr-1*, was present in 52.1 percent of the *E. coli* isolates from raw chicken meat (Aklilu and Raman, 2020). Colistin resistance was found in more in 36.4% of bacteria from poultry chicken and 20% of strains isolated from native chicken in Bangladesh (Islam et al., 2020). In Nepal, it was reported that 27 (22.8%) of colistin-resistant *E. coli* in broiler farms carried the *mcr-1* gene (Joshi et al., 2019). Aside from that, the horizontal transmission is thought to be the main mechanism for the spread of colistin resistance *mcr* genes in *Enterobacteriaceae* worldwide (Gharaibeh and Shatnawi, 2019).

With potent *in vitro* transfer rates and frequently harboured alongside other resistance determinants like β -lactamases, *mcr* genes have been identified on a variety of conjugative plasmids (IncI2, IncHI2, IncX4, and pHNSHP45) (EMA (European Medicine Agencey), 2016). As the mobilized colistin resistance (*mcr*) genes driven by plasmids are quickly emerging, appropriate information on colistin resistance, including the incidence and epidemiological studies of *mcr*-positive cases, is required to apply steps to prevent and manage its dissemination. Therefore, the aim of the study was to determine the prevalence and molecular determinants underlying colistin resistance in *Enterobacteriaceae* (*E. coli, Salmonella* spp., and *Klebsiella pneumoniae*) isolates recovered from poultry and poultry meats in Malaysia.

Materials and methods

Ethics approval

The ethical board of Universiti Putra Malaysia (UPM), Institutional Animal Care and Use Committee (IACUC) approved the research study protocol for collecting cloacal swabs from live poultry (UPM/IACUC/AUP-R091/2019).

Study design and samples

The research study was performed in which chicken meat samples from supermarkets and cloacal swabs, and litter samples from chicken farms within Selangor, Malaysia (Figure 1) were collected from July 2019 to February 2021. Selangor is the densely populated area in Malaysia and most of the poultry farms are located in this state. Sterile plastic bags were used to collect the meat samples. The cloacal swab samples were collected aseptically from the healthy chicken and kept in sterile transport media, Stuart media. Litter samples were collected from the farms' floors using a sterile spoon, and placed in a sterile plastic bag. In total, 543 samples, including 350 chicken meats, 144 cloacal swabs, and 49 litter samples (Table 1), were collected from supermarkets and poultry farms in different areas of Selangor in Malaysia (Figure 1). All collected samples were immediately transported in a sealed icebox to the Bacteriology Laboratory, Faculty of Veterinary Medicine at Universiti Putra Malaysia (UPM), Serdang, Selangor, Malaysia.

Isolation and identification of bacterial strains

In the Enterobacteriaceae family, *Salmonella* spp., *E. coli,* and *K. pneumoniae* have public health importance and are more prevalent with colistin resistance *mcr* genes (Elbediwi et al., 2019). For this reason, *Salmonella* spp., *E. coli,* and *K. pneumoniae,* were isolated and identified phenotypically using the standard protocol of traditional cultural and biochemical tests (Ghafur et al., 2019; Sharma et al., 2019). In the pre-enrichment step, the samples were cultured in buffered peptone water (BPW, Oxoid, United Kingdom), including 25 g of meat in 225 mL, 10 g litter in 90 mL, and cloacal swabs in 10 mL BPW medium, samples were incubated at 37°C for 24 h. The meat samples with BPW were homogenized for 2 min in a stomacher. For *Salmonella* spp. isolation, 100 µL of homogenized BPW was mixed with 10 mL of Rappaport-Vassiliadis (RVS; Oxoid, United Kingdom). Then the RVS mixtures were incubated at 42°C for 24 h. One loop-full RVS of each sample was sub-cultured onto Xylose Lysine Deoxycholate agar (XLD; Oxoid, United Kingdom) and kept at 37°C for 24 h for incubation. On XLD, typically, Salmonella colonies were red with a black centre. One pure colony from XLD was cultured onto nutrient agar (NA, Oxoid, United Kingdom). For presumptive identification, biochemical tests (TSI, Urease, Citrate, and SIM) were performed with pure cultures grown onto NA. Serological confirmation of *Salmonella* spp. was

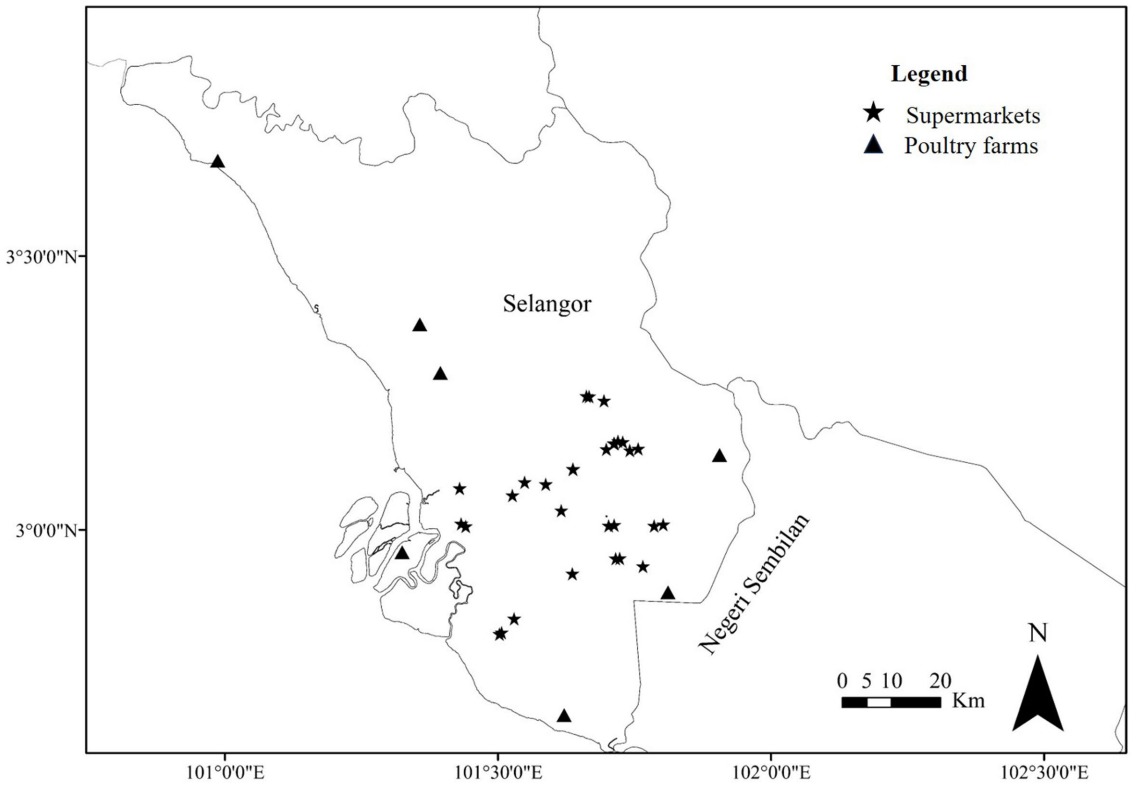

FIGURE 1
Map showing the sampling areas of Selangor, Malaysia. Star (*) and triangle (▲) marks indicating supermarkets and poultry farms, respectively. The geographic information software, ArcGIS v.10.4.1 for Windows was used to generate the sampling spot on the map.

TABLE 1 List of the primers and sequences for the confirmation of *E. coli, Salmonella* spp., and *Klebsiella pneumoniae.*

Organisms	Gene	Primers	Primer sequence	Size (bp)	References
E. coli	16 s rRNA	ECO-1	GACCTCGGTTTAGTTCACAGA	585	Moawad et al. (2018)
		ECO-2	CACACGCTGACGCTGACCA		
Salmonella spp.	*invA*	139-F	GTGAAATTATCGCCACGTTCGGGCAA	284	Rahn et al. (1992)
		141-R	TCATCGCACCGTCAAAGGAACC		
Klebsiella pneumoniae	*mdh*	Pf	ATTTGAAGAGGTTGCAAACGAT	130	Ranjbar et al. (2016)
		Pr1	TTCACTCTGAAGTTTTCTTGTGTTC		

performed using a slide agglutination test using Poly 'O' and 'H' antisera (Remel, United Kingdom). For *E. coli* and *K. pneumoniae* isolation, a loopful of suspension of BPW was inoculated onto MacConkey (Oxoid, United Kingdom). One presumptive colony of *E. coli* and *K. pneumoniae* were then sub-cultured onto NA and subjected to a standard biochemical test for their presumptive confirmation.

Molecular confirmation of *Escherichia coli*, *Salmonella* spp., and *Klebsiella pneumoniae*

The genomic DNA was extracted from the pure culture of the isolates cultured on nutrient agar using the boiling and snap chill method (Pui et al., 2011). The phenotypically positive *E. coli*, *Salmonella* spp., and *Klebsiella pneumoniae* species were then confirmed with conventional PCR with species-specific gene primers (Table 1), in which positive controls included *E. coli* ATCC 25922, *Salmonella* ATCC 14028 and *Klebsiella pneumoniae* ATCC 700603 (Rahn et al., 1992; Ranjbar et al., 2016; Moawad et al., 2018).

Colistin-susceptibility and minimum inhibitory concentration (MIC) assessment

Colistin-susceptibility and MIC in isolates were assessed by the ISO-20776 standard broth microdilution technique (BMD) jointly recommended by the EUCAST (2016a) with few modifications. In brief, a two-fold dilution (0.125–128 μg/mL) of the colistin sulfate salt (Sigma-Aldrich) was prepared on a 96 well microtitre plate. The bacterial inoculum was inoculated in each well with a final concentration of 5×10^5 CFU/mL. Then the microtitre plate was incubated at 37°C for 16–20 h. After the incubation period, 30 μL of 0.015% resazurin solution

was added to each well of the microtitre plate and incubated again at 37C for 1 h, during which the plate was routinely checked every 15 min. The colistin MICs were interpreted with the naked eye and recorded by observing the color change of resazurin (discoloration from blue to pink or purple indicates colistin resistance, while susceptibility is deduced when no color change- blue color). The test was performed in triplicates. During colistin-susceptibility testing, colistin-susceptible *E. coli* ATCC25922 and colistin-resistant (ColR) *E. coli* NCTC 13846 were utilized as negative and positive controls, respectively.

Detection of the colistin resistance determinants, *mcr* genes

Colistin-resistant *Enterobacteriaceae* isolates were identified with MIC values greater than 2 μg/mL colistin (EUCAST, 2016b). The genomic DNA of the colistin-resistant (col-R) isolates was assessed with conventional PCR to detect colistin resistance (*mcr*) gene variants (*mcr-1* to *mcr-10*). According to previous studies, the detection of *mcr-1* to *mcr-5* (Rebelo et al., 2018) and *mcr-6* to *mcr-9* (Borowiak et al., 2020) was performed with multiplex PCR. The uniplex PCR was performed for *mcr-10* (Xu et al., 2021) by the previously designed oligonucleotide primers and the protocol (Table 2).

PCR results analysis

Amplified PCR products were examined on 1.5% agarose (Conda, Madrid, Spain) prepared in 100 mL of 0.5 × TBE Buffer stained with 4 μL of Nucleic Acid stain (ETB "out" Nucleic Acid, Cat. No. FYD007-200P, Yestern Biotech Co. ltd, Taiwan) for *mcr* gene. The expected bands for *mcr-1* to *mcr-10* (Table 2) were visualized and photographed under UV light using AlphaImager 2,200 (AlphaImager, United States).

Confirmation of *mcr* (*mcr-1* and *mcr-5*) gene by sequencing

The amplified PCR products for the *mcr-1* gene of *E. coli* strains, *E. coli* E172, and *mcr-5* gene from one *Salmonella* spp. strain S283 were sent to commercial company for DNA sequencing with the same primers for Sanger sequencing (Table 2) and compared to previously reported *mcr-1* and *mcr-5* sequences in the NCBI database. The consensus sequences of *mcr-1* and *mcr-5* were obtained based on the alignment of the forward and reverse sequences using BioEdit v. 7.2 program (Hall, 1999).

Phylogenetic analysis

The *mcr* gene sequences were used in the phylogenetic tree construction, and analysis was carried out according to Li et al. (2019). The sequences from this study and those from GenBank for the *mcr-1* and *mcr-5* were aligned separately using the MEGA X software (Kumar et al., 2018) to compare their similarities. There are four different types of *mcr-5* gene variants such as *mcr-5.1, mcr-5.2, mcr-5.3* and *mcr-5.4* has been identified in the world. We have selected partial

TABLE 2 List of the primers and sequences for the confirmation of *mcr* genes.

Set	Primers	Primer sequences	Size (bp)	References
Set-1	mcr-1F	AGTCCGTTTGTTCTTGTGGC	320	Rebelo et al. (2018)
	mcr-1R	AGATCCTTGGTCTCGGCTTG		
	mcr-2F	CAAGTGTGTTGGTCGCAGTT	715	
	mcr-2R	TCTAGCCCGACAAGCATACC		
	mcr-3F	AAATAAAAATTGTTCCGCTTATG	929	
	mcr-3R	AATGGAGATCCCCGTTTTT		
	mcr-4F	TCACTTTCATCACTGCGTTG	1,116	
	mcr-4R	TTGGTCCATGACTACCAATG		
	mcr-5F	ATGCGGTTGTCTGCATTTATC	1,644	
	mcr-5R	TCATTGTGGTTGTCCTTTTCTG		
Set-2	mcr-6F-mp	AGCTATGTCAATCCCGTGAT	252	Borowiak et al. (2020)
	mcr-6R-mp	ATTGGCTAGGTTGTCAATC		
	mcr-7F-mp	GCCCTTCTTTTCGTTGTT	551	
	mcr-7R-mp	GGTTGGTCTCTTTCTCGT		
	mcr-8F-mp	TCAACAATTCTACAAAGCGTG	856	
	mcr-8R-mp	AATGCTGCGCGAATGAAG		
	mcr9-F-mp	TTCCCTTTGTTCTGGTTG	1,011	
	mcr9-R-mp	GCAGGTAATAAGTCGGTC		
Set-3	mcr-10-F	AGCCGTCTTGAACATGTGAG	744	Xu et al. (2021)
	mcr-10-R	CATACAGGGCACCGAGACTG		

sequences of these four *mcr-5* variants from GenBank in the NCBI database and analysed with our *mcr-5* sequence data. The phylogenetic tree for *mcr-1* and *mcr-5* was constructed with aligned sequences by the neighbor-joining method using the Kimura 2-parameter model, and Bootstrap values were calculated using 500 replicates.

Statistical analysis

Microsoft Excel sheets (MS-2019) were used to input data, which were then uploaded into the SPSS program v. 25.0 (IBM, Armonk, NY, United States). Descriptive analysis was used to quantify the prevalence, in which level of significance was assessed using the χ^2 test. For statistical significance, *p*- values less than 0.05 ($p < 0.05$) was taken into consideration.

Results

Frequency of *Enterobacteriaceae* isolates

In total, 627 *Enterobacteriaceae* (*E. coli*, *Salmonella* spp., and *K. pneumoniae*) isolates, including 398 isolates from meat samples from supermarkets, 153 isolates from cloacal swabs, and 76 isolates from litter samples from poultry farms, were isolated and identified (Table 3). The 398 isolates from meat samples from supermarkets were classified as *E. coli* ($n = 258$, 73.7%%), *Salmonella* spp. ($n = 122$, 34.9%) and *K. pneumoniae* ($n = 18$, 5.1%). The poultry cloacal swabs from poultry farms yielded *E. coli* ($n = 134$, 93.1%), *Salmonella* spp. ($n = 4$, 2.8%) and *K. pneumoniae* ($n = 15$, 10.4%), and litter samples from poultry farms generated *E. coli* ($n = 44$, 89.8%), *Salmonella* spp. ($n = 14$, 28.6%) and *K. pneumoniae* ($n = 18$, 36.7%). *Salmonella* spp. was highly prevalent in collected chicken meat samples ($p = 0.000$), *E. coli* in cloacal swab ($p = 0.000$), and *K. pneumoniae* was in litter samples ($p = 0.000$) (Table 3). *E. coli, Salmonella* spp., and *K. pneumoniae* isolates were confirmed by PCR showing a band size of 585 bp, 284 bp, and 130 bp, respectively.

Determination of phenotypic colistin susceptibility

Out of 627 *Enterobacteriaceae* isolates, 8.6% ($n = 54$) of isolates exhibited colistin resistance using the broth microdilution assay. Among these, 9.3% ($n = 37$) were isolated from chicken meat, 7.2% ($n = 11$) from the cloacal swab of chicken and 7.9% ($n = 6$) from the litter samples (Table 4). Overall, the phenotypic colistin resistance of the isolates from chicken meat, cloacal swabs, and litter samples was indifferent (Tables 4, $p = 0.712$). On the other hand, 54 colistin-resistant *Enterobacteriaceae* isolates were comprised of *E. coli* ($n = 32$, 7.34%), *Salmonella* spp. ($n = 16$, 11.4%), and *K. pneumoniae* ($n = 6$, 11.76%) (Figure 2).

Detection of colistin resistance determinants, *mcr* gene variants

All 54 isolated colistin-resistant (Col-R) *Enterobacteriaceae* were analyzed to observe the presence of *mcr-1* to *mcr-10*. Overall, 12.96% ($n = 7$) of colistin-resistant *Enterobacteriaceae* isolates were found possessing colistin resistance *mcr* genes comprising 8.1% ($n = 3$), 27.3% ($n = 3$), and 16.67% ($n = 1$) of Col-R isolates from the chicken meat, chicken and litter samples, respectively. Variations of colistin resistance from different sources were not statistically significant (*value of* $p > 0.05$) as shown in Table 4. Out of seven *mcr* harboring Col-R isolates, 11.11% ($n = 6$) and 1.85% ($n = 1$) were found with *mcr-1* and *mcr-5,* respectively. The *E. coli* isolates obtained from chicken meats, cloacal swabs and litter samples were found positive for *mcr-1*, and *Salmonella* spp. originated from the chicken meat sample was observed with *mcr-5*, whereas no *mcr* genes were observed in *K. pneumoniae* strains isolated from any of the collected samples (Figure 3). The other colistin resistance genes, including *mcr-2, mcr-3, mcr-4, mcr-6, mcr-7, mcr-8, mcr-9,* and *mcr-10* were not detected in the studied samples.

Confirmation of *mcr gene* variants

In BLAST analysis, our studied ¬*mcr-1* sequence was found to be 100% identical to the *mcr-1* sequence (Genbank: NG_050417.1) in the NCBI database with 99% query coverage. On the other hand, our studied ¬*mcr-5* sequence was found to be 100% identical to the *mcr-5* sequence (Genbank: NG_055658) in the NCBI database with 98% query coverage.

Minimum inhibitory concentration determination

The broth microdilution test was conducted to assess the MIC value of all isolates following EUCAST guidelines, with the epidemiological cutoff value >2 μg/mL for colistin resistance. Control strains, colistin-resistant isolates *Escherichia coli* NTCC 13846 and susceptible isolate *Escherichia coli* ATCC 25922, showed growth up to 4 μg/mL and 0.5 μg/mL colistin concentration, respectively. The MIC value of isolated colistin-resistant bacteria exhibited 4 to 128 μg/mL of colistin. The *mcr*-carrying isolates were observed with MIC values of 4 and 8 μg/mL colistin (Figure 4). In contrast, *mcr* negative colistin-resistant isolates had extremely high

TABLE 3 Prevalence of *Enterobacteriaceae* isolated from different sources.

Sources (Samples)	Types (Isolates)	*E. coli*	*p*-value	*Salmonella* spp.	*p*-value	*K. pneumoniae*	*p*-value
Supermarkets ($n = 350$)	Chicken meat ($n = 398$)	258 (73.7%)	0.000	122 (34.9%)	0.000	18 (5.1%)	0.000
Poultry farms ($n = 144$) ($n = 49$)	Cloacal swab ($n = 153$)	134 (93.1%)		4 (2.8%)		15 (10.4%)	
	Litter ($n = 76$)	44 (89.8%)		14 (28.6%)		18 (36.7%)	
Total ($n = 543$)	Total ($n = 627$)	436		140		51	

TABLE 4 Phenotypic colistin resistance and mechanism of colistin resistance with *mcr* genes in isolates from chicken meat, chicken and litter.

Source (isolates number)	Phenotypic colistin susceptibility, (%)			*mcr* gene in colistin-resistant isolates, (%)		
	Sensitive	Resistance	*p* value	Present	Absent	*p*-value
Chicken meat ($n=398$)	90.7%	9.3%	0.712	8.1%	91.9%	0.241
Chicken ($n=153$)	92.8%	7.2%		27.3%	72.7%	
Litter ($n=76$)	92.1%	7.9%		16.7%	83.3%	
Total ($n=627$)	91.4%	8.6%		12.96%	87%	

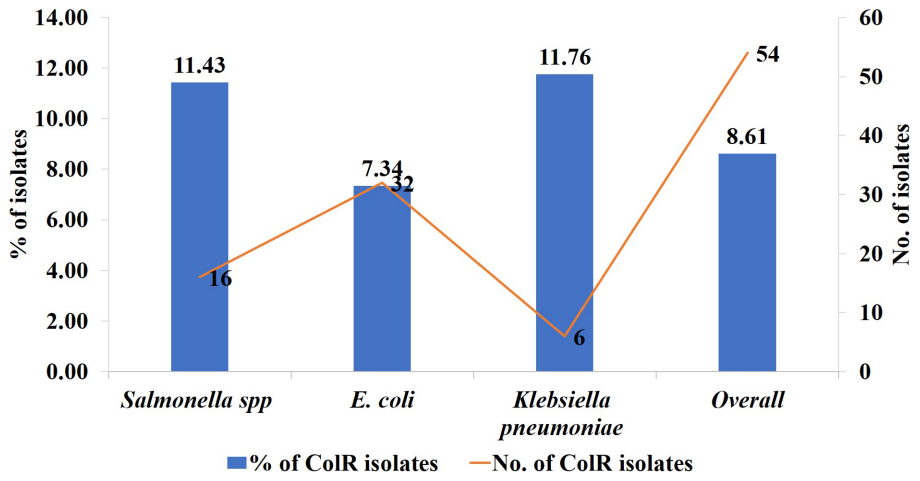

FIGURE 2
The rate trend and number of phenotypically colistin-resistant *Enterobacteriaceae* isolates, *E. coli*, *Salmonella* spp., and *K. pneumoniae*. The blue column = rate trend and red line = number of isolates, left y axis = % of colR isolates, right y axis = number of colR isolates.

MIC levels, 128 μg/mL colistin (Figure 4). Most of the Col-R isolates from three sources exhibited MIC values from 4 to 8 μg/mL of colistin (Supplementary Figure S1).

Phylogenetic comparison

In the phylogeny analysis, it is observed that *mcr-1* genes in the obtained isolates were divided into two clades, named clade A, including subclade I and subclade II, and clade B. The colistin resistance *mcr-1* gene sequence from *E. coli* strains E48, E13, E278, E297, E331 recovered from cloacal swabs and chicken meat samples were clustered in subclade I. These isolates were closely related to subclade II, grouped with *E. coli* and *Salmonella* spp. strains recovered from humans and animals obtained from the NCBI GenBank database. The nucleotide sequence of the *mcr-1* gene of *E. coli* E172 obtained from chicken litter samples was very close to the previously identified isolate in Malaysia and human isolate in China. On the other hand, *mcr-1* sequences of *E. coli* isolates recovered from chicken meats, and chicken cloacal swab samples were grouped in one cluster and were found close to isolates from China and Brazil (Figure 5).

In the phylogeny analysis of the *mcr-5* gene, it was revealed that the nucleotide sequence of the *mcr-5* gene of *Salmonella* spp. obtained from chicken meat has a close relation to the *mcr-5.3* gene in the *E. coli* isolate obtained from the horse in Brazil (Figure 6).

Discussion

The most common bacteria associated with bacterial infections in chickens are *E. coli*, *Salmonella* spp., and *K. pneumoniae*. These microorganisms are known to cause serious health issues, which can result in increased mortality, decreased productivity, and higher costs for both disease prevention and treatment (Ibrahim et al., 2021). *Escherichia coli* isolates were the most prevalent in the collected samples, followed by *Salmonella* spp. and *K. pneumoniae* isolates. *Escherichia coli* isolates were high prevalence in chicken cloacal swabs (93.1%), *Salmonella* spp. were in chicken meats (34.9%), and *K. pneumoniae* isolates were in litter samples (36.7%). Previous studies have also reported 83 and 53.04% of cloacal swabs were found positive for *E. coli* in Malaysia and China, respectively (Suryadevara et al., 2020; Li et al., 2022). In Indonesia, 13.75% of cloacal swabs obtained from broiler chicken farms were found positive for *K. pneumoniae* (Permatasari et al., 2020). Another study in Malaysia showed that the prevalence of *Salmonella* spp. and *E. coli* from cloacal swabs obtained from broilers were 6.5 and 51.8%, respectively (Ibrahim et al., 2021). Backyard chickens in Malaysia were documented with 2.5% of *Salmonella* spp. (Jajere et al., 2019). In contrast, a much higher prevalence of *Salmonella* spp. (48%) in chicken meat samples was observed in Bangladesh (Islam et al., 2016). In Nepal, 33.33% of chicken meat samples were positive for *E. coli* (Joshi et al., 2019) which is lower than our findings, indicating that the frequency of *E. coli* in chicken meat might vary widely. Different levels of hygienic practices in various geographic regions and environmental factors, such as

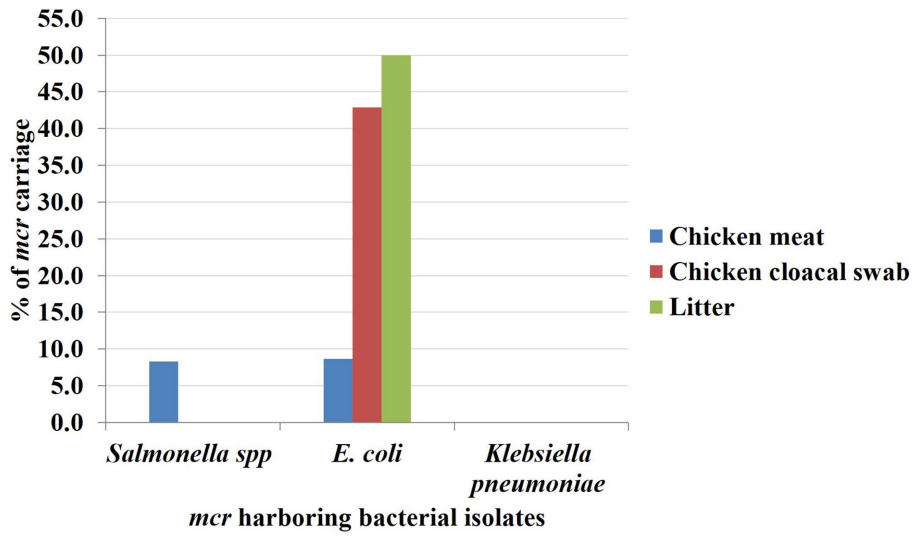

FIGURE 3
The rate of *Enterobacteriaceae* isolates harboring *mcr* gene based on sample sources. The rate of *mcr* genes was marked by blue, red and green bars to the Y-axis for chicken meat, chicken cloacal swab and litter samples, respectively.

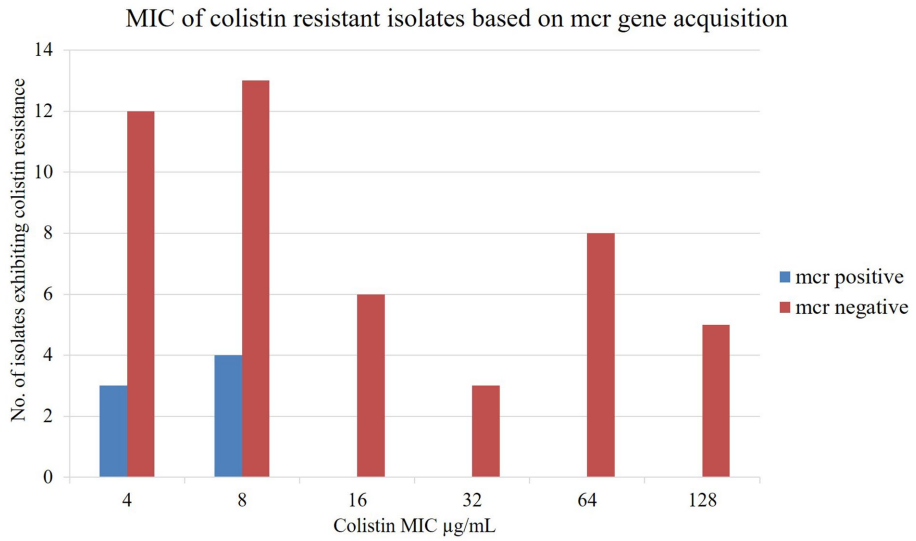

FIGURE 4
Colistin MICs of *Enterobacteriaceae* with the *mcr*-genes.

exposure to poor sanitation, could be the source of the variations in prevalence (Dawadi et al., 2021).

Colistin is being prescribed for the therapeutic purposes of bacterial infection in humans that are resistant to multiple drugs despite its side effects. The introduction of the colistin resistance (*mcr*) gene in bacterial strains that are already resistant to many antibiotics, creates the ineffectiveness of colistin, the last resort drug. In this study, the *Enterobacteriaceae* isolates recovered from various sources, comprising chicken meat from supermarkets and cloacal swabs and litter samples from poultry farms, were prevalent with colistin resistance and *mcr* genes. The MIC value of colistin-resistant isolates ranged from 4 µg/mL to 128 µg/mL of colistin, however, low MIC values were found in *mcr* positive isolates. In previous studies, the *mcr-1* had been documented from *Klebsiella pneumoniae,* and *E. coli* isolates in Malaysia (Yu et al., 2016; Mobasseri et al., 2019; Aklilu and Raman, 2020). The colistin resistance *mcr-1* gene is also observed in *E. coli* isolates from poultry in many countries in Asia (Trung et al., 2017; Joshi et al., 2019; Amin et al., 2020). A greater percentage of *mcr-1* (>94%) was depicted in bacterial strains from turkey and broiler feces in Germany (Irrgang et al., 2016). The colistin resistance gene (*mcr-1*) was found in 25.8% of poultry (turkey and chicken) meats from Italy (5 samples) and Germany (28 samples) but not in any samples (turkey and chicken meats) from Switzerland, Denmark, Austria, or Hungary, according to a Swiss study (Zurfluh et al., 2016). In Brazil, 19.5% of chicken meat and liver samples were positive for *E. coli* harboring *mcr-1* (Monte et al., 2017). All the

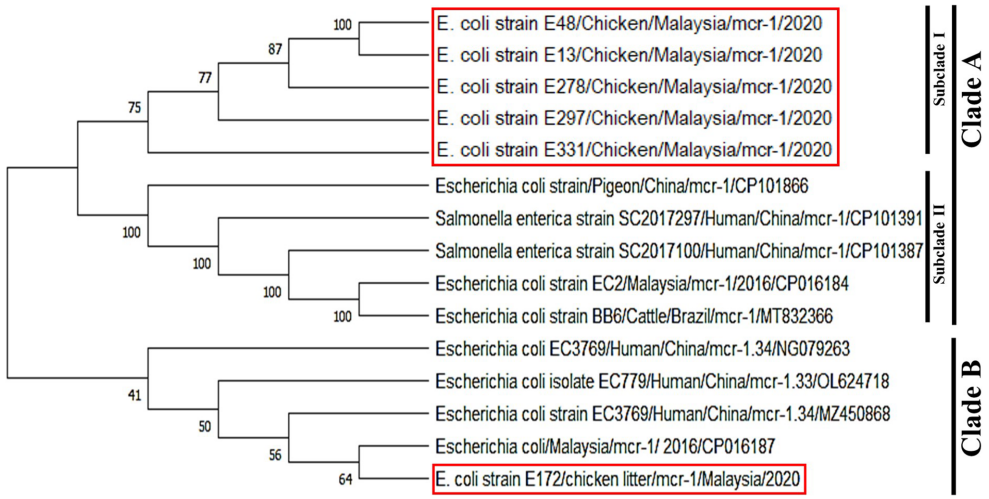

FIGURE 5
Phylogenetic tree of *mcr-1* gene showing the relationship of the partial coding regions of *mcr-1* gene sequences. The studied sequences were marked by red boxes. MEGA X was used to create the phylogenetic tree.

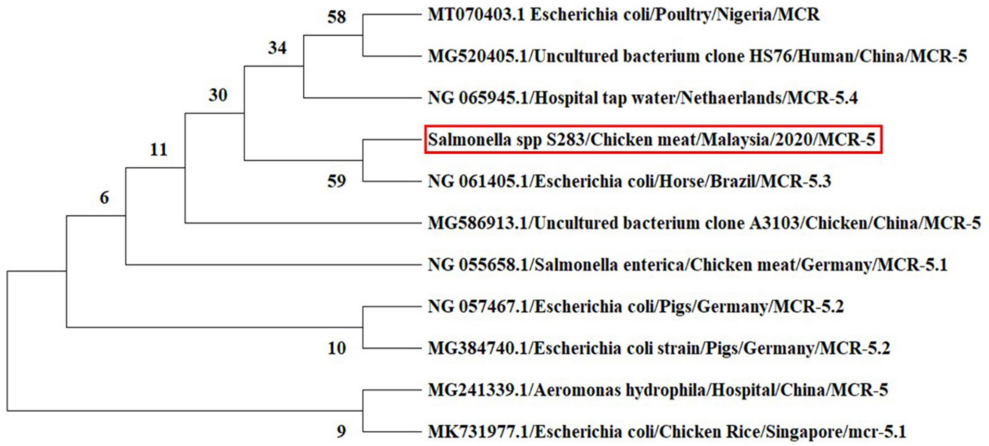

FIGURE 6
Phylogenetic tree inferred from the nucleotide sequences of *mcr-5* gene using the maximum likelihood method for distance calculations using MEGA X software. Bootstrap percentages retrieved in 500 replications are shown at the nodes. The studied sequence is marked by the red box.

colistin-resistant *E. coli* obtained from raw beef and beef products in Egypt were found positive for *mcr-1* (Sabala et al., 2021). In comparison with previous studies, a low prevalence of *mcr-1* gene in colistin-resistant isolates was found in the current research. The explanation for the low incidence in Malaysia isolates is unknown, although other resistance mechanisms, such as chromosomal alteration and modulation in the *mgrB* gene, could be involved (Chen et al., 2017).

The colistin resistance gene, *mcr-5* was detected in *Salmonella* spp. for the first time in Malaysia. There were no reports about this gene in any bacterial strains from animals or humans in Malaysia to the best of our knowledge. In this study, the *mcr-5* gene in *Salmonella* spp. was found at a very low rate. This finding is consistent with a previous report in which 2.5% (8/315) of colistin-resistant *Salmonella* spp. originated from pigs and meats (pork) in Germany (Borowiak et al., 2019), and 0.7% of human vaginal swab samples in Yangzhou in China (Zhang et al., 2018) were found to be positive for the *mcr-5* gene. The *mcr-5* gene was also observed in colistin-resistant *E. coli* strains obtained from cloacal swabs of poultry in Nigeria (Ngbede et al., 2020), veal in Belgium (Timmermans et al., 2021), pork samples in Cambodia (Pungpian et al., 2021) and poultry and pigs samples in Spain and China (García-Meniño et al., 2019). The situation is concerning because these resistant pathogens could be spread to humans through the food chain or close contact with animals (Dawadi et al., 2021).

The *mcr-1* gene was found among the isolates showing MIC values of 4 μg/mL and 8 μg/mL of colistin in this study which is consistent with the previous studies in Bangladesh and China, which showed that colistin-resistant isolates with *mcr-1* had a MIC value of 4 μg/mL, and 8 to 16 μg/mL of colistin, respectively (Islam et al., 2017; Amin et al., 2020).

In nucleotide BLAST, the sequences of the *mcr-1* gene isolated from *E. coli* and the *mcr-5* gene obtained from *Salmonella* spp. were found to be 100% identical to previously reported *mcr-1* and *mcr-5* gene sequences in the NCBI database. In the phylogenetic analysis, *mcr-1* gene sequences were closely related to previous reports, *mcr-1* gene sequence of *E. coli* isolates recovered from chicken in Malaysia (Yu et al., 2016) and *E. coli* strain isolated from human in China (Genbank_MZ450868). This suggests that *mcr-1* gene in *E. coli* has been circulating in Malaysia, which is a threat to animals and public health. The colistin resistance *mcr-5* gene was detected in *Salmonella* spp. isolate for the first time in Malaysia. The various types of *mcr-5* gene variants, including *mcr-5.1* to *mcr-5.4,* were identified in the world (Fleres et al., 2019; Ling et al., 2020). In the phylogeny, the *mcr-5* gene sequence of the current study was closely related to *mcr-5.3* gene recovered from *E. coli* isolates obtained from the horse in Brazil (GenBank database, NG_061405).

Conclusion

The introduction and dissemination of colistin resistance with *mcr* genes in *Enterobacteriaceae* is a major worldwide issue. Colistin-resistant *Enterobacteriaceae* were observed in poultry meats and poultry farms in the present study. The *mcr-1* and *mcr-5* genes were found in colistin-resistant *E. coli* and *Salmonella* spp., respectively. The *mcr-5* has been identified in Malaysia for the first time, which could signal the advent of *mcr-5* harboring bacterial strains for infection. The existence of *mcr*-positive *Enterobacteriaceae* in poultry and poultry meat in Malaysia emphasizes the importance of proper poultry waste disposal and good hygiene practices among people who are exposed to poultry and poultry meats.

Data availability statement

The nucleotide sequences of *mcr-1* and *mcr-5* have been submitted to the GenBank of the NCBI (accession no. OR333822, OR333835). The raw data supporting the findings of this article will be made available by the authors, without undue reservation.

Ethics statement

The animal study was reviewed and approved by the ethical board of Universiti Putra Malaysia (UPM), Institutional Animal Care and Use Committee (IACUC) approved the research study protocol for collecting cloacal swabs from live poultry (UPM/IACUC/AUP-R091/2019).

Author contributions

MK and ZZ: conceptualization, software, investigation, data curation, writing - original draft preparation, visualization, and acquisition. MK, ZZ, LH, NF, and NA: methodology, validation, and writing - review and editing. RK: formal analysis. ZZ: resources, supervision, and project administration. All authors contributed to the article and approved the submitted version.

Funding

This research was funded by the UPM trust fund (grant number: 6282525) in collaboration with Bangladesh Agricultural Research Council (BARC), Dhaka, Bangladesh.

Acknowledgments

The authors would like to thank the authorities of the Bangladesh Agriculture Research Council, Bangladesh, and Universiti Putra Malaysia for their financial support during this research.

Conflict of interest

The authors declare that the research was conducted in the absence of any commercial or financial relationships that could be construed as a potential conflict of interest.

Publisher's note

Supplementary material

The Supplementary material for this article can be found online at: https://www.frontiersin.org/articles/10.3389/fmicb.2023.1208314/full#supplementary-material

References

Aidara-Kane, A., Andremont, A., and Collignon, P. (2013). Antimicrobial resistance in the food chain and the AGISAR initiative. *J. Infect. Public Health* 6, 162–165. doi: 10.1016/j.jiph.2013.04.001

Aklilu, E., and Raman, K. (2020). MCR-1 gene encoded Colistin-resistant *Escherichia coli* in raw chicken meat and bean sprouts in Malaysia. *Int. J. Microbiol.* 2020:8853582. doi: 10.1155/2020/8853582

Amin, M. B., Sraboni, A. S., Hossain, M. I., Roy, S., Mozmader, T. A. U., Unicomb, L., et al. (2020). Occurrence and genetic characteristics of mcr-1-positive colistin-resistant *E. coli* from poultry environments in Bangladesh. *J. Glob. Antimicrob. Resist.* 22, 546–552. doi: 10.1016/j.jgar.2020.03.028

Borowiak, M., Baumann, B., Fischer, J., Thomas, K., Deneke, C., Hammerl, J. A., et al. (2020). Development of a novel mcr-6 to mcr-9 multiplex PCR and assessment of mcr-1 to mcr-9 occurrence in Colistin-resistant *Salmonella enterica* isolates from environment, feed, animals and food (2011–2018) in Germany. *Front. Microbiol.* 11:80. doi: 10.3389/fmicb.2020.00080

Borowiak, M., Hammerl, J. A., Deneke, C., Fischer, J., Szabo, I., and Malorny, B. (2019). Characterization of mcr-5-Harboring *Salmonella enterica* subsp. Enterica Serovar typhimurium isolates from animal and food origin in Germany. *Antimicrob. Agents Chemother.* 63:e00063-19. doi: 10.1128/AAC.00063-19

Cannatelli, A., D'Andrea, M. M., Giani, T., Di Pilato, V., Arena, F., Ambretti, S., et al. (2013). In vivo emergence of colistin resistance in *Klebsiella pneumoniae* producing KPC-type

carbapenemases mediated by insertional inactivation of the PhoQ/PhoP mgrB regulator. *Antimicrob. Agents Chemother.* 57, 5521–5526. doi: 10.1128/AAC.01480-13

Chen, Y., Luo, Y., Pettengill, J., Timme, R., Melka, D., Doyle, M., et al. (2017). Singleton sequence type 382, an emerging clonal Group of *Listeria monocytogenes* associated with three multistate outbreaks linked to contaminated stone fruit, caramel apples, and leafy green salad. *J. Clin. Microbiol.* 55, 931–941. doi: 10.1128/JCM.02140-16

Dawadi, P., Bista, S., and Bista, S. (2021). Prevalence of Colistin-resistant *Escherichia coli* from poultry in south Asian developing countries. *Vet. Med. Int.* 2021, 1–5. doi: 10.1155/2021/6398838

Elbediwi, M., Li, Y., Paudyal, N., Pan, H., Li, X., Xie, S., et al. (2019). Global burden of Colistin-resistant bacteria: mobilized Colistin resistance genes study. *Microorganisms* 7, 1–18. doi: 10.3390/microorganisms7100461

EMA (European Medicine Agency) (2016). Updated Advice on the Use of Colistin Products in Animals within the European Union: Development of Resistance and Possible Impact on Human and Animal Health. European Medicines Agency, Committee for Medicinal Products for Veterinary Use (CVMP); London, UK.

EUCAST (2016a) Recommendations for MIC determination of colistin (polymyxin E) As recommended by the joint CLSI-EUCAST Polymyxin Breakpoints Working Group. Available at: https://Www.Eucast.Org

EUCAST (2016b). *EUCAST breakpoint tables for interpretation of MICs and zone diameters,version 1.0*. Basel: European Committee on Antimicrobial Susceptibility Testing. Version 6.

Ezadi, F., Ardebili, A., and Mirnejad, R. (2019). Antimicrobial susceptibility testing for Polymyxins: challenges, issues, and recommendations. *J. Clin. Microbiol.* 57, 1–20. doi: 10.1128/JCM.01390-18

Fleres, G., Couto, N., Schuele, L., Chlebowicz, M. A., Mendes, C. I., Van Der Sluis, L. W. M., et al. (2019). Detection of a novel mcr-5.4 gene variant in hospital tap water by shotgun metagenomic sequencing. *J. Antimicrob. Chemother.* 74, 3626–3628. doi: 10.1093/jac/dkz363

García-Meniño, I., Díaz-Jiménez, D., García, V., de Toro, M., Flament-Simon, S. C., Blanco, J., et al. (2019). Genomic characterization of prevalent mcr-1, mcr-4, and mcr-5 *Escherichia coli* within swine enteric Colibacillosis in Spain. *Front. Microbiol.* 10:2469. doi: 10.3389/fmicb.2019.02469

Ghafur, A., Shankar, C., GnanaSoundari, P., Venkatesan, M., Mani, D., Thirunarayanan, M. A., et al. (2019). Detection of chromosomal and plasmid-mediated mechanisms of colistin resistance in Escherichia coli and *Klebsiella pneumoniae* from Indian food samples. *J. Glob. Antimicrob. Resist.* 16, 48–52. doi: 10.1016/j.jgar.2018.09.005

Gharaibeh, M. H., and Shatnawi, S. Q. (2019). An overview of colistin resistance, mobilized colistin resistance genes dissemination, global responses, and the alternatives to colistin: a review. *Vet. World* 12, 1735–1746. doi: 10.14202/vetworld.2019.1735-1746

Hall, T. A. (1999). BioEdit: a user-friendly biological sequence alignment editor and analysis program for windows 95/98/NT. *Nucl. Acids. Symp. Ser.* 41, 95–98.

Ibrahim, S., Wei Hoong, L., Lai Siong, Y., Mustapha, Z., CS, C. W. Z., Aklilu, E., et al. (2021). Prevalence of antimicrobial resistance (AMR) salmonella spp. and *Escherichia coli* isolated from broilers in the East Coast of peninsular Malaysia. *Antibiotics* 10. doi: 10.3390/antibiotics10050579

Irrgang, A., Roschanski, N., Tenhagen, B. A., Grobbel, M., Skladnikiewicz-Ziemer, T., Thomas, K., et al. (2016). Prevalence of mcr-1 in *E. coli* from livestock and food in Germany, 2010-2015. *PLoS One* 11:e0159863. doi: 10.1371/journal.pone.0159863

Islam, M. J., Mahbub-E-Elahi, A. T. M., Ahmed, T., and Hasan, M. K. (2016). Isolation and identification of salmonella spp. from broiler and their antibiogram study in Sylhet, Bangladesh. *J. Appl. Biol. Biotechnol.* 4, 046–051. doi: 10.7324/jabb.2016.40308

Islam, A., Rahman, Z., Monira, S., Rahman, M. A., Camilli, A., George, C. M., et al. (2017). Colistin resistant *Escherichia coli* carrying mcr-1 in urban sludge samples: Dhaka, Bangladesh. *Gut Pathog.* 9:77. doi: 10.1186/s13099-017-0227-4

Islam, S., Urmi, U. L., Rana, M., Sultana, F., Jahan, N., Hossain, B., et al. (2020). High abundance of the colistin resistance gene mcr-1 in chicken gut-bacteria in Bangladesh. *Sci. Rep.* 10:17292. doi: 10.1038/s41598-020-74402-4

Jajere, S. M., Hassan, L., Abdul Aziz, S., Zakaria, Z., Abu, J., Nordin, F., et al. (2019). Salmonella in native "village" chickens (Gallus domesticus): prevalence and risk factors from farms in south-central peninsular Malaysia. *Poult. Sci.* 98, 5961–5970. doi: 10.3382/ps/pez392

Joshi, P. R., Thummeepak, R., Paudel, S., Acharya, M., Pradhan, S., Banjara, M. R., et al. (2019). Molecular characterization of Colistin-resistant *Escherichia coli* isolated from chickens: first report from Nepal. *Microb. Drug Resist.* 25, 846–854. doi: 10.1089/mdr.2018.0326

Kumar, S., Stecher, G., Li, M., Knyaz, C., and Tamura, K. (2018). MEGA X: molecular evolutionary genetics analysis across computing platforms. *Mol. Biol. Evol.* 35, 1547–1549. doi: 10.1093/molbev/msy096

Li, J., Liu, S., Fu, J., Yin, J., Zhao, J., Zhong, C., et al. (2019). Co-occurrence of Colistin and Meropenem resistance determinants in a Stenotrophomonas strain isolated from sewage water. *Microb. Drug Resist.* 25, 317–325. doi: 10.1089/mdr.2018.0418

Li, Z., Xin, L., Peng, C., Liu, C., Wang, P., Yu, L., et al. (2022). Prevalence and antimicrobial susceptibility profiles of ESBL-producing *Klebsiella pneumoniae* from broiler chicken farms in Shandong Province, China. *Poult. Sci.* 101:102002. doi: 10.1016/j.psj.2022.102002

Ling, Z., Yin, W., Shen, Z., Wang, Y., Shen, J., and Walsh, T. R. (2020). Epidemiology of mobile colistin resistance genes mcr-1 to mcr-9. *J. Antimicrob. Chemother.* 75, 3087–3095. doi: 10.1093/jac/dkaa205

Liu, Y.-Y., Ang, Y., Walsh, T. R., Yi, L.-X., Zhang, R., Spencer, J., et al. (2016). Emergence of plasmid-mediated colistin resistance mechanism MCR-1 in animals and human beings in China: a microbiological and molecular biological study. *Lancet Infect. Dis.* 16, 161–168. doi: 10.1016/S1473-3099(15)00424-7

Moawad, A. A., Hotzel, H., Neubauer, H., Ehricht, R., Monecke, S., Tomaso, H., et al. (2018). Antimicrobial resistance in Enterobacteriaceae from healthy broilers in Egypt: emergence of colistin-resistant and extended-spectrum β-lactamase-producing *Escherichia coli*. *Gut Pathog.* 10, 1–12. doi: 10.1186/s13099-018-0266-5

Mobasseri, G., Teh, C. S. J., Ooi, P. T., and Thong, K. L. (2019). The emergence of colistin-resistant *Klebsiella pneumoniae* strains from swine in Malaysia. *J. Glob. Antimicrob. Resist.* 17, 227–232. doi: 10.1016/j.jgar.2018.12.015

Monte, D. F., Mem, A., Fernandes, M. R., Cerdeira, L., Esposito, F., Galvão, J. A., et al. (2017). Chicken meat as a reservoir of colistin-resistant *Escherichia coli* strains carrying mcr-1 genes in South America. *Antimicrob. Agents Chemother.* 61, 2–5. doi: 10.1128/AAC.02718-16

Ngbede, E. O., Poudel, A., Kalalah, A., Yang, Y., Adekanmbi, F., Adikwu, A. A., et al. (2020). Identification of mobile colistin resistance genes (mcr-1.1, mcr-5 and mcr-8.1) in Enterobacteriaceae and *Alcaligenes faecalis* of human and animal origin, Nigeria. *Int. J. Antimicrob. Agents* 56:106108. doi: 10.1016/j.ijantimicag.2020.106108

Permatasari, D. A., Witaningrum, A. M., Wibisono, F. J., and Effendi, M. H. (2020). Detection and prevalence of multidrug-resistant *Klebsiella pneumoniae* strains isolated from poultry farms in Blitar, Indonesia. *Biodiversitas* 21, 4642–4647. doi: 10.13057/biodiv/d211024

Pui, C. F., Wong, W. C., Chai, L. C., Nillian, E., Ghazali, F. M., Cheah, Y. K., et al. (2011). Salmonella Typhi and *Salmonella Typhi*murium in sliced fruits using multiplex PCR. *Food Control* 22, 337–342. doi: 10.1016/j.foodcont.2010.05.021

Pungpian, C., Lee, S., Trongjit, S., Sinwat, N., Angkititrakul, S., Prathan, R., et al. (2021). Colistin resistance and plasmid-mediated mcr genes in Escherichia coli and salmonella isolated from pigs, pig carcass and pork in Thailand, Lao PDR and Cambodia border provinces. *J. Vet. Sci.* 22, 1–15. doi: 10.4142/jvs.2021.22.e68

Rahn, K., De Grandis, S. A. A., Clarke, R. C. C., McEwen, S. A. A., Galán, J. E. E., Ginocchio, C., et al. (1992). Amplification of an invA gene sequence of *Salmonella typhimurium* by polymerase chain reaction as a specific method of detection of salmonella. *Mol. Cell. Probes* 6, 271–279. doi: 10.1016/0890-8508(92)90002-F

Ranjbar, R., Izadi, M., Hafshejani, T. T., and Khamesipour, F. (2016). Molecular detection and antimicrobial resistance of *Klebsiella pneumoniae* from house flies (*Musca domestica*) in kitchens, farms, hospitals and slaughterhouses. *J. Infect. Public Health* 9, 499–505. doi: 10.1016/j.jiph.2015.12.012

Rebelo, A. R., Bortolaia, V., Kjeldgaard, J. S., Pedersen, S. K., Leekitcharoenphon, P., Hansen, I. M., et al. (2018). Multiplex PCR for detection of plasmid-mediated colistin resistance determinants, mcr-1, mcr-2, mcr-3, mcr-4 and mcr-5 for surveillance purposes. *Eur. Secur.* 23:17-00672. doi: 10.2807/1560-7917.ES.2018.23.6.17-00672

Sabala, R. F., Usui, M., Tamura, Y., Abd-Elghany, S. M., Sallam, K. I., and Elgazzar, M. M. (2021). Prevalence of colistin-resistant *Escherichia coli* harbouring mcr-1 in raw beef and ready-to-eat beef products in Egypt. *Food Control* 119:107436. doi: 10.1016/j.foodcont.2020.107436

Sharma, J., Kumar, D., Hussain, S., Pathak, A., Shukla, M., Kumar, V. P., et al. (2019). Prevalence, antimicrobial resistance and virulence genes characterization of nontyphoidal salmonella isolated from retail chicken meat shops in northern India. *Food Control* 102, 104–111. doi: 10.1016/j.foodcont.2019.01.021

Suryadevara, N., Yong, K. B., Ganapathy, B., Subramonie, S., Ragavan, N. D., Ramachandiran, M., et al. (2020). Molecular characterization of *Escherichia coli* from chickens in poultry farms of Malaysia. *Res. J. Biotechnol.* 15, 1–10.

Theuretzbacher, U. (2017). Global antimicrobial resistance in gram-negative pathogens and clinical need. *Curr. Opin. Microbiol.* 39, 106–112. doi: 10.1016/j.mib.2017.10.028

Timmermans, M., Wattiau, P., Denis, O., and Boland, C. (2021). Colistin resistance genes mcr-1 to mcr-5, including a case of triple occurrence (mcr-1, −3 and −5), in *Escherichia coli* isolates from faeces of healthy pigs, cattle and poultry in Belgium, 2012–2016. *Int. J. Antimicrob. Agents* 57:106350. doi: 10.1016/j.ijantimicag.2021.106350

Trung, N. V., Matamoros, S., Carrique-Mas, J. J., Nghia, N. H., Nhung, N. T., Chieu, T. T. B., et al. (2017). Zoonotic transmission of mcr-1 Colistin resistance gene from small-scale poultry farms, Vietnam. *Emerg. Infect. Dis.* 23, 529–532. doi: 10.3201/eid2303.161553

Xu, T., Zhang, C., Ji, Y., Song, J., Liu, Y., Guo, Y., et al. (2021). Identification of mcr-10 carried by self-transmissible plasmids and chromosome in Enterobacter roggenkampii strains isolated from hospital sewage water. *Environ. Pollut.* 268:115706. doi: 10.1016/j.envpol.2020.115706

Yu, C. Y., Ang, G. Y., Chin, P. S., Ngeow, Y. F., Yin, W.-F., and Chan, K.-G. (2016). Emergence of mcr-1-mediated colistin resistance in *Escherichia coli* in Malaysia. *Int. J. Antimicrob. Agents* 47, 504–505. doi: 10.1016/j.ijantimicag.2016.04.004

Zhang, J., Chen, L., Wang, J., Butaye, P., Huang, K., Qiu, H., et al. (2018). Molecular detection of colistin resistance genes (mcr-1 to mcr-5) in human vaginal swabs. *BMC. Res. Notes* 11:143. doi: 10.1186/s13104-018-3255-3

Zurfluh, K., Tasara, T., Poirel, L., Nordmann, P., and Stephan, R. (2016). Draft genome sequence of *Escherichia coli* S51, a chicken isolate Harboring a chromosomally encoded mcr-1 gene. *Genome Announc.* 4:e00796-16. doi: 10.1128/genomeA.00796-16

frontiers | Frontiers in Microbiology

TYPE Methods
PUBLISHED 09 August 2023
DOI 10.3389/fmicb.2023.1229542

OPEN ACCESS

EDITED BY
Zuowei Wu,
Iowa State University, United States

REVIEWED BY
Valerio Giaccone,
Dipartimento di Medicina Animale, Produzioni e Salute Università di Padova, Italy
Ruichao Li,
Yangzhou University, China

*CORRESPONDENCE
Rene S. Hendriksen
✉ rshe@food.dtu.dk

RECEIVED 26 May 2023
ACCEPTED 12 July 2023
PUBLISHED 09 August 2023

CITATION
Hendriksen RS, Cavaco LM, Guerra B, Bortolaia V, Agersø Y, Svendsen CA, Nielsen HN, Kjeldgaard JS, Pedersen SK, Fertner M and Hasman H (2023) Evaluation and validation of laboratory procedures for the surveillance of ESBL-, AmpC-, and carbapenemase-producing *Escherichia coli* from fresh meat and caecal samples. *Front. Microbiol.* 14:1229542. doi: 10.3389/fmicb.2023.1229542

Evaluation and validation of laboratory procedures for the surveillance of ESBL-, AmpC-, and carbapenemase-producing *Escherichia coli* from fresh meat and caecal samples

Rene S. Hendriksen[1]*, Lina M. Cavaco[2], Beatriz Guerra[3], Valeria Bortolaia[2], Yvonne Agersø[4], Christina Aaby Svendsen[1], Hanne Nørgaard Nielsen[1], Jette Sejer Kjeldgaard[1], Susanne Karlsmose Pedersen[1], Mette Fertner[1] and Henrik Hasman[2]

[1]National Food Institute, Technical University of Denmark (DTU Food), European Union Reference Laboratory for Antimicrobial Resistance, Research Group for Global Capacity Building, Kgs. Lyngby, Denmark, [2]Department for Bacteria, Parasites and Fungi, Statens Serum Institut, Reference Laboratory for Antimicrobial Resistance, Copenhagen, Denmark, [3]European Food Safety Authority, Parma, Italy, [4]Department of Veterinary and Animal Sciences, University of Copenhagen University, Copenhagen, Denmark

Introduction: Extended-spectrum β-lactamase- (ESBL) and AmpC- β-lactamase-producing *Enterobacterales* are widely distributed and emerging in both human and animal reservoirs worldwide. A growing concern has emerged in Europe following the appearance of carbapenemase-producing *Escherichia coli* (*E. coli*) in the primary production of food animals. In 2013, the European Commission (EC) issued the Implementing Decision on the monitoring and reporting of antimicrobial resistance in zoonotic and commensal bacteria. The European Union Reference Laboratory for Antimicrobial Resistance (EURL-AR) was tasked with providing two laboratory protocols for samples derived from meat and caecal content, respectively, for the isolation of ESBL- and AmpC-producing *E. coli* (part 1) and carbapenemase-producing (CP) *E. coli* (part 2). In this study, we describe the current protocols, including the preparatory work for the development.

Methods: Up to nine laboratory procedures were tested using minced meat as the matrix from beef, pork, and chicken as well as six procedures for the caecal content of cattle, pigs, and chicken. Variables included sample volume, pre-enrichment volume, pre-enrichment broth with and without antimicrobial supplementation, and incubation time/temperature. The procedures were evaluated against up to nine *E. coli* strains harboring different AMR genes and belonging to the three β-lactamase groups.

Results and discussion: The laboratory procedures tested revealed that the most sensitive and specific methodologies were based on a Buffered Peptone Water pre-enrichment of 225 ml to 25 g or 9 ml to 1 g for minced meat and caecal content, respectively, incubated at 37°C overnight, followed by inoculation onto MacConkey agar supplemented with 1 mg/L cefotaxime for detecting ESBL- and AmpC-producing *E. coli* and Chrom ID SMART (Chrom ID CARBA and OXA) for CP *E. coli,* incubated overnight at 37 and 44°C, respectively. We provided two isolation protocols for the EU-specific monitoring of ESBL- and AmpC- producing *E. coli* (part 1) and CP *E. coli* (part 2) from fresh meat (protocol 1) and caecal (protocol 2) samples, which

have been successfully implemented by all EU Member States for the monitoring period 2014–2027 (EU 2020/1729).

KEYWORDS

extended-spectrum beta-lactamase, carbapenemase, isolation method, *Escherichia coli*, protocol, surveillance, European Union

Introduction

Extended-spectrum β-lactamase- (ESBL) and AmpC-β-lactamase-producing *Enterobacterales* are widely distributed and emerging in both human and animal reservoirs worldwide (Madec et al., 2017; Mughini-Gras et al., 2019; Dantas and Ferreira, 2020; Aworh et al., 2022). During the last decade, a growing concern has emerged in Europe following the appearance of carbapenemase-producing (CP) *Escherichia coli* (*E. coli*) and *Salmonella infantis*, harboring the bla_{VIM-1} gene isolated from German pigs and chickens in 2011 (Fischer et al., 2012, 2013, 2017; Guerra et al., 2014; Borowiak et al., 2017; Irrgang et al., 2017, 2019; Madec et al., 2017). Since then, several other examples of CP *Enterobacterales* (CPE) have emerged in primary production in Europe, exemplified by *E. coli* isolated in 2015 from meat products at retail in Belgium harboring bla_{VIM-1} (Garcia-Graells et al., 2020), *E. coli* isolated from poultry and poultry meat in Romania in 2016 harboring bla_{OXA-48}-like ($bla_{OXA-162}$) (Bortolaia et al., 2021), *E. coli* in Italy in 2019 harboring bla_{NDM-4} (Diaconu et al., 2020), *E. coli* in pigs in Germany in 2019 harboring bla_{OXA-48} and bla_{GES-5} (Irrgang et al., 2020b), and *E. coli* in broilers in Austria in 2020 harboring bla_{VIM-1} (European Food Safety Authority European Centre for Disease Prevention Control, 2023). More recent examples include *E. coli* isolated from fattening pigs harboring bla_{OXA-48} and from a veal calf and fattening pigs in Italy in 2021 harboring $bla_{OXA-181}$ (Carfora et al., 2022; European Food Safety Authority European Centre for Disease Prevention Control, 2023), as well as *E. coli* from fattening pigs in Czechia and *E. coli* from fattening pigs and calves in Hungary harboring bla_{NDM-5} (European Food Safety Authority European Centre for Disease Prevention Control, 2023). Similar findings have also been reported to be emerging outside Europe, in China (Li et al., 2019; Shi et al., 2021), Egypt (Hamza et al., 2016), Australia, and India (Kock et al., 2018).

One of the many drivers behind the emergence of ESBL, AmpC-β-lactamase, and CPE is the likely transmission by horizontal gene transfer, which persists among humans and in the primary production of animals, such as broilers, in the EU (Carattoli, 2008; Mughini-Gras et al., 2019).

The World Health Organization (WHO), the World Organization for Animal Health (WOAH), and the European Medicine Agency (EMA) have, thus, all issued lists of critically important antimicrobial agents for human and veterinary medicine (https://www.ema.europa.eu/en/documents/report/categorisation-antibiotics-european-union-answer-request-european-commission-updating-scientific_en.pdf). Both lists define 3rd and 4th generation cephalosporins, as well as carbapenems, as critically important antimicrobials. Hence, the surveillance of antimicrobial resistance against these antimicrobials in sources outside the human reservoir, e.g., in the food chain, is crucial in early warning systems to enable control and prevent further spread to the public.

Striving toward a harmonized and standardized monitoring of antimicrobial resistance among food and food-producing animals in the EU, the European Commission (EC) on 12 November 2013 issued the Implementing Decision on the monitoring and reporting of antimicrobial resistance in zoonotic and commensal bacteria (European Union, 2013), which was repealed in 2021 by the Implementing Decision (EU) 2020/1729 of 17 November 2020 (European Union, 2020). These regulations laid down rules on the specific monitoring of ESBL-, AmpC-, and CP *E. coli* from meat and caecal samples originating from cattle, pigs, and poultry, stipulating that all member states were obliged to follow the protocol of the European Union Reference Laboratory for Antimicrobial Resistance (EURL-AR). Thus, the EURL-AR was tasked with providing a laboratory protocol for the isolation of ESBL-, AmpC-, and CP *E. coli* from meat and caecal samples (https://www.eurl-ar.eu/protocols.aspx).

In this study, we describe the two European Union Reference Laboratory for Antimicrobial Resistance (EURL-AR) protocols, including parts 1 and 2, used in the monitoring and reporting of antimicrobial resistance in zoonotic and commensal bacteria according to the Implementing Decisions 2013/652/EU and 2020/1729, including the preparatory work for the development.

Methods

Sample description

All samples of minced beef, pork, and chicken meat originated from Denmark and were purchased as fresh meat directly from retail supermarkets and transported to the National Food Institute, Technical University of Denmark (DTU Food) in Denmark in polystyrene boxes to maintain the cold chain. Subsequently, the minced meat was stored at 4°C in refrigerators before further processing.

Caecal samples (chicken) and caecal content (pig and cattle) were obtained from Danish slaughterhouses taking part in the EU monitoring. The caecal samples were collected directly from the slaughterhouses and transported to DTU Food in polystyrene boxes to maintain the cold chain. The caecal samples and content were stored at 4°C in refrigerators before further processing, including extracting the caecal content from chickens and pooling five per batch.

Test isolates

When developing the protocols of meat (protocol 1) and caecal content (protocol 2) samples to detect ESBL- and AmpC-producing *E. coli* (part 1) and CP *E. coli* (part 2), the following resistance genes were included in the test panel. *E. coli* isolates harboring relevant and common genes conferring resistance to 3rd generation cephalosporins and carbapenems were used in validation experiments as positive controls: $bla_{CTX-M-1}$ (0412004714_F1), bla_{SHV-12} (0412055161_F131), bla_{TEM-52} (7633094_7), and bla_{CMY-2} (0412056488_F191), all part of DANMAP 2012 (DANMAP, 2012). To detect CP *E. coli*, representative strains carrying bla_{VIM-1} (R178) (Fischer et al., 2012), bla_{NDM-1} (#271) (Poirel et al., 2011), bla_{OXA-48} (KMU AUH), and bla_{KPC-2} (17/11 RKI) were also included in the test panel (Table 1). The *E. coli* ATCC 25922 was used as the susceptible quality control (QC) strain.

Validation experiments for detecting specific ESBL- and AmpC-producing *E. coli* (part 1) — Rationale for the initial set of validation experiments

The final protocols should detect bacteria with reduced susceptibility to 3rd generation cephalosporins (part 1) present in meat and caecal samples. Therefore, a broad selection of *E. coli* isolates carrying various genes related to this reduced susceptibility (including carbapenemases) was included in the first part of the validation experiments.

Spiking procedures of the minced meat samples

From nine batches of 1,500 g retailed minced meat, one batch per nine *E. coli* isolates was divided into six portions of 190 g and six portions of 10 g. The different portions were labeled with the isolate number and with one of the following concentrations: 0, 0.1, 1, 10, 100, and 1,000 CFU/g. One 10 g sample labeled 0 CFU/g for each of the nine 1,500 g retailed minced meat samples was selected as the negative control to ensure that the meat was not already contaminated with an ESBL-producing, AmpC-producing, and CP organism (CPO). The remaining five 10 g samples of each of the nine 1,500 g retailed minced meat samples were spiked individually with one of the nine *E. coli* test strains. The samples were spiked with 0.9% NaCl suspensions containing each of the nine individual *E. coli* test strains to contain 0.1, 1, 10, 100, and 1,000 CFU/g per final weight of 200 g. The lowest dilution step of 0.1 CFU/g was included to ensure an extra dilution in case the experiment did not provide a precise CFU count. In brief, the spiking was prepared as follows: individual *E. coli* test strains were cultured overnight (o/n) at 37°C in 10 ml Luria-Bertani (LB) broth (Sigma-Aldrich) supplemented with 1 mg/L cefotaxime, except for the susceptible control strain (*E. coli* ATCC 25922) and the bla_{OXA-48} strain. The o/n cultures were cooled on ice for 30 min before centrifugation (8,000 g, 10 min) in 10 ml cold 0.9% NaCl. Subsequently, the optical density (OD) was adjusted to OD600 = 0.25 by using 1–4 ml of saline as a starting point (dilution 0). Further serial 10-fold dilutions (10^{-2} to 10^{-6}) were prepared from the stock by transferring 1 ml into 9 ml cold 0.9% NaCl and thoroughly mixing it for 20 s between each dilution. After preparing the dilutions, the CFU was assessed in dilutions of 10^{-4}, 10^{-5}, and 10^{-6} in triplicates. Briefly, 100 µl of each dilution was plated onto LB agar plates (nine plates in total) and incubated at 37°C o/n. Subsequently, the CFUs were enumerated and recorded.

The previously prepared suspensions were used for spiking by mixing 2 mL of different dilutions of pre-adjusted bacterial suspensions (final dilutions between 10^{-3} and 10^{-7} containing between 20 and 2×10^5 bacteria per 2 mL) in 200 g of meat samples to obtain meat samples with the intended CFU count per gram.

The 10 g spiked minced meat samples were homogenized using a stomacher with the corresponding 190 g minced meat samples to make up the final weight of 200 g.

Minced beef

Initially, a full study design was prepared using minced beef as the matrix, which included six laboratory procedures (MM-1 to MM-6) evaluated against all nine *E. coli* strains producing various types of 3rd-generation cephalosporinases or carbapenemases. The initial design was based on the recommendation from the European Food Safety Authority's (EFSA) Scientific Opinion "on the public health risks of bacterial strains producing extended-spectrum β-lactamases and/or AmpC β-lactamases in food and food-producing animals" (EFSA Panel on Biological Hazards, 2011). In this study, the initial six laboratory procedures (MM-1 to MM-6) were conducted in duplicates and varied in terms of (1) pre-enrichment broths and associated incubation temperatures, (2) selective/non-selective antimicrobial supplements, and (3) selective agar plates in the assessment of sensitivity (growth) and specificity (gene detected) of the different strains (Table 2; Figure 1).

The pre-enrichment assessment included the following variations: 25 g of spiked minced beef in 225 ml of Buffered Peptone Water (BPW) recommended for the food analysis of *Salmonella* spp. (Danish Standard Associaation, 2017) vs. 5 g of spiked minced beef in 45 ml of MacConkey broth (MB) [Purple, Oxoid CM0505 (CM5a)] aligned with the procedure for isolating *E. coli* in the Danish national surveillance program, DANMAP (Bager et al., 2015) (Table 2; Figure 1).

The pre-enrichment broths were with or without a supplement of third-generation cephalosporins (cefotaxime vs. ceftriaxone of 1 mg/L) and incubated for 18–24 h at either 37 or 44°C, the latter temperature was included to test the ability to inhibit the growth of background flora with reduced susceptibility to third-generation cephalosporins (Table 1; Figure 1). Plating was conducted by applying three continuous streaks onto MacConkey agar (MA) (BD Difco Ref 212123) (supplemented with 1 mg/L of either cefotaxime or ceftriaxone and incubated for 18–24 h at 44°C (Table 2; Figure 1).

The sensitivity of the six laboratory procedures was evaluated and categorized based on a semi-quantitative measure according to the load of bacterial growth on the MacConkey plates (0:

10.3389/fmicb.2023.1229542

TABLE 1 MIC (mg/L) determination and antimicrobial resistance genes of the test strains used for the spiking experiments.

Target gene	Strain no	Ampicillin	Temocillin	Cefoxitin	Cefotaxime	Cefotaxime clavulanic acid	Ceftazidime	Ceftazidime/ clavlanic acid	Cefepime	Ertapenem	Imipenem	Meropenem
$bla_{CTX-M-1}$	0412004714_F1	>32	4	16	32	0.12/4	2	0.25/4	8	0.12	≤0.12	≤0.03
bla_{SHV-12}	0412055161_F131	>32	8	8	4	≤0.06/4	32	≤0.12/4	1	≤0.015	0.25	≤0.03
bla_{TEM-52}	7633094_7	>32	8	16	8	0.12/4	8	≤0.12/4	1	16	≤0.12	≤0.03
bla_{CMY-2}	0412056488_F191	>32	4	64	8	8/4	8	8	0.25	0.06	0.12	≤0.03
bla_{VIM-1}	R178	>32	32	32	16	16/4	64	32/4	4	0.06	0.5	0.12
bla_{NDM-1}	271	>32	>128	>64	>64	>64/4	>128	>128/4	>32	>2	8	>16
bla_{OXA-48}	KMU AUH	>32	128	>64	32	32/4	32	32/4	16	>2	1	4
bla_{KPC-2}	17/11 RKI	>32	16	>64	64	32/4	16	8/4	8	>2	1	2
Quality Control	ATCC 25922	4	16	2	≤0.25	0.12/4	≤0.25	0.25/4	≤0.12/4	≤0.015	≤0.12	≤0.03

TABLE 2 Laboratory procedures testing methodologies for the detection of ESBL- and AmpC-producing *E. coli* in minced meat from cattle, pigs, and chickens.

Method	Sample origin	Sample amount (g)	Pre-enrichment broth	AB supplement in borth	Amount of broth (ml)	Incubation temp (°C)	MacC agar with AB supplement	CHROM ID SMART agar	CHROM ID OXA agar	CHROM ID CARBA agar	Incubation temp (°C)
MM-1	Beef	25	BPW		225	37	CRO and CTX				44
	Pork										
	Chicken meat										
MM-2	Beef	25	BPW	CRO	225	37	CRO				44
MM-3	Beef	25	BPW	CTX	225	37	CTX				44
MM-4	Beef	5	MB		45	44	CRO and CTX				44
	Pork										
MM-5	Beef	5	MB	CRO	45	44	CRO				44
	Pork										
MM-6	Beef	5	MB	CTX	45	44	CTX				44
MM-7	Beef	25	BPW		225	37		X	X	X	37
	Pork										
	Chicken meat										
MM-8	Beef	5	MB		45	44		X	X	X	37
	Pork										
MM-9	Pork	5	MB	CRO	45	44		X	X	X	37

MM, minced meat procedure; AB, antimicrobials; BPW, buffered peptone water; MB, MacConkey broth; MacC, MacConkey; CRO, ceftriaxone; CTX, cefotaxime.

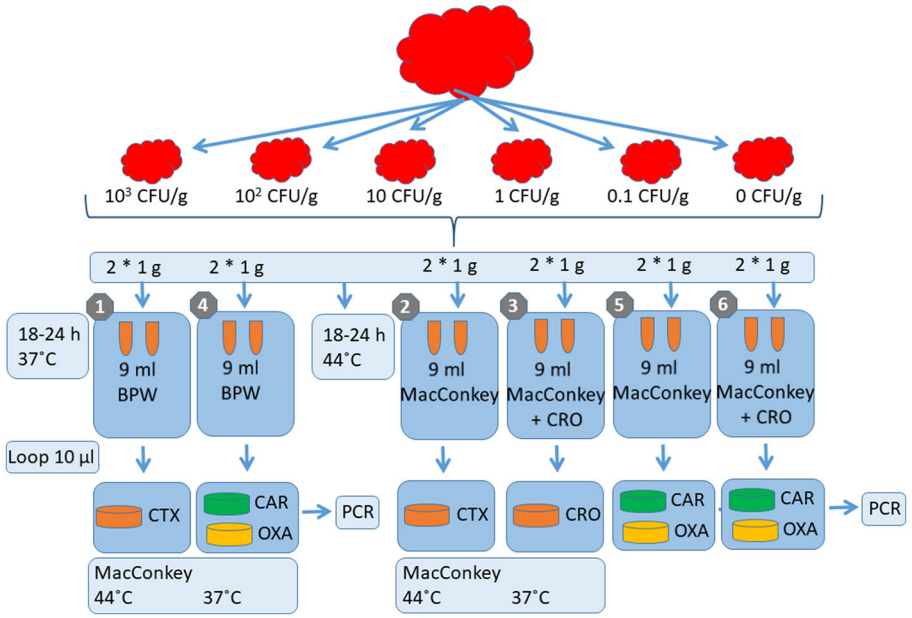

FIGURE 1
Validation scheme for the comparison of the different detection methods on minced meat content. CFU/g, colony-forming unit per Gram; g, Gram; C, Celsius; h, hour; ml, milliliter; BPW, Buffered Peptone Water; CAR, ChromID CARBA medium; OXA, ChromID OXA media; MacConkey, MacConkey broth or agar; CTX, cefotaxime; CRO, ceftriaxone; PCR, Polymerase chain reaction.

No growth, 1: bacterial growth in the first streak of plating, 2: bacterial growth in the first and second streaks of plating, and 3: bacterial growth in the first, second, and third streaks of plating). For each of the six laboratory procedures, 24 bacterial colonies were selected from the selective semi-quantitative MacConkey agar plates to confirm the presence of the spiked strains by identifying the respective antimicrobial resistance genes by PCR using the primers and Polymerase chain reaction design available from the EURL-AR website (www.eurl-ar.eu). For each of the nine bacterial strains, we evaluated the performance of the laboratory methods against sensitivity by assessing the lowest detection limit (0.1, 1, 10, 100, and 1,000 CFU/g) combined with the highest bacterial growth (0–3), as well as the specificity by assessing the recovery of the spiked *E. coli* isolates harboring the following antimicrobial resistance genes: $bla_{CTX-M-1}$, bla_{SHV-12}, bla_{TEM-52}, bla_{CMY-2}, bla_{VIM-1}, bla_{NDM-1}, bla_{OXA-48}, and bla_{KPC-2} (Table 1).

Minced pork

Based on the results obtained from the initial study on minced beef, the study design for minced pork was reduced to include only three laboratory procedures, MM-1, MM-4, and MM-5 (Table 2; Figure 1), the two most commonly detected third-generation cephalosporinases in food animals ($bla_{CTX-M-1}$ and bla_{CMY-2}) and three carbapenemases (bla_{VIM-1}, bla_{OXA-48}, and bla_{KPC-2}).

In brief, the reduced assessment included the following variations: 25 g of spiked minced pork in 225 ml of BPW without antimicrobial supplementation and incubated for 18–24 h at 37°C (MM-1) vs. 5 g of spiked minced pork in 45 ml of MB without antimicrobial supplementation (MM-4), as well as with the supplementation of 1 mg/L of ceftriaxone (MM-5) incubated for 18–24 h at 44°C for both methods (Table 2; Figure 1). Plating was conducted using MacConkey agar supplemented with 1 mg/L of cefotaxime and/or ceftriaxone and incubated for 18–24 h at 44°C (Table 2; Figure 1). The sensitivity was evaluated and categorized based on a semi-quantitative measurement according to the load of bacterial growth. Bacterial colonies were selected from the selective semi-quantitative MacConkey agar plates to confirm the presence of the spiked strains by PCR.

The reduced procedure was tested on five *E. coli* test strains, $bla_{CTX-M-1}$ (0412004714_F1), bla_{CMY-2} (0412056488_F191), bla_{VIM-1} (R178) (Fischer et al., 2012), bla_{OXA-48} (KMU AUH), and bla_{KPC-2} (17/11 RKI) (Table 1). The *E. coli* ATCC 25922 was used as the susceptible QC strain. The reason for the reduction was the highly similar results obtained previously for the tested methodologies on minced beef samples; another reason was to reduce the workload. In addition, the number of CFU concentrations tested was reduced to include the following five concentrations: 0, 1, 10, 100, and 1,000 CFU/g, since the dilution step of 1 CFU/g was sufficient to provide a precise CFU count.

All other procedures followed the procedure described above for the minced beef experiments.

Spiking procedures of the caecal content samples

From five batches of caecal content, one batch per five *E. coli* isolates ($bla_{CTX-M-1}$, bla_{CMY-2}, bla_{VIM-1}, bla_{OXA-48} and one susceptible control *E. coli* ATCC 25922) (Table 1) were divided into five smaller portions of 1 g. The different portions were labeled with the isolate number and with one of the following concentrations: 0, 1, 10, 100, and 1,000 CFU/g. One of the 1 g samples labeled 0

CFU/g for each of the five portions of caecal content was selected as the negative control to ensure that the caecal content was not already contaminated with an ESBL-producing organism, an AmpC-producing organism, and CPO.

The remaining four portions of 1 g each of caecal content were spiked individually with 0.010 mL of a 0.9% NaCl suspension containing each of the five individual *E. coli* test strains to contain a final concentration of 1, 10, 100, and 1,000 CFU/g per final weight of 1 g following the above procedure (Figure 2). Subsequently, the 1 g spiked caecal content samples were homogenized using a sterile spatula.

Caecal samples from pigs and cattle

Based on the results obtained from the minced pork experiment, the study design for caecal samples from pigs and cattle focused solely on the concept of the three laboratory procedures, MM-1, MM-4, and MM-5, testing the five *E. coli* isolates ($bla_{CTX-M-1}$, bla_{CMY-2}, bla_{VIM-1}, $bla_{OXA-48,}$ and one susceptible control *E. coli* ATCC 25922) (Tables 1, 2; Figure 1).

In brief, the procedure included testing of 1 g of spiked caecal content from pigs and cattle in 9 ml of BPW without antimicrobial supplementation and incubating for 18–24 h at 37°C (C-1) vs. 1 g of spiked caecal content from cattle alone in 9 ml of MB without antimicrobial supplementation (C-2), as well as with the supplementation of 1 mg/L of ceftriaxone (C-3) incubated for 18–24 h at 44°C for both methods (Table 3; Figure 2). Plating was conducted using MacConkey agar supplemented with 1 mg/L of cefotaxime or ceftriaxone and incubated for 18–24 h at 44°C (Table 3; Figure 2). Sensitivity was evaluated and categorized based on a semi-quantitative measure according to the load of bacterial growth, as previously explained. Bacterial colonies were selected from the selective semi-quantitative MacConkey agar plates to confirm the presence of the spiked strains by PCR.

All other procedures followed the procedure described in the minced beef experiment above.

Chicken meat and caecal samples

Based on the results obtained from the minced beef and pork as well as caecal samples originating from cattle and pigs, one laboratory procedure was tested for minced poultry meat (MM-1) and caecal samples from chickens (C-1), respectively (Tables 2, 3; Figures 1, 2). The laboratory procedure used for both spiking and validation was identical to the point of the minced pork and caecal sample study designs testing five *E. coli* isolates ($bla_{CTX-M-1}$, bla_{CMY-2}, bla_{VIM-1}, $bla_{OXA-48,}$ and one susceptible control *E. coli* ATCC 25922) (Table 1) with a few exceptions.

In brief, 25 g of spiked minced chicken meat and 1 g of spiked caecal content were transferred to 225 and 9 ml of BPW without antimicrobial supplementation, respectively, and incubated for 18–24 h at 37°C (Tables 2, 3; Figures 1, 2). Plating was conducted using MacConkey agar supplemented with 1 mg/L of cefotaxime and incubated for 18–24 h at 44°C (Tables 2, 3; Figures 1, 2). The sensitivity was evaluated and categorized based on a semi-quantitative measure according to the load of bacterial growth. Bacterial colonies were selected from the selective semi-quantitative MacConkey agar plates to confirm the presence of the spiked strains by PCR.

Validation experiments for detecting specific carbapenemase *E. coli* (part 2) — Rationale for the initial set of validation experiments

The final protocols should specifically detect bacteria with reduced susceptibility to carbapenems that are present in meat and caecal samples. Therefore, a selection of *E. coli* isolates producing various carbapenemases (including OXA-48, which is not a cephalosporinase) was included in the second part of the validation experiments.

Spiking procedures of the minced beef, pork, and chicken meat, as well as the bovine, porcine, and chicken caecal content samples

The spiking procedures of the minced beef, pork, and chicken meat, as well as the bovine, porcine, and chicken caecal content, were performed similarly to the procedures previously described for the section on ESBL- and AmpC-producing *E. coli*.

A full study design was prepared using minced beef, pork, and chicken meat as well as bovine, porcine, and chicken caecal content as matrices, which included two laboratory procedures and an evaluation against four and five *E. coli* strains for minced meat and caecal samples, respectively.

Minced beef and bovine caecal content samples

The design was based on the recommendation from the EFSA Scientific Opinion "on carbapenem resistance in food animal ecosystems" (EFSA BIOHAZ Panel, 2013) and on previous experience gained from a validation pilot study performed at the Federal Institute for Risk Assessment within the RESET project (http://www.reset-verbund.de/), in which different combinations of pre-enrichment (selective and non-selective), selective media (MacConkey agar supplemented with 0.125 and 0.5 mg/L of meropenem and commercial CP-selective plates), incubation conditions (37 vs. 44°C), and *E. coli* and *Salmonella* isolated from livestock used as test strains were tested as described by San José et al. (2014) and Hasman et al. (2015). From these studies, the best results (detection limit 1 CFU/g) were obtained using a non-supplemented BPW incubated at 37°C, followed by inoculation on a ChromID CARBA medium (bioMérieux), while selective pre-enrichment by MEM 0.125 mg/L was not recommended. Thus, in this present study, two laboratory procedures were conducted in duplicates and varied in terms of testing (1) different pre-enrichment broths, (2) selective/non-selective antimicrobial supplements, (3) incubation temperatures

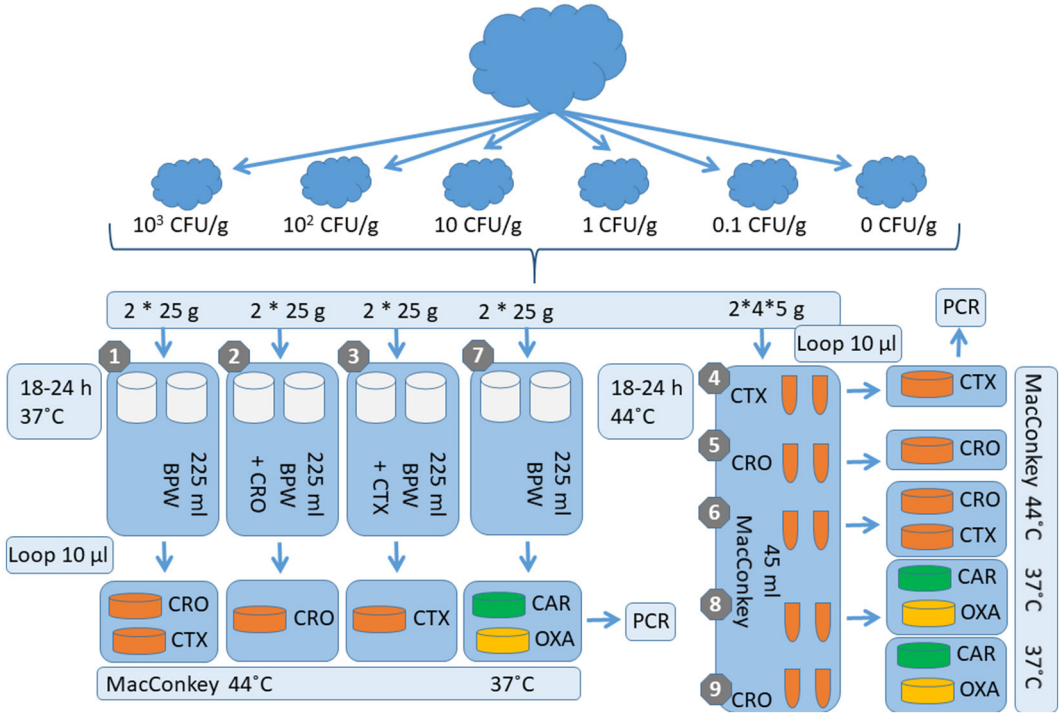

FIGURE 2
Validation scheme for the comparison of the different detection methods on caecal content. CFU/g, colony-forming unit per Gram; g, Gram; C, Celsius; h, hour; ml, milliliter; BPW, Buffered Peptone Water; CAR, ChromID CARBA medium; OXA, ChromID OXA media; MacConkey, MacConkey broth or agar; CTX, cefotaxime; CRO, ceftriaxone; PCR, Polymerase chain reaction.

of 37 and 44°C, and (4) selective agar plates in the assessment of sensitivity (growth) and specificity (gene detected) of the different strains.

The two laboratory procedures included pre-enrichment with the following variations: 25 g of spiked minced beef in 225 ml of BPW (MM-7) vs. 5 g of spiked minced beef in 45 ml of MB without AB selection (MM-8), as well as 1 g of spiked bovine caecal content in 9 ml of BPW (C-4) vs. 1 g of spiked caecal content in 9 ml of MB without AB selection (C-5) (Tables 2, 3; Figures 1, 2). The pre-enrichment broths were incubated for 18–24 h at either 37°C (MM-7 and C-4) or 44°C [MM-8, C-5, and C-6 (C-6 was supplemented with 1 mg/L of ceftriaxone)], and the latter temperature was included to test the ability to inhibit the growth of background flora with reduced susceptibility to third-generation cephalosporins (Tables 1, 2; Figures 1, 2). Plating was conducted by applying three continuous streaks onto ChromID SMART, CARBA agar, and ChromID OXA (bioMérieux) incubated for 18–24 h at 37°C (Tables 2, 3; Figures 1, 2).

The sensitivity of the two laboratory procedures was evaluated and categorized based on the semi-quantitative measure according to the load of bacterial growth, similarly to the previous description for the section on ESBL- and AmpC-producing *E. coli* in meat and caecal samples. For both laboratory procedures, 24 bacterial colonies were selected from the selective semi-quantitative MC agar plates to confirm the presence of the spiked strains by identifying the respective antimicrobial resistance genes by PCR. For each of the bacterial strains, the performance of the laboratory methods was evaluated against sensitivity by assessing the lowest detection limit (1, 10, 100, and 1,000 CFU/g) combined with the highest bacterial growth (0–3), as well as the specificity by assessing the recovery of the spiked *E. coli* isolates harboring bla_{VIM-1}, bla_{NDM-1}, bla_{KPC-2}, and bla_{OXA-48} (Table 1).

Minced pork and caecal content samples

The procedure was similar to the minced beef and bovine caecal content samples, except for a few changes. In addition to the methods MM-7, MM-8, C-4, C-5, and C-6, 5 g of spiked minced pork was also mixed in 45 ml of MB supplemented with 1 mg/L of ceftriaxone (MM-9) (Table 2; Figure 1). The pre-enrichment broth (MM-9) was incubated for 18–24 h at 37°C. The plating was similar to the minced beef and bovine caecal content samples where three continuous streaks were applied solely onto the commercial selective plates ChromID CARBA agar, ChromID OXA agar, and ChromID SMART agar (bioMérieux). All plates were incubated for 18–24 h at 37°C (Table 2; Figure 1).

Minced chicken meat and caecal content samples

Considering the results of the experiments using minced beef and pork and caecal content as matrices, the study design for minced chicken meat and caecal content samples was prepared as a continuation of these. Thus, the study design was set up to solely confirm if the selected MM-7 indicated using 25 g of spiked minced chicken meat in 225 ml of BPW had the expected sensitivity and specificity when using the commercial selective plates ChromID CARBA agar, ChromID OXA agar, and ChromID

10.3389/fmicb.2023.1229542

TABLE 3 Laboratory procedures testing methodologies for the detection of ESBL- and AmpC-producing *E. coli* from the caecal content of cattle, pigs, and chickens.

Method	Sample origin	Sample amount (g)	Pre-enrichment broth	AB supplement in borth	Amount of broth (ml)	Incubation temp (°C)	MacC agar with AB supplement	CHROM ID SMART agar	CHROM ID OXA agar	CHROM ID CARBA agar	Incubation temp (°C)
C-1	Cattle	1	BPW		9	37	CTX				44
	Pig										
	Chicken										
C-2	Cattle	1	MB		9	44	CTX				44
	Pig										
C-3	Cattle	1	MB	CRO	9	44	CRO				44
	Pig										
C-4	Cattle	1	BPW		9	37			X	X	37
	Pig							X	X	X	
	Chicken								X	X	
C-5	Cattle	1	MB		9	44			X	X	37
	Pig							X			
	Chicken										
C-6	Cattle	1	MB	CRO	9	44			X	X	37
	Pig							X	X	X	

C, caecal content procedure; AB, antimicrobials; BPW, buffered peptone water; MB, MacConkey broth; MacC, MacConkey; CRO, ceftriaxone; CTX, cefotaxime; MEM, meropenem.

SMART agar (bioMérieux). No experiments were conducted for the caecal content (Table 2; Figure 1).

Results

ESBL-producing *E. coli*, AmpC-producing *E. coli*, and CP *E. coli* in minced beef

Assessing the ability of methods MM-1 to MM-3 (see Table 2; Figure 1 for details regarding all the methods) to isolate ESBL-producing *E. coli*, AmpC-producing *E. coli,* and CP *E. coli* in minced beef samples by evaluating the detection limits of the methods as well as the semi-quantitative measurements, we found no differences between using a supplemented or non-supplemented antimicrobial pre-enrichment broth; we also found no difference upon using different third-generation cephalosporins in the selective agar plates (Table 4). However, the detection limits differed slightly depending on the antimicrobial resistance gene tested with bla_{SHV-12}, bla_{TEM-52}, and $_{NDM-1}$ having a detection limit (1 CFU/g) that was one dilution step higher than $bla_{CTX-M-1}$, bla_{CMY-2}, bla_{VIM-1}, and bla_{KPC-2}, all of which had a detection limit of 0.1 CFU/g (Table 4). Due to the selective principles, no growth was detected when bla_{OXA-48} and the susceptible *E. coli* ATCC 25922 strain were tested (Table 4).

The ability of methods MM-4 to MM-6 to isolate ESBL-producing *E. coli*, AmpC-producing *E. coli*, and CP *E. coli* in minced beef samples was further assessed by applying the same evaluation criteria. This assessment also showed no differences between using a supplemented or non-supplemented antimicrobial pre-enrichment broth; it also showed no difference when using different third-generation cephalosporins in the selective agar plates. The detection limits also differed, as observed in MM-1 to MM-3, slightly depending on the antimicrobial resistance gene tested with either the same detection limit as in MM-1 to MM-3 or one level higher for bla_{CMY-2} and bla_{VIM-1}, having an overall detection limit at 1 CFU/g for MM-4 to MM-6 (Table 4). Thus, the laboratory procedure MM-1 described by a sample size of 25 g minced beef in 225 ml of BPW without supplemented antimicrobial pre-enrichment broth was selected for the protocol.

ESBL-producing *E. coli*, AmpC-producing *E. coli*, and CP *E. coli* in minced pork

Due to the results of the minced beef experiments, minced pork was assessed based on methods MM-1, MM-4, and MM-5 alone. The ability of all three methods to isolate ESBL- and

TABLE 4 Detection and bacterial growth of ESBL- and AmpC-producing *E. coli* in minced meat from cattle, pigs, and chickens.

Antimicrobial classes			ESBLs			AmpC	CPE				QC
Method	Sample origin	Agar type	CTX-M-1	SHV-12	TEM-52	CMY-2	VIM-1	BDM-1	KPC-2	OXA-48	ATCC 25922
MM-1	Beef	MacConkey+CRO	0.1 (2)	1 (2)	1 (1)	0.1 (2)	0.1 (2)	1 (1)	0.1 (3)	BD	BD
	Pork	MacConkey+CTX	1 (2)			1 (3)	1 (2)			BD	BD
	Chicken meat		0.1 (1)			0.1 (2)	0.1(2)			BD	BD
MM-2	Beef		0.1 (3)	1 (2)	1 (1)	0.1 (2)	0.1 (2)	1 (3)	0.1 (3)	BD	BD
MM-3	Beef		0.1 (3)	1 (2)	0.1 (2)	0.1 (2)	0.1 (2)	1 (2)	0.1 (2)	BD	BD
	Pork	MacConkey+CTX	0.1 (1)	1 (2)	1 (2)	1 (1)	1 (1)	1 (1)	0.1 (3)		
			1 (3)			1 (2)	1 (1)			BD	BD
MM-5	Beef		0.1 (3)	1 (2)	1 (1)	1 (1)	1 (1)	1 (1)	0.1 (2)	BD	BD
	Pork		1 (2)			1 (1)	10 (1)			BD	BD
MM-6	Beef		0.1 (3)	1 (1)	1 (1)	1 (1)	1 (1)	1 (1)	0.1 (3)	BD	BD
	Chicken meat										
MM-7	Beef	CHROM ID OXA agar	BD							1 (1)	
		CHROM ID CARBA agar	BD						0.1 (1)		
	Pork	CHROM ID OXA agar				BD	BD			1 (1)	BD
		CHROM ID CARBA agar				BD	1 (1)			BD	BD
	Chicken meat	CHROM ID OXA agar	BD			BD	BD			10 (1)	BD
		CHROM ID CARBA agar	BD			BD	BD			BD	BD
MM-8	Beef	CHROM ID OXA agar	BD							BD	
		CHROM ID CARBA agar	BD						1 (1)		
	Pork	CHROM ID OXA agar				BD	BD			1 (1)	BD
		CHROM ID CARBA agar				BD	1 (1)			BD	BD
MM-9	Pork	CHROM ID OXA agar				BD	BD			BD	BD
		CHROM ID CARBA agar				BD	1 (1)			BD	BD

The detection limit of bacteria is presented as the minimum concentration (CFU/g) in which bacteria were identified from both double-tested cultures. Bacterial growth presented in brackets is semi-quantified as growth in the first (1), second (2), or third (3) strike on the agar plate. BD, Below detection limit.

10.3389/fmicb.2023.1229542

AmpC-producing *E. coli* in minced pork samples showed similar detection limits.

Overall, the detection limit of MM-1, MM-4, and MM-5 showed a detection limit at 1 CFU/g testing $bla_{CTX-M-1}$, bla_{CMY-2}, and bla_{VIM-1}, except for MM-5 testing bla_{VIM-1} and having a detection limit of 10 CFU/g (Table 4). Thus, the laboratory procedure MM-1 described by a sample size of 25 g minced beef in 225 ml of BPW without supplemented antimicrobial pre-enrichment broth was selected for the protocol.

ESBL-, AmpC-, and CP *E. coli* from caecal samples from pig and cattle

Assessing the ability of methods C-1 to C-3 to isolate ESBL- and AmpC-producing *E. coli* from caecal samples of cattle by evaluating the detection limits of the methods as well as the semi-quantitative measurements, we found no differences between using a supplemented or non-supplemented antimicrobial pre-enrichment broth; we also found no difference when using different third-generation cephalosporins in the selective agar plates (Table 5). However, the detection limits differed slightly depending on the antimicrobial resistance gene tested with $bla_{CTX-M-1}$ having a detection limit of 10 CFU/g (C-1 to C-3), bla_{CMY-2} having a detection limit of 10 CFU/g for C-1 to C-2 and 1 CFU/g for C-3, and bla_{VIM-1} having a detection limit of 1 CFU/g (C-1 to C-3) (Table 5). The ability of method C-1 to isolate ESBL-producing *E. coli*, AmpC-producing *E. coli*, and CP *E. coli* from caecal samples of pigs showed identical results to the C-1 method applied to the caecal samples obtained from cattle (Table 5). Due to the selective principles, no growth was detected when bla_{OXA-48} and the ATCC strain were tested for both sample types (Table 5). Thus, the laboratory procedure C-1 described by a sample size of 1 g of caecal content from pigs and cattle in 9 ml of BPW without antimicrobial supplementation and incubated for 18–24 h at 37°C was selected for the protocol.

ESBL-producing *E. coli*, AmpC- producing *E. coli*, and CP *E. coli* in minced chicken meat and caecal content

Minced chicken meat and caecal content were solely assessed based on methods MM-1 and C-1 due to the results of the previously conducted experiments. The results for the ability of method MM-1 to isolate ESBL- and AmpC-producing *E. coli* in minced chicken meat showed similar detection limits to those for the minced beef samples with 0.1 CFU/g for $bla_{CTX-M-1}$, bla_{CMY-2}, and bla_{VIM-1} (Table 4). In contrast, the ability of method C-1 to isolate ESBL- and AmpC-producing *E. coli* from caecal content showed a 1- to 2-fold difference in the detection limit (100 CFU/g for $bla_{CTX-M-1}$, bla_{CMY-2}, and bla_{VIM-1}) compared to the detection limits in the caecal content originating from cattle and pigs beef samples (Table 5).

Thus, the laboratory procedures MM-1 and C-1 described by a sample size of 25 g minced chicken meat in 225 ml of BPW and 1 g of caecal content in 9 ml of BPW without antimicrobial supplementation and incubated for 18–24 h at 37°C was selected for the protocol.

Overall, despite the minute difference in the detection limit of MM-1 to MM-3 as well as C-1 to C-3, testing the minced meat and caecal content, MM-1 and C-1 were selected for the protocol. This did not include a supplemented antimicrobial pre-enrichment broth, allowing the users to further use the pre-enrichment broth, BPW, for other parts of the AMR monitoring than the specific monitoring of ESBL-producing *E. coli*, AmpC- producing *E. coli*, and CP *E. coli* from meat and caecal samples originating from cattle, pigs, and poultry, specifically, e.g., commensal *E. coli* and *Salmonella*.

CP *E. coli* in minced beef

Assessing the ability of methods MM-7 and MM-8 to isolate CP *E. coli* in minced beef samples by evaluating the detection limits of the methods as well as the semi-quantitative measurements, we found one dilution step difference between using 25 g of minced beef in 225 ml of BPW (MM-7) and using 5 g of minced beef in 45 ml of MB (MM-8) (Table 4). Thus, the detection limit for MM-8 was one dilution step higher than that for MM-7 with a detection limit of 0.1 CFU/g for bla_{KPC-2}, whereas bla_{OXA-48} was observed to grow (detection limit of 1 CFU/g) only when method MM-7 was applied compared to MM-8 (Table 5). Due to the selective principles, no growth was detected testing $bla_{CTX-M-1}$ and the *E. coli* ATCC 25922 strain (Table 5). Thus, procedure MM-7 starting with a sample of 25 g of minced beef in 225 ml of BPW without antimicrobial supplementation and incubated for 18–24 h at 37°C was selected for the protocol.

CP *E. coli* in minced pork

The minced pork was assessed based on methods MM-7, MM-8, and MM-9 and showed the ability of all three methods to isolate CP *E. coli* with a detection limit of 1 CFU/g for bla_{VIM-1} and bla_{OXA-48} (no growth in MM-9, expected considering its phenotype) (Table 5). Thus, the detection limit for MM-8 was one dilution step higher than that for MM-7. Due to the selective principles, no growth was detected when $bla_{CTX-M-1}$ and the susceptible *E. coli* ATCC 25922 strain were tested (Table 5). Thus, similar to beef, the laboratory procedure MM-7, starting with a sample of 25 g minced pork in 225 ml of BPW without supplemented antimicrobial pre-enrichment broth, was selected to be included in the protocol.

CP *E. coli* from the caecal samples of pig and cattle

When assessing the ability of methods C-4 to C-6 to isolate CP *E. coli* from the caecal samples of pig and cattle by evaluating

10.3389/fmicb.2023.1229542

TABLE 5 Detection and bacterial growth of ESBL- and AmpC-producing *E. coli* from the caecal content of cattle, pigs, and chickens.

Antimicrobial classes			ESBLs	AmpC	CPE		QC
Method	Sample origin	Agar type	CTX-M-1	CMY-2	VIM-1	OXA-48	ATCC 25922
C-1	Cattle		10 (2)	10 (2)	1 (1)	BD	BD
	Pig		10 (1)	10 (1)	1 (1)	BD	BD
	Chicken		100 (1)	100 (1)	100 (1)	BD	BD
C-2	Cattle		10 (1)	10 (1)	1 (1)	BD	BD
	Pig		BD	BD	BD	BD	BD
C-3	Cattle		10 (3)	1 (2)	1 (2)	BD	BD
	Pig		BD	BD	BD	BD	BD
	Cattle	CHROM ID OXA agar	BD	BD	BD		1 (1)
		CHROM ID CARBA agar	BD	BD	1 (1)		BD
	Pig	CHROM ID OXA agar	BD	BD	BD		100 (1)
		CHROM ID CARBA agar	BD	BD	10 (1)		BD
	Chicken	CHROM ID OXA agar					
C-5		CHROM ID SMART agar					
		CHROM ID CARBA agar	BD	BD	1 (1)		BD
		CHROM ID SMART agar			BD/BD		BD/BD
		CHROM ID CARBA agar	BD	BD	BD		BD
		CHROM ID SMART agar					
		CHROM ID CARBA agar					
C-6		CHROM ID SMART agar					
		CHROM ID CARBA agar	BD	BD	1 (1)		BD
		CHROM ID SMART agar			BD/BD		BD/BDg
		CHROM ID CARBA agar	BD	BD	BD		BD
		CHROM ID SMART agar					
		CHROM ID CARBA agar					

The detection limit of bacteria is presented as the minimum concentration (CFU/g) in which bacteria were identified from both double-tested cultures. Bacterial growth presented in brackets is semi-quantified as growth in the first (1), second (2), or third (3) strike on the agar plate. BD, below detection limits. An underline values are indicate the CFU/g.

the detection limits of the methods as well as the semi-quantitative measurements, no growth was obtained with either method C5 (unexpected) or C-6 (expected considering the resistance phenotype of the isolate). Similarly, no growth was observed when assessing the ability of methods C-5 and C-6 by testing bla_{VIM-1} for the caecal samples of pigs; the detection limit for caecal samples obtained from cattle was 1 CFU/g (Table 5). C-4 was assessed to have the ability to isolate CP *E. coli* from caecal samples with a detection limit of 1 CFU/g for both bla_{VIM-1} and bla_{OXA-48} obtained from cattle, as opposed to a detection limit of 10 CFU/g (bla_{VIM-1}) and 100 CFU/g (bla_{OXA-48}) from pigs (Table 5). Due to the selective principles, no growth was detected when $bla_{CTX-M-1}$, bla_{CMY-2}, and the susceptible *E. coli* ATCC 25922 strain were tested (Table 4). Thus, laboratory procedure C-4 described by a sample size of 1 g caecal content in 9 ml of BPW without supplemented antimicrobial pre-enrichment broth was selected for the protocol.

CP *E. coli* in minced chicken meat

The minced chicken meat was assessed for the ability to detect CP *E. coli* using method MM-7 due to the results of the previously conducted experiments. The ability of method MM-7 to isolate CP *E. coli* in minced chicken meat showed no growth for bla_{VIM-1} (See Discussion section), whereas it showed a detection limit one dilution step higher than that for minced beef and pork with 10 CFU/g for bla_{OXA-48} (Table 4).

Thus, the laboratory procedure MM-7, which started with a sample of 25 g minced chicken meat in 225 ml of BPW without antimicrobial supplementation that was incubated for 18–24 h at 37°C was selected for the protocol.

Overall, after testing the minced meat and caecal content, MM-7 and C-4 were selected for the protocol. This did not include a supplemented antimicrobial pre-enrichment broth, allowing the users to further use the pre-enrichment broth and BPW for other

parts of the monitoring than the specific monitoring of ESBL-producing *E. coli*, AmpC-producing *E. coli,* and CP *E. coli* from meat and caecal samples originating from cattle, pigs, and poultry, specifically, e.g., commensal *E. coli* and *Salmonella*.

Discussion

To ensure a harmonized approach to monitoring, standardized laboratory protocols are essential. When considering which laboratory protocol is to be used for monitoring a specific pathogen, the advantages and disadvantages of the protocol must be accounted for, such as test sensitivity and specificity. Additionally, laboratory and infrastructure practicalities as well as any economic aspects must also be considered. For example, whether or not a pre-enrichment broth for a given laboratory procedure targeting a specific phenotype and species will also be useful for other species must be considered. In general, a selective pre-enrichment step increases sensitivity whenever an antimicrobial-resistant bacteria of concern is present in extremely low numbers. The inclusion of a selective pre-enrichment step, however, may facilitate horizontal gene transfer and may limit the use of the broth for detecting other bacteria under surveillance, even though this principle has been challenged recently (Lopatkin et al., 2016).

The preparatory work when developing the two EURL-AR protocols for meat (protocol 1) and caecal (protocol 2) samples, respectively, of the specific monitoring of ESBL- and AmpC-producing *E. coli* (part 1) and CP *E. coli* (part 2) originating from cattle, pigs, and poultry in the EU used in the Implementing Decision on the monitoring and reporting of antimicrobial resistance in zoonotic and commensal bacteria (2013/652/EU) (European Union, 2013), which was repealed in 2021 by the Implementing Decision (EU) 2020/1729 of 17 November 2020 (European Union 2020), showed that method MM-1 (protocol 1) and C-1 (protocol 2) were the most optimal protocols among the tested approaches for minced meat and caecal content sample, with a detection limit ranging from 0.1 to 100 CFU/g, depending on the matrix and test strains. Of note, the detection limits are presented in the most conservative way to include the minimum value for both double-tested samples. Hence, if the detection limit for one sample is 10 CFU/g and the other is 1 CFU/g, only the highest concentration (10 CFU/g) is presented.

Both MM-1 and C-1 included a non-selective pre-enrichment broth based on BPW and subsequent plating on selective agar plates, MacConkey agar supplemented with 1 mg/L cefotaxime for the detection of ESBL- and AmpC-producing *E. coli* and Chrom ID SMART (Chrom ID CARBA and OXA) for CP *E. coli.* ChromID CARBA (bioMérieux) is known to have the highest specificity (76%) and sensitivity (96%), and in our experience, this medium performs better as single plates rather than in combined half-plates with Chrom ID OXA in the Chrom ID SMART plates. An in-house media (e.g., MacConkey agar) supplemented with a carbapenem or a chromogenic medium could also be applied as a selective agar for isolating CP *E. coli.* These chromogenic media, however, generally show difficulties when detecting $bla_{\text{OXA}-48}$ producers due to the low carbapenem MICs. Therefore, ChromID OXA (bioMérieux) was developed for the specific detection of $bla_{\text{OXA}-48}$ producers as it prohibits the growth of class A and B carbapenemases. However, it should be used in combination with another selective medium (EFSA BIOHAZ Panel, 2013), e.g., ChromID SMART (bioMérieux).

Recently, a similar protocol, the Tricycle Protocol (Jacob et al., 2020; World Health Organization, 2021), was published as a screening tool in the global surveillance of ESBL-producing *E. coli*; it is based on the principle of MacConkey agar with higher selection pressure (cefotaxime 4 mg/L). In our experience, a cefotaxime concentration at 4 mg/L is too high to detect some enzymes, such as $bla_{\text{TEM}-20}$, $bla_{\text{TEM}-52}$, and $bla_{\text{CMY}-2}$; thus, as of this study, we would propose the use of a concentration of 1 mg/L cefotaxime as screening cut-off, as also recommended by EUCAST to detect ESBL- and AmpC-producing *E. coli* (https://www.eucast.org/fileadmin/src/media/PDFs/EUCAST_files/Resistance_mechanisms/EUCAST_detection_of_resistance_mechanisms_170711.pdf). The Tricycle Protocol further addressed the need for a standardized MacConkey recipe, as MacConkey agar varies substantially between manufacturers, which may influence the growth of *E. coli* (Jacob et al., 2020).

It would be of utmost importance to perform follow-up research based on the results of the current study, with further investigation on the test sensitivity and specificity of the two suggested laboratory protocols concerning media and selection pressure.

In developing this protocol, the laboratory testing of the different methodologies was designed as a "cascade assessment," where the testing and variables were reduced for the next experiment based on the results of the preceding experiment, e.g., the minced pork experiment was reduced based on the outcome of the minced beef experiment. This was implemented due to the lack of time, enabling the publication of the protocols before the legislation came into force. Nonetheless, we observed during the experiment that most methods detected the spiked test strain, with the exception of where growth should not be expected, e.g., genes conferring resistance to third-generation cephalosporins should not grow on media containing carbapenems Chrom ID agar, and strains containing $bla_{\text{OXA}-48}$ should not grow on Chrom ID CARBA as opposed to Chrom ID OXA and vice versa for strains harboring $bla_{\text{VIM}-1}$, for example. In a single case in the method for detecting CP *E. coli*, one of the test strains ($bla_{\text{VIM}-1}$ producing *E. coli* strain R178) did not grow. This might be related to the specific strain harboring the $bla_{\text{VIM}-1}$, which had an extremely low MIC for carbapenems, e.g., in this study, ertapenem MIC = 0.06, imipenem MIC = 0.5, and meropenem MIC = 0.12 or the strain harboring the $bla_{\text{VIM}-1}$, which originated from a different animal species than the matrix to which the spiked strain belonged. Multiple times, when preparing reference material for the EURL-AR iterations of the External Quality Assessment schemes on the selective isolation of presumptive ESBL-producing *E. coli*, AmpC- producing *E. coli*, and CP *E. coli* from meat and caecal samples (Matrix EQAS) (https://www.eurl-ar.eu/reports.aspx), we made similar observations. In this study, we observed that$bla_{\text{VIM}-1}$, e.g., present in a strain originating from a chicken sample did not survive well the spiking into a matrix of pig caeca. Based on this, we speculated whether the caeca in these examples contained some sort of inhibitor responsible for killing the strain isolated from the caecum of a different animal species (no data available). Thus, we decided to

still recommend the C-1 procedure despite the lack of growth by the *bla*$_{VIM-1}$ strain based on the results obtained by a previous study conducted within the RESET Project (San José et al., 2014).

During the experiments, we also observed that, for the meat samples, the BPW methods tended to generate more background growth of accompanying flora than the MacConkey methods. This was opposed to the MacConkey methods showing no growth in all of the pig caecal samples when pre-incubating in MB. This interesting and limiting observation was perhaps due to the presence of bile salts in the caecal samples from pigs combined with the bile salts in the MB, which could have killed the bacteria. Nonetheless, this observation was considered and judged to be a greater limitation than background growth with the application of the BPW. It is noteworthy that another issue that could contribute to the increased psychotropic background flora could be related to the time in which the samples were maintained in the refrigerator before analysis. In our experience (data not shown), those samples spiked after a couple of days and presented higher background flora mainly the previous study conducted within the RESET Project (San José et al., 2014), which must be considered when investigating the samples during the monitoring program.

An advantage of selecting a method based on BPW (MM-1 and C-1) was the opportunity taken by many NRLs to use the BPW for other parts of the Implementing Decision (EU) 2020/1729 of 17 November 2020 (European Union, 2020). A recent questionnaire survey with participation from 34 European National Reference Laboratories and affiliated laboratories, representing 32 countries, investigated the extent to which the pre-enrichment broth for ESBL was re-used in the surveillance of other pathogens. The survey results showed that the pre-enrichment broth for caecal content was used to identify *Salmonella*, commensal *E. coli*, and enterococci by 66, 32, and 50%, respectively, of the laboratories. Similarly, the pre-enrichment broth from meat samples was used to identify *Salmonella*, commensal *E. coli*, and enterococci by 71, 58%, and 50%, respectively, of the laboratories (https://www.eurl-ar.eu/CustomerData/Files/Folders/25-resourcer/593_survey-eurl-ar-esblprotocol.pdf). The numbers for enterococci, however, represent relatively few laboratories testing for enterococci regularly for both caecal contents (10 laboratories) and meat samples (six laboratories).

Several considerations and limitations were introduced while developing the protocols, which may have affected the outcome. A cephalosporin, such as cefotaxime or ceftriaxone, could be added to the pre-enrichment buffer to potentially enrich ESBL/AmpC producers before plating. This selective pre-enrichment could, however, exclude some *bla*$_{OXA-48}$-group producers, if a cephalosporinase-encoding gene is not harbored simultaneously. Furthermore, the inclusion of a cephalosporin or carbapenem in the media could trigger horizontal gene transfer during pre-enrichment (Liu et al., 2019). Similarly, a low concentration of a carbapenem could have been used as a supplement to the pre-enrichment broth; however, this might have resulted in the growth of a substantial part of background flora, such as *Pseudomonas* spp., with intrinsic resistance to certain carbapenems, thereby making the isolation and detection of CPEs challenging. For the detection of CPE in extremely low numbers for control efforts, a selective pre-enrichment including a carbapenem in low concentration (e.g., meropenem 0.125 mg/L) may be required. This approach could potentially increase sensitivity while excluding any presence of OXA-48 and similar producers, as well as other isolates expressing low resistance to carbapenems close to the screening cut-off/ECOFFs, as the *bla*$_{VIM-1}$ isolate used in this study (Fischer et al., 2012).

Considering that the presence of CP *E. coli* is still rare in food-producing animals and the meat thereof and that the methodology proposed could have a low detection limit for some types of carbapenemases, for almost a decade, after the implementation in 2014, the isolation protocol has facilitated the detection of CP *E. coli* from meat and caecal samples in a few EU MSs (Borowiak et al., 2017; Irrgang et al., 2017, 2020a,b; Madec et al., 2017; Diaconu et al., 2020; Garcia-Graells et al., 2020; Bortolaia et al., 2021; Carfora et al., 2022; European Food Safety Authority European Centre for Disease Prevention Control, 2023). Thus, the EURL-AR protocols have been proven to fulfill the purpose of facilitating the monitoring and reporting of antimicrobial resistance in zoonotic and commensal bacteria according to the Implementing Decisions 2013/652/EU and 2020/1729, for the specific isolation of ESBL-producing *E. coli*, AmpC-producing *E. coli*, and CP *E. coli* from meat and caecal samples. The protocols are contributing to the detection of this slow but emerging threat in the food chain in a harmonized way.

Conclusion

We evaluated and validated several laboratory procedures based on EFSA recommendations to provide two isolation protocols for fresh meat and caecal samples, respectively, used for the EU-specific monitoring of ESBL-producing *E. coli*, AmpC-producing *E. coli*, and CP *E. coli*.

The laboratory procedures tested revealed that the most sensitive and specific methodology was a procedure based on a BPW pre-enrichment step, followed by inoculation onto MacConkey agar supplemented with cefotaxime for detecting ESBL- and AmpC-producing *E. coli* and Chrom ID for detecting CP *E. coli*. The protocol also allows for the BPW pre-enrichment to be used for other parts of the EU monitoring due to non-supplementation with antimicrobials. For specific field and control studies for the detection of CP *E. coli*, the sensitivity and specificity might be enhanced by supplementing the pre-enrichment with carbapenem, although this will not be proficient for detecting *bla*$_{OXA-48}$-like enzymes. The protocol continues to be used by all EU MSs for the present monitoring period (2021–2027).

Data availability statement

The original contributions presented in the study are included in the article/supplementary material, further inquiries can be directed to the corresponding author.

Author contributions

HH, LC, BG, VB, and YA designed the study and discussed the results gained. CS and HN conducted the lab experiments and generated the data. JK and SP revised the protocol. RH and MF drafted the first version of the manuscript whereas HH

and BG assisted with the last version the manuscript as well as revised the manuscript. All authors have read and approved the final manuscript.

Funding

This work was supported by funding for the European Union Reference Laboratory for Antimicrobial Resistance (EURL AR) (http://www.eurl-ar.eu/).

Acknowledgments

We are grateful to P. Nordmann, Mikala Wang at AUH Skejby, Yvonne Pfeifer, and Jennie Fischer for sharing the following isolates: 271 harboring the *bla*$_{NDM-1}$, KMU AUH with *bla*$_{OXA-48}$, 17/11 RKI containing *bla*$_{KPC-2,}$ and R178 harboring *bla*$_{VIM-1}$, respectively.

Conflict of interest

The authors declare that the research was conducted in the absence of any commercial or financial relationships that could be construed as a potential conflict of interest.

Publisher's note

All claims expressed in this article are solely those of the authors and do not necessarily represent those of their affiliated organizations, or those of the publisher, the editors and the reviewers. Any product that may be evaluated in this article, or claim that may be made by its manufacturer, is not guaranteed or endorsed by the publisher.

Author disclaimer

BG is currently employed by the European Food Safety Authority (EFSA) in its BIOHAW Unit, which provides scientific and administrative support to EFSA's scientific activities in the area of Microbial Risk Assessment. The positions and opinions presented in this manuscript are those of the authors alone and are not intended to represent the views or scientific works of EFSA. Some of the studies performed at DTU Food run in parallel with those from the RESET project at the Federal Institute for Risk Assessment, where BG was working at that time.

References

Aworh, M. K., Ekeng, E., Nilsson, P., Egyir, B., Owusu-Nyantakyi, C., and Hendriksen, R. S. (2022). Extended-spectrum ÃŸ-lactamase-producing escherichia coli among humans, beef cattle, and abattoir environments in Nigeria. *Front. Cell Infect. Microbiol.* 12, 869314. doi: 10.3389/fcimb.2022.869314

Bager, F., Birk, T., Borck Høg, B., Jensen, L. B., Jensen, A. N., de Knegt, L., et al. (2015). *DANMAP 2014 - Use of Antimicrobial Agents and Occurrence of antImicrobial Resistance in Bacteria From Food aniMals, Food and Humans in Denmark*. DANMAP. Available online at: http://www.danmap.org/$\sim$/media/Projekt%20sites/Danmap/DANMAP%20reports/DANMAP%202014/Danmap_2014.ashx (accessed July 31, 2023).

Borowiak, M., Szabo, I., Baumann, B., Junker, E., Hammerl, J. A., Kaesbohrer, A., et al. (2017). VIM-1-producing Salmonella Infantis isolated from swine and minced pork meat in Germany. *J. Antimicrob. Chemother.* 72, 2131–2133. doi: 10.1093/jac/dkx101

Bortolaia, V., Ronco, T., Romascu, L., Nicorescu, I., Milita, N. M., Vaduva, A. M., et al. (2021). Co-localization of carbapenem (blaOXA-162) and colistin (mcr-1) resistance genes on a transferable IncHI2 plasmid in *Escherichia coli* of chicken origin. *J. Antimicrob. Chemother.* 76, 3063–3065. doi: 10.1093/jac/dkab285

Carattoli, A. (2008). Animal reservoirs for extended spectrum beta-lactamase producers. *Clin. Microbiol. Infect.* 14 (Suppl. 1), 117–123. doi: 10.1111/j.1469-0691.2007.01851.x

Carfora, V., Diaconu, E. L., Ianzano, A., Di, M. P., Amoruso, R., Dell'Aira, E., et al. (2022). The hazard of carbapenemase (OXA-181)-producing *Escherichia coli* spreading in pig and veal calf holdings in Italy in the genomics era: risk of spill over and spill back between humans and animals. *Front. Microbiol.* 13, 1016895. doi: 10.3389/fmicb.2022.1016895

Danish Standard Associaation. (2017). *ISO 6579-1:2017 Microbiology of the food chain — Horizontal method for the detection, enumeration and serotyping of Salmonella — Part 1: Detection of Salmonella sp*. Available online at: https://www.iso.org/standard/56712.html (accessed July 31, 2023).

DANMAP (2012). *Use of Antimicrobial Agents and Occurrence of Antimicrobial Resistance in Bacteria From Food Animals, Food and Humans in Denmark*. Avaialble online at: https://www.danmap.org/reports/2012 (accessed July 31, 2023).

Dantas, P. J., and Ferreira, H. M. N. (2020). Extended-spectrum beta-lactamase (ESBL)-producing Enterobacteriaceae in cattle production - a threat around the world. *Heliyon* 6, e03206. doi: 10.1016/j.heliyon.2020.e03206

Diaconu, E. L., Carfora, V., Alba, P., Di, M. P., Stravino, F., Buccella, C., et al. (2020). Novel IncFII plasmid harbouring blaNDM-4 in a carbapenem-resistant Escherichia coli of pig origin, Italy. *J. Antimicrob. Chemother.* 75, 3475–3479. doi: 10.1093/jac/dkaa,374

EFSA BIOHAZ Panel (2013). Scientific Opinion on Carbapenem resistance in food animal ecosystems. *EFSA J.* 11, 3501. doi: 10.2903/j.efsa.2013.3501

EFSA Panel on Biological Hazards (2011). Scientific Opinion on the public health risks of bacterial strains producing extended-spectrum β-lactamases and/or AmpC β-lactamases in food and food-producing animals. *EFSA J.* 9, 2322. doi: 10.2903/j.efsa.2011.2322

European Food Safety Authority and European Centre for Disease Prevention and Control (2023). The European Union Summary Report on Antimicrobial Resistance inzoonotic and indicator bacteria from humans, animals and food in 2020/2021. *EFSA J.* 21, 7867. doi: 10.2903/j.efsa.2023.7867

European Union (2013). Commission Implementing Decision of 12 November 2013 on the monitoring and reporting of antimicrobial resistance in zoonotic and commensal bacteria (2013/652/EU). *Off J. Eur Union*. 26–39.

European Union (2020). Commission Implementing Decision (EU) 2020/1729 of 17 November 2020 on the monitoring and reporting of antimicrobial resistance in zoonotic and commensal bacteria and repealing Implementaing Decision 2013/652/EU. (2020/1729/EU). *Off J Eur Union* 8–21.

Fischer, J., Rodriguez, I., Schmoger, S., Friese, A., Roesler, U., Helmuth, R., et al. (2012). *Escherichia coli* producing VIM-1 carbapenemase isolated on a pig farm. *J. Antimicrob. Chemother.* 67, 1793–1795. doi: 10.1093/jac/dks108

Fischer, J., Rodriguez, I., Schmoger, S., Friese, A., Roesler, U., Helmuth, R., et al. (2013). Salmonella enterica subsp. enterica producing VIM-1 carbapenemase isolated from livestock farms. *J. Antimicrob. Chemother.* 68, 478–480. doi: 10.1093/jac/dks393

Fischer, J., San, J. M., Roschanski, N., Schmoger, S., Baumann, B., Irrgang, A., et al. (2017). Spread and persistence of VIM-1 Carbapenemase-producing Enterobacteriaceae in three German swine farms in 2011 and 2012. *Vet. Microbiol.* 200, 118–123. doi: 10.1016/j.vetmic.2016.04.026

Garcia-Graells, C., Berbers, B., Verhaegen, B., Vanneste, K., Marchal, K., Roosens, N. H. C., et al. (2020). First detection of a plasmid located carbapenem resistant bla(VIM-1) gene in *E. coli* isolated from meat products at retail in Belgium in 2015. *Int. J. Food Microbiol.* 324, 108624. doi: 10.1016/j.ijfoodmicro.2020.108624

Guerra, B., Fischer, J., and Helmuth, R. (2014). An emerging public health problem: acquired carbapenemase-producing microorganisms are present in food-producing animals, their environment, companion animals and wild birds. *Vet. Microbiol.* 171, 290–297. doi: 10.1016/j.vetmic.2014.02.001

Hamza, E., Dorgham, S. M., and Hamza, D.A. (2016). Carbapenemase-producing Klebsiella pneumoniae in broiler poultry farming in Egypt. *J. Glob. Antimicrob. Resist.* 7, 8–10. doi: 10.1016/j.jgar.2016.06.004

Hasman, H., Agers ø, Y., Cavaco, L., Svendsen, C. A., Nielsen, H., San Jose, M., et al. (2015). *Evaluation of Methods for Enrichment of Carbapenemase-Producing E. coli in Pork Meat and Cecal Samples of Porcine and Bovine Origin: EV0266. Abstract From 25th European Congress of Clinical Microbiology and Infectious Diseases*. Copenhagen: ECCMID.

Irrgang, A., Fischer, J., Grobbel, M., Schmoger, S., Skladnikiewicz-Ziemer, T., Thomas, K., et al. (2017). Recurrent detection of VIM-1-producing *Escherichia coli* clone in German pig production. *J. Antimicrob. Chemother.* 72, 944–946. doi: 10.1093/jac/dkw479

Irrgang, A., Pauly, N., Tenhagen, B. A., Grobbel, M., Kaesbohrer, A., and Hammerl, A.J.A. (2020a). Spill-over from public health? First detection of an OXA-48-producing *Escherichia coli* in a German Pig Farm. *Microorganisms* 8, 855. doi: 10.3390/microorganisms8060855

Irrgang, A., Tausch, S. H., Pauly, N., Grobbel, M., Kaesbohrer, A., and Hammerl, J.A. (2020b). First detection of GES-5-producing *Escherichia coli* from livestock-an increasing diversity of carbapenemases recognized from german pig production. *Microorganisms* 8, 1593. doi: 10.3390/microorganisms8101593

Irrgang, A., Tenhagen, B. A., Pauly, N., Schmoger, S., Kaesbohrer, A., and Hammerl, J.A. (2019). Characterization of VIM-1-producing *E. coli* isolated from a German fattening pig farm by an improved isolation procedure. *Front. Microbiol.* 10, 2256. doi: 10.3389/fmicb.2019.02256

Jacob, M. E., Keelara, S., Idara-Kane, A., Matheu, A. Jr., and Fedorka-Cray, P.J. (2020). Optimizing a screening protocol for potential extended-spectrum Î²-lactamase *Escherichia* coli on macconkey agar for use in a global surveillance program. *J. Clin. Microbiol.* 58, e01039–e01019. doi: 10.1128/JCM.01039-19

Kock, R., Niels-Haardt, I., Becker, K., Mellmann, A., Friedrich, A. W., Mevius, D., et al. (2018). Carbapenem-resistant Enterobacteriaceae in wildlife, food-producing, and companion animals: a systematic review. *Clin, Microbiol. Infect.* 24, 1241–1250. doi: 10.1016/j.cmi.2018.04.004

Li, J., Bi, Z., Ma, S., Chen, B., and Cai, C., He, J., et al. (2019). Inter-host transmission of carbapenemase-producing *Escherichia coli* among humans and backyard animals. *Environ. Health Perspect.* 127, 107009. doi: 10.1289/EHP5251

Liu, G., Bogaj, K., Bortolaia, V., Olsen, J. E., and Thomsen, L.E. (2019). Antibiotic-induced, increased conjugative transfer is common to diverse naturally occurring ESBL plasmids in *Escherichia coli*. *Front. Microbiol.* 10, 2119. doi: 10.3389/fmicb.2019.02119

Lopatkin, A. J., Huang, S., Smith, R. P., Srimani, J. K., Sysoeva, T. A., Bewick, S., et al. (2016). Antibiotics as a selective driver for conjugation dynamics. *Nat. Microbiol.* 1, 16044. doi: 10.1038/nmicrobiol.2016.44

Madec, J. Y., Haenni, M., Nordmann, P., and Poirel, L. (2017). Extended-spectrum Î²-lactamase/AmpC- and carbapenemase-producing Enterobacteriaceae in animals: a threat for humans? *Clin. Microbiol. Infect.* 23, 826–833. doi: 10.1016/j.cmi.2017.01.013

Mughini-Gras, L., Dorado-Garcia, A., van, D. E., van den, B. G., Dierikx, C. M., Bonten, M. J. M., et al. (2019). Attributable sources of community-acquired carriage of Escherichia coli containing Î²-lactam antibiotic resistance genes: a population-based modelling study. *Lancet Planet Health* 3, e357–e369. doi: 10.1016/S2542-5196(19)30130-5

Poirel, L., Walsh, T. R., Cuvillier, V., and Nordmann, P. (2011). Multiplex PCR for detection of acquired carbapenemase genes. *Diagn. Microbiol. Infect. Dis.* 70, 119–123. doi: 10.1016/j.diagmicrobio.2010.12.002

San José, M., Hasman, H., Fischer, J., Agerso, Y., Schmoger, S., Jahn, S., et al. (2014). *Evaluation of Methods for Detection of VIM-1-Carbapenemase-Producing Enterobacteriaceae in Bovine Minced Meat. (ECCMID 2014 - eP334)*. Barcelona: ECCMID.

Shi, X., Li, Y., Yang, Y., Shen, Z., Cai, C., Wang, Y., et al. (2021). High prevalence and persistence of carbapenem and colistin resistance in livestock farm environments in China. *J. Hazard Mater.* 406, 124298. doi: 10.1016/j.jhazmat.2020.124298

World Health Organization (2021). *WHO Integrated Global Surveillance on ESBL-Producing E. coli Using a "One Health" Approach: Implementation and Opportunities*. World Health Organization. Available online at: https://apps.who.int/iris/handle/10665/340079 (accessed July 31, 2023).

frontiers | Frontiers in Microbiology

TYPE Original Research
PUBLISHED 19 September 2023
DOI 10.3389/fmicb.2023.1237825

OPEN ACCESS

EDITED BY
Guyue Cheng,
Huazhong Agricultural University, China

REVIEWED BY
Yuan Liu,
Yangzhou University, China
Xinhai Chen,
Shenzhen Bay Laboratory, China

*CORRESPONDENCE
Binghu Fang
✉ fangbh@scau.edu.cn

RECEIVED 10 June 2023
ACCEPTED 29 August 2023
PUBLISHED 19 September 2023

CITATION
Zhu C, Zhou Y, Kang J, Yang H, Lin J and Fang B (2023) Alkaline arginine promotes the gentamicin-mediated killing of drug-resistant *Salmonella* by increasing NADH concentration and proton motive force.
Front. Microbiol. 14:1237825.
doi: 10.3389/fmicb.2023.1237825

Alkaline arginine promotes the gentamicin-mediated killing of drug-resistant *Salmonella* by increasing NADH concentration and proton motive force

Chunyang Zhu[1,2], Yanhong Zhou[1,2], Jian Kang[3], Heng Yang[1,2], Jinglin Lin[3] and Binghu Fang[1,2]*

[1]Guangdong Provincial Key Laboratory of Veterinary Pharmaceutics Development and Safety Evaluation, South China Agricultural University, Guangzhou, China, [2]National Risk Assessment Laboratory for Antimicrobial Resistance of Animal Original Bacteria, South China Agricultural University, Guangzhou, China, [3]School of Animal Science and Technology, Guangdong Polytechnic of Science and Trade, Guangzhou, China

Introduction: Antimicrobial resistance, especially the development of multidrug-resistant strains, is an urgent public health threat. Antibiotic adjuvants have been shown to improve the treatment of resistant bacterial infections.

Methods: We verified that exogenous L-arginine promoted the killing effect of gentamicin against *Salmonella in vitro* and *in vivo*, and measured intracellular ATP, NADH, and PMF of bacteria. Gene expression was determined using real-time quantitative PCR.

Results: This study found that alkaline arginine significantly increased gentamicin, tobramycin, kanamycin, and apramycin-mediated killing of drug-resistant *Salmonella*, including multidrug-resistant strains. Mechanistic studies showed that exogenous arginine was shown to increase the proton motive force, increasing the uptake of gentamicin and ultimately inducing bacterial cell death. Furthermore, in mouse infection model, arginine effectively improved gentamicin activity against *Salmonella typhimurium*.

Discussion: These findings confirm that arginine is a highly effective and harmless aminoglycoside adjuvant and provide important evidence for its use in combination with antimicrobial agents to treat drug-resistant bacterial infections.

KEYWORDS

Salmonella, arginine, gentamicin, resistance, proton motive force

1. Introduction

Infections with drug-resistant bacteria, including multidrug-resistant (MDR) strains, are becoming a greater threat to human health and the farming industry. The emergence of a few superbugs has cost most extant antimicrobials to lose their efficacy (Ciorba et al., 2015). *Salmonella* spp. is a common and widely distributed zoonotic pathogen that can cause severe disease in both humans and animals. The more recent spread of MDR *Salmonella* spp. has made it more difficult to contain these infections (Hogberg et al., 2010). Thus, there is an urgent need to develop measures to contain the occurrence and spread of drug-resistant bacteria.

Antibiotic adjuvants, substances that do not have their own antibacterial effects but can increase the potency of antibiotics, are shown to be effective against drug-resistant microbes

(Liu et al., 2019a). Clavulanate and sulbactam are prominent adjuvants that increase the effect of penicillin by inhibiting β-lactamase. Given that the metabolic status of bacteria impacts antimicrobial efficacy, metabolic regulators (Stokes et al., 2019), a class of antibiotic adjuvants, used in combination with antimicrobial agents, is considered a potential strategy for treating MDR bacteria (Liu et al., 2019b).

Metabolic regulators were first used to treat *Escherichia coli* and *Staphylococcus aureus* persisters (Allison et al., 2011). Specifically, glucose, fructose, mannitol, or pyruvate were used to fuel bacterial glycolysis, promote NADH generation, activate the electron transport chain (ETC), and increase the cell membrane proton motive force (PMF), facilitating the uptake of gentamicin and ultimately leading to bacterial cell death. Peng et al. (2015) demonstrated that alanine, glucose, or fructose promote kanamycin activity using a similar mechanism against drug-resistant *Edwardsiella tarda* (Su et al., 2015). Several metabolic regulators are also shown that enhance the activity of beta-lactam, fluoroquinolones, and aminoglycosides against *E. coli*, *Pseudomonas aeruginosa*, *Klebsiella pneumoniae*, and *Vibrio alginolyticus* (Meylan et al., 2017; Liu et al., 2021; Zhao et al., 2021). To date, however, few studies have identified metabolic regulators that synergize with antimicrobial agents used to treat *Salmonella* spp., including persisters and drug-resistant cells.

Aminoglycosides are highly potent and broad-spectrum antimicrobials that are used to treat a wide range of pathogens (Poulikakos and Falagas, 2013). However, the PMF of bacterial cell membranes is needed to aid the internalization of these drugs (Taber et al., 1987). Our previous study found that some amino acids and sugars can regulate the metabolic state of bacteria and promote PMF, eventually increasing the uptake of aminoglycosides (Yong et al., 2021; Zhou et al., 2022). Alkalinized media can also provide bacterial cells with a transmembrane pH difference (ΔpH) and increase PMF (Sabath and Toftegaard, 1974; Letoffe et al., 2014). For example, lysine, a basic amino acid that can confer the transmembrane difference in H + concentration to bacteria, is shown to increase aminoglycoside-mediated killing of MDR *Acinetobacter baumannii*, *Escherichia coli*, and *Klebsiella pneumoniae* (Deng et al., 2020). Similarly, alkaline arginine promotes the activity of gentamicin against *Staphylococcus aureus*, *E. coli*, and *Pseudomonas aeruginosa* persisters both *in vitro* and *in vivo*. The existence of pH-independent factors that promote arginine-mediated antimicrobial activity has also been proposed (Lebeaux et al., 2014). Further studies are needed to identify the mechanism by which arginine synergizes with antibiotics.

Our previous study confirmed that arginine biosynthesis and metabolism are disrupted in gentamicin-resistant *Salmonella*, and arginine levels are reduced in resistant cells. D-ribose, which facilitates gentamicin-mediated killing of drug-resistant *Salmonella*, was similarly suppressed in resistant bacteria (Zhou et al., 2022). Thus, we speculated that arginine could promote gentamicin activity against drug-resistant *Salmonella*.

The current study confirmed that the basic amino acid, arginine, can promote the activity of aminoglycosides against drug-resistant *Salmonella* spp. including clinically isolated MDR strains. Arginine was able to enhance aminoglycoside function by affecting the electrical potential across the membrane ($\Delta\psi$) and the transmembrane difference in H + concentration (ΔpH). The findings confirm that arginine is a highly effective and harmless aminoglycoside adjuvant and further previous findings of arginine-mediated antimicrobial potentiation. Overall, this study provides important evidence for the use of arginine in combination with antimicrobial agents to combat drug-resistant bacteria.

2. Materials and methods

2.1. Chemicals

All antibiotics were purchased from Shanghai Macklin Biochemical Technology Co., Ltd (Shanghai, China). Mueller Hinton (MH) Agar, MH Broth, Tryptic Soy Agar (TSA), Luria-Bertani (LB) broth, and MacConkey Agar were purchased from Guangdong Huankai Microbial Sci & Tech. Co., Ltd. (Guangdong, China). Arginine purchased from Beijing Solarbio Science & Technology Co., Ltd. (Beijing, China). Mouse serum were purchased from Guangzhou Ruite Biotechnology Co., Ltd.

2.2. Bacterial strains and growth conditions

Escherichia coli (ATCC25922) Standard strain was purchased from American Type Culture Collection (Manassas, VA, United States). *Salmonella* typhimurium (CICC 21484) Standard strain was purchased from China Center of Industrial Culture Collection (Beijing, China). The standard *S.* typhimurium (CICC 21484) strain was sequentially propagated with or without gentamicin and drug-resistant bacteria were selected (STM-R). The clinical strains, SR-1 (*S.* Derby), SR-2 (*S.* 1, 4, [5], 12: i:-), SR-7 (*S.* typhimurium), and SR-8 (London) were isolated from swine farms in South China (Guangdong Province, China). These strains confer resistance to most clinical antimicrobials, including β-lactams, aminoglycosides, tetracyclines, and sulfonamides (**Table 1**).

2.3. Antibiotic bactericidal assays

The antibacterial assay was carried out as described previously (Allison et al., 2011). In brief, bacterial cells were cultured in LB broth for 8 h. After centrifugation at 13,000 × *g* for 5 min at 4°C, the precipitate was washed twice with sterile PBS buffer and resuspended to 1 × 10^6 colony-forming units (CFU)/mL in M9 minimal media. Gentamicin-resistant *Salmonella* was inoculated into 3 mL of M9 broth containing gentamicin, gentamicin plus arginine, respectively. For all CCCP experiments, the cells were preincubated with 20 μM CCCP for 5 min before the addition of metabolites or antibiotics. The remaining inhibitors, malonate, and rotenone were added at the same time as the metabolites or antibiotics. The bacteria were counted at 0, 2, 4, 6, and 8 h, and bacterial survival curves were drawn. Percentage survival was determined by the ratio of CFU obtained from the test and control samples. To investigate the effect of arginine on the bactericidal activity of Gentamicin against *Salmonella* in mouse serum culture medium. The experimental strains (STM-R, SR-1, SR-2, SR-7, and SR-8) were treated with Gentamicin (1 MIC), and with or without arginine (10 mM) for 8 h in mouse serum medium.

TABLE 1 MIC value of different antimicrobials against *Salmonella* (μ g/mL).

	STM-S	STM-R	SR-1	SR-2	SR-7	SR-8
Gentamicin	0.25	32	32	64	32	64
Tobramycin	0.5	8	32	64	32	32
Kanamycin	1	4	512	256	512	32
Apramycin	2	8	128	128	128	128
Ampicillin	2	2	128	512	512	64
Colistin	0.5	0.5	1	0.5	1	1
Sulfisoxazole	2	2	512	512	512	512
Tetracycline	0.5	0.5	32	128	32	64
Florfenicol	1	1	256	256	128	256
Sulfamethoxazole/trimethoprim	0.5/9.5	0.5/9.5	4/76	4/76	4/76	4/76
Cefotaxifur	0.25	0.25	1	0.5	0.5	1
Ciprofloxacin	0.05	0.05	8	0.5	8	0.5
Enrofloxacin	0.03	0.03	4	1	4	0.5
Amoxicillin/clavulanic acid	2/1	2/1	32/16	16/8	16/8	32/16
Meropenem	0.05	0.05	0.03	0.03	0.03	0.03
Ceftazidime	0.5	0.5	1	0.5	0.5	0.25

2.4. Synergistic antibacterial effect in a mouse infection model

The mouse infection model was established according to previously described methods (Yong et al., 2021). The 6-week-old female KM mice (body weight b.w., 18–22 g) were intraperitoneally injected with *Salmonella* typhimurium STM-R and SR-7 (10^7 CFU/mL for both), mice were divided into 4 groups, 6 mice in each group. Investigate the therapeutic effect of arginine combined with gentamicin on a mouse infection model. Investigate treatment with 0.9% saline (control, 0.1 mL), arginine (100 mg/kg b.w.), gentamicin (10 mg/kg b.w.), and arginine plus gentamicin (100 mg/kg plus10 mg/kg b.w.), administered the same dose 12 h after the first administration. Twelve hours after the second administration, six mice were randomly selected and sacrificed by cervical dislocation. The blood, liver, kidney and spleen samples of mice were collected for bacterial count, and the bacterial load of each organ was counted to investigate the therapeutic effect of arginine combined with gentamicin on mice. Ethics Statement: This study was approved by the Animal Ethics Committee of South China Agricultural University (application NO:2023b020) and was carried out in accordance with the ARRIVE guidelines.

2.5. Measurement of NADH and ATP

The intracellular NADH concentration of *Salmonella* was detected as previously described (Peng et al., 2015). NADH concentration was detected using an NAD + /NADH assay kit (BioAssay Systems, Hayward, CA, United States). The bacteria were cultured in M9 medium with or without a final concentration of 10 mM arginine for 8 h. After that, 1 mL of the bacterial solution was collected and centrifuged at 13,000 × *g* for 5 min at 4°C to collect the precipitate. The supernatant was discarded, and the pellet was washed three times with PBS. NADH extraction buffer (100 μL) was added, the extract was heated at 60°C for 5 min, and 20 μL assay buffer and 100 μL NAD + extraction buffer were added to neutralize the extract. After centrifugation, NADH was measured in the supernatant according to the manufacturer's instructions. ATP concentration was measured using an ATP assay kit (Beyotime, China) as described previously (Liu et al., 2021). After co-culturing the bacteria (1×10^6 CFU/mL) and 10 mM arginine for 4 h, the bacterial solution was centrifuged at 4°C and 12,000 × *g* for 5 min. The supernatant was discarded, and the pellet is carefully resuspended in PBS and washed twice. ATP levels were determined using a commercially available kit following the manufacturer's instructions.

2.6. Measurement of membrane potential

Arginine was added into the M9 medium of Gentamicin-resistant *Salmonella*. The mixture was then incubated at 37°C for 8 h. After incubation, 1 mL of bacterial solution was removed and centrifuge at 20,000 × *g* for 5 min at −10°C. The supernatant was discarded. The precipitate was washed twice with PBS and then diluted to approximately 1×10^6 CFU/mL with PBS. The membrane potential was examined using a BacLight Bacterial Membrane Potential Kit (Life Technologies, Carlsbad, CA, United States) as previously described (Zhou et al., 2022).

2.7. Measurement of intracellular gentamicin

Intracellular gentamicin levels were determined as previously described (Zhou et al., 2022). In brief, bacterial cells were cultured

in LB broth until the late exponential phase. After centrifugation, the precipitates were collected and resuspended in 10 mL of M9 minimal media to 1×10^6 CFU/mL with or without antibiotics and arginine. The reaction samples were incubated at 37°C for 6 h, and the precipitates were harvested by centrifugation, washed twice with PBS, and resuspended in 1 mL of PBS. The solution was sonicated for 10 min and the insoluble substances were removed by centrifugation. Gentamicin was quantified in the supernatant using a gentamicin ELISA kit (Shanghai Enzymelinked Biotechnology Co., Ltd., Shanghai, China).

2.8. Quantitative RT-PCR analysis

Bacteria were cultured in 50 mL M9 medium with or without 10 mM arginine for 8 h. The bacteria cells were collected following centrifugation at 8,000 rpm for 10 min (4°C, discard the supernatant). The pellet washed three times with sterile PBS buffer. The bacterial samples were snap frozen by liquid nitrogen and stored at −80°C until analysis. RT-qPCR assay was in agreement with the previous method (Wang et al., 2023). The specific primers are listed in the (**Supplementary Table 1**).

2.9. Statistical analysis

Results are presented as means ± SD. The statistical analysis was performed using SPSS Statistics 26.0 software (IBM Corp., Armonk, NY, United States). Statistical significance was set as $^*p < 0.05$, $^{**}p < 0.01$ (use the *t*-test or one-way ANOVA). Three biological repeats were carried out.

3. Results

3.1. Exogenous arginine promotes aminoglycoside activity against drug-resistant *Salmonella*

Exogenous arginine promotes the gentamicin-mediated killing of *E. coli* and *Staphylococcus aureus* persister cells both *in vitro* and *in vivo*. We speculated that arginine can also promote gentamicin-mediated killing of drug-resistant *Salmonella*. Four clinical *Salmonella* isolates with different serotypes, including *Salmonella* typhimurium, London, Derby, and 1, 4, [5], 12: i: -, which are resistant to almost all common antibiotics, were used to test this hypothesis. Arginine was shown to significantly increase the killing of gentamicin-resistant *Salmonella* in a dose-dependent manner. Specifically, STM-R cell viability was reduced 3.48-, 17.85-, and 1327.29-fold when treated with 2.5, 5, and 10 mM arginine plus 1 MIC gentamicin, respectively. When the fixed arginine concentration at 10 mM, the survival rate of STM-R decreases with the increase of Gentamicin concentration. In addition, STM-R cell viability was reduced by increasing doses of gentamicin with or without 10 mM arginine (**Figures 1A–C**). Arginine also enhanced gentamicin activity against clinically isolated MDR *S.* Derby (SR-1), *S.* 1, 4, [5], 12: i:–(SR-2), *S.* typhimurium (SR-7) and *S.* London (SR-8) (**Figures 1D–G**), and increased tobramycin-, kanamycin-, and apramycin-mediated killing of MDR *Salmonella* (**Supplementary Figures 1–3**). Furthermore, the efficacy of the treatment was also observed in mouse serum. Mouse serum showed little or no clearance of the different Salmonella strains (compared with M9 medium). When no substance was added, the number of bacteria in the two media (M9 and serum) was increased to the power of 108 CFU/mL after 8 h, although the serum group showed a small inhibitory effect. The statistical analysis did not constitute a significant difference (*T*-test). When treated with a combination of 10 mM arginine and 1 MIC gentamicin, the viability of *Salmonella* of different serotypes decreased significantly. The survival rates of STM-R, SR-1, SR-2, SR-7, and SR-8 decreased by 1584.42-, 1126.98-, 72.49-, 761.90-, and 1027.03-fold, respectively (**Supplementary Figure 4**). The arginine-potentiated aminoglycoside-mediated killing of drug-resistant *Salmonella* was both dose and incubation period-dependent. These findings show that arginine could effectively enhance aminoglycoside activity against MDR *Salmonella*.

3.2. Synergistic antibacterial effect in a mouse infection model

Mice were injected intraperitoneally with *Salmonella* typhimurium STM-R and SR-7 to establish a mouse model of drug-resistant bacterial infection. To investigate the potential synergistic effect of gentamicin and arginine in eliminating *Salmonella* typhimurium in mice. The bacterial loads were monitored, respectively, in the liver, spleen, kidney and blood. In a mouse model of infection with STM-R, the results show that the arginine plus gentamicin (test group) were significantly lower than in those treated with gentamicin alone. Compared with gentamicin alone, the bacterial load of blood, spleen, liver and kidney was reduced by 14.5, 18.2, 28.8, and 13.5-fold, respectively. At SR-7 mouse infection model, the test group had similar results (**Figures 2A–H**). These results indicate that arginine promotes gentamicin against drug-resistant *Salmonella in vivo*, including lab-evolved and clinically isolated multidrug-resistant *Salmonella*.

3.3. Arginine-induced PMF enhances gentamicin uptake

Exogenous metabolites promote the uptake of aminoglycosides by increasing the bacterial cell membrane PMF and causing cell death. Thus, several assays were performed to confirm whether arginine could increase the PMF of drug-resistant *Salmonella*. Drug-resistant cells were cultured in M9 minimal media with or without arginine for 8 h and the PMF was assessed using the BacLight bacterial membrane potential lit. The PMF of STM-R increased by 9.17, 9.4, and 12.93% in response to 2.5, 5, and 10 mM arginine, respectively. In contrast, PMF decreased by 15.49, 12.43, 11.53, and 9.14% in response to 20 μM CCCP and 2.5, 5, or 10 mM arginine, respectively (**Figure 3A**). CCCP is a proton ionophore that inhibits PMF. Similar results were obtained when clinical MDR *Salmonella* cells were incubated with various doses of exogenous arginine (**Supplementary Figure 5**). These results

10.3389/fmicb.2023.1237825

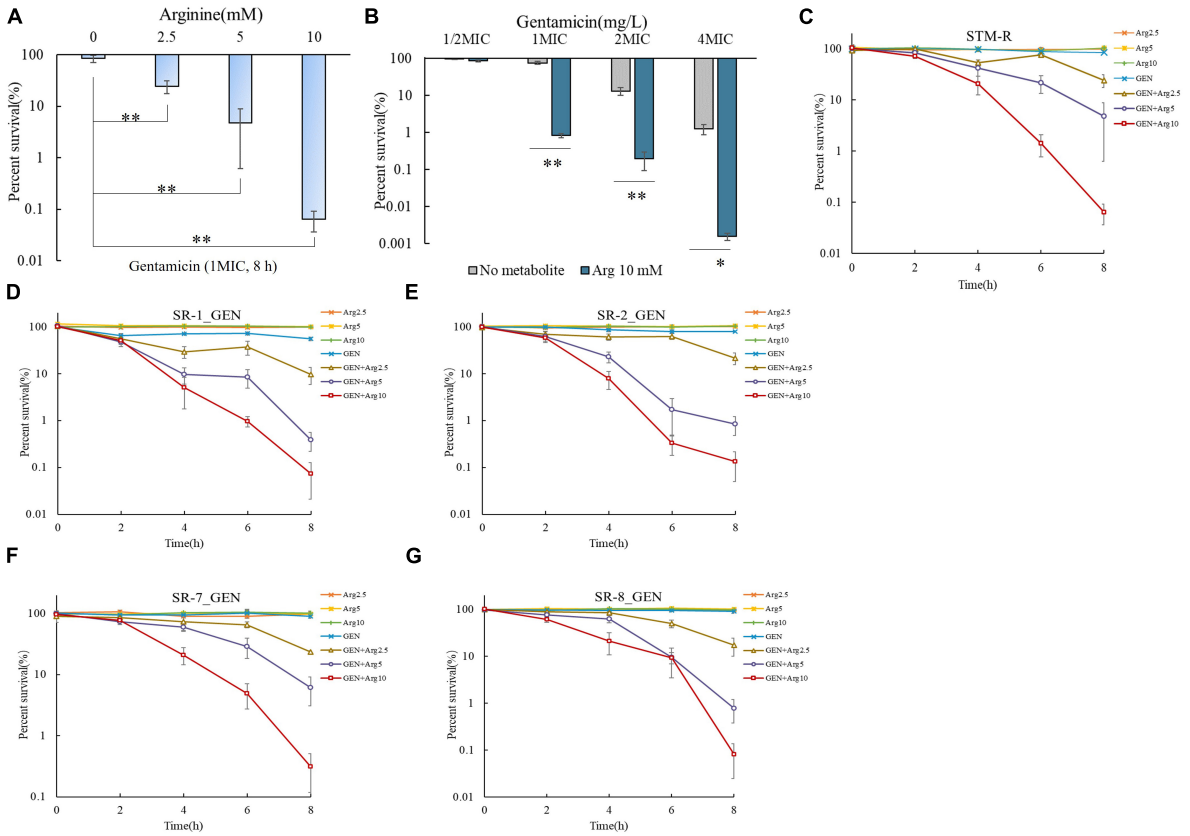

FIGURE 1
Arginine induces gentamicin-mediated killing in drug-resistance *Salmonella*. **(A)** Percent survival of STM-R in the presence of the indicated concentration of arginine and 1 MIC gentamicin. **(B)** Percent survival of STM-R in the presence of the indicated concentration of gentamicin and with or without 10 mM arginine. Percent survival of lab-evolved STM-R **(C)** and clinical isolates SR-1 **(D)**, SR-2 **(E)**, SR-7 **(F)**, and SR-8 **(G)** in the presence of gentamicin(1MIC) by arginine dose. Results are displayed as the mean ± SD and three biological repeats are carried out. Significant differences are identified (*$p < 0.05$ and **$p < 0.01$ as determined by *t*-test).

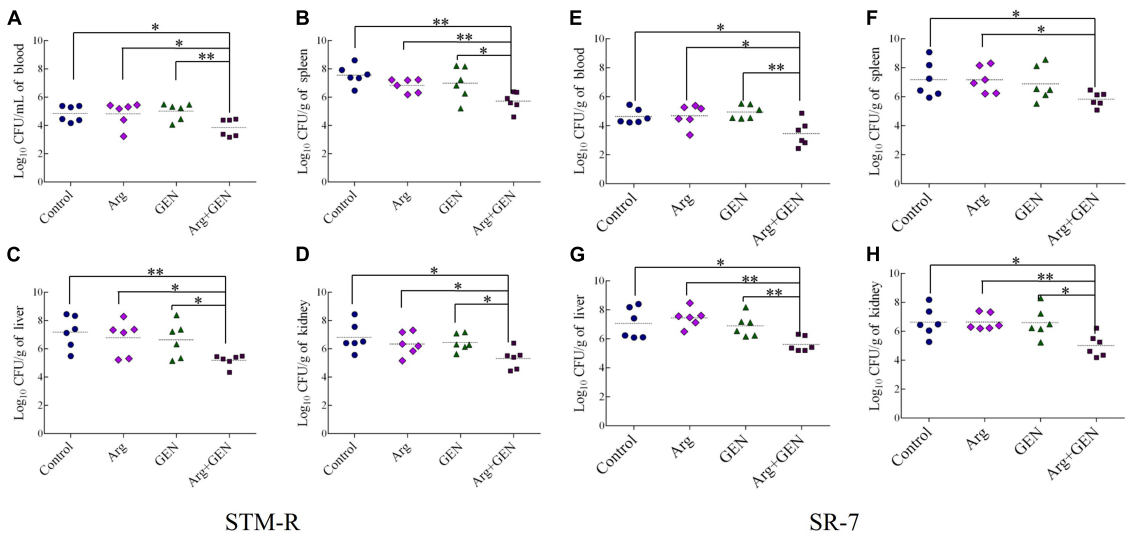

FIGURE 2
Arginine induces gentamicin-mediated killing in a mouse infection model with drug-resistance *Salmonella*. Bacterial density of blood **(A)**, spleen **(B)**, liver **(C)**, and kidney **(D)** in mice infected with STM-R after treatment with different therapeutic schedule. Bacterial density of blood **(E)**, spleen **(F)**, liver **(G)**, and kidney **(H)** in mice infected with SR-7 after treatment with different therapeutic schedule. Results are displayed as the mean ± SD and three biological repeats are carried out. Significant differences are identified (*$p < 0.05$ and **$p < 0.01$ as determined by *t*-test).

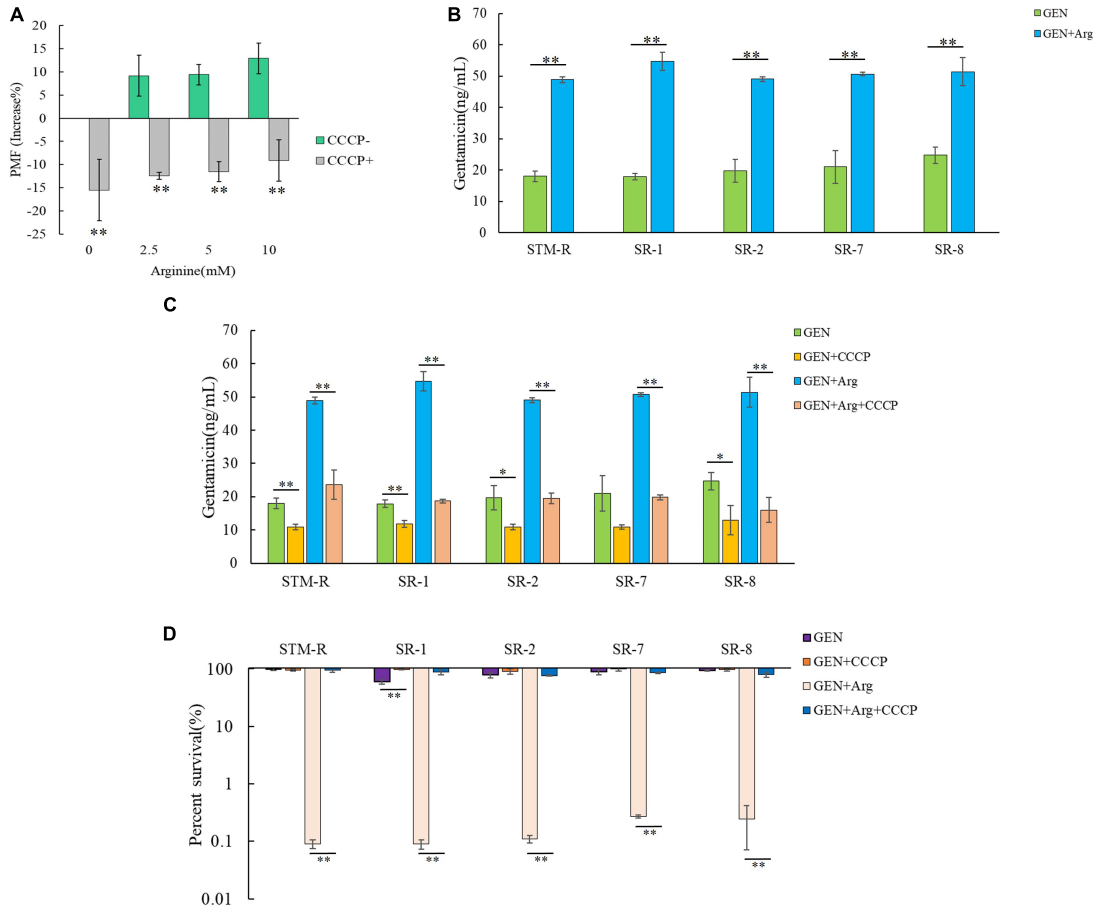

FIGURE 3
Effect of exogenous arginine on ponton motive force of *Salmonella*. **(A)** Variation of PMF in STM-R by arginine dose with or without CCCP. **(B)** Intracellular concentration of gentamicin in STM-R and clinical isolates in the presence of 10 mM arginine. **(C)** Intracellular concentration of gentamicin in STM-R and clinical isolates in the presence of 10 mM arginine with or without CCCP. GEN, gentamicin. **(D)** Percent survival of STM-R and clinical isolates in the presence or absence of CCCP and 1 MIC gentamicin plus 10 mM arginine. GEN, gentamicin. Results are displayed as the mean ± SD and three biological repeats are carried out. Significant differences are identified (*$p < 0.05$ and **$p < 0.01$ as determined by *t*-test).

indicated that arginine was able to enhance the PMF of drug-resistant *Salmonella*. To confirm that arginine-potentiated PMF facilitated drug uptake by bacterial cells, intracellular drug levels were measured using a gentamicin ELISA kit. The intracellular concentration of gentamicin in STM-R and MDR isolates increased significantly in the presence of 10 mM arginine (Figures 3B, C). The gentamicin-mediated killing was abolished by CCCP in the presence and absence of arginine (Figure 3D). These results indicated that arginine-potentiated PMF facilitated drug uptake by bacterial cells and induced cell death.

3.4. pH-dependent increase in PMF causes bacterial cell death

The PMF is composed of both the electrical potential across the membrane ($\Delta\psi$) and the transmembrane difference in H + concentration (ΔpH). The basic amino acids arginine and lysine can increase the PMF of bacterial cells depending on the ΔpH. Thus, it is probable that arginine can alkalinize media, inducing PMF and leading to cell death. To test this, drug-resistant *Salmonella* cells were incubated for 8 h in alkalinized medium with AMPSO buffer adjusted to a pH of ~7.21 (a pH value equivalent to 10 mM arginine) (Figure 4A). Cell viability was significantly reduced in the alkalinized media containing gentamicin, suggesting that the increased pH promoted the gentamicin-mediated killing of drug-resistant *Salmonella*. However, the pH-mediated potentiation of gentamicin was weaker than the arginine-mediated potentiation even when the pH value was the same. On the other hand, buffered arginine (pH = 7.0) was able to enhance gentamicin-mediated killing (Figure 4B). These findings suggest that basic arginine may provide the ΔpH to enhance the PMF of the cell membrane and that some pH-independent factors may also be involved in this process.

3.5. The activated electron transport chain is responsible for increasing the PMF

This study confirmed that pH-independent factors are involved in promoting the gentamicin-mediated killing of drug-resistant

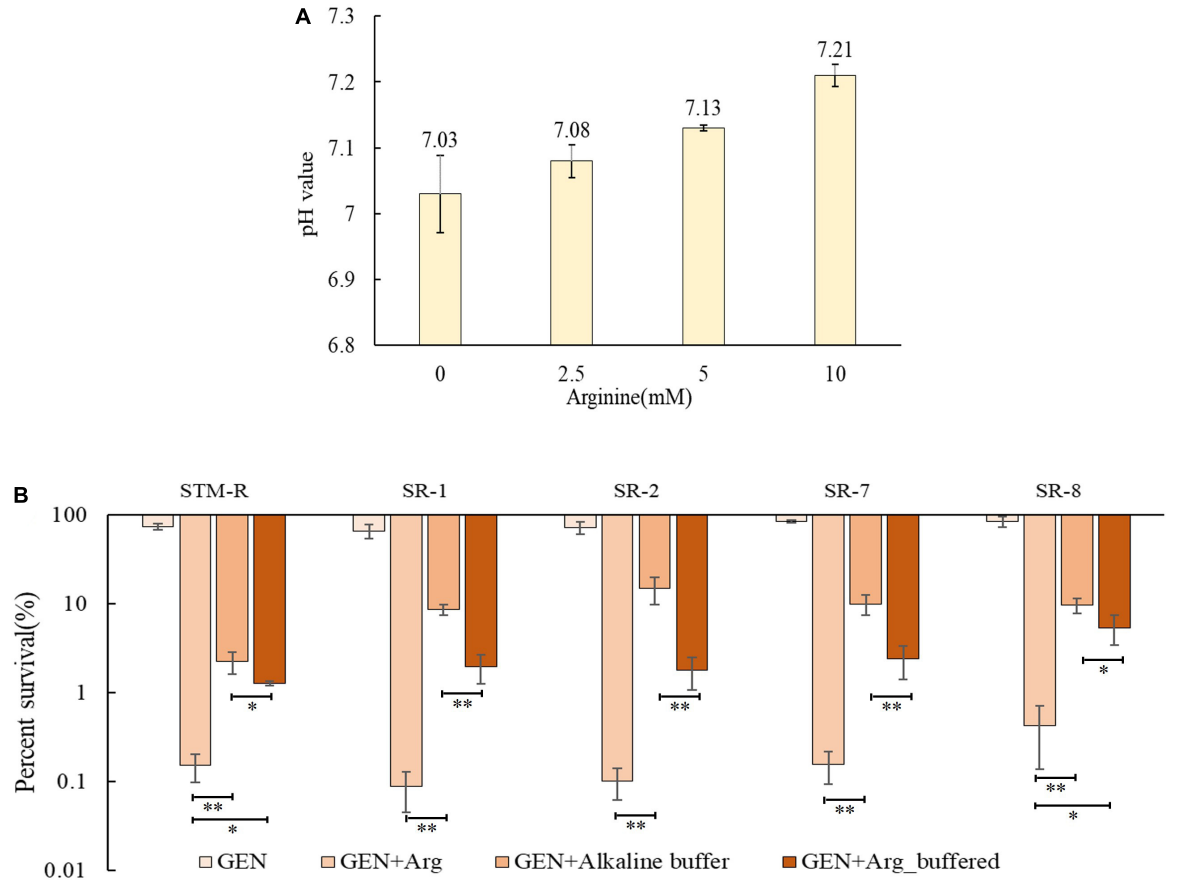

FIGURE 4
pH-induced elevated PMF promotes gentamicin-mediated killing. **(A)** pH value of M9 media with different dose arginine. **(B)** Percent survival of *Salmonella* in M9 media with buffered arginine and alkalized. Results are displayed as the mean ± SD and three biological repeats are carried out. Significant differences are identified [$*p < 0.05$ and $**p < 0.01$ as determined by one way-ANOVA, **(B)**].

Salmonella. Several studies have shown that amino acids and sugars can elevate intracellular NADH, which activates the ETC and elevates the PMF. To test this in drug-resistant *Salmonella*, intracellular NADH levels were measured and shown to increase in response to arginine in a dose-dependent manner. While intracellular NADH levels increased markedly in response to 5 and 10 mM arginine, the increase was less apparent in response to 2.5 mM arginine (Figure 5A). This finding indicated that the arginine-mediated increase in NADH involved a threshold arginine dose. In addition, the ETC inhibitor, rotenone, partially abolished the arginine-potentiated gentamicin-mediated killing of drug-resistant *Salmonella* (Figure 5B). When the electron transport chain pumps electrons across the membrane to form a potential difference, ATP provides energy as the end product of the electron transport chain life activity. NADH as a substrate in the electron transport chain, is also affected by arginine, which may increase the intracellular ATP concentration. The intracellular ATP concentration was measured, as shown in the Supplementary Figure 6, the intracellular ATP concentration was significantly increased after arginine addition compared to the control group. These results suggested that exogenous arginine can elevate intracellular NADH, it promotes ATP production and enhances bacterial metabolic activity, which activates the ETC and ultimately elevates the PMF.

3.6. Arginine fuels the TCA cycle and drives aminoglycoside-mediated killing

Intracellular NADH is generated through partial reactions in central carbon metabolism (the TCA cycle, glycolysis/gluconeogenesis, pentose phosphate pathway) and ultimately undergoes redox reactions to activate the ETC, facilitating the PMF of the cell membrane. Thus, it was assumed that arginine activates central carbon metabolism to promote the generation of NADH. To test this, qRT-PCR was used to examine genes involved in central carbon metabolism (17 associated with the TCA cycle, 7 associated with glycolysis/gluconeogenesis, and 8 involved in the pentose phosphate pathway). Genes involved in glycolysis/gluconeogenesis and the pentose phosphate pathway remained unchanged, while nine genes involved in the TCA cycle, *mdh*, *acnB*, *icdA*, *sucA*, *sucC*, *sdhA*, *sdhC*, *frdC*, and *frdB* were upregulated in the presence of 10 mM arginine (Figure 6A). Of these, *mdh*, *icdA*, and *sucA* encoded malate dehydrogenase, isocitrate dehydrogenase, and α-ketoglutarate dehydrogenase, respectively, which are involved in NADH generation during the TCA cycle. The enzymes encoded by *sdhA*, *sdhC*, *frdB*, and *frdC* are involved in the ETC and are important for maintaining membrane potential. QRT-PCR results showed that arginine is involved in

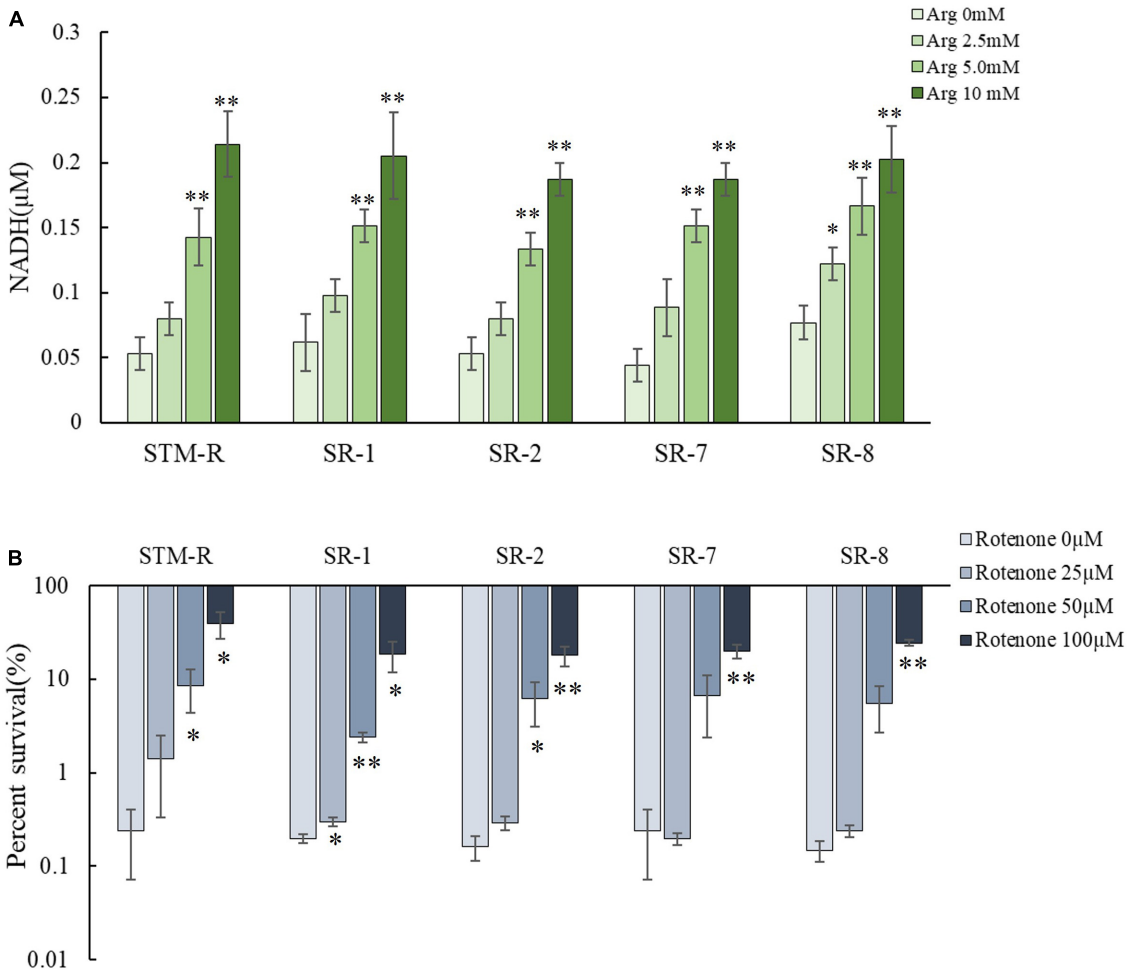

FIGURE 5
Arginine activates the ETC. **(A)** The intracellular NADH concentration of *Salmonella* by different arginine dose and 1 MIC gentamicin. **(B)** Percent survival of *Salmonella* by rotenone dose and 1 MIC gentamicin plus 10 mM arginine. Results are displayed as the mean ± SD and three biological repeats are carried out. Significant differences are identified (*$p < 0.05$ and **$p < 0.01$ as determined by *t*-test).

activating the TCA cycle but not the glycolysis/gluconeogenesis and pentose phosphate pathways. We also assessed the enzymatic activity of intracellular isocitrate dehydrogenase (IDH) and α-ketoglutarate dehydrogenase (KGDH) and found that the activity of both enzymes in drug-resistant *Salmonella* was elevated in the presence of 10 mM arginine (Figures 6B, C).

The TCA cycle inhibitor, malonate, which competitively inhibits succinate dehydrogenase, was used to further verify the impact of the TCA cycle on arginine-mediated potentiation. Drug-resistant *Salmonella* was incubated for 8 h in M9 media with 10 mM arginine plus malonate. As expected, arginine induced the PMF, and NADH was inhibited by malonate in a dose-dependent manner. The arginine-mediated potentiation of gentamicin was similarly inhibited by malonate. Malonate increased drug-resistant *Salmonella* cell viability in a dose-dependent manner even in the presence of arginine and gentamicin (Figures 6D–F).

These findings suggested that in addition to providing ΔpH to increase the PMF, arginine affects the *Salmonella* TCA cycle, inducing NADH and polarizing the ETC (Figure 7). This increases the PMF and promotes drug uptake and cell death.

4. Discussion

There is a critical need for the development of effective strategies to cope with worsening antimicrobial resistance. The use of antibiotic adjuvants may be a better alternative to the development of new antimicrobial agents for the treatment of drug-resistant bacterial infections. This study found that basic arginine significantly increased the gentamicin-, tobramycin-, kanamycin-, and apramycin-mediated killing of drug-resistant *Salmonella*, including MDR strains. The findings provide evidence for the use of arginine as a harmless and highly effective antibiotic adjuvant. Interestingly, arginine also exhibits a positive synergistic effect in mice. However, the metabolic mechanism of arginine *in vivo* is still unclear, which is a topic worth further research.

At first, we tried to explore the mechanism of synergistic effect of arginine and gentamicin by inhibiting arginine decomposition. We conducted experiments using two inhibitors, L-NMMA and BEC. However, the results obtained from these experiments did not provide an explanation for the mechanism under study (Supplementary Figure 7). So, we selected the succinate

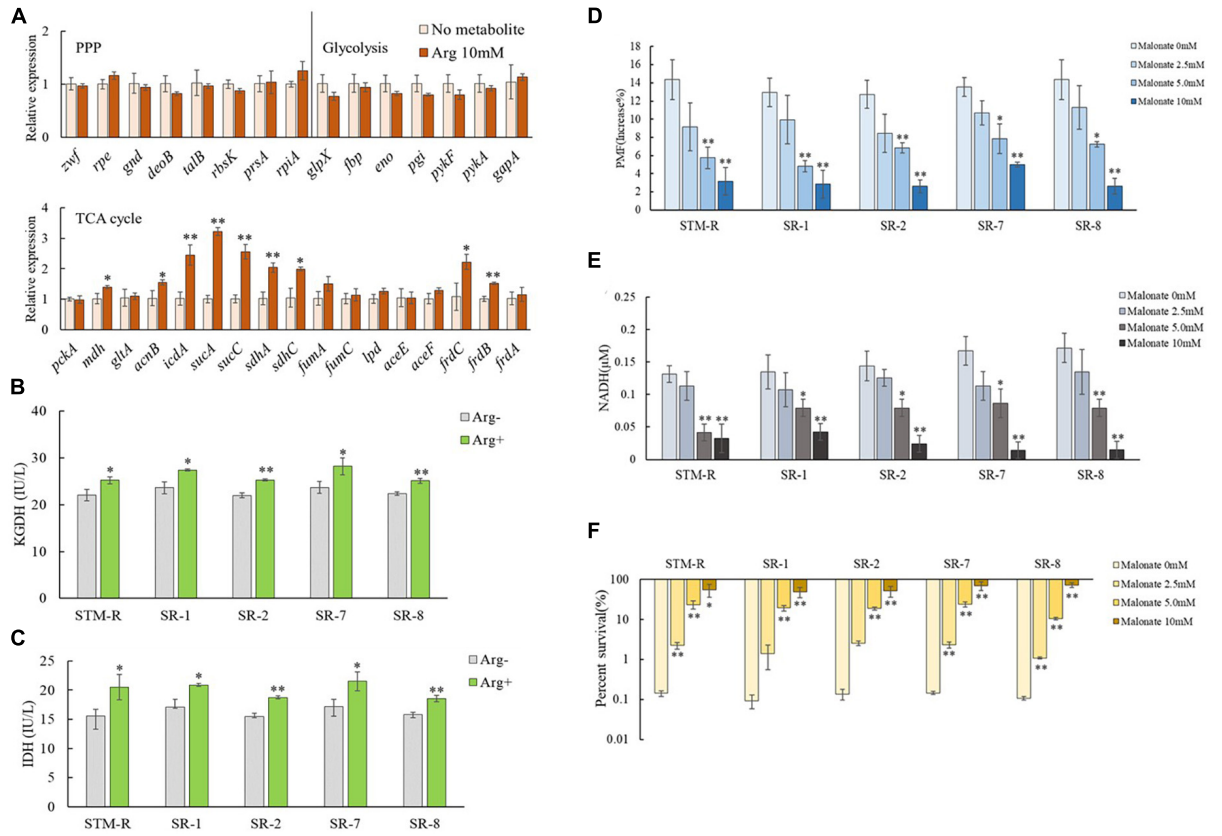

FIGURE 6
Effect of exogenous arginine on central carbon metabolism. **(A)** QRT-PCR for expression of key central carbon metabolism genes in the presence of 10 mM arginine. **(B,C)** Activity of IDH and KGDH in STM-R and clinical isolates with or without arginine. **(D–F)** The PMF, intracellular NADH and percent survival of *Salmonella* by malonate dose with 10 mM arginine. Results are displayed as the mean ± SD and three biological repeats are carried out. Significant differences are identified (*$p < 0.05$ and **$p < 0.01$ as determined by *t*-test).

dehydrogenase inhibitors (malonate), ETC inhibitors (rotenone) and PMF uncoupler (CCCP) for verification selected by many studies. These reagents have been proven to be reliable through several studies, with the relevant literature being referenced in the article. We used three inhibitors to elucidate our mechanism, suggesting that the synergistic effect of arginine is closely related to PMF. Bacterial cell membrane proton motive force (PMF), which is composed of ΔpH (the transmembrane pH difference) and Δψ (the electrical potential across the membrane), is required for the internalization of aminoglycosides (Taber et al., 1987; Sun et al., 2011). Thus, a rise in PMF that occurs due to changes in the ΔpH and/or Δψ can promote the antibacterial effects of aminoglycosides. This is illustrated by the increased susceptibility of bacteria to aminoglycosides in alkaline media and their decreased susceptibility to aminoglycosides in acidic media (Sabath and Toftegaard, 1974; Letoffe et al., 2014). Interestingly, while a dose-dependent effect of arginine was observed *in vitro*, a dose-dependent effect of PMF was not evident. These interesting results may prompt us that PMF is not the only mechanism by which arginine promotes killing effects. However, it is worth noting that the addition of arginine did lead to an increase in PMF, indicating that arginine does plays a significant role in elevating PMF. Indeed, Lebeaux et al. (2014) reported that basic arginine can alkalinize media and increase gentamicin-mediated killing of *E. coli* persisters and *S. aureus* biofilms both *in vitro* and *in vivo*. Alkaline lysine is also shown to assist aminoglycosides in eliminating drug-resistant *Acinetobacter baumannii*, *E. coli*, and *Klebsiella pneumoniae* (Deng et al., 2020). These studies indicate that arginine and lysine can increase aminoglycoside potentiation depending on the ΔpH. The current study similarly found that basic arginine could alkalize media, and promote gentamicin, tobramycin, kanamycin, and apramycin activity against drug-resistant *Salmonella*. These findings suggest that the use of basic substances such as arginine or lysine, to alkalize media, is an effective strategy to improve the activity of aminoglycosides.

Distinct from the ΔpH-induced PMF increase, the Δψ-dependent increase results from a series of biochemical reactions in bacterial cells (Gao et al., 2019). The Δψ, a part of the PMF, improves aminoglycoside activity. Many metabolites also increase the efficacy of aminoglycosides against persisters or drug-resistant bacteria, including glucose, fructose, alanine, and glutamic acid (Allison et al., 2011; Peng et al., 2015). Metabolite-mediated potentiation works by promoting cells to generate more NADH, activating ETC and providing the Δψ needed to elevate the PMF. While Lebeaux et al. (2014) attributed basic arginine-mediated enhancement to the ΔpH, buffered arginine was also found to partially increase gentamicin-mediated killing. The current study found that buffered arginine also promoted the

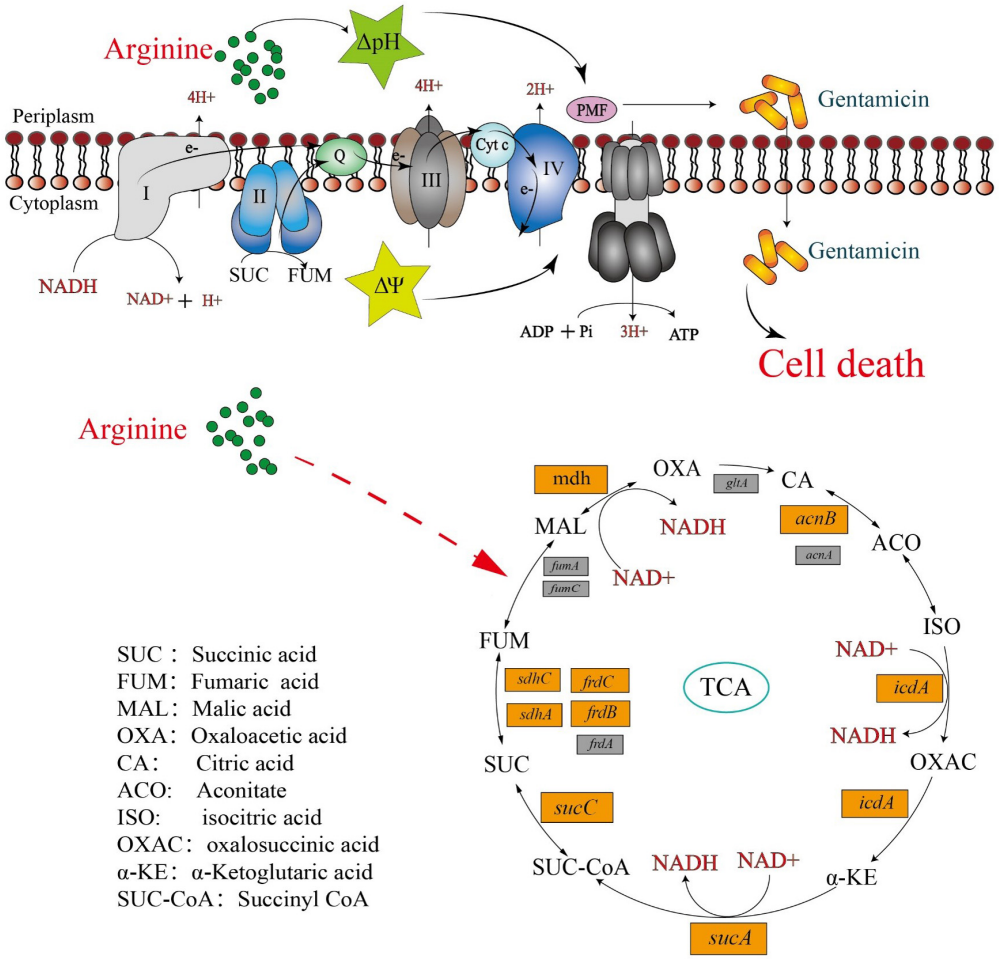

FIGURE 7
Mechanism of exogenous alkaline arginine promotes gentamicin treatment of drug-resistant *Salmonella*.

activity of gentamicin against *Salmonella*, suggesting that there is a pH-independent mechanism for arginine-mediated fortification. Interestingly, the ETC inhibitor, rotenone, partially saved the *Salmonella* cells, highlighting the direct effect of membrane potential on aminoglycoside activity. These results suggest that in addition to pH, Δψ can aid arginine-mediated aminoglycoside function.

Central carbon metabolism, which includes glycolysis, the pentose phosphate pathway (PPP), and the TCA cycle, is required for the generation of intracellular NADH (Baughn and Rhee, 2014; Dolan et al., 2020). Glucose, fructose, and pyruvate entering glycolysis can promote intracellular NADH production in *E. coli*, activate ETC, and induce the PMF. However, the entry of D-ribose into the PPP does not have a similar effect (Allison et al., 2011). Interestingly, our previous study found that D-ribose provides NADH to drug-resistant *Salmonella* through feeding the PPP, and then activates and finally promotes gentamicin activity (Zhou et al., 2022). Peng et al. (2015) demonstrated that metabolites such as alanine, glutamate, fructose, and glucose were able to stimulate the TCA cycle in drug-resistant *Edwardsiella tarda*, promote NADH production, and induce higher PMF to facilitate the uptake of kanamycin (Su et al., 2015). These studies suggested that central carbon metabolism is an important target for metabolite-mediated antimicrobial potentiation. To determine whether arginine influence central carbon metabolism in drug-resistant *Salmonella*, qPCR was performed for genes associated with this pathway in the presence or absence of arginine. Arginine was shown to fuel the TCA cycle but not glycolysis and PPP. Thus, we hypothesized that alkaline arginine provides both ΔpH and activates ETC through the TCA cycle for resistant cells, increasing the PMF of resistant bacteria using both the ΔpH and Δψ, promoting the uptake of gentamicin, and ultimately causing bacterial death.

In summary, arginine is a crucial amino acid that plays an indispensable role in promoting growth and development. The research has indicated that arginine exhibits superior immunomodulatory and anti-inflammatory properties (Kuo et al., 2018; Chen et al., 2022). We developed a strategy for eradicating drug-resistant *Salmonella* and provided evidence to support its use. Arginine was shown to serve as an effective aminoglycoside adjuvant, increasing the PMF of drug-resistant bacteria by modulating both the transmembrane chemical gradient and the electrical potential across the membrane. This increased drug uptake and led to *Salmonella* cell death.

Data availability statement

The original contributions presented in this study are included in the article/**Supplementary material**, further inquiries can be directed to the corresponding author.

Ethics statement

The animal study was approved by the Animal Ethics Committee of South China Agricultural University. The study was conducted in accordance with the local legislation and institutional requirements.

Author contributions

CZ carried out the main experiments and data analysis and wrote the manuscript. YZ and JK participated in the *in vitro* validation tests. HY and JL participated in the isolation and identification of clinical drug-resistant bacteria. BF conceived and designed the experiments. All authors contributed to the article and approved the submitted version.

Funding

This work was funded by the Local Innovative and Research Teams Project of Guangdong Pearl River Talents Program (No. 2019BT02N054).

Acknowledgments

We thank the native English-speaking scientists of Charlesworth Data Services (Beijing) Co., Ltd. (Beijing, China) for editing the manuscript.

Conflict of interest

The authors declare that the research was conducted in the absence of any commercial or financial relationships that could be construed as a potential conflict of interest.

Publisher's note

All claims expressed in this article are solely those of the authors and do not necessarily represent those of their affiliated organizations, or those of the publisher, the editors and the reviewers. Any product that may be evaluated in this article, or claim that may be made by its manufacturer, is not guaranteed or endorsed by the publisher.

Supplementary material

The Supplementary Material for this article can be found online at: https://www.frontiersin.org/articles/10.3389/fmicb.2023.1237825/full#supplementary-material

References

Allison, K. R., Brynildsen, M. P., and Collins, J. J. (2011). Metabolite-enabled eradication of bacterial persisters by aminoglycosides. *Nature* 473, 216–220. doi: 10.1038/nature10069

Baughn, A. D., and Rhee, K. Y. (2014). Metabolomics of central carbon metabolism in *Mycobacterium tuberculosis*. *Microbiol. Spectr.* 2:2.3.02. doi: 10.1128/microbiolspec.MGM2-0026-2013

Chen, Y. L., Lin, M. T., Wang, W. H., Yeh, S. L., and Yeh, C. L. (2022). Intravenous arginine administration attenuates the inflammatory response and improves metabolic profiles in diet-induced obese mice after sleeve Gastrectomy. *Metabolites* 12:153. doi: 10.3390/metabo12020153

Ciorba, V., Odone, A., Veronesi, L., Pasquarella, C., and Signorelli, C. (2015). Antibiotic resistance as a major public health concern: Epidemiology and economic impact. *Ann. Ig* 27, 562–579. doi: 10.7416/ai.2015.2048

Deng, W., Fu, T., Zhang, Z., Jiang, X., Xie, J., Sun, H., et al. (2020). L-lysine potentiates aminoglycosides against *Acinetobacter baumannii* via regulation of proton motive force and antibiotics uptake. *Emerg. Microbes Infect.* 9, 639–650. doi: 10.1080/22221751.2020.1740611

Dolan, S. K., Kohlstedt, M., Trigg, S., Vallejo Ramirez, P., Kaminski, C. F., Wittmann, C., et al. (2020). Contextual flexibility in *Pseudomonas aeruginosa* central carbon metabolism during growth in single carbon sources. *mBio* 11:e02684-19. doi: 10.1128/mBio.02684-19

Gao, M., Yi, J., Zhu, J., Minikes, A. M., Monian, P., Thompson, C. B., et al. (2019). Role of mitochondria in Ferroptosis. *Mol. Cell* 73, 354.e3–363.e3. doi: 10.1016/j.molcel.2018.10.042

Hogberg, L. D., Heddini, A., and Cars, O. (2010). The global need for effective antibiotics: Challenges and recent advances. *Trends Pharmacol. Sci.* 31, 509–515. doi: 10.1016/j.tips.2010.08.002

Kuo, Y. F., Yeh, C. L., Shih, J. M., Shih, Y. M., and Yeh, S. L. (2018). Arginine pretreatment enhances circulating endothelial progenitor cell population and attenuates inflammatory response in high-fat diet-induced obese mice with limb ischemia. *Nutr. Res.* 53, 67–76. doi: 10.1016/j.nutres.2018.03.010

Lebeaux, D., Chauhan, A., Letoffe, S., Fischer, F., de Reuse, H., Beloin, C., et al. (2014). pH-mediated potentiation of aminoglycosides kills bacterial persisters and eradicates *in vivo* biofilms. *J. Infect. Dis.* 210, 1357–1366. doi: 10.1093/infdis/jiu286

Letoffe, S., Audrain, B., Bernier, S. P., Delepierre, M., and Ghigo, J. M. (2014). Aerial exposure to the bacterial volatile compound trimethylamine modifies antibiotic resistance of physically separated bacteria by raising culture medium pH. *mBio* 5:e00944-13. doi: 10.1128/mBio.00944-13

Liu, Y., Li, R., Xiao, X., and Wang, Z. (2019a). Antibiotic adjuvants: An alternative approach to overcome multi-drug resistant Gram-negative bacteria. *Crit. Rev. Microbiol.* 45, 301–314. doi: 10.1080/1040841X.2019.1599813

Liu, Y., Li, R., Xiao, X., and Wang, Z. (2019b). Bacterial metabolism-inspired molecules to modulate antibiotic efficacy. *J. Antimicrob Chemother.* 74, 3409–3417. doi: 10.1093/jac/dkz230

Liu, Y., Yang, K., Jia, Y., Shi, J., Tong, Z., and Wang, Z. (2021). Thymine sensitizes gram-negative pathogens to antibiotic killing. *Front. Microbiol.* 12:622798. doi: 10.3389/fmicb.2021.622798

Meylan, S., Porter, C. B. M., Yang, J. H., Belenky, P., Gutierrez, A., Lobritz, M. A., et al. (2017). Carbon sources tune antibiotic susceptibility in *Pseudomonas aeruginosa* via Tricarboxylic acid cycle control. *Cell Chem. Biol.* 24, 195–206. doi: 10.1016/j.chembiol.2016.12.015

Peng, B., Su, Y. B., Li, H., Han, Y., Guo, C., Tian, Y. M., et al. (2015). Exogenous alanine and/or glucose plus kanamycin kills antibiotic-resistant bacteria. *Cell Metab.* 21, 249–262. doi: 10.1016/j.cmet.2015.01.008

Poulikakos, P., and Falagas, M. E. (2013). Aminoglycoside therapy in infectious diseases. *Expert Opin. Pharmacother.* 14, 1585–1597. doi: 10.1517/14656566.2013.806486

Sabath, L. D., and Toftegaard, I. (1974). Rapid microassays for clindamycin and gentamicin when present together and the effect of pH and of each on the antibacterial activity of the other. *Antimicrob. Agents Chemother.* 6, 54–59. doi: 10.1128/AAC.6.1.54

Stokes, J. M., Lopatkin, A. J., Lobritz, M. A., and Collins, J. J. (2019). Bacterial metabolism and antibiotic efficacy. *Cell Metab.* 30, 251–259. doi: 10.1016/j.cmet.2019.06.009

Su, Y. B., Peng, B., Han, Y., Li, H., and Peng, X. X. (2015). Fructose restores susceptibility of multidrug-resistant *Edwardsiella tarda* to kanamycin. *J. Proteome Res.* 14, 1612–1620. doi: 10.1021/pr501285f

Sun, M., Wartel, M., Cascales, E., Shaevitz, J. W., and Mignot, T. (2011). Motor-driven intracellular transport powers bacterial gliding motility. *Proc. Natl. Acad. Sci. U.S.A.* 108, 7559–7564. doi: 10.1073/pnas.1101101108

Taber, H. W., Mueller, J. P., Miller, P. F., and Arrow, A. S. (1987). Bacterial uptake of aminoglycoside antibiotics. *Microbiol. Rev.* 51, 439–457. doi: 10.1128/mr.51.4.439-457.1987

Wang, X., Xing, C., Li, G., Dai, X., Gao, X., Zhuang, Y., et al. (2023). The key role of proteostasis at mitochondria-associated endoplasmic reticulum membrane in vanadium-induced nephrotoxicity using a proteomic strategy. *Sci. Total Environ.* 869, 161741. doi: 10.1016/j.scitotenv.2023.161741

Yong, Y., Zhou, Y., Liu, K., Liu, G., Wu, L., and Fang, B. (2021). Exogenous Citrulline and glutamine contribute to reverse the resistance of *Salmonella* to Apramycin. *Front. Microbiol.* 12:759170. doi: 10.3389/fmicb.2021.759170

Zhao, X. L., Chen, Z. G., Yang, T. C., Jiang, M., Wang, J., Cheng, Z. X., et al. (2021). Glutamine promotes antibiotic uptake to kill multidrug-resistant uropathogenic bacteria. *Sci. Transl. Med.* 13:eabj0716. doi: 10.1126/scitranslmed.abj0716

Zhou, Y., Yong, Y., Zhu, C., Yang, H., and Fang, B. (2022). Exogenous D-ribose promotes gentamicin treatment of several drug-resistant *Salmonella*. *Front. Microbiol.* 13:1053330. doi: 10.3389/fmicb.2022.1053330

frontiers | Frontiers in Microbiology

TYPE Original Research
PUBLISHED 12 October 2023
DOI 10.3389/fmicb.2023.1280012

OPEN ACCESS

EDITED BY
Jie Feng,
Lanzhou University Medical College, China

REVIEWED BY
Manmohit Kalia,
Binghamton University, United States
Silvia Giono Cerezo,
National Polytechnic Institute (IPN), Mexico

*CORRESPONDENCE
Yang Li
✉ 11418092@zju.edu.cn
Yunzhong Wang
✉ 2248797907@qq.com

†These authors have contributed equally to this work and share first authorship

RECEIVED 19 August 2023
ACCEPTED 29 September 2023
PUBLISHED 12 October 2023

CITATION
Zhang X, Zhu Y, Gao Y, Li W, Wang Y and Li Y (2023) Evaluation and analysis of multidrug resistance- and hypervirulence-associated genes in carbapenem-resistant *Pseudomonas aeruginosa* strains among children in an area of China for five consecutive years. *Front. Microbiol.* 14:1280012. doi: 10.3389/fmicb.2023.1280012

Evaluation and analysis of multidrug resistance- and hypervirulence-associated genes in carbapenem-resistant *Pseudomonas aeruginosa* strains among children in an area of China for five consecutive years

Xin Zhang[1,2,3†], Yunfen Zhu[1†], Yuanyuan Gao[1], Wei Li[1], Yunzhong Wang[1,3*] and Yang Li[1,2,3*]

[1]Department of Clinical Laboratory, Children's Hospital of Soochow University, Suzhou, China, [2]Institute of Pediatric Research, Children's Hospital of Soochow University, Suzhou, Jiangsu, China, [3]Clinical Medical College of Pediatrics, Soochow University, Suzhou, Jiangsu, China

Introduction: Carbapenem-resistant *Pseudomonas aeruginosa* (CRPA) is a growing threat. It is urgent to investigate the multidrug resistance and high virulence of CRPA to provide a basis for infection control and rational use of antibiotics.

Methods: A retrospective study of 56 nonduplicated CRPA isolates was conducted.

Results: CRPA mainly came from the intensive care unit (ICU) and was mostly isolated from sputum samples. The carbapenem resistance rates of *P. aeruginosa* were 21.37% (2016), 10.62, 5.88, 10 and 13.87% from 2016 to 2020, respectively. Carbapenem-resistant enzymes and aminoglycoside-modifying enzyme-encoding genes were detected in all isolates, and extended-spectrum β-lactamase and cephalosporin enzyme-encoding genes were present in 96.43 and 80.38% of isolates, respectively. The detection rate of *OprM* showed a statistically significant difference ($p < 0.05$) between the ICU and other wards. Genes related to biofilms, membrane channel proteins, I integrons and efflux systems were detected in all isolates, with detection rates greater than 90%. CRPA was strongly virulent, and over 80% of isolates carried hypervirulence-associated genes (*exoU*, *exoS*, *exoT*, and *exoY*). The drug resistance rates of cefepime and piperacillin/tazobactam showed a statistically significant difference ($p < 0.05$) between strains with *exoU* (+) and *exoU* (–) ($p < 0.05$). Notably, out of the 7 individuals who died, 4 had extensively drug-resistant *P. aeruginosa* (57.14%).

Discussion: The detection rates of various resistance and virulence genes were high, and the coexistence phenomenon was serious. In clinical practice, antibiotics should be used reasonably based on different drug resistance genes to ensure the rationality and safety of patient medication.

KEYWORDS

***Pseudomonas aeruginosa*, children, carbapenem resistance, hypervirulence, gene, type III secretion system, epidemiology**

1. Introduction

Pseudomonas aeruginosa (*P. aeruginosa*) is a common opportunistic pathogen in hospital-acquired infections. In 2017, the *World Health Organization* listed *P. aeruginosa* as a top priority pathogen. Many previous studies of *P. aeruginosa* infections have focused on adult patients. To date, there is less information about *P. aeruginosa* infections in children than in adults. *P. aeruginosa* infection usually has serious consequences for children, especially for those admitted to the intensive care unit (ICU). *P. aeruginosa* can be transmitted through multiple routes, causing infections in multiple parts of the human body, including the respiratory tract, circulatory system, urinary tract and wound surfaces (Hall et al., 2022). Antibiotic treatment is an effective method for treating *P. aeruginosa* infection. The introduction of antibiotics at the beginning of the 20th century revolutionized medicine, greatly reducing the incidence rate and mortality of bacterial infections. However, the increase in drug-resistant strains is occurring much more rapidly than the development of effective antibiotics. Due to the overuse of antibiotics, studies in various regions have shown an increase in drug resistance rates (Walkty et al., 2017; Sader et al., 2018; Lyu et al., 2023). Bacteria have been found to have severe resistance and are often multidrug resistant (MDR). At present, carbapenems are often the preferred antibiotics for terminal treatment of *P. aeruginosa* infections in clinical practice due to their broad antibacterial spectrum, strong antibacterial activity, and rapid action. However, the presence of carbapenem-resistant *Pseudomonas aeruginosa* (CRPA) isolates increases the incidence and mortality rates, length of hospital stay and treatment costs (Ponce de Leon et al., 2020). According to reports, the resistance of *P. aeruginosa* to carbapenems in other developing countries is approximately 50% (Sharifi et al., 2019). The latest data released by the *National Drug Resistance Monitoring Network*[1] show that in the isolation rate of Gram-negative bacteria in hospitals in 2021, *P. aeruginosa* still ranked third, accounting for 11.8%. In terms of drug resistance, the national average resistance rate of *P. aeruginosa* to carbapenems is 17.7%, and the drug resistance rate in Jiangsu Province is higher than the national average level (24.3%). According to the CDC's 2019 Antibiotic Resistance Threats Report, CRPA is listed as an urgent threat (CDC, 2019). According to the survey results of the *Chinese Children's Bacterial Resistance Monitoring Group*, the resistance rate of *P. aeruginosa* to carbapenem antibiotics is rising rapidly, and it also has high resistance to other common antibiotics (Pan et al., 2021). With the widespread use of antibiotics, the numbers of multidrug-resistant *P. aeruginosa* (MDR-PA) and extensively drug-resistant *P. aeruginosa* (XDR-PA) strains are constantly increasing. However, very few antibiotics can effectively treat infections caused by MDR-PA and XDR-PA (Tamma et al., 2022). Therefore, it is of great importance to analyze the clinical distribution and drug resistance of *P. aeruginosa* for early antibiotic treatment.

At present, there are very limited effective antibiotics for CRPA, and a deep understanding of the resistance mechanism of CRPA is important for conducting new drug research and the rational clinical use of antibiotics. *P. aeruginosa* has both natural and acquired multidrug resistance, and its complex resistance mechanisms mainly include loss of outer membrane barrier pore protein ($OprD_2$), overexpression of the efflux system, and production of β-lactam enzymes (BLEs) and aminoglycoside-modifying enzymes (AMEs). $OprD_2$ is the only pore protein found in *P. aeruginosa* that is conducive to the passage of antibiotics (Chevalier et al., 2017). The downregulation of $OprD_2$ usually leads to resistance to common carbapenem antibiotics (such as imipenem and meropenem). Therefore, the deletion or mutation of the gene encoding $OprD_2$ can reduce drug uptake by *P. aeruginosa*. The efflux pumps are formed by a combination of *OprM*, which is found in the outer membrane, with *MexA* and *MexB* to form a stable complex at the inner membrane (Coșeriu et al., 2023). The most common efflux pump family in *Pseudomonas* is the resistance nodulation-division. *MexAB-OprM* plays an important role in the inherent resistance of *P. aeruginosa* (Ma et al., 2021). By overexpressing the MexAB-OprM complex, bacteria can acquire resistance to cephalosporins, penicillin, carbapenems, phenols, and most fluoroquinolones (Zahedi Bialvaei et al., 2021). The *MexR* gene is a regulator of the efflux pump *MexAB-OprM*. *MexA* and *MexB* are regulated by *MexR* on the operator of the efflux system. The production of BLEs is an important drug resistance mechanism of *P. aeruginosa*. BLEs include extended-spectrum β-lactamases (ESBLs), carbapenemases (MBLs), and cephalosporin enzymes (AmpC). ESBL production is an important mechanism of resistance of drug-resistant bacteria to penicillins, cephalosporins and aztreonam. MBLs are the most important drug resistance mechanism of CRPA (Elshafiee et al., 2019). Resistance to carbapenem antibiotics is mainly caused by Class B enzymes (Kim et al., 2016), and their resistance can be horizontally transmitted to other species. The genes encoding MBLs are usually part of the class I integron structure and are transmitted by mobile genetic elements (Palzkill, 2013). Integrins are a genetic structure that exists on bacterial plasmids, chromosomes, or transposons. They can capture drug resistance genes and make bacteria exhibit multiple-antibiotic resistance, which is also an important reason for the rapid development of bacterial multidrug resistance. Class I integrons represented by *intI-1* and *qacE△1-sul1* are the most common in clinical isolates. Whether *P. aeruginosa* can cause infection upon entering the body depends on two factors: one is the body's defense ability, and the other is the pathogenic ability of the bacteria. Domestic and foreign studies have shown that the main pathogenesis of *P. aeruginosa* is closely related to its encoded polymorphic secretion system (Golovkine et al., 2018). The exoenzymes produced through the type III secretion system (T3SS) are an important virulence system for the pathogenicity of *P. aeruginosa*, which can lead to apoptosis of alveolar epithelial cells, macrophages, and fibroblasts, exacerbate inflammatory reactions, and increase the mortality rate of infection (Horna and Ruiz, 2021). Most *P. aeruginosa* have a functional T3SS, which contains virulence genes such as *exoS*, *exoT*, *exoU*, and *exoY*, which secrete effector proteins such as ExoS, ExoT, ExoU, and ExoY, respectively. Recently, a study showed that the detection rates of *exoA*, *exoS*, and *exoU* in *P. aeruginosa* were relatively high (Zarei et al., 2020), which poses great challenges to clinical treatment due to the widespread resistance of *P. aeruginosa*. The identification of virulence gene profiles is crucial for developing effective anti-*P. aeruginosa* infection strategies.

Due to the existence of multiple drug resistance mechanisms, the drug resistance rate of *P. aeruginosa* remains high, and it can secrete a large number of virulence factors, leading to a substantial increase in the incidence rate and mortality (Ponce de Leon et al., 2020).

1 http://www.carss.cn/

Exploring the coexistence of drug resistance genes and virulence genes is of great importance for the treatment of patients. Although there is currently information on the resistance and virulence genes of *P. aeruginosa*, the characteristics of various strains vary due to factors such as different targets of action, different sample sources, and different regions (Takata et al., 2018; de Sousa et al., 2023; Poursina et al., 2023). There are still few research papers and reviews on the correlation between CRPA infection in children in the Suzhou area. Therefore, we conducted a 5-year retrospective study to evaluate the epidemiological characteristics, resistance genes (*VIM*, *GIM*, *IMP*, *BIC*, *AIM*, *SPM*, *NDM*, *OXA*, *OXA-2*, *OXA-10*, *KPC*, *PER*, *VEB*, *SHV*, *TEM*, *CIT-1*, *MOX-1*, *EBC-1*, *ant(2″)-I*, *ant(2″)-Ia*, *ant(3″)-I*, *aac(3)-II*, *aac(3)-IIc*, *ant(4′)-Ia*, *aac(6′)-I*, *aac(6′)-Ib*, *aac(6′)-II*, *OprM*, *MexB*, *mucB*, *intI-1*, *qacE△1-sul1*, $OprD_2$) and hypervirulence-associated genes (*exoU*, *exoS*, *exoT* and *exoY*) of *P. aeruginosa* infection in children in the Suzhou area to explore the reasons for the resistance and high virulence of CRPA at the molecular level and promote the rational use of antibiotics in clinical practice based on the detected virulence and resistance gene carriers.

2. Materials and methods

2.1. Study site

This study was conducted at the Children's Hospital of Soochow University (CHSU), which is a children's medical center in East China and the only provincial tertiary children's hospital in Jiangsu Province. CHSU has 1,500 beds and serves >70,000 inpatients and > 2 million outpatients annually.

2.2. General information

From January 2016 to December 2020, a total of 82 CRPA strains were isolated, of which 56 nonduplicated CRPA strains were selected as the research subjects. *P. aeruginosa* isolates were confirmed by mass spectrometry (Microflex LT/SH, Germany). An automatic bacterial detection and analysis system (VITEK®2 Compact, France) and Kirby-Bauer (KB) method were used for the drug sensitivity test. The results were analyzed according to the guidelines of the Clinical and Laboratory Standards Institute. The quality control strains were *P. aeruginosa* (ATCC 27853) which were purchased from the clinical testing center of the National Health Commission. This study was approved by the ethics committee of CHSU (No. 2021CS158).

2.3. Determination of drug-resistant *Pseudomonas aeruginosa*

The judgment criteria of CRPA were *P. aeruginosa* resistant to imipenem and one of the following eight categories of antibiotics, including cephalosporin (such as ceftazidime and cefepime), quinolones (such as levofloxacin and ciprofloxacin), carbapenem (such as imipenem and meropenem), β-lactam enzyme inhibitors (such as piperacillin/tazobactam and cefoperazone/sulbactam), aminoglycosides (such as gentamicin, tobramycin, and amikacin), monobactams (aztreonam), phosphates (fosfomycin), and polymyxin (polymyxin B). Resistant to 3 and more than three antibiotics are considered MDR, resistant to 6 and more than six are considered XDR, and strains showing resistance to all the tested drugs are considered pan-drug resistant (Magiorakos et al., 2012).

2.4. Detection of virulence and resistance genes

Focusing on the analysis of the resistance and virulence genes, specific gene sequences can be found in Supplementary Table S1. Bacterial DNA was extracted by the boiling method, as described in the literature (Wei et al., 2007). The specific steps were as follows: a ring of colonies was picked from the inoculation ring, placed in an EP tube containing 1 mL of sterile water, shaken and mixed evenly. Then, the colonies were boiled in a 100°C metal bath for 30 min and cooled in a −20°C refrigerator for 30 min to lyse the cells, completely thawed at room temperature, and centrifuged at 15000 rpm for 5 min. The supernatant was collected and stored. After measuring its concentration and purity by UV spectrophotometry, it was placed in a refrigerator at −20°C as a template for storage.

2.5. Data analysis

SPSS 20.0 and WHONET v5.6 software (WHO Collaborating Centre for Surveillance of Antimicrobial Resistance, Boston, MA, USA) were used to analyze the data. The counting data were expressed as the number of cases (n) and rate (%). The χ^2 test was used in univariate analysis. The comparison between groups was carried out by the χ^2 test, with $p < 0.05$ indicating a statistically significant difference.

3. Results

3.1. Clinical information analysis of 56 CRPA strains

A total of 56 CRPA isolates were collected. Among them, 33 strains were isolated from the ICU, 39 isolates were isolated from sputum, and 7 strains were isolated from deceased patients. The source of the specimen showed a statistically significant difference ($p < 0.05$) between the ICU and other wards. The probability of patients admitted to the ICU being infected with other pathogens was significantly higher than that of patients in other wards (Table 1).

3.2. The detection and carbapenem-resistance rate of *Pseudomonas aeruginosa*

In this study, the detection of *P. aeruginosa* fluctuated between 2016 and 2020, with the lowest amount of CRPA isolates detected in 2018 (Figure 1A). The carbapenem resistance rates of *P. aeruginosa* were 21.37, 10.62, 5.88, 10 and 13.87% from 2016 to 2020, respectively. The carbapenem resistance rate in the local children's medical center was significantly lower than that in Jiangsu Province and the whole country of China (Figure 1B).

10.3389/fmicb.2023.1280012

TABLE 1 Epidemiology in this study [n (%)].

Classification		ICU ($n = 33$)	Other wards* ($n = 23$)	χ^2	P
Specimen	Sputum ($n = 39$)	27 (69.23)	12 (30.77)	**5.634**	**0.018**
	Blood ($n = 4$)	1 (25)	3 (75)	2.049	0.152
	Alveolarlavage fluid ($n = 5$)	4 (80)	1 (20)	1.007	0.316
	Urine ($n = 4$)	0 (0)	4 (100)	**6.181**	**0.013**
	Others specimen* ($n = 4$)	1 (25)	3 (75)	2.049	0.152
Age	0 ~ <3Y ($n = 39$)	24 (61.54)	15 (38.46)	0.362	0.548
	3 ~ <14Y ($n = 16$)	9 (56.25)	7 (43.75)	0.066	0.797
	14 ~ <18Y ($n = 1$)	0 (0)	1 (100)	1.461	0.227
Survival state	Survival ($n = 49$)	27 (55.10)	22 (44.90)	2.372	0.124
	Death ($n = 7$)	6 (85.71)	1 (14.29)		
Gender	Male ($n = 36$)	20 (55.56)	16 (44.44)	0.474	0.491
	Female ($n = 20$)	13 (65)	7 (35)		
Length of hospitalization	0 ~ <15 d ($n = 8$)	4 (50)	4 (50)	0.307	0.579
	15 ~ <30 d ($n = 11$)	4 (36.36)	7 (63.64)	2.880	0.090
	30 ~ <60 d ($n = 25$)	17 (68)	8 (32)	1.536	0.215
	> = 60 d ($n = 12$)	8 (66.67)	4 (33.33)	0.378	0.539
Basic disease	Pneumonia ($n = 20$)	11 (55)	9 (45)	0.198	0.656
	Hematological system diseases ($n = 14$)	7 (50)	7 (50)	0.615	0.433
	Heart disease ($n = 12$)	10 (83.33)	2 (16.67)	3.758	0.053
	Other infections* ($n = 5$)	2 (40)	3 (60)	0.813	0.367
	Other diseases* ($n = 5$)	3 (60)	2 (40)	0.003	0.959
Any combined infection with other pathogenic bacteria	Gram-positive bacteria ($n = 7$)	4 (57.14)	3 (42.86)	0.011	0.918
	Gram-negative bacteria ($n = 25$)	12 (48)	13 (52)	2.229	0.135
	Mixed infection of Gram-negative/positive bacteria or fungi ($n = 11$)	11 (100)	0 (0)	**9.541**	**0.002**
	No combined infection ($n = 13$)	6 (46.15)	7 (53.85)	1.142	0.285

Bold values highlight meaningful results. *Other specimens included pharyngeal swabs and pus. Other infections included encephalitis, laryngitis, urinary tract infection, and lymphadenitis. Other diseases included epilepsy, genetic metabolic disease, foreign body inhalation asphyxia, and neonatal respiratory distress syndrome. Other wards included the departments of hematology, neonatology, and respiratory care. d, days; Y, years.

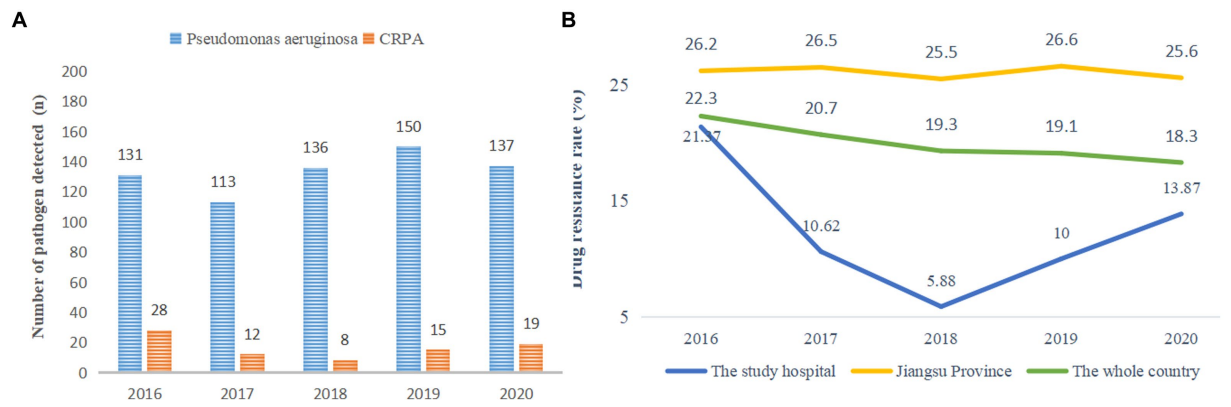

FIGURE 1
(A) Detection of pathogenic bacteria. **(B)** Carbapenem resistance rate of *P. aeruginosa* from 2016 to 2020. * The carbapenem resistance rate of *P. aeruginosa* in the whole country came from the National Drug Resistance Monitoring Network. The member units that report the data are mainly tertiary hospitals, which report the monitoring data from October of the current year to September of the next year every year. The principle of retaining the first strain of the same bacteria from the same patient is to eliminate duplicate strains.

10.3389/fmicb.2023.1280012

TABLE 2 Analysis of the drug resistance of 56 CRPA isolates.

Antibiotic		Number of drug-resistant bacteria	Percentage (%)
Carbapenems	Imipenem	56	100
Monobactams	Aztreonam	28	50
Extended-spectrum cephalosporin	Cefotetan	56	100
	Ceftazidime	18	32.14
	Ceftriaxone	56	100
	Cefepime	9	16.07
Penicillins	Ampicillin	56	100
	Piperacillin	20	35.71
	Ticarcillin	40	71.43
Enzyme inhibitor complexes	Ampicillin/sulbactam	56	100
	Piperacillin/tazobactam	17	30.36
	Cefoperazone/sulbactam	18	32.14
Aminoglycosides	Gentamicin	0	0
	Amikacin	0	0
	Tobramycin	0	0
Sulfonamides	Compoundsulfamethoxazole	56	100
Fluoroquinolones	Ciprofloxacin	4	7.14
	Levofloxacin	4	7.14

3.3. Analysis of antimicrobial susceptibility

A total of 56 CRPA isolates exhibited a higher drug resistance rate to various antibiotics but fluoroquinolone antibiotics, as shown in Table 2. They showed a 100% resistance rate to carbapenems (imipenem), extended-spectrum cephalosporins (cefotetan, ceftriaxone), enzyme inhibitor complexes (ampicillin/sulbactam), penicillins (ampicillin), and sulfonamides (compound sulfamethoxazole). The resistance rate to fluoroquinolones (ciprofloxacin and levofloxacin) was only 7.14%.

3.4. Detection of BLEs genes in 56 CRPA isolates

BLEs genes include carbapenem resistance genes, ESBLs genes and AmpC genes. In Table 3, the detection rates of *VIM*, *OXA*, *GIM*, *BIC* and *IMP* were 98.21, 57.14, 55.36, 30.36, and 17.86%, respectively. NDM, *AIM*, *SPM*, *KPC*, *OXA-2* and *OXA-10* were not detected. See Supplementary Table S2 for the details of resistance genes carried by the 56 isolates.

3.5. Detection of other main genes of the 56 CRPA isolates

AMEs genes and other resistance genes were analyzed. As seen in Table 4, *ant(2″)-I*, *mucB*, *OprD*$_2$, *intI-1*, *qacE*$\triangle$*1-sul1*, and *MexB* were detected in all isolates. See Supplementary Table S2 for the details of resistance genes carried by the 56 isolates.

3.6. Detection of hypervirulence-associated genes of 56 CRPA isolates

In Tables 4, 5 hypervirulence-associated genes were analyzed. *exoS, exoT, and exoY* were present in 100% of the isolates. In addition, 83.93% of the strains carried *exoU*. See Supplementary Table S3 for the details of hypervirulence-associated genes carried by the 56 isolates.

3.7. The correlation between carrying exoU and antibiotic resistance of 56 CRPA isolates

As shown in Table 6, there were differences in cefepime and piperacillin/tazobactam resistance among strains carrying *exoU*, while there was no difference in other antibiotics.

3.8. Differential analysis between the survival group and death groups

Comparison of data between the survival and death groups showed that there was no statistically significant difference in the detection rates of major drug resistance genes or hypervirulence-associated genes

TABLE 3 The results of BLEs gene detection in 56 CRPA isolates [n (%)].

Gene	Type	Number of isolates with detected genes			χ^2	*P*
		Total	ICU (*n* = 33)	Other wards* (*n* = 23)		
Carbapenem-resistant genes	*VIM*	55 (98.21)	32 (57.14)	23 (41.07)	0.71	0.4
	OXA	32 (57.14)	18 (32.14)	14 (25)	0.221	0.638
	GIM	31 (55.36)	17 (30.36)	14 (25)	0.48	0.488
	BIC	17 (30.36)	10 (17.86)	7 (12.5)	0	0.992
	IMP	16 (17.86)	10 (17.86)	6 (10.71)	0.118	0.731
	AIM	0	0	0	–	–
	SPM	0	0	0	–	–
	NDM	0	0	0	–	–
	KPC	0	0	0	–	–
	OXA-2	0	0	0	–	–
	OXA-10	0	0	0	–	–
ESBLs genes	*SHV*	54 (96.43)	31 (55.36)	23 (41.07)	1.446	0.229
	VEB	0	0	0	–	–
	PER	0	0	0	–	–
	TEM	0	0	0	–	–
AmpC genes	*EBC-1*	43 (76.79)	25 (44.65)	18 (32.14)	0.048	0.827
	CIT-1	32 (57.14)	22 (39.29)	10 (17.86)	2.976	0.085
	MOX-1	0	0	0	–	–

*Other wards included the departments of hematology, neonatology, and respiratory care.

(Table 7). Notably, out of the 7 individuals who died, 4 had XDR bacteria detected.

4. Discussion

Pseudomonas aeruginosa can rapidly mutate and acquire resistance to adapt to the environment, making it one of the main pathogens causing hospital infections. Carbapenem antibiotics are currently the "ace killer" of Gram-negative bacteria due to their strong selectivity and low toxicity to host cells. However, with the widespread use of antibiotics, the detection rate of *P. aeruginosa* resistant to multiple antibiotics is increasing yearly (Litwin et al., 2020). The emergence of CRPA has made hospital infection control increasingly difficult. CRPA has a high mortality rate, is prone to cross-infection, and is extremely difficult to treat. Its drug resistance genes are easily transmitted between strains, leading to the production of drug-resistant bacteria and thus affecting treatment effectiveness. In addition, very few antibiotics can effectively treat infections caused by multidrug-resistant *P. aeruginosa* (Wanqing et al., 2022). The emergence, prevention, and treatment of hospital infections and new drug-resistant bacteria are extremely important.

In the present work, 56 CRPA strains mainly came from three key departments: the ICU, neonatal pediatrics, and hematology. The proportion of CRPA originating from the ICU exceeded 50%, which may be related to the rapid spread of CRPA among ICU patients. This result is consistent with a recent survey on CRPA infections in critically ill children in a large tertiary pediatric hospital in China (Huang et al., 2023). The incidence of infection among ICU patients was 5-7-fold higher than that among general inpatients, contributing to 20–25% of all nosocomial infections in hospitals (Alfouzan et al., 2021). Subsequently, statistical analysis was conducted on the types of specimens, and it was found that most CRPA isolates were detected in sputum specimens, accounting for 69.64%, which is consistent with reports that CRPA is mainly isolated from sputum (Gill et al., 2022). There was a statistically significant difference in the detection of CRPA detected in sputum and urine between the ICU and other wards. From an age group perspective, detection was mainly concentrated among children aged 0 ~ <3 years. The proportion of CRPA isolated from males was slightly higher than that isolated from females. Patients who had been hospitalized for more than 30 days had a higher proportion of CRPA detection (66.07%). Analysis of 7 CRPA strains isolated from deceased children found that 6 strains originated from sputum and 1 strain from blood. The mortality rate in the sputum sample group was 15.38% (6/39), while in the blood group, the mortality rate was 25% (1/4). The mortality rate of bloodstream infections caused by CRPA is high. Special attention should be given to CRPA detected in the blood circulation system (Recio et al., 2020). Among the clinical cases corresponding to the 56 CRPA strains, pneumonia, hematological system diseases, and heart disease accounted for the highest proportion of diseases. Children admitted to the ICU were more likely to develop mixed infections ($p = 0.002$). In response to the upstream situation, clinical practitioners should pay attention to high-risk factors, take timely response measures, isolate and protect, and perform early prevention, detection, and treatment.

To further explore the detection of *P. aeruginosa* and the discovery of carbapenem antibiotic resistance, from 2016 to 2020, the carbapenem resistance rate of *P. aeruginosa* showed a downward and

10.3389/fmicb.2023.1280012

TABLE 4 The results of other main gene detection in 56 CRPA isolates [n (%)].

Gene	Type	Number of isolates with detected genes			χ^2	*P*
		Total	ICU (*n* = 33)	Other wards* (*n* = 23)		
AMEs genes	*ant(2″)-I*	56 (100)	33 (58.93)	23 (41.07)	–	–
	aac(6′)-II	48 (85.71)	27 (48.21)	21 (37.5)	0.996	0.318
	aac(3)-IIc	35 (62.5)	21 (37.5)	14 (25)	0.044	0.833
	ant(2″)-Ia	30 (53.57)	18 (32.14)	12 (21.43)	0.031	0.861
	aac(6′)-Ib	28 (50)	20 (35.71)	8 (14.29)	3.615	0.057
	aac(6′)-I	6 (10.71)	4 (7.14)	2 (3.57)	0.166	0.683
	ant(4′)-Ia	0	0	0	–	–
	ant(3″)-I	0	0	0	–	–
	aac(3)-II	0	0	0	–	–
Biofilm-related genes	*mucB*	56 (100)	33 (58.93)	23 (41.07)	–	–
Membrane channel protein-related genes	*OprD*$_2$	56 (100)	33 (58.93)	23 (41.07)	–	–
I integron	*intI-1*	56 (100)	33 (58.93)	23 (41.07)	–	–
	qacE△1-sul1	56 (100)	33 (58.93)	23 (41.07)	–	–
Genes related to the efflux system	*MexB*	56 (100)	33 (58.93)	23 (41.07)	–	–
	OprM	52 (92.86)	33 (58.93)	19 (33.93)	**6.181**	**0.013**

Bold values highlight meaningful results. *Other wards included the departments of hematology, neonatology, and respiratory care.

TABLE 5 The results of virulence gene detection in 56 CRPA isolates [n (%)].

Hypervirulence-associated genes	Number of isolates with detected genes			χ^2	*P*
	Total	ICU (*n* = 33)	Other wards* (*n* = 23)		
exoU	47 (83.93)	26 (55.32)	21 (44.68)	1.574	0.210
exoS	56 (100)	33 (58.93)	23 (41.07)	–	–
exoT	56 (100)	33 (58.93)	23 (41.07)	–	–
exoY	56 (100)	33 (58.93)	23 (41.07)	–	–

*Other wards included the departments of hematology, neonatology, and respiratory care.

then upward trend, which was consistent with a previous report (Feng et al., 2021) and far lower than the drug resistance rate shown in another study (Sharifi et al., 2019). However, the drug resistance rate continued to increase from 2018 to 2020, which was inconsistent with the downward trend reported by the *National Drug Resistance Monitoring Network* (*CHINET*) (see text footnote 1) (Hu et al., 2021). The resistance of *P. aeruginosa* to imipenem is primarily caused by the production of metalloenzymes and efflux pumps and the lack of OprD$_2$ (Memar et al., 2021), which may be related to the widespread use of imipenem in clinical practice in recent years, and resistance is gradually increasing. According to feedback from the *Chinese Children's Bacterial Resistance Monitoring Group*, the detection rate of CRPA in 2020 was 9.5% (Leiyan et al., 2021), lower than the 13.87% in this study and the national rate (18.3%). This indicates that the drug resistance rate of *P. aeruginosa* in children's hospitals is still relatively high. If hypervirulence-associated genes are combined, it will be tremendously difficult to make diagnoses and provide treatment. Therefore, special attention needs to be paid to the infection situation of CRPA in children.

Exploring the drug resistance mechanism of CRPA and analyzing its high toxicity and pathogenicity need to be performed. Subsequently, the related resistance genes (including production of BLEs and AMEs, loss of OprD$_2$ and overexpression of the efflux system) and hypervirulence-associated genes were analyzed. The PCR results indicated that among 56 CRPA isolates, the proportion of BLE-producing strains was quite high. Carbapenem resistance genes were detected in 56 strains. The most prevalent gene detected in this study was *VIM*, in agreement with other study (Gill et al., 2022). There is evidence that the rapid dissemination of MBL-producing *P. aeruginosa* is mainly due to *VIM* and *NDM* (Urbanowicz et al., 2019). Very few studies have reported on the coexistence of VIM and NDM in the same bacterium (Jaggi et al., 2012). Regarding differences in drug resistance genes detected in different regions, different types of carbapenem resistance (*IMP, NDM, DIM* and so on) among

10.3389/fmicb.2023.1280012

TABLE 6 Correlation analysis between the resistance rate and *exoU* [n (%)].

Antibiotics	Number of drug resistant bacteria		χ^2	*P*
	exoU (+)* (*n* = 47)	*exoU* (–) (*n* = 9)		
Imipenem	47 (83.93)	9 (16.07)	–	–
Aztreonam	25 (44.64)	3 (5.36)	1.191	0.275
Cefotetan	47 (83.93)	9 (16.07)	–	–
Ceftazidime	17 (30.36)	1 (1.78)	2.175	0.140
Ceftriaxone	47 (83.93)	9 (16.07)	–	–
Cefepime	9 (16.07)	0	**8.640**	**0.003**
Ampicillin	47 (83.93)	9 (16.07)	–	–
Piperacillin	18 (32.14)	2 (3.57)	0.850	0.356
Ticarcillin	35 (62.5)	5 (8.93)	1.324	0.250
Ampicillin/sulbactam	47 (83.93)	9 (16.07)	–	–
Piperacillin/tazobactam	17 (30.36)	0	**4.674**	**0.031**
Cefoperazone/sulbactam	16 (28.57)	2 (3.57)	0.484	0.487
Gentamicin	0	0	–	–
Amikacin	0	0	–	–
Tobramycin	0	0	–	–
Compoundsulfamethoxazole	47 (83.93)	9 (16.07)	–	–
Ciprofloxacin	4 (7.14)	0	0.825	0.364
Levofloxacin	4 (7.14)	0	0.825	0.364

Bold values highlight meaningful results. **exoU* (+) represents the detection of this gene.

P. aeruginosa strains have been detected in Europe (Paul et al., 2016). ESBLs genes were detected in 54 strains, and AmpC genes were detected in 45 strains. ESBL-producing Gram-negative pathogens are a major cause of resistance to ESBL antibiotics. In the past, *TEM* and *SHV*-type ESBLs were the predominant families of ESBLs. In this work, *SHV* was the only main ESBL gene, accounting for 96.43%. *VEB, PER and TEM* were not detected. Currently, *CTX-M*-type enzymes are the most commonly found ESBLs type (Castanheira et al., 2021). AmpC enzyme is a type of β-lactam enzyme mediated by chromosomes or plasmids, including *ACC*, *DHA*, *CIT*, *EBC*, *FOX* and *MOX*. As shown in Table 2, the detection rates of *EBC-1, CIT-1* and *MOX-1* were 76.79, 57.14% and 0, respectively. This is somewhat different from the results reported in other studies (Miao et al., 2019), indicating that CRPA from different regions and sample sources may have different drug resistance rates and drug resistance gene carriers.

Pseudomonas aeruginosa forms drug resistance by producing AMEs. Reportedly, *aac(6′)-I*, *aac(6′)-II*, *ant(2″)-I* and *aph(3′)* are the most common AMEs genes in *P. aeruginosa* (Asghar and Ahmed, 2018). According to the report by Cabrera, the *aac(3)-Ia, aac(3)-Ic, aac(6″)-Ib* and *ant(2″)-Ia* genes were associated with aminoglycoside-resistant strains (Cabrera et al., 2022). The results showed that *aac(6′)-Ib* was the most commonly (26/43, 60.4%) identified AME-encoding gene (Ahmadian et al., 2021). A total of 11 AMEs genes were analyzed in 56 isolates of CRPA. *ant(2″)-I* plays an important role in aminoglycoside-resistant antibiotics. The PCR results showed that *MexB* was present in 100% of the 56 isolates. Comparative analysis of *OprM* gene detection between the ICU and other departments found that the gene was detected in all 33 CRPA strains isolated from the ICU, while only 19 CRPA strains from other departments had the gene, with a statistically significant difference ($p = 0.013$). The *MexAB-OprM* efflux pump system can transport β-lactams, quinolones and macrolides, causing *P. aeruginosa* to have a wide range of drug resistance (Henrichfreise et al., 2007). There is a need for vigilance of the spread of drug-resistant bacteria in ICU wards. Other resistance genes (*mucB*, $OprD_2$, *intI-1*, *qacE*△*1-sul1*) were present in 100% of the 56 CRPA isolates. These above results indicate that the resistance of 56 strains of CRPA was closely related to the formation of efflux pump systems and biofilms, suggesting the development of corresponding technologies or drugs from these aspects to improve the effectiveness of clinical treatment of CRPA.

In addition to the existence of multiple drug resistance genes, a large number of virulence factors also significantly increase the invasion and pathogenicity of the bacterium, leading to an increase in the incidence rate and mortality (Takata et al., 2018). A report by Omid et al. showed that the detection rate of hypervirulence-associated genes in *P. aeruginosa* isolates is high, and multidrug-resistant and highly virulent *P. aeruginosa* poses great challenges to clinical treatment (Zarei et al., 2020). The identification of virulence gene profiles is crucial for developing effective anti-*P. aeruginosa* infection strategies. The exozymes produced by the type III secretion system (T3SS) are important virulence systems for the pathogenicity of *P. aeruginosa*. Therefore, analyzing whether patients carry corresponding virulence genes will help clinicians focus on the patient's condition and prevent serious clinical symptoms leading to death. Some studies have shown that *exoU* gene-positive *P. aeruginosa* shows higher multidrug resistance and more significant mortality than other T3SS gene-expressing *P. aeruginosa* (Takata et al., 2018; Khodayary et al., 2019). The results showed that *exoS*, *exoT* and *exoY* were present in all isolates, except for *exoU* (83.93%). Further analysis of *exoU* toxicity showed that a total of 12 children had CRPA detected in at least two specimens, of which 11 children had CRPA carrying *exoU*, accounting for 91.67% (11/12). This indicates that strains carrying *exoU* have strong virulence

10.3389/fmicb.2023.1280012

TABLE 7 Related comparative analysis of the survival group and death group [n (%)].

Classification		Survival group ($n = 49$)	Death group ($n = 7$)	χ^2	P
Carbapenem-resistant genes	*VIM* ($n = 55$)	48 (87.27)	7 (12.73)	0.145	0.703
	OXA ($n = 32$)	27 (84.38)	5 (15.62)	0.667	0.414
	GIM ($n = 31$)	27 (87.1)	4 (12.9)	0.01	0.919
	BIC ($n = 17$)	16 (94.12)	1 (5.88)	0.977	0.323
	IMP ($n = 16$)	12 (75)	4 (25)	3.200	0.074
ESBLs genes	*SHV* ($n = 54$)	47 (87.04)	7 (12.96)	0.296	0.586
AmpC genes	*EBC-1* ($n = 43$)	37 (86.05)	6 (13.95)	0.358	0.550
	CIT-1 ($n = 32$)	27 (84.38)	5 (15.62)	0.667	0.414
AMEs genes	*aac(6′)-II* ($n = 48$)	42 (87.5)	6 (12.5)	0	1
	aac(3)-IIc ($n = 35$)	30 (85.71)	5 (14.29)	0.27	0.602
	ant(2″)-Ia ($n = 30$)	26 (86.67)	4 (13.33)	0.041	0.839
	aac(6′)-Ib ($n = 28$)	23 (82.14)	5 (17.86)	1.469	0.225
	aac(6′)-I ($n = 6$)	5 (83.33)	1 (16.67)	0.107	0.744
Genes related to the efflux system	*OprM* ($n = 52$)	45 (86.54)	7 (13.46)	0.615	0.433
Hypervirulence-associated genes	*exoU* (+) ($n = 47$)	41 (87.23)	6 (12.77)	0.019	0.891
Any combined infection with other pathogenic bacteria	Gram-positive bacteria ($n = 7$)	7 (100)	0 (0)	1.143	0.285
	Gram-negative bacteria ($n = 25$)	23 (92)	2 (8)	0.836	0.361
	Mixed infection of Gram-negative/positive bacteria or fungi ($n = 11$)	8 (72.73)	3 (27.27)	2.731	0.098
	No combined infection ($n = 13$)	11 (84.62)	2 (15.38)	0.129	0.720
Basic disease	Pneumonia ($n = 20$)	19 (95)	1 (5)	1.600	0.206
	Hematological system diseases ($n = 14$)	10 (71.43)	4 (28.57)	**4.408**	**0.036**
	Heart disease ($n = 12$)	11 (91.67)	1 (8.33)	0.242	0.622
	Other infections* ($n = 5$)	5 (100)	0 (0)	0.784	0.376
	Other diseases* ($n = 5$)	4 (80)	1 (20)	0.282	0.595

Bold values highlight meaningful results. *exoU (+) represents the detection of this gene. Other infections included encephalitis, laryngitis, urinary tract infection, and lymphadenitis. Other diseases included epilepsy, genetic metabolic disease, foreign body inhalation asphyxia, and neonatal respiratory distress syndrome.

and are prone to penetrating cells and invading other parts, leading to infection. The coexistence of resistance and high virulence factors in CRPA is an alarming threat. This finding underlines the importance of monitoring multidrug resistance to determine optimal therapeutic options against such infections.

The correlation between the drug resistance rate of 56 CRPA strains and the *exoU* gene was further analyzed. The results of the drug sensitivity test showed that the 56 CRPA isolates exhibited a higher drug resistance rate to various antibiotics, but it was lower than that in a recent study that analyzed CRPA isolated from children (Huang et al., 2023). The drug resistance rates of cefepime and piperacillin/tazobactam were related to whether they carried *exoU*, and the difference was statistically significant ($p < 0.05$). *P. aeruginosa* has natural resistance to many kinds of antibiotics and easily develops acquired resistance in the course of treatment, so a combination of drugs is the first choice for the clinical treatment of *P. aeruginosa*. In addition, this study found that the resistance rate of 56 CRPA strains to fluoroquinolones (ciprofloxacin and levofloxacin) was only 7.14%, and the resistance rate to aminoglycoside antibiotics, such as amikacin, tobramycin, and gentamicin, was 0. The abovementioned drugs have a relatively high degree of harm to children and are less commonly used in clinical practice (Lin et al., 2016), resulting in a lower resistance rate, which is consistent with the expected results. AMEs genes are associated with resistance to multiple antibiotics (Atassi et al., 2023). Combined with the analysis of genetic testing results, the detection rate of AMEs genes and *MexB* was high, while the resistance rate of corresponding aminoglycoside antibiotics was 0, which suggests that there may be potential resistance factors, and the relationship between resistance genes and antibiotics needs to be further explored. In view of this, carbapenem drugs or combination drugs should be used reasonably in the treatment of CRPA infections, such as β-lactam in combination with aminoglycosides or β-lactam combined with fluoroquinolones, but the dosage should be reasonably controlled. The drug sensitivity results suggest that it is necessary to strengthen the monitoring of bacterial resistance in clinical practice and actively promote and guide the rational use of antibiotics.

To determine the risk factors for CRPA infection in children, a retrospective case–control study was conducted that included 56 patients with CRPA infection. This study consisted of 56 MDR-PA strains and 31 XDR-PA strains. The clinical outcome of children

infected with CRPA was poor, with a mortality rate of 12.5%, which is lower than the mortality rate reported by Lodise et al. (2022) (20.0% ~ 30.8%). Comparison of data between the survival and death groups showed that there was no statistically significant difference in the detection rates of major drug resistance genes or hypervirulence-associated genes. Strains carrying the *exoU* are more virulent, as they can encode and produce a strong toxin protein, which can lead to cell necrosis and apoptosis (Zhu et al., 2023). There was no statistically significant difference in the detection of an exoU gene between the survival group and the death group. Patients with hematological system diseases are themselves a high-risk population infected with carbapenem-resistant Gram-negative bacteria (Zhao et al., 2020). Among the 7 deceased children, 4 children suffered from hematological diseases. Comparing the data on hematological diseases between the survival group and the death group, the difference was statistically significant ($p = 0.036$). An interesting finding of this study is that out of the 7 deceased children, 4 children had isolated XDR-PA, accounting for 57.14% (4/7). Special attention needs to be paid to the detection of MDR-PA and XDR-PA and timely control of infection to avoid exacerbating the condition of children.

In summary, CRPA, as an important nosocomial infectious pathogen, was mainly isolated from sputum and ICU patients. CRPA has gradually increased in drug resistance and virulence, making treatment more difficult. The coexistence of resistance and high virulence factors in CRPA is an alarming threat. Analyzing the multiple drug resistance- and hypervirulence-associated genes carried by CRPA can help clinicians gain a deeper understanding of the coexistence mechanism of drug resistance and virulence genes. However, there are some limitations in this study. Due to limited testing conditions, only representative resistance- and hypervirulence-associated genes were selected, resulting in limited clinical value. In future research, it is necessary to collect more strains and expand the scope of gene analysis, conduct in-depth research on the resistance mechanism and virulence of CRPA, and understand the correlation between multidrug resistance and high virulence.

Data availability statement

The datasets used and/or analyzed during the current study available from the corresponding author on reasonable request.

Ethics statement

The studies involving humans were approved by the Medical Ethics Committee of the Children's Hospital of Soochow University (ethics batch number: 2021CS158). The studies were conducted in accordance with the local legislation and institutional requirements. Written informed consent for participation was not required from the participants or the participants' legal guardians/next of kin because simple retrospective analysis of data does not involve patient privacy.

Author contributions

XZ: Conceptualization, Data curation, Formal analysis, Methodology, Writing – original draft. YZ: Conceptualization, Formal analysis, Methodology, Writing – original draft, Writing – review & editing. YG: Data curation, Formal analysis, Writing – original draft. WL: Data curation, Methodology, Writing – original draft. YW: Conceptualization, Formal analysis, Writing – review & editing. YL: Conceptualization, Funding acquisition, Writing – review & editing, Formal analysis.

Funding

The author(s) declare financial support was received for the research, authorship, and/or publication of this article. This study was supported by grants from the Special Foundation for National Science and Technology Basic Research Program of China (2019FY101200), the High-level Innovative and Entrepreneurial Talents Introduction Program of Jiangsu Province (2020-30191), the Natural Science Foundation of the Jiangsu Higher Education Institutions of China (20KJB310012), the Medical Research Project of Jiangsu Commission of Health (M2020027), National Tutorial System Project of Suzhou Health Young Backbone Talents (Qngg2022011), the Science and Technology Program of Suzhou (SYS2020163 and SYSD2019120).

Acknowledgments

We thank the staff from the Department of Clinical Laboratory, Children's Hospital of Soochow University, who took part in the study.

Conflict of interest

The authors declare that the research was conducted in the absence of any commercial or financial relationships that could be construed as a potential conflict of interest.

Publisher's note

Author disclaimer

The views, opinions, assumptions, or any other information set out in this article are solely those of the authors and should not be attributed to the funders or any other person connected with the funders.

Supplementary material

The Supplementary material for this article can be found online at: https://www.frontiersin.org/articles/10.3389/fmicb.2023.1280012/full#supplementary-material

References

Ahmadian, L., Norouzi Bazgir, Z., Ahanjan, M., Valadan, R., and Goli, H. R. (2021). Role of aminoglycoside-modifying enzymes (AMEs) in resistance to aminoglycosides among clinical isolates of *Pseudomonas aeruginosa* in the north of Iran. *Biomed. Res. Int.* 2021:7077344. doi: 10.1155/2021/7077344

Alfouzan, W., Dhar, R., Abdo, N. M., Alali, W. Q., and Rabaan, A. A. (2021). Epidemiology and microbiological profifile of common healthcare associated infections among patients in the intensive care unit of a general hospital in Kuwait: a retrospective observational study. *J. Epidemiol. Glob. Health* 11, 302–309. doi: 10.2991/jegh.k.210524.001

Asghar, A. H., and Ahmed, O. B. (2018). Prevalence of aminoglycoside resistance genes in *Pseudomonas aeruginosa* isolated from a tertiary care hospital in Makkah, KSA. *Clin. Pract.* 15, 541–547. doi: 10.4172/clinical-practice.1000391

Atassi, G., Medernach, R., Scheetz, M., Nozick, S., Rhodes, N. J., Murphy-Belcaster, M., et al. (2023). Genomics of aminoglycoside resistance in *Pseudomonas aeruginosa* bloodstream infections at a United States academic hospital. *Microbiol. Spectr.* 11:e0508722. doi: 10.1128/spectrum.05087-22

Cabrera, R., Fernández-Barat, L., Vázquez, N., Alcaraz-Serrano, V., Bueno-Freire, L., Amaro, R., et al. (2022). Resistance mechanisms and molecular epidemiology of *Pseudomonas aeruginosa* strains from patients with bronchiectasis. *J. Antimicrob. Chemother.* 77, 1600–1610. doi: 10.1093/jac/dkac084

Castanheira, M., Simner, P. J., and Bradford, P. A. (2021). Extended-spectrum β-lactamases: an update on their characteristics, epidemiology and detection. *JAC Antimicrob Resist* 3:dlab092. doi: 10.1093/jacamr/dlab092

CDC. *Antibiotic resistance threats in the United States; centers for disease control*. Atlanta, GA: CDC. (2019). *9*.

Chevalier, S., Bouffartigues, E., Bodilis, J., Maillot, O., Lesouhaitier, O., Feuilloley, M. G. J., et al. (2017). Structure, function and regulation of *Pseudomonas aeruginosa* porins. *FEMS Microbiol. Rev.* 41, 698–722. doi: 10.1093/femsre/fux020

Coșeriu, R. L., Vintilă, C., Pribac, M., Mare, A. D., Ciurea, C. N., Togănel, R. O., et al. (2023). Antibacterial effect of 16 essential oils and modulation of mex efflux pumps gene expression on multidrug-resistant *Pseudomonas aeruginosa* clinical isolates: is cinnamon a good fighter? *Antibiotics* 12:163. doi: 10.3390/antibiotics12010163

de Sousa, T., Hébraud, M., Alves, O., Costa, E., Maltez, L., Pereira, J. E., et al. (2023). Study of antimicrobial resistance, biofilm formation, and motility of *Pseudomonas aeruginosa* derived from urine samples. *Microorganisms*. 11:1345. doi: 10.3390/microorganisms11051345

Elshafiee, E. A., Nader, S. M., Dorgham, S. M., and Hamza, D. A. (2019). Carbapenem-resistant *Pseudomonas aeruginosa* originating from farm animals and people in Egypt. *J. Vet. Res.* 63, 333–337. doi: 10.2478/jvetres-2019-0049

Feng, W., Huang, Q., Wang, Y., Yuan, Q., Li, X., Xia, P., et al. (2021). Changes in the resistance and epidemiological characteristics of *Pseudomonas aeruginosa* during a ten-year period. *J. Microbiol. Immunol. Infect.* 54, 261–266. doi: 10.1016/j.jmii.2019.08.017

Gill, C. M., and Nicolau, D. P.ERACE-PA Global Study Group (2022). Carbapenem-resistant *Pseudomonas aeruginosa*: an assessment of frequency of isolation from ICU versus non-ICU, phenotypic and genotypic profiles in a multinational population of hospitalized patients. *Antimicrob. Resist. Infect. Control* 11:146. doi: 10.1186/s13756-022-01187-8

Golovkine, G., Reboud, E., and Huber, P. (2018). *Pseudomonas aeruginosa* takes a multi-target approach to achieve junction breach. *Front. Cell. Infect. Microbiol.* 7:532. doi: 10.3389/fcimb.2017.00532

Hall, K. M., Pursell, Z. F., and Morici, L. A. (2022). The role of the *Pseudomonas aeruginosa* hypermutator phenotype on the shift from acute to chronic virulence during respiratory infection. *Front. Cell. Infect. Microbiol.* 12:943346. doi: 10.3389/fcimb.2022.943346

Henrichfreise, B., Wiegand, I., Pfister, W., and Wiedemann, B. (2007). Resistance mechanisms of multiresistant *Pseudomonas aeruginosa* strains from Germany and correlation with hypermutation. *Antimicrob. Agents Chemother.* 51, 4062–4070. doi: 10.1128/AAC.00148-07

Horna, G., and Ruiz, J. (2021). Type 3 secretion system of *Pseudomonas aeruginosa*. *Microbiol. Res.* 246:126719. doi: 10.1016/j.micres

Hu, F., Guo, Y., Zhu, D., Wang, F., Jiang, X., Xu, Y., et al. (2021). CHINET surveillance of bacterial resistance: results of 2020. *Chin. J. Infect. Chemother.* 21, 377–387. doi: 10.16718/j.1009-7708.2021.04.001

Huang, W., Wei, X., Xu, G., Zhang, X., and Wang, X. (2023). Carbapenem-resistant *Pseudomonas aeruginosa* infections in critically ill children: prevalence, risk factors, and impact on outcome in a large tertiary pediatric hospital of China. *Front. Public Health* 11:1088262. doi: 10.3389/fpubh.2023.1088262

Jaggi, N., Sissodia, P., and Sharma, L. (2012). Control of multidrug resistant bacteria in a tertiary care hospital in India. *Antimicrob. Resist. Infect. Control* 1:23. doi: 10.1186/2047-2994-1-23

Khodayary, R., Nikokar, I., Mobayen, M. R., Afrasiabi, F., Araghian, A., Elmi, A., et al. (2019). High incidence of type III secretion system associated virulence factors (exoenzymes) in *Pseudomonas aeruginosa* isolated from Iranian burn patients. *BMC. Res. Notes* 12:28. doi: 10.1186/s13104-019-4071-0

Kim, H., Sung, J. Y., Yong, D., Jeong, S. H., Song, W., Lee, K., et al. (2016). Disk carbapenemase test for the rapid detection of KPC-, NDM-, and other metallo-β-lactamase-producing gram-negative bacilli. *Ann. Lab. Med.* 36, 434–440. doi: 10.3343/alm.2016.36.5.434

Leiyan, H., Pan, F., Xia, W., Chuanqing, W., Hui, Y., and Hongmei, Xu, et al. (2021). Antimicrobial resistance profile of clinical strains isolated from children in China: a report from the ISPED program of 2020. *Chin. J. Evidence Based Pediatr.* 16, 414–420. doi: 10.3969/j.issn.1673-5501.2021.06.002

Lin, K. Y., Lauderdale, T. L., Wang, J. T., and Chang, S. C. (2016). Carbapenem-resistant *Pseudomonas aeruginosa* in Taiwan: prevalence, risk factors, and impact on outcome of infections. *J. Microbiol. Immunol. Infect.* 49, 52–59. doi: 10.1016/j.jmii.2014.01.005

Litwin, A., Fedorowicz, O., and Duszynska, W. (2020). Characteristics of microbial factors of healthcare-associated infections including multidrug-resistant pathogens and antibiotic consumption at the university intensive care unit in Poland in the years 2011-2018. *Int. J. Environ. Res. Public Health* 17:6943. doi: 10.3390/ijerph17196943

Lodise, T. P., Bassetti, M., Ferrer, R., Naas, T., Niki, Y., Paterson, D. L., et al. (2022). All-cause mortality rates in adults with carbapenem-resistant gram-negative bacterial infections: a comprehensive review of pathogen-focused, prospective, randomized, interventional clinical studies. *Expert Rev. Anti-Infect. Ther.* 20, 707–719. doi: 10.1080/14787210.2022.2020099

Lyu, J., Chen, H., Bao, J., Liu, S., Chen, Y., Cui, X., et al. (2023). Clinical distribution and drug resistance of *Pseudomonas aeruginosa* in Guangzhou, China from 2017 to 2021. *J. Clin. Med.* 12:1189. doi: 10.3390/jcm12031189

Ma, M., Lustig, M., Salem, M., Mengin-Lecreulx, D., Phan, G., and Broutin, I. (2021). MexAB-OprM efflux pump interaction with the peptidoglycan of *Escherichia coli* and *Pseudomonas aeruginosa*. *Int. J. Mol. Sci.* 22:5328. doi: 10.3390/ijms22105328

Magiorakos, A. P., Srinivasan, A., Carey, R. B., Carmeli, Y., Falagas, M. E., Giske, C. G., et al. (2012). Multidrug-resistant, extensively drug-resistant and pandrug-resistant bacteria: an international expert proposal for interim standard definitions for acquired resistance. *Clin. Microbiol. Infect.* 18, 268–281. doi: 10.1111/j.1469-0691.2011.03570.x. Epub 2011 Jul 27

Memar, M. Y., Adibkia, K., Farajnia, S., Samadi Kafil, H., Khalili, Y., Azargun, R., et al. (2021). In-vitro effect of imipenem, fosfomycin, colistin, and gentamicin combination against carbapenem-resistant and biofilm-forming *Pseudomonas aeruginosa* isolated from burn patients. *Iran J. Pharm. Res.* 20, 286–296. doi: 10.22037/ijpr.2020.111824.13380

Miao, M., Wen, H., Xu, P., Niu, S., Lv, J., Xie, X., et al. (2019). Genetic diversity of carbapenem-resistant enterobacteriaceae (CRE) clinical isolates from a tertiary Hospital in Eastern China. *Front. Microbiol.* 9:3341. doi: 10.3389/fmicb.2018.03341

Palzkill, T. (2013). Metallo-β-lactamase structure and function. *Ann. N. Y. Acad. Sci.* 1277, 91–104. doi: 10.1111/j.1749-6632.2012.06796.x

Pan, F., Leiyan, H., Chuanqing, W., Hui, Y., Hongmei, X., Chunmei, J., et al. (2021). Antimicrobial resistance profile of clinical isolates in pediatric hospitals in China: report from the ISPED surveillance program in 2019. *Chinese J. Evid. Based Pediatr.* 16, 43–49. doi: 10.3969/j.issn.1673-5501.2021.01.002

Paul, D., Dhar, D., Maurya, A. P., Mishra, S., Sharma, G. D., Chakravarty, A., et al. (2016). Occurrence of co-existing blaVIM-2 and blaNDM-1 in clinical isolates of *Pseudomonas aeruginosa* from India. *Ann. Clin. Microbiol. Antimicrob.* 15:31. doi: 10.1186/s12941-016-0146-0

Ponce de Leon, A., Merchant, S., Raman, G., Avendano, E., Chan, J., Tepichin Hernandez, G., et al. (2020). Pseudomonas infections among hospitalized adults in Latin America: a systematic review and meta-analysis. *BMC Infect. Dis.* 20:250. doi: 10.1186/s12879-020-04973-0.

Poursina, S., Ahmadi, M., Fazeli, F., and Ariaii, P. (2023). Assessment of virulence factors and antimicrobial resistance among the *Pseudomonas aeruginosa* strains isolated from animal meat and carcass samples. *Vet. Med. Sci.* 9, 315–325. doi: 10.1002/vms3.1007

Recio, R., Mancheño, M., Viedma, E., Villa, J., Orellana, M. Á., Lora-Tamayo, J., et al. (2020). Predictors of mortality in bloodstream infections caused by *Pseudomonas aeruginosa* and impact of antimicrobial resistance and bacterial virulence. *Antimicrob. Agents Chemother.* 64:e01759-19. doi: 10.1128/AAC.01759-19

Sader, H. S., Castanheira, M., Duncan, L. R., and Flamm, R. K. (2018). Antimicrobial susceptibility of *Enterobacteriaceae* and *Pseudomonas aeruginosa* isolates from United States medical centers stratified by infection type: results from the international network for optimal resistance monitoring (INFORM) surveillance program, 2015-2016. *Diagn. Microbiol. Infect. Dis.* 92, 69–74. doi: 10.1016/j.diagmicrobio.2018.04.012

Sharifi, H., Pouladfar, G., Shakibaie, M. R., Pourabbas, B., Mardaneh, J., and Mansouri, S. (2019). Prevalence of β-lactamase genes, class 1 integrons, major virulence factors and clonal relationships of multidrug-resistant *Pseudomonas aeruginosa* isolated from hospitalized patients in southeast of Iran. *Iran. J. Basic Med. Sci.* 22, –812. doi: 10.22038/ijbms.2019.35063.8340

Takata, I., Yamagishi, Y., and Mikamo, H. (2018). Association of the exoU genotype with a multidrug non-susceptible phenotype and mRNA expressions of resistance genes in *Pseudomonas aeruginosa*. *J. Infect. Chemother.* 24, 45–52. doi: 10.1016/j.jiac.2017.08.018

Tamma, P. D., Aitken, S. L., Bonomo, R. A., Mathers, A. J., van Duin, D., and Clancy, C. J. (2022). Infectious Diseases Society of America 2022 guidance on the treatment of extended-spectrum β-lactamase producing enterobacterales (ESBL-E), carbapenem-resistant enterobacterales (CRE), and *Pseudomonas aeruginosa* with difficult-to-treat resistance (DTR-*P. aeruginosa*). *Clin. Infect. Dis.* 75, 187–212. doi: 10.1093/cid/ciac268

Urbanowicz, P., Izdebski, R., Baraniak, A., Żabicka, D., Ziółkowski, G., Hryniewicz, W., et al. (2019). *Pseudomonas aeruginosa* with NDM-1, DIM-1 and PME-1 β-lactamases, and RmtD3 16S rRNA methylase, encoded by new genomic islands. *J. Antimicrob. Chemother.* 74, 3117–3119. doi: 10.1093/jac/dkz262

Walkty, A., Lagace-Wiens, P., Adam, H., Baxter, M., Karlowsky, J., Mulvey, M. R., et al. (2017). Antimicrobial susceptibility of 2906 *Pseudomonasaeruginosa* clinical isolates obtained from patients in Canadian hospitals over a period of 8 years: results of the Canadian Ward surveillance study (CANWARD), 2008-2015. *Diagn. Microbiol. Infect. Dis.* 87, 60–63. doi: 10.1016/j.diagmicrobio.2016.10.003

Wanqing, N., Janshe, Y., Juanli, C., and Jingshui, L. (2022). Research hotspots and trends of Pseudomonas aeruginosa drug resistance:a study based on CiteSpace. *Microbiology.* 49, 4942–4956. doi: 10.13344/j.microbiol.china.220336

Wei, H., Sun, L., Zhu, J., Zhang, X., Zhu, C., Zhao, L., et al (2007). Effects of different DNA extraction methods on ERIC-PCR identification of two common nosocomial infectious bacteria. *Chinese Journal of Nosocomiology.* 17, 1044–1047. doi: 10.3321/j.issn:1005-4529.2007.09.002

Zahedi Bialvaei, A., Rahbar, M., Hamidi-Farahani, R., Asgari, A., Esmailkhani, A., Mardani Dashti, Y., et al. (2021). Expression of RND efflux pumps mediated antibiotic resistance in *Pseudomonas aeruginosa* clinical strains. *Microb. Pathog.* 153:104789. doi: 10.1016/j.micpath.2021.104789

Zarei, O., Mahmoudi, H., Bardbari, A. M., Karami, P., and Alikhani, M. Y. (2020). Detection of virulence factors and antibiotic resistance pattern of clinical and intensive care unit environmental isolates of *Pseudomonas aeruginosa*. *Infect. Disord. Drug Targets* 20, 758–762. doi: 10.2174/1871526520666191231124717

Zhao, Y., Lin, Q., Liu, L., Ma, R., Chen, J., Shen, Y., et al. (2020). Risk factors and outcomes of antibiotic-resistant *Pseudomonas aeruginosa* bloodstream infection in adult patients with acute leukemia. *Clin. Infect. Dis.* 71, S386–S393. doi: 10.1093/cid/ciaa1522.

Zhu, Y., Kang, Y., Zhang, H., Yu, W., Zhang, G., Zhang, J., et al. (2023). Emergence of ST463 exoU-positive, imipenem-nonsusceptible *Pseudomonas aeruginosa* isolates in China. *Microbiol. Spectr.* 11:e0010523. doi: 10.1128/spectrum.00105-23

frontiers | Frontiers in Microbiology

TYPE Original Research
PUBLISHED 02 November 2023
DOI 10.3389/fmicb.2023.1276314

OPEN ACCESS

EDITED BY
Liang-xing Fang,
South China Agricultural University, China

REVIEWED BY
Renjie Wu,
Fujian Academy of Agriculture Sciences, China
Percy Schröttner,
Technische Universität Dresden, Germany
Xing-Ping Li,
Henan University of Science and Technology, China

*CORRESPONDENCE
Xuejun Guo
✉ xuejung2021@163.com
Lingwei Zhu
✉ lingweiz@126.com

†These authors have contributed equally to this work and share first authorship

RECEIVED 11 August 2023
ACCEPTED 23 October 2023
PUBLISHED 02 November 2023

CITATION
Guan J, Zhou W, Guo J, Zheng L, Lu G, Hua F, Liu M, Ji X, Sun Y, Zhu L and Guo X (2023) A *Wohlfahrtiimonas chitiniclastica* with a novel type of *bla*$_{VEB-1}$-carrying plasmid isolated from a zebra in China.
Front. Microbiol. 14:1276314.
doi: 10.3389/fmicb.2023.1276314

A *Wohlfahrtiimonas chitiniclastica* with a novel type of *bla*$_{VEB-1}$-carrying plasmid isolated from a zebra in China

Jiayao Guan[1,2†], Wei Zhou[3†], Jingyi Guo[4], Lin Zheng[2], Gejin Lu[2], Fuyou Hua[5], Mingwei Liu[2], Xue Ji[2], Yang Sun[2], Lingwei Zhu[2*] and Xuejun Guo[2*]

[1]College of Veterinary Medicine, Jilin Agricultural University, Changchun, China, [2]Key Laboratory of Jilin Province for Zoonosis Prevention and Control, Changchun Veterinary Research Institute, Chinese Academy of Agricultural Sciences, Changchun, China, [3]Center for Animal Disease Control and Prevention of Ordos, Ordos, China, [4]The Second Hospital of Jilin University, Jilin University, Changchun, China, [5]Shenzhen Safari Park, Shenzhen, China

Background: *Wohlfahrtiimonas chitiniclastica* is an emerging fly-borne zoonotic pathogen, which causes infections in immunocompromised patients and some animals. Herein, we reported a *W. chitiniclastica* BM-Y from a dead zebra in China.

Methods: The complete genome sequencing of BM-Y showed that this isolate carried one chromosome and one novel type of *bla*$_{VEB-1}$-carrying plasmid. Detailed genetic dissection was applied to this plasmid to display the genetic environment of *bla*$_{VEB-1}$.

Results: Three novel insertion sequence (IS) elements, namely IS*Woch1*, IS*Woch2*, and IS*Woch3*, were found in this plasmid. *aadB*, *aacA1*, and *gcuG* were located downstream of *bla*$_{VEB-1}$, composing a gene cassette array *bla*$_{VEB-1}$–*aadB*–*aacA1*–*gcuG* bracketed by an intact IS*Woch1* and a truncated one, which was named the *bla*$_{VEB-1}$ region. The 5′-RACE experiments revealed that the transcription start site of the *bla*$_{VEB-1}$ region was located in the intact IS*Woch1* and this IS provided a strong promoter for the *bla*$_{VEB-1}$ region.

Conclusion: The spread of the *bla*$_{VEB-1}$-carrying plasmid might enhance the ability of *W. chitiniclastica* to survive under drug selection pressure and aggravate the difficulty in treating infections caused by *bla*$_{VEB-1}$-carrying *W. chitiniclastica*. To the best of our knowledge, this is the first report of the genetic characterization of a novel *bla*$_{VEB-1}$-carrying plasmid with new ISs from *W. chitiniclastica*.

KEYWORDS

***Wohlfahrtiimonas chitiniclastica*, *bla*$_{VEB-1}$, plasmid, drug resistance, zoonotic bacteria, mobile genetic element**

Abbreviations: VEB, Vietnamese extended-spectrum β-lactamase; OD, optical density; MIC, minimum inhibitory concentration; ANI, average nucleotide identity; ORF, open reading frame; RACE, rapid amplification of cDNA end; GSP, gene-specific primer; *rep*, replication; *par*, partition; IS, insertion sequence; GCA, gene cassette array; CS, conserved segment; DR, direct repeat; *rlx*, relaxase; *oriT*, origin of conjugative replication; *pri*, primase; *cpl*, coupling protein; T4SS, type IV secretion system; TU, translocatable unit.

1. Introduction

Wohlfahrtiimonas chitiniclastica is an emerging fly-borne pathogen that causes bacteremia (Rebaudet et al., 2009), sepsis (Almuzara et al., 2011), cellulitis (de Dios et al., 2015), osteomyelitis (Suryalatha et al., 2015), wound infections (Nogi et al., 2016), and soft tissue and bone infections (Kõljalg et al., 2015) in humans and bacteremia (Thaiwong et al., 2014), endocarditis (Josue et al., 2015), and hoof fetlow (Qi et al., 2016) in animals. It was first identified from both the homogenate of the third-stage larvae of the parasitic fly *Wohlfahrtia magnifica* and the foregut of a third-stage maggot of *W. magnifica* collected from an infested vulval wound of a Romney sheep in Hungary in 2008 (Tóth et al., 2008). Since then, *W. chitiniclastica* has been associated with several obligate parasitic flies, including *W. magnifica* (Tóth et al., 2008), *Chrysomya megacephala* (Cao et al., 2013), *Lucilia sericata* (Campisi et al., 2015), *Musca domestica* (Gupta et al., 2012), and *Lucilia illustris* (Iancu et al., 2020). These flies can transmit *W. chitiniclastica* to humans and animals, which causes local or systemic infections originating from wounds infested with fly larvae. Diverse risk factors have been identified among infected patients and animals, including homelessness, alcoholism, tobacco abuse, poor hygiene, chronic open wounds, proximity to livestock, increasing age, low socioeconomic status, immunocompromised patients, chronic cardiovascular/circulatory disease, and neurological disease (Schröttner et al., 2017). To date, *W. chitiniclastica* has been identified in 10 countries in Europe (Tóth et al., 2008; Rebaudet et al., 2009; Campisi et al., 2015; Kõljalg et al., 2015; Schröttner et al., 2017; Pablo-Marcos et al., 2019; Dovjak et al., 2021; Hladík et al., 2021; De Smet et al., 2022; Karaca et al., 2022), four in Asia (Suryalatha et al., 2015; Zhou et al., 2016; Suraiya et al., 2017; Katanami et al., 2018), two in South America (Almuzara et al., 2011; Matos et al., 2016), one in North America (Thaiwong et al., 2014), one in Oceania (Connelly et al., 2019), and one in Africa (Hoffman et al., 2016).

It is speculated that *W. chitiniclastica* is intrinsically resistant to fosfomycin due to the fosfomycin efflux proteins, the gene homolog encoding for transferases, and the gene homologous to *mdtG* that related to fosfomycin resistance (Kopf et al., 2021). In addition, research has revealed that *W. chitiniclastica* shows resistance to amikacin (Kopf et al., 2021), tetracycline (Snyder et al., 2020), and tobramycin (Kopf et al., 2021), and it is intermediate to ampicillin (Qi et al., 2016). However, *W. chitiniclastica* is susceptible to the majority of the known antibiotics including β-lactams, quinolones, and trimethoprim/sulfamethoxazole (Kopf et al., 2022). Therefore, these three categories of antimicrobials may be the best options for treating *W. chitiniclastica* infections (Schröttner et al., 2017).

bla_{VEB-1} was initially identified from a clinical *Escherichia coli* isolated from Vietnam, and it encodes Vietnamese extended-spectrum β-lactamase (VEB-1) that displays high-level resistance to amoxicillin, piperacillin, cefotaxime, ceftazidime, and aztreonam (Poirel et al., 1999). Since then, bla_{VEB-1} has been found in IncA/C (Papagiannitsis et al., 2012), IncF (Paul et al., 2017), IncK (Paul et al., 2017), and IncP plasmids (Siebor et al., 2021) and in plasmids with undetermined Inc type from various Gram-negative species, including *Enterobacteriaceae* (Poirel et al., 1999), *Morganellaceae* (Oikonomou et al., 2016), *Acinetobacter* (e.g., *Acinetobacter baumannii* with the accession number LC107425), *Aeromonas* (e.g., *Aeromonas caviae* with the accession number KU886278), *Shewanella* (e.g., *Shewanella algae* with the accession number CP033574), *Vibrio alginolyticus* (Ye et al., 2016), *Pseudomonas aeruginosa* (Naas et al., 1999), *Achromobacter xylosoxidans* (with the accession number DQ393569), and *Pasteurella multocida* (with the accession number CP014157), but not in *W. chitiniclastica*. Generally, bla_{VEB-1} is carried by integrons, and *aadB* encoding an aminoglycoside adenyltransferase is located downstream of bla_{VEB-1} (Naas et al., 1999, 2000).

This study showed the complete genome sequences of a *W. chitiniclastica* from the pancreas of a dead zebra in China, which carried one chromosome and one novel type of bla_{VEB-1}-carrying plasmid. Detailed genetic dissection was applied to this plasmid to display the genetic environment of bla_{VEB-1}. The transcription start site and the promoter of the bla_{VEB-1} region were identified. The data presented here provided a deeper genomics and bioinformatics understanding of *W. chitiniclastica* for clinical treatment and pathogenesis research. To the best of our knowledge, this is the first report of the genetic characterization of a novel bla_{VEB-1}-carrying plasmid from *W. chitiniclastica*.

2. Materials and methods

2.1. Bacterial isolation

The blood, heart, liver, spleen, lung, kidney, and pancreas specimens from a dead zebra were collected from Shenzhen Safari Park in 2013 and transferred to our laboratory in Changchun under sterile conditions for bacterial isolation. For each specimen, the tissue was plated onto brain heart infusion agar medium, 5% sheep blood agar medium, and MacConkey agar medium. The sample was then incubated at 37°C for 18 h under aerobic conditions.

The *W. chitiniclastica* strain DSM 18708 (Leibniz Institute DSMZ-German Collection of Microorganisms and Cell Cultures GmbH, Germany), isolated from artificial culture of *W. magnifica* in Hungary, was used as the reference strain in this study (Kõljalg et al., 2015).

2.2. Bacterial identification and phenotypic characteristics

Gram staining, BD Phoenix^{TM}-100 Automated Microbiology System (Becton, Dickinson and Company, USA) detection, PCR amplification of the 16S rRNA, *rpoB*, and *gyrB* genes followed by sequencing, and matrix-assisted laser desorption ionization-time of flight mass spectrometry (MALDI-TOF MS, Bruker Daltonics, USA) were conducted for bacterial identification.

A transmission electron microscopy investigation was carried out. The motility of the bacteria was tested on motility agar (Tittsler and Sandholzer, 1936). To determine the bacterial growth curves, the optical density at 600 nm (OD_{600}) was monitored for each culture with a 1-h interval during the first 12 h and a 2-h interval during the last 12 h using the NanoPhotometer N60 (Implen, Germany).

The minimum inhibitory concentrations (MICs) of piperacillin-tazobactam, ceftazidime, cefotaxime, cefepime,

aztreonam, imipenem, meropenem, amikacin, gentamicin, ciprofloxacin, levofloxacin, tetracycline, chloramphenicol, and trimethoprim-sulfamethoxazole were determined using the BD Phoenix^{TM}-100 Automated Microbiology System. The *E. coli* ATCC 25922 was used as an internal quality control.

The biochemical characteristics were tested using the BD Phoenix^{TM}-100 Automated Microbiology System, and the cellular fatty acid composition was detected using gas chromatography (Hewlett Packard 6890, USA) and identified using the Sherlock Microbial Identification System (MIDI, USA).

2.3. Sequencing and sequence assembly

The bacterial genomic DNA was isolated using the UltraClean microbial kit (Qiagen, Germany) and sequenced with a PacBio RS II sequencer (Pacific Biosciences, USA) (Fu et al., 2022; Li et al., 2022). The reads were assembled *de novo* using SMARTdenovo.[1]

2.4. Bacterial precise species identification

Bacterial precise species identification was conducted using pairwise average nucleotide identity (ANI) analysis between the bacterial genomic DNA sequenced in this study and the reference genome.[2] A cutoff of $\geq$ 95% ANI was used to define a bacterial species (Richter and Rosselló-Móra, 2009).

2.5. Phylogenetic analysis

The core genes and specific genes of the bacterial genomes were analyzed using the CD-HIT rapid clustering of similar proteins software with a threshold of 50% pairwise identity and 0.7 length difference cutoff in amino acid (Li et al., 2001, 2002; Li and Godzik, 2006). The core amino acid sequences were extracted and aligned using MUSCLE (Edgar, 2004). Based on the core amino acid sequences, a maximum-likelihood phylogenetic tree was constructed using TreeBeST[3] with a bootstrap iteration of 1,000.

2.6. Sequence annotation

RAST 2.0 (Brettin et al., 2015), blastp/blastn (Boratyn et al., 2013), and DANMEL (Wang et al., 2022) searches were used to predict open reading frames (ORFs). The online databases CARD (Jia et al., 2017), ResFinder (Zankari et al., 2012), ISfinder (Siguier et al., 2006), and INTEGRALL (Moura et al., 2009) were used to find resistance genes and mobile elements. Inkscape 1.0 was used to draw gene organization diagrams.[4]

1 http://github.com/ruanjue/smartdenovo
2 http://www.ezbiocloud.net/tools/ani
3 http://treesoft.sourceforge.net/treebest.shtml
4 http://inkscape.org/en/

2.7. Identification of the transcription start site and the promoter of the *bla*$_{VEB-1}$ region

The total RNA of the bacterial isolates was extracted using the RNeasy maxi kit (Qiagen, Germany). Rapid amplification of cDNA ends (RACE) was performed using 5′-RACE system version 2.0 (Invitrogen, USA) according to the manufacturer's instructions. Three gene-specific primers GSP1 (5′-ATCCTTCTCATTGCTG-3′), GSP2 (5′-CTCCTATTCTGGCATTTTTTG-3′), and GSP3 primer (5′-AAGTTGTCAGTTTGAGCATTT-3′) were used. The final PCR products were cloned into the pMD18-T vector, and then, the positive clones were identified and sequenced. The 5′-RACE experiment was repeated three times. Five clones were selected randomly and sequenced each time. The transcription start site was determined according to the sequence comparison between the positive clones and the *bla*$_{VEB-1}$ region. The online database BPROM (Cassiano and Silva-Rocha, 2020) was used for promoter prediction.

2.8. Conjugation and electroporation experiments

Conjugal transfer and electroporation were performed as described previously (Liang et al., 2018; Guan et al., 2022).

2.9. Data availability statement

The complete sequences of the chromosome of BM-Y and the plasmid pBM-Y were submitted to GenBank under the accession numbers CP115969 and CP115970, respectively.

3. Results

3.1. Identification of *W. chitiniclastica* BM-Y and its phenotypic characteristics

BM-Y was isolated from the pancreas specimens of a dead zebra. According to Gram staining and the sequences of the amplicon of the 16S rRNA, *rpoB*, and *gyrB* genes, BM-Y was identified as the Gram-negative bacteria *W. chitiniclastica*. The MALDI-TOF MS score of BM-Y was 2.418, confirming *W. chitiniclastica*. Scores above 2.300 represent a highly probable species identification. No other bacterial isolates were discovered in this study. BM-Y has a 97.19% ANI value with the reference genome DSM 18708 (accession number AQXD01000000). BM-Y contained one chromosome (2.0 Mb in length) and one plasmid pBM-Y (42.3 Kb in length), and they were fully sequenced herein. The chromosome carried no resistance genes. The plasmid pBM-Y harbored *bla*$_{VEB-1}$, *aadB*, *aacA1*, and *tetA*(H).

Colonies of BM-Y were small (colony diameter 0.8–1.0 mm), entire, convex, smooth, and glistening and were composed of short, straight, and non-motile rods (0.1–0.2 × 1.0–1.5 μm, **Figure 1**), which did not produce hemolysin on 5% sheep blood agar medium.

10.3389/fmicb.2023.1276314

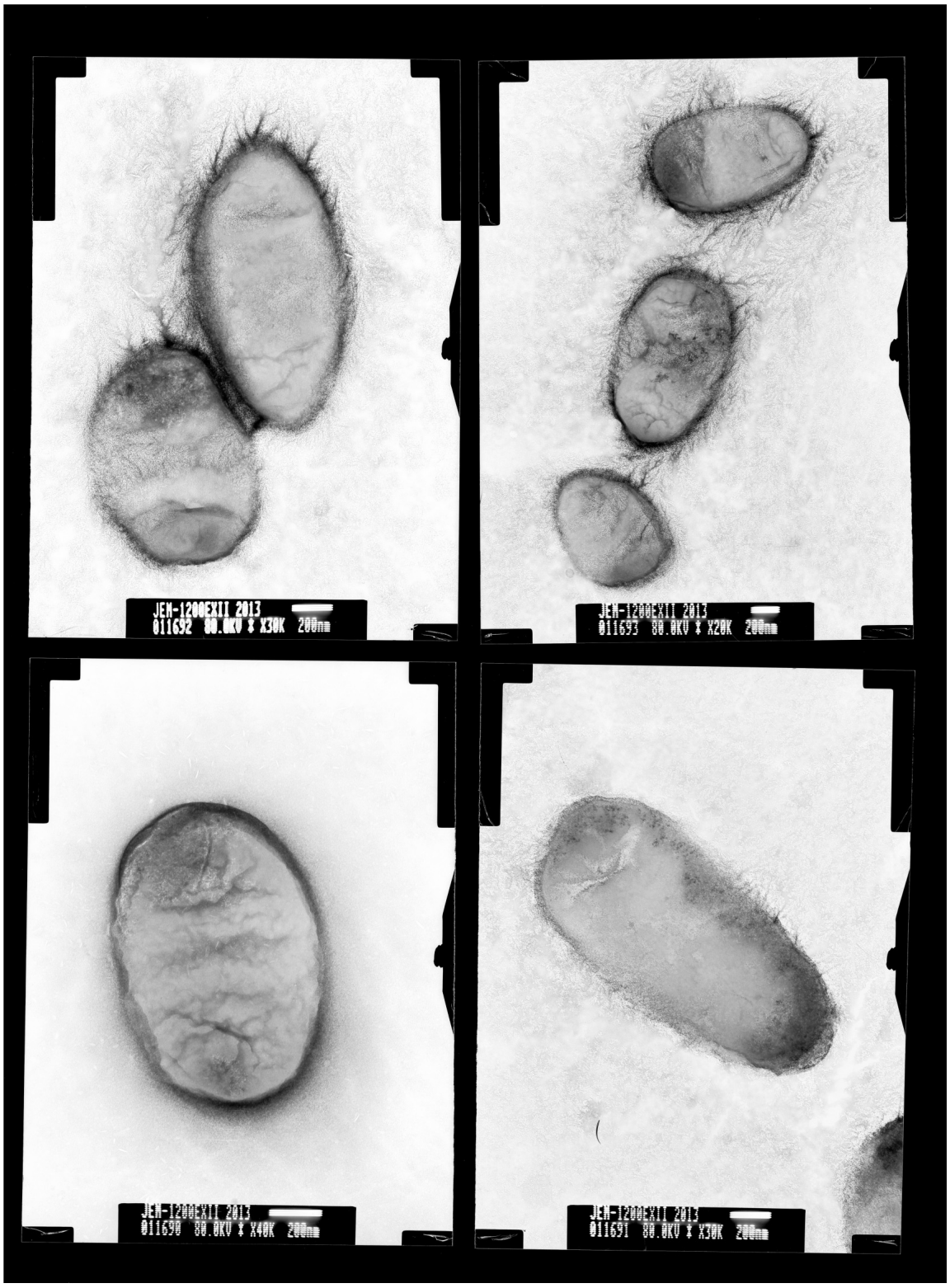

FIGURE 1
Transmission electron micrographs of *Wohlfahrtiimonas chitiniclastica* BM-Y. BM-Y was incubated on a brain heart infusion agar medium at 37°C for 18 h.

Both BM-Y and DSM 18708 reached the middle logarithmic phase (OD_{600} value of about 1.0) and the stationary stage at the fifth hour and the 12th hour, respectively (Figure 2).

The MICs of ceftazidime, cefotaxime, cefepime, aztreonam, gentamicin, and tetracycline of BM-Y were higher than that of DSM 18708. The MICs of 14 antimicrobial drugs are shown in Table 1.

10.3389/fmicb.2023.1276314

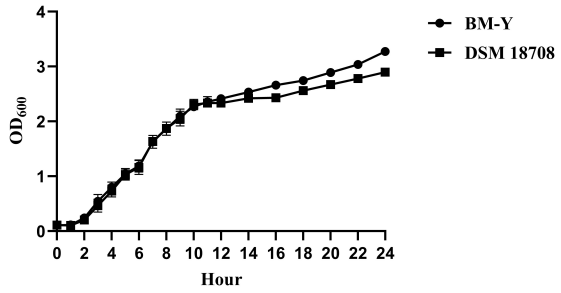

FIGURE 2
Bacterial growth curves of *W. chitiniclastica* BM-Y and DSM 18708.

TABLE 1 Minimum inhibitory concentrations of 14 antimicrobial drugs.

Antibiotics	Minimum inhibitory concentration (MIC, μg/mL)		
	BM-Y	DSM 18708	ATCC 25922
Piperacillin-tazobactam	< 4/4	> 64/4	< 4/4
Ceftazidime	> 16	16	< 1
Cefotaxime	8	< 1	< 1
Cefepime	> 16	8	< 2
Aztreonam	> 16	8	< 2
Imipenem	< 1	< 1	< 1
Meropenem	< 1	< 1	< 1
Amikacin	16	16	< 8
Gentamicin	8	4	< 2
Ciprofloxacin	< 0.5	< 0.5	< 0.5
Levofloxacin	< 1	< 1	< 1
Tetracycline	> 8	< 2	< 2
Chloramphenicol	< 4	< 4	> 16
Trimethoprim/ sulfamethoxazole	< 0.5/9.5	< 0.5/9.5	< 0.5/9.5

The biochemical test results of BM-Y and DSM 18708 are shown in Table 2. A varied reaction between these two strains was observed for acetate, polymyxin B, and glycine. The cellular fatty acid profile (Table 3) of BM-Y revealed a proportionally high level of $C_{18:1}\omega7c$, $C_{14:0}$, and $C_{16:0}$, which was consistent with DSM 18708.

3.2. Phylogenetic analysis

Based on the bacterial core/pan-genome analysis, we conducted the phylogenetic analysis of 27 sequenced *W. chitiniclastica* isolates (Supplementary Table 1), including one complete genome sequence from this study and 26 draft genome sequences from GenBank (last accessed March 17, 2023). Construction of a phylogenetic tree (Figure 3) based on core genes (1602/3597, 44.53%) of 27 *W. chitiniclastica* genomes revealed that all strains clustered in one subclade with the reference genome DSM 18708, and BM-Y shared the closest genetic relationship with MUWRP0946 from Uganda. This result indicated a surprisingly

TABLE 2 Biochemical characteristics of BM-Y and DSM 18708.

Substrates	BM-Y	DSM 18708
Arginine	–	–
Glutaryl-glycine-arginine	–	–
L-leucine	+	+
L-pyroglutamic acid	–	–
Acetate	–	+
Colistin	+	+
Malonate	–	–
4MU-N-acetyl-BD-glucosaminide	–	–
PNP-BD-glucoside	–	–
β-gentiobiose	–	–
D-galactose	–	–
Sorbitol	–	–
L-arabinose	–	–
Maltulose	–	–
Ornithine	–	–
Glycine-proline	–	–
L-arginine	–	–
L-phenylalanine	+	+
L-tryptophan	–	–
Adonitol	–	–
D-mannitol	–	–
Polymyxin B	–	+
γ-glutamyl-NA	–	–
Bis (PNP) phosphate	+	+
Dextrose	–	–
D-gluconic acid	–	–
Sucrose	–	–
L-rhamnose	–	–
N-acetyl-galactosamine	–	–
Urea	–	–
Glycine	–	+
L-glutamic acid	–	–
L-proline	–	–
Lysine-alanine	–	–
Citrate	–	–
α-ketoglutaric acid	+	+
Tiglic acid	–	–
L-proline-NA	+	+
β-allose	–	–
D-fructose	–	–
D-melibiose	–	–
Galacturonic acid	–	–
Methyl-B-glucoside	–	–
N-acetyl-glucosamine	–	–
Esculin	–	–

+, positive; –, negative.

TABLE 3 Cellular fatty acid profiles of BM-Y and DSM 18708.

Fatty acids		BM-Y (%)	DSM 18708 (%)
Saturated acids	$C_{12:0}$	5.68	5.10
	$C_{14:0}$	17.70	14.40
	$C_{16:0}$	6.57	15.60
	$C_{18:0}$	tr	1.30
Unsaturated	C18:1ω7*c*	50.03	47.30
Branched acids	$C_{12:0}$ 3-OH	3.23	1.00
	cyclo-$C_{19:0}$ω8*c*	5.68	7.60
Summed features	Summed feature 1	3.08	1.33
	Summed feature 2	5.64	2.86

tr, trace amount (< 0.5%). Summed features represent two or three fatty acids that could not be separated by the Microbial Identification System. Summed feature 1 comprises $C_{14:0}$ 3-OH/iso-$C_{16:1}$. Summed feature 2 comprises $C_{16:1}$ω7*c*/iso-C_{15} 2-OH.

conserved core/pan genome without clear host or geographical clustering, suggesting a potential spread and transmission. This is in line with Kopf's report (Kopf et al., 2022).

3.3. Organization of the *bla*$_{VEB-1}$-carrying plasmid pBM-Y

The modular structure of pBM-Y (Figure 4) was separated into the backbone and the accessory modules. The backbone contained three different *rep* (replication) with no similar DNA sequences (nucleotide identity < 95%) in GenBank, two *parA* (partition) with different sequences, three groups of *relBE* (a toxin–antitoxin system) with low nucleotide identities, one group of *yefM/yoeB* (a toxin–antitoxin system), and one group of *hsdMSR* (a type I restriction–modification system). No conjugal transfer genes were identified in the backbone. The accessory modules were composed of a *bla*$_{VEB-1}$ region, a *tetA*(H) region, and intact or truncated insertion sequences (ISs) IS*Woch2* and IS*Woch3*.

bla$_{VEB-1}$ was originally found in Tn*2000* in the plasmid pNLT1 from *E. coli* MG-1 (Poirel et al., 1999; Naas et al., 2001). Tn*2000* was an IS*26*-composite transposon composed of ΔIn53 and was used as a reference herein. A detailed sequence comparison (Figure 5) was applied to the *bla*$_{VEB-1}$-carrying ΔIn53 from Tn*2000* and the *bla*$_{VEB-1}$ region from pBM-Y. Both ΔIn53 and the *bla*$_{VEB-1}$ region harbored the *bla*$_{VEB-1}$ cassette (with a 133-bp attachment site of the cassette, *attC*), the *aadB* cassette (with a 60-bp *attC*), and the *aacA1/gcuG* fusion gene cassette (with a 118-bp *attC*) (Naas et al., 2001), but they showed three major modular variations: (i) an intact *attC_aacA1/gcuG* in ΔIn53, while an interrupted one in the *bla*$_{VEB-1}$ region; (ii) a gene cassette array (GCA) *qacL–aadB–aacA1–gcuG–bla*$_{VEB-1}$*–aadB–arr-2–cmlA5–bla*$_{OXA-10}$*–aadA1* in ΔIn53, while a GCA *bla*$_{VEB-1}$*–aadB–aacA1–gcuG* in the *bla*$_{VEB-1}$ region; and (iii) a truncated 5′-conserved segment (5′-CS) and a 3′-CS were upstream and downstream, respectively, of the GCA in ΔIn53, while a novel IS element IS*Woch1* and a truncated one were upstream and downstream, respectively, of the GCA in the *bla*$_{VEB-1}$ region. No direct repeats (DRs) were identified at the ends of the *bla*$_{VEB-1}$ region from pBM-Y.

IS*Woch1*, IS*Woch2*, and IS*Woch3* were named based on the first four letters of the species in which they were first discovered (*Wohlfahrtiimonas chitiniclastica*) and had IR of 37, 45, and 21 bp, respectively (Figure 4). IS*Woch1* and IS*Woch2* encoded two transposases, while IS*Woch3* carried a single one. No DNA sequences similar (nucleotide identity < 95%) to these transposases were found using blastn analysis. The promoter of IS*Woch1* was determined using 5′-RACE experiments. Fourteen of 15 positive clones were successfully sequenced. GACCT (Figure 6), the transcription start site of the *bla*$_{VEB-1}$ region, was identified through multiple sequence alignments. This site was found in IS*Woch1* and located 173 bp upstream of the initiation codon of *bla*$_{VEB-1}$. A promoter with the −10/−35 region (TATAAT/TTAGCA) was located upstream of this site (Figure 5). The spacing between the −10/−35 region was 18 bp. Based on the results of the promoter prediction, IS*Woch2* contained a −10/−35 region (TATCAT/ATACCA, with a 21-bp spacer), and IS*Woch3* carried a −10/−35 region (TAAAAT/TTATCA, with a 19-bp spacer). IS*Woch1–bla*$_{VEB-1}$*–aadB–aacA1–gcuG–*ΔIS*Woch1* was composed of the *bla*$_{VEB-1}$ region (Figure 5). IS*Woch2* was located upstream of the truncated IS*Woch3* and downstream of the *repA*. Three intact IS*Woch3* and three truncated ones were found in pBM-Y. IS*Woch3–orf405–tetR*(H)*–tetA*(H)*–orf423* formed the *tetA*(H) region.

3.4. Conjugation and electroporation experiments

The *bla*$_{VEB-1}$-carrying transconjugants could not be obtained, regardless of the number of times the conjugation experiments were performed. This result might be due to the absence of the essential conjugal transfer genes, including *rlx* (relaxase), *oriT* (origin of conjugative replication), *pri* (DNA primase), and *cpl* (coupling protein), and the type IV secretion system (T4SS) in pBM-Y.

The *bla*$_{VEB-1}$-carrying electroporants were not obtained, no matter how many times the electroporation experiments were conducted. Because we failed to extract the plasmid pBM-Y from strain BM-Y.

4. Discussion

Wohlfahrtiimonas chitiniclastica is an emerging fly-borne zoonotic pathogen, which is often carried by different species of flies, and it causes infections in immunocompromised patients and some animals (Almuzara et al., 2011; Thaiwong et al., 2014), leading to bacteremia, sepsis, and other infections. β-lactams, quinolones, and trimethoprim/sulfamethoxazole are used to treat patients and animals infected by *W. chitiniclastica* (Schröttner et al., 2017).

Herein, BM-Y was isolated from the pancreas of a dead zebra in Shenzhen Safari Park in China in 2013. We speculated that *W. chitiniclastica* was possibly transferred to this park through either or both internal and international transport routes. Notably, *W. chitiniclastica* was first isolated and identified in China from *C. megacephala* captured from the Pudong International Airport in 2011 (Cao et al., 2013). This fly is one of the most common species found in South China (Liu et al., 2009), and it may have become

10.3389/fmicb.2023.1276314

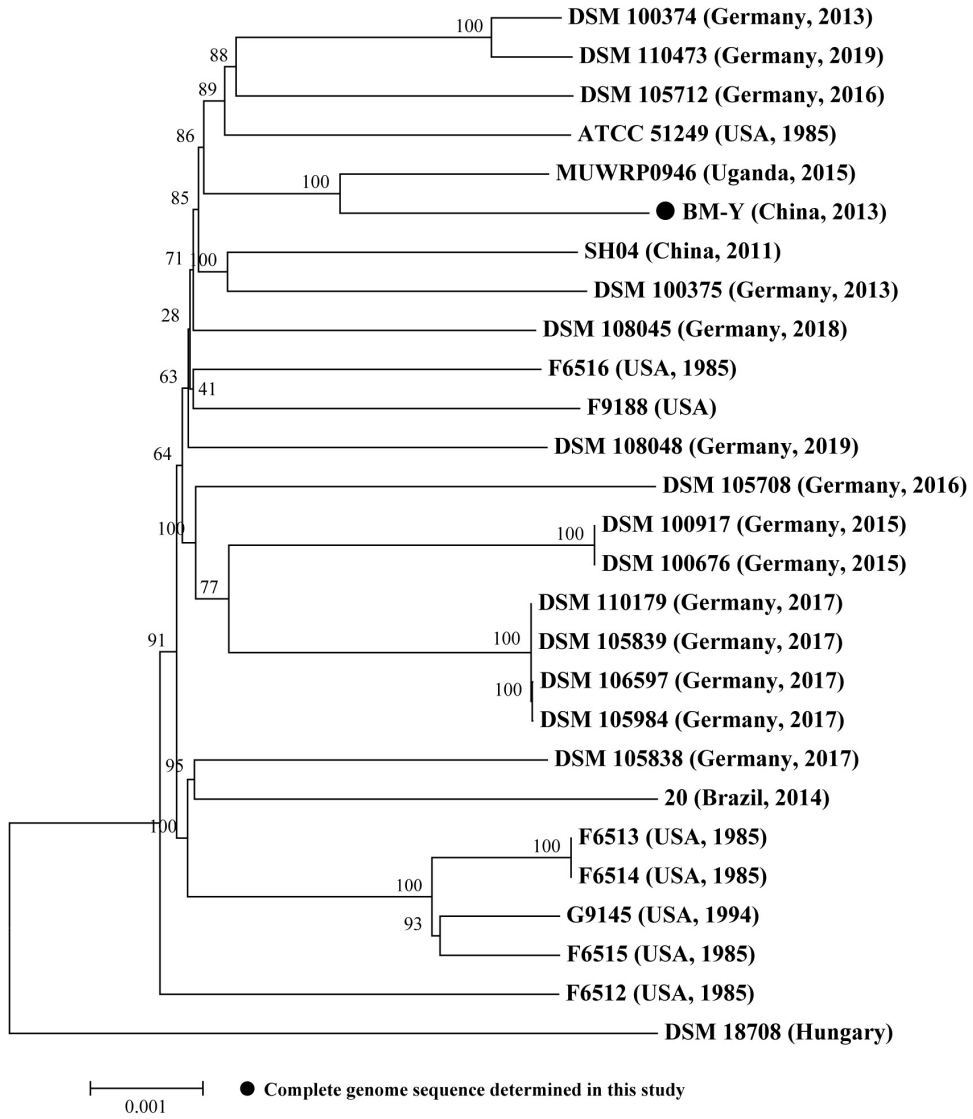

FIGURE 3
Maximum-likelihood phylogenetic tree of 27 *W. chitiniclastica* isolates. The numbers above branches indicate bootstrap values of 1,000 times. The bar corresponds to a scale of sequence divergence.

the depositor of *W. chitiniclastica* in China. However, BM-Y shares the closest genetic relationship with MUWRP0946 from Uganda. *W. chitiniclastica* is more likely to be transferred from other countries to this park through international food (animal- and plant-based) trade or travel. We failed to isolate *W. chitiniclastica* from the flies collected in Shenzhen Safari Park, although we made several attempts.

We are not sure whether BM-Y was associated with the death of the zebra because we failed to find the maggots from the zebra. Generally, flies transmit *W. chitiniclastica* to the host by laying eggs that subsequently hatch into larvae inside an open wound (Schröttner et al., 2017). In this study, neither an open wound nor a maggot was found, but the flies might have carried *W. chitiniclastica* to deposit the eggs on the mucosal surfaces of the zebra (Schröttner et al., 2017). It is necessary to continuously monitor the spread of *W. chitiniclastica*, especially the ones that carry antimicrobial resistance genes, in the future.

pBM-Y is a very specific plasmid. It carries three different and novel *rep* genes. Currently, no other similar genes can be found in GenBank. pBM-Y encodes two toxin–antitoxin systems: RelBE and YefM/YoeB, which have been shown to increase plasmid maintenance (Gotfredsen and Gerdes, 1998). The HsdMSR type I restriction–modification system is also identified in pBM-Y. This system can stabilize plasmids by degrading the unmethylated incoming DNA (Oliveira et al., 2014). It is speculated herein that the loss of the toxin–antitoxin or restriction–modification system might lead to the instability of pBM-Y. No conjugative genes were identified; so, pBM-Y is putatively mobilized by the conjugative plasmids (Xu et al., 2021).

The MICs of ceftazidime, cefotaxime, cefepime, aztreonam, gentamicin, and tetracycline of BM-Y were higher than that of DSM 18708, which was related to the resistance genes bla_{VEB-1}, *aadB*, *aacA1*, and *tetA*(H). These genes were identified in pBM-Y using the CARD and ResFinder online databases. This indicates that these

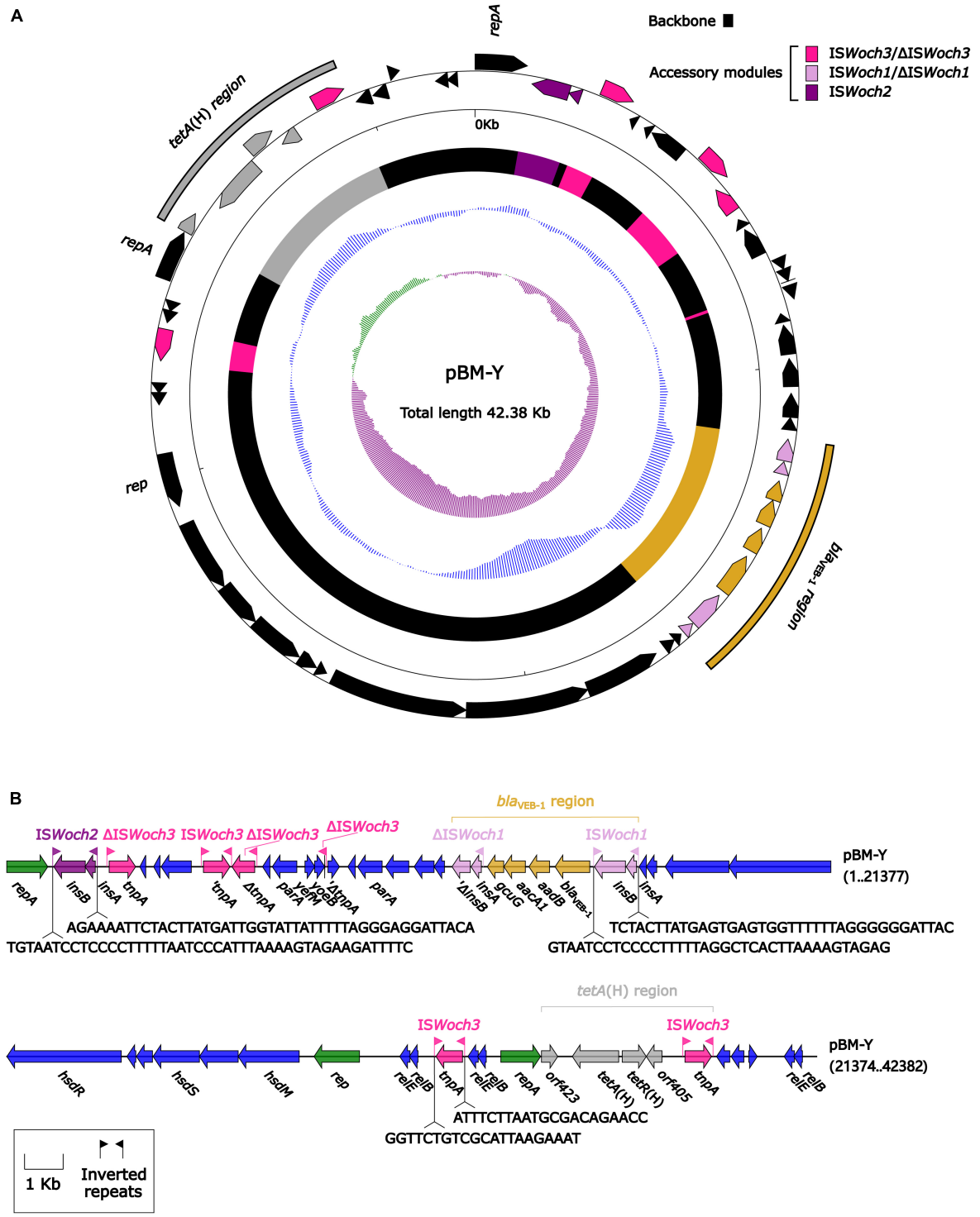

FIGURE 4
Organization of the plasmid pBM-Y. **(A)** Schematic map of pBM-Y. Genes are denoted by arrows, and the backbone and accessory module regions are highlighted in black and color, respectively. The innermost circle presents the GC-skew [(G−C)/(G+C)], with a window size of 500 bp and a step size of 20 bp. The next-to-innermost circle presents the GC content. **(B)** Linear structure of pBM-Y. Genes are denoted by arrows. The genes, accessory genetic elements (AGEs), and other features are colored based on their functional classification. The numbers in brackets indicate nucleotide positions within pBM-Y.

genes can express effectively and are involved in the increase in MICs. The bla_{VEB-1} gene cassette, the *aadB* gene cassette, and the *aacA1*/*gcuG* fusion cassette are individual mobile units and are usually found inserted into an integron (Partridge et al., 2018). In this study, they formed a GCA (bla_{VEB-1}–*aadB*–*aacA1*–*gcuG*) different from that (*qacL*–*aadB*–*aacA1*–*gcuG*–bla_{VEB-1}–*aadB*–*arr-2*–*cmlA5*–bla_{OXA-10}–*aadA1*) in ΔIn53 from Tn*2000* (Naas et al., 2001). This demonstrates that these gene cassettes might undergo

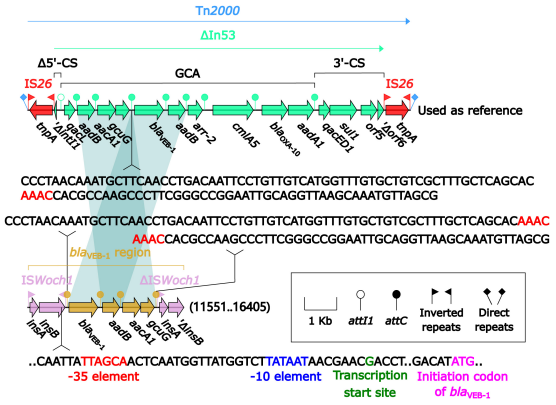

FIGURE 5
Comparison of the bla_{VEB-1} region from pBM-Y and bla_{VEB-1}-carrying Tn*2000*. Genes are denoted by arrows. The genes, AGEs, and other features are colored based on their functional classification. The shading in light blue denotes regions of homology (nucleotide identity ≥ 95%). The 3′ fragment of *attC_aacA1*/*gcuG* is upstream of bla_{VEB-1}, while the 5′ fragment is downstream of *gcuG*. The numbers in the brackets indicate the nucleotide positions within pBM-Y. Tn*2000* (Naas et al., 2001) (accession number AF205943) was used as a reference.

reassembly via homologous recombination. An intact and a truncated IS*Woch1* were at the 5′ and 3′ ends of bla_{VEB-1}–*aadB*–*aacA1*–*gcuG* in pBM-Y, respectively, which indicated that this GCA might be captured by IS*Woch1* to form a translocatable unit (TU, one copy of IS*Woch1* and an adjacent region) (Partridge et al., 2018). Then, this TU inserts into a recipient that lacks IS*Woch1* (intermolecular replicative transposition) or targets an existing copy of IS*Woch1* (intermolecular conservative transposition) (Partridge et al., 2018). However, one copy of IS*Woch1* has been truncated during transposition.

Two copies of IS*Woch1* participated in the movement of bla_{VEB-1}–*aadB*–*aacA1*–*gcuG*. A single IS can also move an adjacent region that includes one or more resistance genes by forming a TU (Partridge et al., 2018). Herein, IS*Woch3* was located upstream of *orf405*–*tetR*(H)–*tetA*(H)–*orf423*, indicating that it might be involved in the mobilization of *tetA*(H), and this *tetA*(H) region might preferentially insert next to an existing copy of IS*Woch3* in the recipient molecule, generating a structure of IS*Woch3*–*orf405*–*tetR*(H)–*tetA*(H)–*orf423*–IS*Woch3* (Partridge et al., 2018). It should also be noted that six intact or truncated copies of IS*Woch3* were presented in pBM-Y, demonstrating that they participated in complex homologous recombination events and promoted the assembly of complex structures as observed in pBM-Y. A promoter was found or predicted in each of IS*Woch1*, IS*Woch2*, and IS*Woch3*, meaning these three ISs might provide a promoter for captured genes. Taken together, IS*Woch1*, IS*Woch2*, and IS*Woch3* might promote the dissemination of drug resistance genes and affect the expression of these genes to regulate antimicrobial resistance (Noel et al., 2022). Surveillance studies for these three ISs are necessary.

The promoter region (containing the −10 and −35 elements) of the bla_{VEB-1} region was located in IS*Woch1*. The optimal spacing between the −10 and 35 elements is 16–18 bp (Aoyama et al., 1983), and in this study, it was 18 bp. This indicates that IS*Woch1* provides a strong promoter for the bla_{VEB-1} region. Therefore, BM-Y can express β-lactamase and show resistance to ceftazidime, cefepime, and aztreonam. This means that some β-lactams are not suitable for treating infections caused by bla_{VEB-1}-carrying *W. chitiniclastica*, while quinolones and trimethoprim/sulfamethoxazole can still be the first choices.

To the best of our knowledge, this is the first report of the genetic characterization of a novel bla_{VEB-1}-carrying plasmid with three new ISs from *W. chitiniclastica*. The acquisition of this plasmid can give bacteria the fitness advantage for adapting to mammals and enable bacteria to acquire new antimicrobial resistance genes. The resistance of *W. chitiniclastica* to ceftazidime, cefepime, aztreonam, and tetracycline might enhance its ability to survive under drug selection pressure and aggravate the difficulty in treating infections caused by *W. chitiniclastica*. It is necessary to continuously monitor the spread of the bla_{VEB-1}-carrying *W. chitiniclastica* and the possibility of acquiring other drug resistance genes in *W. chitiniclastica*.

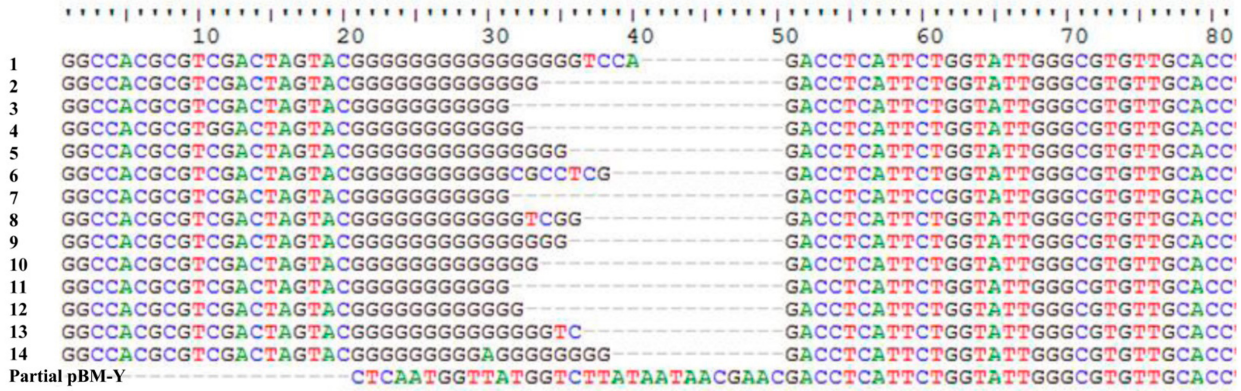

FIGURE 6
Identification of the transcription start site of the bla_{VEB-1} region. Multiple sequence alignments of 14 positive clones and partial pBM-Y.

Data availability statement

The datasets presented in this study can be found in online repositories. The names of the repository/repositories and accession number(s) can be found in this article/**Supplementary material**.

Ethics statement

The animal study was approved by the Laboratory Animal Welfare and Ethics Committee of the Changchun Veterinary Research Institute, Chinese Academy of Agricultural Sciences. The study was conducted in accordance with the local legislation and institutional requirements.

Author contributions

JiaG: Formal analysis, Investigation, Writing – original draft. WZ: Formal analysis, Writing – original draft. JinG: Formal analysis, Writing – original draft. LZhe: Investigation, Writing – original draft. GL: Formal analysis, Writing – original draft. FH: Resources, Writing – original draft. ML: Formal analysis, Writing – original draft. XJ: Investigation, Writing – original draft. YS: Investigation, Writing – original draft. LZhu: Conceptualization, Writing – review and editing. XG: Conceptualization, Writing – review and editing.

Funding

The authors declare financial support was received for the research, authorship, and/or publication of this article. This work was supported by the National Natural Science Foundation of China (31872486).

Acknowledgments

We are grateful to Professor Dongsheng Zhou from the State Key Laboratory of Pathogen and Biosecurity, Beijing Institute of Microbiology and Epidemiology for the assistance with the drawing of the gene organization diagrams.

Conflict of interest

The authors declare that the research was conducted in the absence of any commercial or financial relationships that could be construed as a potential conflict of interest.

Publisher's note

All claims expressed in this article are solely those of the authors and do not necessarily represent those of their affiliated organizations, or those of the publisher, the editors and the reviewers. Any product that may be evaluated in this article, or claim that may be made by its manufacturer, is not guaranteed or endorsed by the publisher.

Supplementary material

The Supplementary Material for this article can be found online at: https://www.frontiersin.org/articles/10.3389/fmicb.2023.1276314/full#supplementary-material

References

Almuzara, M. N., Palombarani, S., Tuduri, A., Figueroa, S., Gianecini, A., Sabater, L., et al. (2011). First case of fulminant sepsis due to *Wohlfahrtiimonas chitiniclastica*. *J. Clin. Microbiol.* 49, 2333–2335. doi: 10.1128/JCM.00001-11

Aoyama, T., Takanami, M., Ohtsuka, E., Taniyama, Y., Marumoto, R., Sato, H., et al. (1983). Essential structure of *E. coli* promoter: Effect of spacer length between the two consensus sequences on promoter function. *Nucleic Acids Res.* 11, 5855–5864.

Boratyn, G. M., Camacho, C., Cooper, P. S., Coulouris, G., Fong, A., Ma, N., et al. (2013). BLAST: A more efficient report with usability improvements. *Nucleic Acids Res.* 41, W29–W33. doi: 10.1093/nar/gkt282

Brettin, T., Davis, J. J., Disz, T., Edwards, R. A., Gerdes, S., Olsen, G. J., et al. (2015). RASTtk: A modular and extensible implementation of the RAST algorithm for building custom annotation pipelines and annotating batches of genomes. *Sci. Rep.* 5:8365. doi: 10.1038/srep08365

Campisi, L., Mahobia, N., and Clayton, J. J. (2015). *Wohlfahrtiimonas chitiniclastica* bacteremia associated with myiasis, United Kingdom. *Emer. Infect. Dis.* 21, 1068–1069. doi: 10.3201/eid2106.140007

Cao, X., Chen, T., Xu, L., Yao, L., Qi, J., Zhang, X., et al. (2013). Complete genome sequence of *Wohlfahrtiimonas chitiniclastica* strain SH04, isolated from *Chrysomya megacephala* collected from Pudong International Airport in China. *Genome Announc.* 1:e0011913. doi: 10.1128/genomeA.00119-13

Cassiano, M. H. A., and Silva-Rocha, R. (2020). Benchmarking bacterial promoter prediction tools: Potentialities and limitations. *MSystems* 5, e439–e420. doi: 10.1128/mSystems.00439-20

Connelly, K. L., Freeman, E., Smibert, O. C., and Lin, B. (2019). *Wohlfahrtiimonas chitiniclastica* bloodstream infection due to a maggot-infested wound in a 54-year-old male. *J. Glob. Infect. Dis.* 11, 125–126. doi: 10.4103/jgid.jgid_58_18

de Dios, A., Jacob, S., Tayal, A., Fisher, M. A., Dingle, T. C., and Hamula, C. L. (2015). First report of *Wohlfahrtiimonas chitiniclastica* isolation from a patient with cellulitis in the United States. *J. Clin. Microbiol.* 53, 3942–3944. doi: 10.1128/JCM.01534-15

De Smet, D., Goegebuer, T., Ho, E., Vandenbroucke, M., and Lemmens, A. (2022). First case of *Wohlfahrtiimonas chitiniclastica* isolation from a patient with a foot ulcer infection in Belgium. *Acta Clin. Belg.* 78, 245–247. doi: 10.1080/17843286.2022.2090770

Dovjak, P., Kroißenbrunner, M., and Iglseder, B. (2021). Myiasis absent *Wohlfahrtiimonas chitiniclastica* bacteremia in a lung cancer patient: A case report. *Eur. J. Med. Res.* 26:101. doi: 10.1186/s40001-021-00576-w

Edgar, R. C. (2004). MUSCLE: Multiple sequence alignment with high accuracy and high throughput. *Nucleic Acids Res.* 32, 1792–1797.

Fu, J., Zhang, J., Yang, L., Ding, N., Yue, L., Zhang, X., et al. (2022). Precision methylome and *in vivo* methylation kinetics characterization of *Klebsiella pneumoniae*. *Genomics Proteomics Bioinform.* 20, 418–434. doi: 10.1016/j.gpb.2021.04.002

Gotfredsen, M., and Gerdes, K. (1998). The *Escherichia coli relBE* genes belong to a new toxin-antitoxin gene family. *Mol. Microbiol.* 29, 1065–1076.

Guan, J., Li, L., Zheng, L., Lu, G., Wang, Y., Lakoh, S., et al. (2022). First report of the colistin resistance gene *mcr-10.1* carried by $Inc_{pA1763-KPC}$ plasmid pSL12517-mcr10.1 in *Enterobacter cloacae* in Sierra Leone. *Microbiol. Spect.* 10:e0112722. doi: 10.1128/spectrum.01127-22

Gupta, A. K., Nayduch, D., Verma, P., Shah, B., Ghate, H. V., Patole, M. S., et al. (2012). Phylogenetic characterization of bacteria in the gut of house flies (*Musca domestica* L.). *FEMS Microbiol. Ecol.* 79, 581–593. doi: 10.1111/j.1574-6941.2011.01248.x

Hladík, M., Lipovy, B., Kaloudova, Y., Hanslianova, M., Vitkova, I., Deissova, T., et al. (2021). Human infections by *Wohlfahrtiimonas chitiniclastica*: A mini-review and the first report of a burn wound infection after accidental myiasis in Central Europe. *Microorganisms* 9:1934. doi: 10.3390/microorganisms9091934

Hoffman, R., Fortuin, F., Newton-Foot, M., and Singh, S. (2016). First report of *Wohlfahrtiimonas chitiniclastica* bacteraemia in South Africa. *S. Afr. Med. J.* 106:1062. doi: 10.7196/SAMJ.2016.v106i11.11449

Iancu, L., Necula-Petrareanu, G., and Purcarea, C. (2020). Potential bacterial biomarkers for insect colonization in forensic cases: Preliminary quantitative data on *Wohlfahrtiimonas chitiniclastica* and *Ignatzschineria indica* dynamics. *Sci. Rep.* 10:8497. doi: 10.1038/s41598-020-65471-6

Jia, B., Raphenya, A. R., Alcock, B., Waglechner, N., Guo, P., Tsang, K. K., et al. (2017). CARD 2017: Expansion and model-centric curation of the comprehensive antibiotic resistance database. *Nucleic Acids Res.* 45, D566–D573. doi: 10.1093/nar/gkw1004

Josue, D.-D., Eva, S., Isabel, V. A., Lucas, D., Marisa, A., Manuel, A., et al. (2015). Endocarditis associated with *Wohlfahrtiimonas chitiniclastica* in a short-beaked common dolphin (*Delphinus delphis*). *J. Wildlife Dis.* 51, 283–286. doi: 10.7589/2014-03-072

Karaca, M. O., Gürler, M., Afacan, M., Terzi, M. M., Evren, E., Çınar Aydın, G., et al. (2022). *Wohlfahrtiimonas chitiniclastica*-related soft-tissue infection and osteomyelitis: A rare case report. *Ulus. Travma Acil Cerrahi Derg. Turk. J. Trauma Emerg. Surg.* 28, 1038–1041. doi: 10.14744/tjtes.2022.01409

Katanami, Y., Kutsuna, S., Nagashima, M., Takaya, S., Yamamoto, K., Takeshita, N., et al. (2018). *Wohlfahrtiimonas chitiniclastica* bacteremia hospitalized homeless man with squamous cell carcinoma. *Emerg. Infect. Dis.* 24, 1746–1748. doi: 10.3201/eid2409.170080

Kõljalg, S., Telling, K., Huik, K., Murruste, M., Saarevet, V., Pauskar, M., et al. (2015). First report of *Wohlfahrtiimonas chitiniclastica* from soft tissue and bone infection at an unusually high northern latitude. *Folia Microbiol.* 60, 155–158. doi: 10.1007/s12223-014-0355-x

Kopf, A., Bunk, B., Coldewey, S. M., Gunzer, F., Riedel, T., and Schröttner, P. (2021). Identification and antibiotic profiling of *Wohlfahrtiimonas chitiniclastica*, an underestimated human pathogen. *Front. Microbiol.* 12:712775. doi: 10.3389/fmicb.2021.712775

Kopf, A., Bunk, B., Coldewey, S. M., Gunzer, F., Riedel, T., and Schröttner, P. (2022). Comparative genomic analysis of the human pathogen *Wohlfahrtiimonas Chitiniclastica* provides insight into the identification of antimicrobial resistance genotypes and potential virulence traits. *Front. Cell. Infect. Microbiol.* 12:912427. doi: 10.3389/fcimb.2022.912427

Li, C., Jiang, X., Yang, T., Ju, Y., Yin, Z., Yue, L., et al. (2022). Genomic epidemiology of carbapenemase-producing *Klebsiella pneumoniae* in China. *Genomics Proteomics Bioinform.* 20, 1154–1167. doi: 10.1016/j.gpb.2022.02.005

Li, W., and Godzik, A. (2006). Cd-hit: A fast program for clustering and comparing large sets of protein or nucleotide sequences. *Bioinformatics (Oxford, England)* 22, 1658–1659.

Li, W., Jaroszewski, L., and Godzik, A. (2001). Clustering of highly homologous sequences to reduce the size of large protein databases. *Bioinformatics (Oxford, England)* 17, 282–283.

Li, W., Jaroszewski, L., and Godzik, A. (2002). Tolerating some redundancy significantly speeds up clustering of large protein databases. *Bioinformatics (Oxford, England)* 18, 77–82.

Liang, Q., Jiang, X., Hu, L., Yin, Z., Gao, B., Zhao, Y., et al. (2018). Sequencing and genomic diversity analysis of IncHI5 plasmids. *Front. Microbiol.* 9:3318. doi: 10.3389/fmicb.2018.03318

Liu, X., Shi, Y., Wang, H., and Zhang, R. (2009). Determination of malathion levels and its effect on the development of *Chrysomya megacephala* (Fabricius) in South China. *Forensic Sci. Int.* 192, 14–18. doi: 10.1016/j.forsciint.2009.07.005

Matos, J., Queiroga, A. P., de Oliveira Pedroza Bindi dos Reis, C. C., Ribeiro, R. L., Teixeira, L. M., Albano, R. M., et al. (2016). First report of the emerging zoonotic agent *Wohlfahrtiimonas chitiniclastica* isolated from a retail frozen chicken in Rio de Janeiro, Brazil. *Antonie Van Leeuwenhoek* 109, 729–734. doi: 10.1007/s10482-016-0673-x

Moura, A., Soares, M., Pereira, C., Leitão, N., Henriques, I., and Correia, A. (2009). INTEGRALL: A database and search engine for integrons, integrases and gene cassettes. *Bioinformatics (Oxford, England)* 25, 1096–1098. doi: 10.1093/bioinformatics/btp105

Naas, T., Benaoudia, F., Massuard, S., and Nordmann, P. (2000). Integron-located VEB-1 extended-spectrum β-lactamase gene in a *Proteus mirabilis* clinical isolate from Vietnam. *J. Antimicrob. Chemother.* 46, 703–711.

Naas, T., Mikami, Y., Imai, T., Poirel, L., and Nordmann, P. (2001). Characterization of In53, a class 1 plasmid- and composite transposon-located integron of *Escherichia coli* which carries an unusual array of gene cassettes. *J. Bacteriol.* 183, 235–249.

Naas, T., Poirel, L., Karim, A., and Nordmann, P. (1999). Molecular characterization of In50, a class 1 integron encoding the gene for the extended-spectrum β-lactamase VEB-1 in *Pseudomonas aeruginosa*. *FEMS Microbiol. Lett.* 176, 411–419.

Noel, H. R., Petrey, J. R., and Palmer, L. D. (2022). Mobile genetic elements in *Acinetobacter* antibiotic-resistance acquisition and dissemination. *Ann. N. Y. Acad. Sci.* 1518, 166–182. doi: 10.1111/nyas.14918

Nogi, M., Bankowski, M. J., and Pien, F. D. (2016). *Wohlfahrtiimonas chitiniclastica* infections in 2 elderly patients, Hawaii. *Emerg. Infect. Dis.* 22, 567–568. doi: 10.3201/eid2203.151701

Oikonomou, O., Liakopoulos, A., Phee, L. M., Betts, J., Mevius, D., and Wareham, D. W. (2016). *Providencia stuartii* isolates from Greece: Co-carriage of cephalosporin (bla_{SHV-5}, bla_{VEB-1}), carbapenem (bla_{VIM-1}), and aminoglycoside (*rmtB*) resistance determinants by a multidrug-resistant outbreak clone. *Microb. Drug Resistance (Larchmont, N.Y.)* 22, 379–386. doi: 10.1089/mdr.2015.0215

Oliveira, P. H., Touchon, M., and Rocha, E. P. C. (2014). The interplay of restriction-modification systems with mobile genetic elements and their prokaryotic hosts. *Nucleic Acids Res.* 42, 10618–10631. doi: 10.1093/nar/gku734

Pablo-Marcos, D., Siller-Ruiz, M., Fernandez-Ayala, M., Agüero, J., and Calvo, J. (2019). First case of infection by *Wohlfahrtiimonas chitiniclastica* described in Spain. *Rev. Esp. Quimioter.* 32, 558–560.

Papagiannitsis, C. C., Miriagou, V., Kotsakis, S. D., Tzelepi, E., Vatopoulos, A. C., Petinaki, E., et al. (2012). Characterization of a transmissible plasmid encoding VEB-1 and VIM-1 in *Proteus mirabilis*. *Antimicrob. Agents Chemother.* 56, 4024–4025. doi: 10.1128/AAC.00470-12

Partridge, S. R., Kwong, S. M., Firth, N., and Jensen, S. O. (2018). Mobile genetic elements associated with antimicrobial resistance. *Clin. Microbiol. Rev.* 31, e88–e17. doi: 10.1128/CMR.00088-17

Paul, D., Ingti, B., Bhattacharjee, D., Maurya, A. P., Dhar, D., Chakravarty, A., et al. (2017). An unusual occurrence of plasmid-mediated bla_{OXA-23} carbapenemase in clinical isolates of *Escherichia coli* from India. *Int. J. Antimicrob. Agents* 49, 642–645. doi: 10.1016/j.ijantimicag.2017.01.012

Poirel, L., Naas, T., Guibert, M., Chaibi, E. B., Labia, R., and Nordmann, P. (1999). Molecular and biochemical characterization of VEB-1, a novel class A extended-spectrum beta-lactamase encoded by an *Escherichia coli* integron gene. *Antimicrob. Agents Chemother.* 43, 573–581.

Qi, J., Gao, Y., Wang, G., Li, L., Li, L., Zhao, X., et al. (2016). Identification of *Wohlfahrtiimonas chitiniclastica* isolated from an infected cow with hoof fetlow, China. *Infect. Genetics Evol. J. Mol. Epidemiol. Evol. Genet. Infect. Dis.* 41, 174–176. doi: 10.1016/j.meegid.2016.04.008

Rebaudet, S., Genot, S., Renvoise, A., Fournier, P. E., and Stein, A. (2009). *Wohlfahrtiimonas chitiniclastica* bacteremia in homeless woman. *Emer. Infect. Dis.* 15, 985–987. doi: 10.3201/eid1506.080232

Richter, M., and Rosselló-Móra, R. (2009). Shifting the genomic gold standard for the prokaryotic species definition. *Proc. Natl. Acad. Sci. U.S.A.* 106, 19126–19131. doi: 10.1073/pnas.0906412106

Schröttner, P., Rudolph, W. W., Damme, U., Lotz, C., Jacobs, E., and Gunzer, F. (2017). *Wohlfahrtiimonas chitiniclastica*: Current insights into an emerging human pathogen. *Epidemiol. Infect.* 145, 1292–1303. doi: 10.1017/S0950268816003411

Siebor, E., de Curraize, C., Varin, V., Magallon, A., and Neuwirth, C. (2021). Mobilisation of plasmid-mediated bla_{VEB-1} gene cassette into distinct genomic islands of *Proteus mirabilis* after ceftazidime exposure. *J. Glob. Antimicrob. Resist.* 27, 26–30. doi: 10.1016/j.jgar.2021.07.011

Siguier, P., Perochon, J., Lestrade, L., Mahillon, J., and Chandler, M. (2006). ISfinder: The reference centre for bacterial insertion sequences. *Nucleic Acids Res.* 34, D32–D36.

Snyder, S., Singh, P., and Goldman, J. (2020). Emerging pathogens: A case of *Wohlfahrtiimonas chitiniclastica* and *Ignatzschineria indica* bacteremia. *IDCases* 19:e00723. doi: 10.1016/j.idcr.2020.e00723

Suraiya, S., Zuraina, N., Ahmad, F., and Rahman, Z. A. (2017). Fatal *Wohlfahrtiimonas chitiniclastica* bacteremia in an immunocompromised patient. *Clin. Microbiol. Newslett.* 39, 172–173. doi: 10.1016/j.clinmicnews.2017.07.003

Suryalatha, K., John, J., and Thomas, S. (2015). *Wohlfahrtiimonas chitiniclastica*-associated osteomyelitis: A rare case report. *Fut. Microbiol.* 10, 1107–1109. doi: 10.2217/fmb.15.44

Thaiwong, T., Kettler, N. M., Lim, A., Dirkse, H., and Kiupel, M. (2014). First report of emerging zoonotic pathogen *Wohlfahrtiimonas chitiniclastica* in the United States. *J. Clin. Microbiol.* 52, 2245–2247. doi: 10.1128/JCM.00382-14

Tittsler, R. P., and Sandholzer, L. A. (1936). The use of semi-solid agar for the detection of bacterial motility. *J. Bacteriol.* 31, 575–580.

Tóth, E. M., Schumann, P., Borsodi, A. K., Kéki, Z., Kovács, A. L., and Márialigeti, K. (2008). *Wohlfahrtiimonas chitiniclastica* gen. nov., sp. nov., a new gammaproteobacterium isolated from *Wohlfahrtia magnifica* (Diptera: Sarcophagidae). *Int. J. Systematic Evol. Microbiol.* 58(Pt 4), 976–981. doi: 10.1099/ijs.0.65324-0

Wang, P., Jiang, X., Mu, K., Jing, Y., Yin, Z., Cui, Y., et al. (2022). DANMEL: A manually curated reference database for analyzing mobile genetic elements associated with bacterial drug resistance. *mLife* 1, 460–464. doi: 10.1002/mlf2.12046

Xu, Y., Zhang, J., Wang, M., Liu, M., Liu, G., Qu, H., et al. (2021). Mobilization of the nonconjugative virulence plasmid from hypervirulent *Klebsiella pneumoniae*. *Genome Med.* 13:119. doi: 10.1186/s13073-021-00936-5

Ye, L., Li, R., Lin, D., Zhou, Y., Fu, A., Ding, Q., et al. (2016). Characterization of an IncA/C multidrug resistance plasmid in *Vibrio alginolyticus*. *Antimicrob. Agents Chemother.* 60, 3232–3235. doi: 10.1128/AAC.00300-16

Zankari, E., Hasman, H., Cosentino, S., Vestergaard, M., Rasmussen, S., Lund, O., et al. (2012). Identification of acquired antimicrobial resistance genes. *J. Antimicrob. Chemother.* 67, 2640–2644. doi: 10.1093/jac/dks261

Zhou, W., Li, M., Zhu, L., Hua, F., Ji, X., Sun, Y., et al. (2016). Complete genome sequence of *Wohlfahrtiimonas chitiniclastica* strain BM-Y, isolated from the pancreas of a zebra in China. *Genome Announc.* 4, e643–e616. doi: 10.1128/genomeA.00643-16

frontiers | Frontiers in Microbiology

TYPE Original Research
PUBLISHED 10 November 2023
DOI 10.3389/fmicb.2023.1278821

OPEN ACCESS

EDITED BY
Guyue Cheng,
Huazhong Agricultural University, China

REVIEWED BY
Yolande Proroga,
Experimental Zooprophylactic Institute of Southern Italy (IZSM), Italy
Shenye Yu,
Chinese Academy of Agricultural Sciences (CAAS), China
Eelco Franz,
Center for Infectious Disease Control (RIVM), Netherlands

*CORRESPONDENCE
Ahmed E. Yousef
✉ yousef.1@osu.edu

RECEIVED 16 August 2023
ACCEPTED 18 October 2023
PUBLISHED 10 November 2023

CITATION
Abdelhamid AG and Yousef AE (2023) Egg-associated *Salmonella enterica* serovar Enteritidis: comparative genomics unveils phylogenetic links, virulence potential, and antimicrobial resistance traits. *Front. Microbiol.* 14:1278821. doi: 10.3389/fmicb.2023.1278821

Egg-associated *Salmonella enterica* serovar Enteritidis: comparative genomics unveils phylogenetic links, virulence potential, and antimicrobial resistance traits

Ahmed G. Abdelhamid[1,2] and Ahmed E. Yousef[1,3]*

[1]Department of Food Science and Technology, The Ohio State University, Columbus, OH, United States, [2]Botany and Microbiology Department, Faculty of Science, Benha University, Benha, Egypt, [3]Department of Microbiology, The Ohio State University, Columbus, OH, United States

Salmonella enterica serovar Enteritidis (SE) remains a frequent cause of foodborne illnesses associated with the consumption of contaminated hen eggs. Such a food–pathogen association has been demonstrated epidemiologically, but the molecular basis for this association has not been explored. Comparative genomic analysis was implemented to decipher the phylogenomic characteristics, antimicrobial resistance, and virulence potential of eggs-associated SE. Analyzing 1,002 genomes belonging to 841 sequence types of food-isolated SE strains suggests a high genomic similarity within the egg-related lineage, which is phylogenetically close to SE strains isolated from poultry but is different from those isolated from beef. Core genome- and single nucleotide polymorphism (SNP)-based phylogeny of 74 SE strains of egg origin showcased two distinct sublineages. Time-scaled phylogeny supported the possibility of a common ancestor of egg-related SE lineages. Additionally, genome mining revealed frequent antibiotic resistance due to the presence of *aac(6')-Iaa* and *mdsAB* encoded on the genomes of egg-associated SE strains. For virulence gene profiling, 103–113 virulence determinants were identified in the egg-associated SE, which were comparable to 112 determinants found in human-associated SE, emphasizing the capacity of egg-associated strains to infect humans and cause diseases. The findings of this study proved the genomic similarity of egg-associated SE strains, and these were closely related to poultry strains. The egg-associated strains also harbor virulence genes equivalent to those found in human-associated SE strains. The analysis provided critical insights into the genetic structure, phylogenomics, dynamics of virulence, and antibiotic resistance of *Salmonella* Enteritidis, circulating in eggs and emphasizing the necessity of implementing anti-*Salmonella* intervention strategies, starting at the production stage of the poultry supply chain.

KEYWORDS

whole genome sequencing, *Salmonella* Enteritidis, salmonellosis, foodborne disease outbreaks, eggs, egg safety, comparative genomics

1. Introduction

Non-typhoidal *Salmonella enterica* is estimated to cause 153 million illnesses and 57,000 deaths annually worldwide (Healy and Bruce, 2019). According to the European Food Safety Authority (EFSA) and European Center for Disease Prevention and Control (ECDC), *Salmonella* was involved in 30.7% of foodborne disease outbreaks in 2018, and salmonellosis is the second most reported disease and the second cause of death due to the consumption of contaminated food (EFSA and ECDC, 2019). In the United States, it was estimated that 1 million cases of non-typhoidal salmonellosis occurred in 2013; this infection level accounted for 24% of the economic burden of all foodborne diseases (USDA, 2019). Certain foods are disproportionately linked to salmonellosis outbreaks. Eggs and egg products accounted for 45.6% of salmonellosis outbreaks in the European Union (EFSA and ECDC, 2019). In a recent report by EFSA and ECDC, salmonellosis was the second most reported zoonoses in humans, *Salmonella* Enteritidis remained the most frequent causative agent of foodborne outbreaks, and *Salmonella* serovars in eggs and egg products were of the most concern (EFSA and ECDC, 2022). Similarly, the *Salmonella*–egg combination caused most of the salmonellosis outbreaks in the United States (Dewey-Mattia et al., 2018). In fact, *Salmonella* Enteritidis has been the main serovar associated with human salmonellosis (Ferrari et al., 2019), including those associated with eggs, and the serovar has been associated with disease outbreaks in several countries (Cardoso et al., 2021). The terms "egg" or "eggs," used in the current study, refer to hen whole shell eggs, egg components such as white and yolk, or raw whole liquid egg.

Despite the obvious *Salmonella* Enteritidis–egg epidemiological association, there is a knowledge gap about the genetic basis for the colonization and survival of *Salmonella* Enteritidis in eggs. Several researchers attempted to determine the underlying genetic mechanisms governing the ability of this serovar to colonize internal egg contents. Previous research showed that non-motile mutants (Δ*fliC*, Δ*fljB*, and Δ*fliH*), compared with the wild-type strain, were impaired in the survival of egg albumin (Cogan et al., 2004; Shah et al., 2012). In addition to motility, genes involved in curli fimbriae production (*agfA*), DNA replication, repair, and recombination (e.g., *yafD*) were significantly important for the survival of the pathogen in egg albumin (Lu et al., 2003; Cogan et al., 2004). In a previous study (Clavijo et al., 2006), screening 2,850 libraries of *Salmonella* Enteritidis mutants revealed the importance of 32 genes, broadly involved in cell wall structure and nucleic acid and amino acid metabolism, for survivability of the serovar in egg albumin. Adaptation of *Salmonella* Enteritidis to egg yolk has been investigated. Passage of *Salmonella* Enteritidis in egg yolk increased intestinal colonization in a colitis mouse model, but the infection dose of the pathogen and the mode of action were not reported in the study (Moreau et al., 2016). In a recent research, the growth of *Salmonella* Enteritidis in egg yolk, in comparison with growth in a synthetic microbiological medium, increased virulence of the pathogen in mice, and a dose of only 280 CFU in yolk was sufficient to kill 50% of the mice (Xu et al., 2022). However, it is still unknown whether *Salmonella* Enteritidis strains isolated from eggs share genomic similarities or can be phylogenomically distinguishable from those isolated from other sources. It is not known whether egg-associated *Salmonella* Enteritidis strains possess important genetic traits (e.g., virulence and antimicrobial resistance) in a similar manner to strains associated with human illnesses. To reduce this knowledge gap, the current study was conducted to provide insight into phylogenetic characteristics, antimicrobial resistance, virulence, and genetic signatures of *Salmonella* Enteritidis associated with eggs.

2. Materials and methods

2.1. Selection of *Salmonella* strains

To evaluate the distinct global genomic characteristics of *Salmonella* Enteritidis, compared with other serovars isolated from food sources, a dataset consisting of 10,869 strains characterized by 9,235 core-genome multilocus sequence types was extracted from the EnteroBase database. This dataset was subsequently utilized to construct a phylogenetic tree using the rapid neighbor-joining model integrated in EnteroBase, thereby elucidating potential genetic distinctions. Additionally, to further underscore the genetic distinctiveness of *Salmonella* Enteritidis strains originated from eggs compared with those from other food sources, a subset of 1,002 strains represented by 841 core-genome multilocus sequence types was extracted from the EnteroBase database. A minimum spanning tree model, integrated in EnteroBase, was then employed to construct a phylogenetic tree.

For a focused assessment of the phylogenetic attributes, antimicrobial resistance genetic determinants, and virulence traits of *Salmonella* Enteritidis strains associated with eggs, we selected strains from the National Center for Biotechnology Information (NCBI) due to their adequate metadata and the comprehensive genomic sequence information. The selection of *Salmonella* Enteritidis strains was based on a defined set of criteria, ensuring that the strains are representative and suitable for analysis. A total of 94 *Salmonella* Enteritidis strains submitted to NCBI between 2015 and 2021 were used to represent the following two groups, egg-related and non-related groups. The quality of the selected genomes was also performed by assessing the N_{50} and coverage values of the genomes. The ranges of coverage and N_{50} for the selected genomes were 29–301x and 32 kb–4.7 Mb, respectively (Supplementary File 1). The egg-related group included 74 strains isolated from 23 whole raw liquid egg samples, 20 shell eggs, and 31 raw egg yolk samples. These were all the strains that met the selection criteria below and retrieved from the NCBI pathogen isolates database.[1] The isolates, which were (a) associated with "egg" in their "isolation source," (b) originated from different single nucleotide polymorphism (SNP) clusters, and (c) not belonging to the same outbreak, were retrieved from NCBI in November 2022. Among the selected egg-related strains, three shell egg isolates (*Salmonella* Enteritidis PT8, PT13, and ODA 99-30581-13) were sequenced in our laboratory at The Ohio State University, Columbus, United States, as described in a previous study (Xu et al., 2021). The second group was a control group (non-egg-related) integrated into the analysis to provide a comparative baseline against egg-related strains. The control group consisted of 19 clinical strains originating from human feces and one strain originating from a farm environment. These strains were selected from geographical regions that were different from those

1 https://www.ncbi.nlm.nih.gov/pathogens/isolates/

of the egg-related group, and their isolation source metadata explicitly indicated no association with eggs. Detailed information about the investigated strains is presented in Supplementary File 1.

2.2. Reference-based single nucleotide polymorphism calling and phylogeny

For SNP calling, genomes of the 94 *Salmonella* Enteritidis strains were uploaded as Fasta files into CSI Phylogeny 4.1.0 tool (available at the Center for Genomic Epidemiology; https://cge.cbs.dtu.dk/services/CSIPhylogeny/; Kaas et al., 2014) and mapped against a reference genome of *Salmonella* Enteritidis strain P125109 (accession number GCA_015240635.1). SNPs were called at default settings (minimum SNP quality of 30, and minimum map quality of 25). CSI phylogeny yields a Newick maximum likelihood phylogenetic tree inferred by FastTree 2.1.7, and the tree was visualized using the interactive Tree Of Life tool (iTOL; https://itol.embl.de/; Letunic and Bork, 2019).

2.3. Core-genome-based phylogeny

Pangenomic analysis was performed utilizing the 94 *Salmonella* Enteritidis strains in addition to the reference genome of the P125109 strain using the Roary pipeline (Page et al., 2015). The whole genomes of all strains were annotated using Prokka program, version 1.13 (Seemann, 2014), which yields annotated genomes in the GFF3 format; these genomes were used as an input for Roary that created a multi-FASTA alignment of the core genes with MAFFT (version 7.477; Katoh et al., 2002) at a minimum BLAST percentage identity of 95. The alignment was used to infer a maximum likelihood phylogeny using IQ-TREE (version 1.5.4; Nguyen et al., 2015), and the phylogenetic tree was visualized and annotated with iTOL.

2.4. Time-scaled phylogeny

The SNP-based maximum likelihood phylogenetic tree produced by CSI phylogeny tool was time-scaled and rooted by LSD2 (version 1.4.2.2.; To et al., 2016), as described previously (Carroll et al., 2021) using the default settings with modifications as follows: (i) a substation rate of 2.79×10^{-7} substitutions/site/year, a rate that corresponds to the estimate determined for *Salmonella* Typhimurium DT104 in a previous study (Leekitcharoenphon et al., 2016); (ii) tip dates corresponding to the collection year for each strain; (iii) genome sequence length of the reference strain *Salmonella* Enteritidis P125109 (4,685,848 bp); and (iv) variances of input branch lengths. The resulting time-scaled phylogenetic tree was visualized and annotated using iTOL.

2.5. Identifying antimicrobial resistance and virulence determinants

For AMR determinants, two different genome-mining analyses were applied to *Salmonella* Enteritidis genomes. First, ABRicate (version 1.0.1) in GalaxyTrakr pipeline (Gangiredla et al., 2021) was used to identify the AMR determinants in the 94 *Salmonella* Enteritidis genomes, in addition to the reference genome, *Salmonella* Enteritidis P125109, using the Resfinder database with 80% minimum DNA identity and coverage for each gene. Second, AMRFinderplus (version 3.8.28; Feldgarden et al., 2019) was used to detect AMR and stress response genes using the following settings: AMRFinderplus database (version 2020-09-30.1), *Salmonella* organism option, minimum coverage percentage of 50, and minimum identity threshold of 75. In addition, plasmid replicons, in *Salmonella* Enteritidis genomes, were screened using ABRicate (version 1.0.1) and PlasmidFinder databases with an identity and coverage percentage of 80. For virulence factor determination in the *Salmonella* Enteritidis genomes, ABRicate (version 1.0.1) was implemented against the Virulence Factor Database (VFDB) with a minimum coverage and identity percentage of 80. The presence or absence of AMR and virulence genes were represented as heatmaps using GraphPad Prism software (version 9.4.1; GraphPad Software, San Diego, CA, United States).

3. Results

3.1. Global genomic diversity of *Salmonella enterica* isolated from food

To gain a global overview of the genetic diversity of *S. enterica* isolated from food, we investigated the population structure and genomic diversity of non-typhoidal *S. enterica* isolated from "food" as a "source niche" according to the EnteroBase database. A neighbor-joining phylogenetic tree (Figure 1) was constructed based on cgMLST and allelic differences; this tree comprised 10,869 strains belonging to 9,235 sequence types (STs) of more than 30 *Salmonella* serovars. The *S. enterica* strains, included in this analysis, were geographically dispersed and originated from more than 30 countries located in Europe, North America, South America, Asia, Africa, and Oceania. Food-associated *S. enterica* strains formed separate clusters when based on the serovar. It was obvious that "Enteritidis," "Heidelberg," and "Typhimurium" were the most common serovars in food, each of which formed a distinct lineage in this cgMLST-based phylogenetic tree (Figure 1). The emphasis in this manuscript will be on serovar "Enteritidis" strains from food. By analyzing 1,002 *Salmonella* Enteritidis strains belonging to 841 STs and isolated from more than 20 food sources, the strains were grouped into different lineages (Figure 2), among which one single lineage contained all strains isolated from eggs or egg products (Figure 2, red-colored clusters). This observation indicates relatively small genomic diversity within the egg-related strains. Nevertheless, the egg-related group clustered closely with the poultry-associated strains and distantly from the beef-associated strains (Figure 2).

3.2. Phylogenetic relationships within egg-associated *Salmonella* Enteritidis

A maximum likelihood phylogenetic tree (Figure 3) was constructed based on 2,164 SNPs detected in the core genome regions of 94 *Salmonella* Enteritidis strains (74 from eggs, 19 from human feces, and one from farm environment for comparison) against

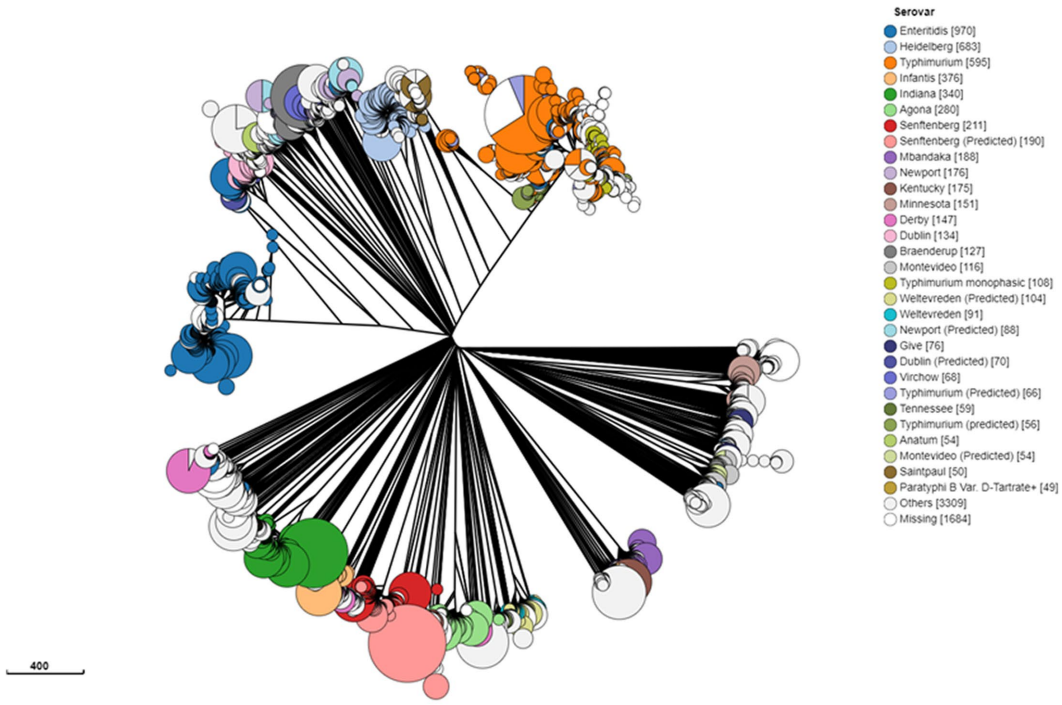

FIGURE 1
Genomic diversity of *Salmonella enterica* isolated from food worldwide, as determined by a neighbor-joining tree of 10,869 strains of 9,235 core-genome multilocus sequence types, according to EnteroBase. Each node represents a unique sequence type, and the size of each node corresponds to the number of strains within that node. *Salmonella* strains are color-coded by serovar, and the number of isolates is presented between brackets. The scale bar indicates 400 core-genome multilocus sequence-type alleles.

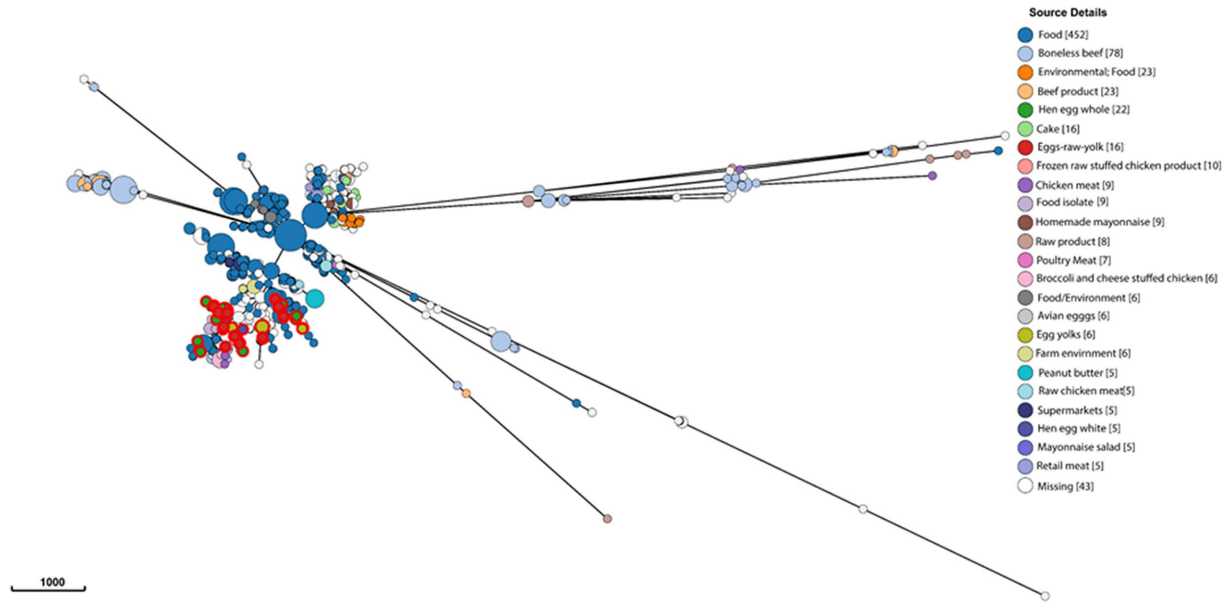

FIGURE 2
Genomic diversity of *Salmonella* Enteritidis isolated from food, according to the EnteroBase database, and determined by the minimum spanning tree of 1,002 strains of 841 core-genome multilocus sequence types. Each node represents a unique sequence type, and the node size corresponds to the number of *Salmonella* Enteritidis strains within that node. *Salmonella* strains are color-coded by EnteroBase-defined isolation source details (the number of isolates is presented between brackets), and the scale bar indicates 1,000 core-genome multilocus sequence type alleles. Reference to "food" in the legend indicates that the food types were not specified in the EnteroBase.

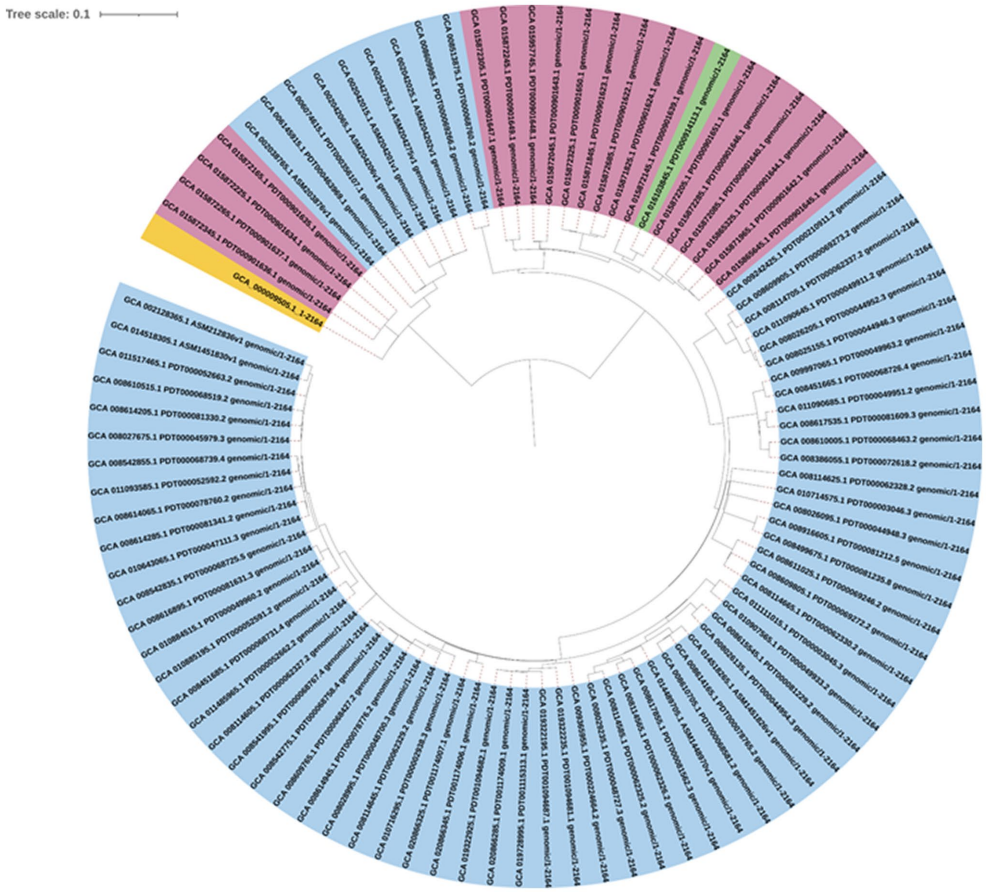

FIGURE 3
Maximum likelihood phylogeny constructed based on core single nucleotide polymorphism (SNPs; $n = 2{,}164$) among 94 *Salmonella* Enteritidis genomes. The strains were color-shaded according to their source as follows: eggs (blue), pink (human feces), green (farm environment), and yellow (reference genome of *Salmonella* Enteritidis P125109). Core SNPs were determined by CSI Phylogeny v.4.1.0, whereas the phylogenetic tree was inferred using FastTree v.2.1.7. The scale bar denotes substitutions per site.

Salmonella Enteritidis P125109 reference strain. Pairwise comparisons between strains showed a range of SNPs varying from 2 to 542. The SNP-based phylogeny demonstrated that most of the egg-associated strains formed a distinct sublineage from the human-associated strains (Figure 3). These findings were confirmed by constructing a phylogeny (Figure 4A), based on the core genome sequences, in all 94 Enteritidis strains, in addition to the reference P125109 strain. The phylogenetic tree comprised two major clades, and the egg-associated strains formed unique sublineages separated from the human and farm-associated strains (Figure 4A).

A time-scaled phylogeny was built to infer the possible timing of the emergence of the egg-associated *Salmonella* Enteritidis (Figure 4B). The SNP-based time-scaled phylogenetic tree demonstrated the presence of two major clades containing the egg-related strains. A small clade "Clade I" contained a sublineage of seven egg-associated strains that shared a common most recent ancestor dated to approximately 1,920 as determined by the LSD v.2.0.0 tool. The large clade "Clade II" encompassed most egg-associated strains, which formed a distinct sublineage that shared a common most recent ancestor dated approximately to 1,516. Additionally, these findings illustrate the genetic distinctiveness of egg-associated *Salmonella* Enteritidis since most of these strains were clustered in Clade II. Genetic distinction of egg-associated *Salmonella* Enteritidis would become more apparent when more genome sequences from eggs become available in public databases.

3.3. Antibiotic resistance and virulence determinants in *Salmonella* Enteritidis from eggs

Two genome mining approaches, Resfinder and AMRFinderplus, identified AMR determinants in the genomes of egg-associated *Salmonella* Enteritidis while selected human-associated strains ($n = 19$) were used for comparison. AMR results from Resfinder showed that egg-associated *Salmonella* Enteritidis showcased two AMR genes, *aac(6′)-Iaa* and *mdsAB* (Figure 5A), which confer resistance to aminoglycosides and other antibiotics (e.g., chloramphenicol, cephalosporin, and monobactam). These AMR genes were also conserved in the investigated human-related strains. Exceptionally, the egg isolate *Salmonella* Enteritidis PT13 (GCA_014518265.1) harbored genes conferring resistance to aminoglycosides (*aph(3″)-Ib* and *aph(6)-Id*), beta lactams (*blaTEM-1b*), sulfonamide (*sul2*), and tetracycline (*tetA*). With

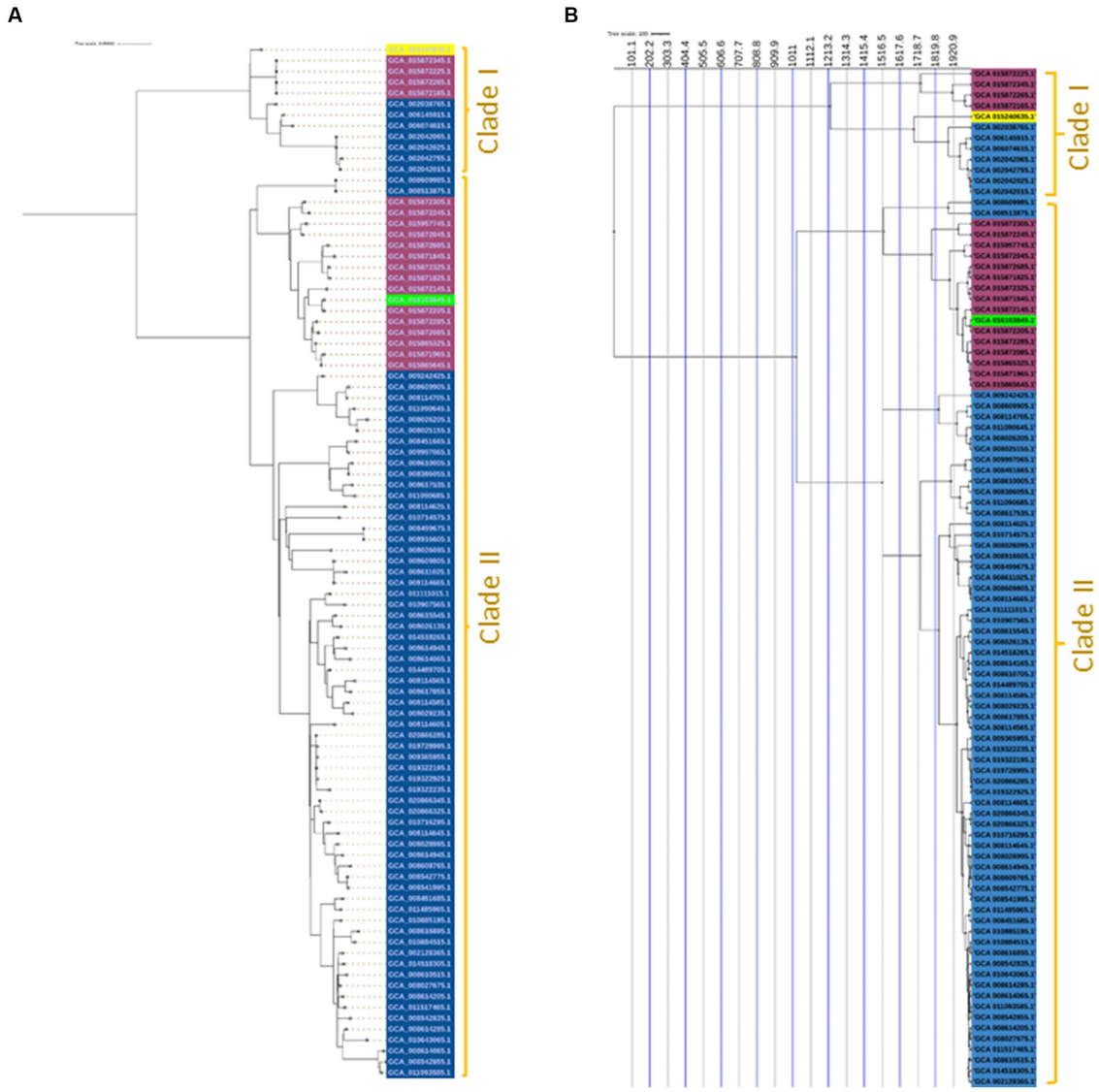

FIGURE 4
Core-genome and time-scaled phylogeny of *Salmonella* Enteritidis from eggs. **(A)** Maximum likelihood phylogeny of 94 *Salmonella* Enteritidis strains, constructed using the core-genes sequence alignment determined by the Roary pipeline and inferred by IQ-TREE v.1.5.4; **(B)** Time-scaled maximum likelihood phylogeny constructed using core SNPs identified among the 94 *Salmonella* Enteritidis strains; the phylogeny was rooted and scaled using LSD2 with scale bar reported in years. The strains were color-shaded according to their source as follows: eggs (blue), pink (human feces), green (farm environment), and yellow (reference genome of *Salmonella* Enteritidis P125109).

AMRFinderplus analysis, the results (Figure 5B) revealed the presence of a colonization factor (*sinH*), and some stress response genes (*golS* and *golT*) that confer resistance to metal ions (i.e., gold and copper). These genes were similarly found in egg- and human-related strains. Moreover, two *gyrA* mutations (D87Y and S83F) were found in a few *Salmonella* Enteritidis strains isolated from eggs and human feces, and these gene mutations mediate quinolone resistance.

Genomic screening was conducted for plasmid replicons known to harbor antibiotic-resistant genes in *Salmonella* genomes. Out of eight different plasmid replicons identified in *Salmonella* Enteritidis genomes, IncFIB(S)_1 and IncFII(S)_1 were detected in 86 genomes (Supplementary File 2). The plasmid replicons IncN_1, Col156_1, ColRNAI_1, and ColpVC_1 were detected in 2–3 genomes while IncX1_1 and IncX4_2 were found in 10–11 genomes. Most of the egg-associated *Salmonella* Enteritidis genomes harbored IncFIB(S)_1 and IncFII(S)_1, and 9–10 of the genomes harbored IncX1_1 and IncX4_2 plasmid replicons (Supplementary File 2). The presence of such plasmid replicons indicates a potential antibiotic resistance capability of egg-associated *Salmonella* Enteritidis.

Profiling of virulence genes using the ABRicate tool against the virulence factor database revealed that the egg-associated *Salmonella* Enteritidis possessed 103–113 virulence factors in their genomes, mainly encoded on the *Salmonella* pathogenicity islands (SPIs), such as SPI-1, SPI-2, SPI-3, SPI-4, and SPI-5; these SPIs are indispensable for disease onset in the host. Comparably, the human-associated strains harbored 112 virulence genes (Figure 6). These results augment the notion that egg-associated *Salmonella* Enteritidis strains possess

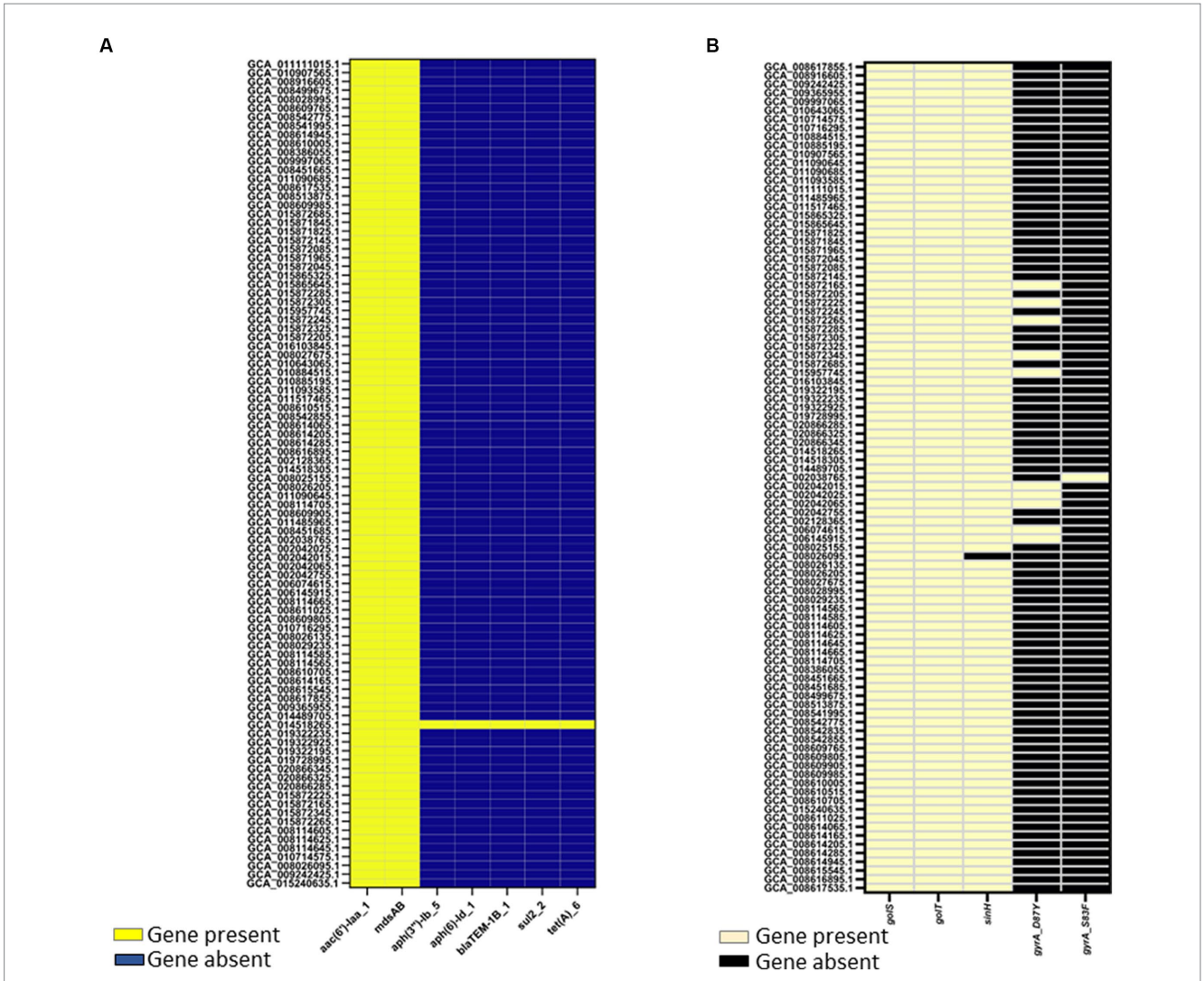

FIGURE 5
Antimicrobial resistance (AMR) determinants identified in 94 *Salmonella* Enteritidis strains including the 74 strains from eggs. AMR determinants were identified as "present" using ABRicate with the Resfinder database **(A)** at a minimum 80% identity and coverage, or **(B)** AMRFinderplus v.3.8.28 with the AMRFinderplus database at a minimum threshold of 50 and 75% for coverage and identity, respectively. Genes present in *Salmonella* Enteritidis genomes were colored "yellow" in the heatmap illustrations.

putative AMR determinants and the essential virulence factors required for causing human diseases.

3.4. Pangenomic analysis highlighted genetic features in *Salmonella* Enteritidis from eggs

The annotated genomes obtained with the Prokka tool were used as an input for the Roary pipeline to infer the pangenome, which is the entire set of genes within the investigated *Salmonella* Enteritidis strains. The pangenome results produced a gene presence/absence matrix by comparing the presence of 6,148 genes with the 94 *Salmonella* Enteritidis genomes (74 for the egg-, 19 for the human-, and one for the farm-associated strains), in addition to the reference *Salmonella* Enteritidis P125109 genome. Our findings (Table 1) showed that two genes (*oadA2* and *oadB2*), involved in sodium ion transport and anaerobic growth, were identified in 30 genomes of the egg-associated strains but were absent in the human-associated group. Additional genes (Table 1) involved in cellular processes, such as DNA-dependent transcription, DNA repair, and conjugal transfer, were identified only in 12–13 of the egg-associated *Salmonella* Enteritidis group but were absent in the human-associated group.

4. Discussion

Salmonella Enteritidis is the main *S. enterica* serovar that causes frequent disease outbreaks linked to food, particularly eggs and other poultry products (Rodrigue et al., 1990). The historical dilemma of *Salmonella* Enteritidis–egg association remains unresolved, and understanding the biological mechanisms behind the serovar fitness in such a food matrix is still insufficiently explored. It is unknown whether *Salmonella* Enteritidis strains associated with eggs are genetically identical. Analysis of the global lineages of non-typhoidal *Salmonella* isolated from food (Figure 1) suggests that *Salmonella* Enteritidis is genetically different from the rest of the serovars, and the genomes of the serovar formed a unique cluster. The analysis also

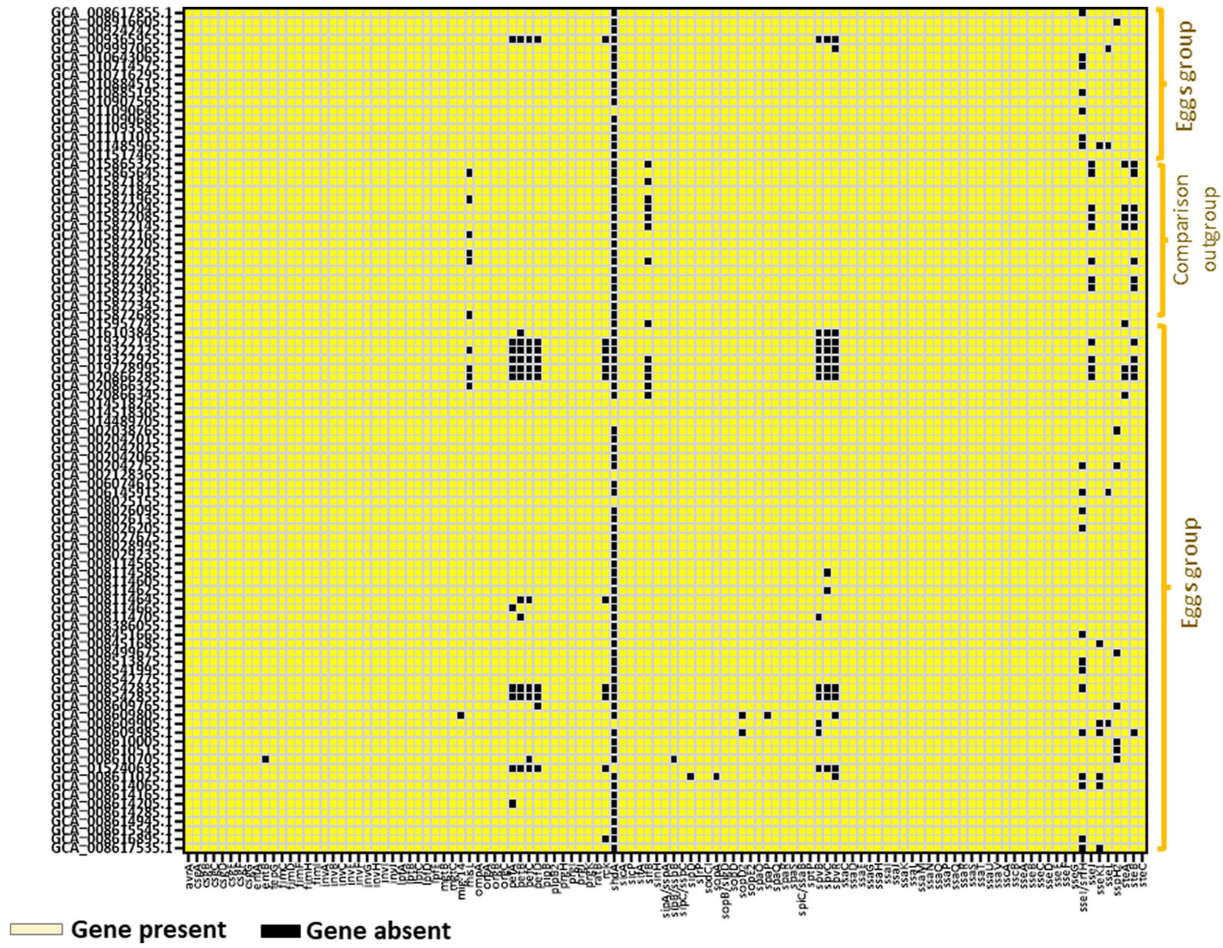

FIGURE 6
Virulence gene profiling in 94 *Salmonella* Enteritidis strains including the 74 strains from eggs. Up to 113 virulence determinants were identified as "present" using ABRicate with the Virulence Factor database at a minimum of 80% identity and coverage. Virulence genes reported as "present" were colored "yellow" in the heatmap illustration.

showed that *Salmonella* Enteritidis strains from eggs and poultry are closely related genomically (Figure 2), and both are relatively different from the beef-related strains of that serovar. This obvious genetic relatedness emphasizes the importance of the *Salmonella* Enteritidis vertical transmission route, i.e., from breeding chicken to hatching eggs (Gantois et al., 2009). According to a recent study, poultry breeding stocks drove the dispersal of *Salmonella* Enteritidis globally, and that hatching eggs were the key driver for the global spread of this pathogen (Li et al., 2021). The latter study provided evidence that the intercontinental spread of *Salmonella* Enteritidis arose from centralized origins because the global lineages of this pathogen were similar to the strains that were isolated originally from poultry products in the United States and Europe, where the first industrialized poultry production appeared. Moreover, surveys conducted in the United States in 1991 highlighted the presence of *Salmonella* on eggshells from breeder hatcheries (Cox et al., 1991). Together, these findings explain the genomic similarity between *Salmonella* Enteritidis strains from eggs and poultry sources. Intriguingly, *Salmonella* Enteritidis strains from eggs were genetically distinct from those isolated from beef, indicating that beef is an unlikely transmission vehicle of this serovar to eggs.

In the current study, the egg-associated *Salmonella* Enteritidis strains found in the NCBI database (as of November 2022) were included in our analyses. Most of these strains were isolated in the United States; this coincides with the fact that the United States was one of the earliest exporters of chicken breeding stocks to the world (Li et al., 2021). Our SNP- and core-genome-based phylogeny demonstrated that *Salmonella* Enteritidis strains from eggs displayed limited intra-genomic diversity, and these strains were closely related phylogenetically, indicating that they may have a common ancestor. The time-scaled phylogeny constructed in the current study (Figure 4) suggests that the egg-related strains may have naturally evolved from a common ancestor. Comparably, a recent study found that *Salmonella* Enteritidis ST11 lineage from Africa shared a common ancestor dated to 1,551–1,801 (Carroll et al., 2021).

Our findings showcased *Salmonella* Enteritidis strains from eggs to be a reservoir of antibiotic resistance genes, mainly *aac(6′)-Iaa* and *mdsAB*, which encode aminoglycoside acetyl transferase and efflux pump complex, respectively; these genetic traits confer resistance to aminoglycosides and other antibiotics (Alcaine et al., 2007; Song et al., 2014; Nair et al., 2018). The identification of such antibiotic-resistant determinants (Figure 5), in addition to several

TABLE 1 Proteins and corresponding genes uniquely found in genomes of *Salmonella enterica* serovar Enteritidis from eggs.

Protein (corresponding gene)	Number of genomes** of eggs-associated strains	Biological process
Oxaloacetate decarboxylase alpha chain (*oadA2*)*	30	Sodium transport/Biotin binding (Translocase)
Oxaloacetate decarboxylase beta chain (*oadB2*)*	30	Sodium transport (Translocase)
Hypothetical proteins	12–14	Unknown
Heme exporter protein C (*ccmC*)	13	Cytochrome complex assembly
Tyrosine recombinase XerC (*xerC*)	13	Cell cycle, cell division, DNA integration, and DNA recombination
Putative transposon Tn552 DNA-invertase bin3 (*bin3*)	12	DNA integration, DNA Recombination
mRNA interferase toxin RelE (*relE*)	12	Toxin-antitoxin system
Transcription antitermination protein RfaH (*rfaH*)	12	Transcription/Transcription regulation
Type IV secretion system protein VirB4 (*virB4*)	12	Conjugal transfer ATPase
Type IV secretion system protein VirB9 (*virB9*)	12	Conjugative transfer
Protein VirD4 (*virD4*)	12	Conjugal transfer
Type IV secretion system protein VirB11 (*virB11*)	12	Conjugal transfer
mRNA interferase HigB (*higB*)	12	Regulation of DNA-dependent transcription, and regulation mRNA stability
Antitoxin HigA (*higA*)	12	Regulation of DNA-dependent transcription
Protein TraL (*traL*)	12	Pilus assembly
Cytochrome c-type biogenesis protein CcmE (*ccmE*)	12	Cytochrome complex assembly
Elongation factor Tu 1 (*tuf1*)	12	Translational elongation, response to antibiotics
DNA topoisomerase 3 (*topB2*)	12	DNA topological change

*Anaerobic growth; **Data represent the number of eggs-associated *Salmonella* Enteritidis genomes positive for a given protein that was absent in human-associated strains of the serovar. The term "genome" refers to chromosomal DNA and does not include plasmid DNA.

plasmid replicons (Supplementary File 2), including IncFIB(S)_1, IncFII(S)_1, IncX1_1, and IncX4_1, which have been associated with harboring antibiotic resistance genes (van den Berg et al., 2019; Hull et al., 2022), suggests that the egg-associated *Salmonella* Enteritidis could harbor and possibly disseminate antibiotic resistance genes via plasmid-mediated gene transfer. Antibiotic resistance among *Salmonella* Enteritidis strains from eggs can be explained by the intense use of antibiotics during poultry production (Sapkota et al., 2014). This is consistent with a previous study, which concluded that the prevalence of antibiotic-resistant *Salmonella* was reduced when a conventional farm was converted to organic farming (Sapkota et al., 2014). In addition to that assumption, antibiotic resistance genes can spread among *Salmonella* Enteritidis strains via horizontal transfer of antibiotic-resistant plasmids or chromosomal acquisition of transposons that carry antibiotic-resistant genes (Domingues et al., 2012). The prevalence of *golS* and *golT* in *Salmonella* Enteritidis genomes from eggs highlights the strains' ability to confer metal ion resistance; the two genes were also implicated in regulating antibiotic resistance efflux pumps (Pontel et al., 2007). These findings alert the egg industry sector to revise the egg/poultry production regimes to reduce the spread of antibiotic resistance among associated pathogens such as *Salmonella* Enteritidis. Our genome (Chromosomal DNA) mining analysis also uncovered a comprehensive virulence machinery in *Salmonella* Enteritidis strains from eggs, which implies the capability of these strains to infect humans and cause diseases.

From a pathogen–food adaptive perspective, the pangenome analysis revealed the abundance of *oadA* and *oadB* and other genes (e.g., *xerC* and *higB*; Table 1) in egg-associated *Salmonella* Enteritidis. These genes enhance the capacity of *Salmonella* to grow anaerobically (similar to the eggshell environment) and in assisting nucleic acid-related processes such as DNA repair in response to damage encountered in environments such as egg white (Woehlke and Dimroth, 1994; Huang et al., 2019). These hypotheses have been overlooked and are now worth further investigation.

5. Conclusion

Salmonella Enteritidis is a predominant causative agent of egg-associated foodborne disease outbreaks and leads to a multitude of human illnesses and economic losses. This study utilized comparative genomic analysis for an understanding of the phylogenomic links, genomically encoded virulence and antimicrobial resistance traits, and genomic landscape of *Salmonella* Enteritidis strains that were historically associated with disease outbreaks in eggs or egg products. The genetic homology within the egg-associated *Salmonella* Enteritidis indicates a possible common ancestry origin for the circulating strains in egg products, presumably due to the trading of poultry breeding stocks. A whole genome-based comparison gave a glimpse of the virulence aspect of *Salmonella* Enteritidis associated with poultry eggs, and such assessment confirmed the need for advancing the anti-*Salmonella* intervention strategies, starting at the poultry production chain. Further investigations utilizing genome-wide association studies could underpin specific genetic targets characteristics of *Salmonella* Enteritidis associated with eggs.

Data availability statement

The datasets presented in this study can be found in online repositories. The names of the repository/repositories and accession number(s) can be found in the article/Supplementary material.

Author contributions

AA: Conceptualization, Data curation, Formal analysis, Investigation, Methodology, Writing – original draft, Writing – review & editing. AY: Conceptualization, Funding acquisition, Project administration, Supervision, Writing – review & editing.

Funding

The author(s) declare financial support was received for the research, authorship, and/or publication of this article. This study is supported by the USDA National Institute of Food and Agriculture, AFRI project 2020-67017-30794.

Conflict of interest

The authors declare that the research was conducted in the absence of any commercial or financial relationships that could be construed as a potential conflict of interest.

Publisher's note

Supplementary material

The Supplementary material for this article can be found online at: https://www.frontiersin.org/articles/10.3389/fmicb.2023.1278821/full#supplementary-material

References

Alcaine, S. D., Warnick, L. D., and Wiedmann, M. (2007). Antimicrobial resistance in nontyphoidal *Salmonella*. *J. Food Prot.* 70, 780–790. doi: 10.4315/0362-028X-70.3.780

Cardoso, M. J., Nicolau, A. I., Borda, D., Nielsen, L., Maia, R. L., Møretrø, T., et al. (2021). *Salmonella* in eggs: from shopping to consumption—a review providing an evidence-based analysis of risk factors. *Compr. Rev. Food Sci. Food Saf.* 20, 2716–2741. doi: 10.1111/1541-4337.12753

Carroll, L. M., Pierneef, R., Mathole, M., and Matle, I. (2021). Genomic characterization of endemic and ecdemic non-typhoidal *Salmonella enterica* lineages circulating among animals and animal products in South Africa. *Front. Microbiol.* 12:748611. doi: 10.3389/fmicb.2021.748611

Clavijo, R. I., Loui, C., Andersen, G. L., Riley, L. W., and Lu, S. (2006). Identification of genes associated with survival of *Salmonella enterica* Serovar Enteritidis in chicken egg albumen. *Appl. Environ. Microbiol.* 72, 1055–1064. doi: 10.1128/AEM.72.2.1055-1064.2006

Cogan, T. A., Jørgensen, F., Lappin-Scott, H. M., Benson, C. E., Woodward, M. J., and Humphrey, T. J. (2004). Flagella and curli fimbriae are important for the growth of *Salmonella enterica* serovars in hen eggs. *Microbiology* 150, 1063–1071. doi: 10.1099/MIC.0.26791-0

Cox, N. A., Bailey, J. S., Mauldin, J. M., Blankenship, L. C., and Wilson, J. L. (1991). Extent of *salmonellae* contamination in breeder hatcheries. *Poult. Sci.* 70, 416–418. doi: 10.3382/PS.0700416

Dewey-Mattia, D., Manikonda, K., Hall, A. J., Wise, M. E., and Crowe, S. J. (2018). Surveillance for foodborne disease outbreaks—United States, 2009–2015. *MMWR Surveill. Summ.* 67, 1–11. doi: 10.15585/mmwr.ss6710a1

Domingues, S., da Silva, G. J., and Nielsen, K. M. (2012). Integrons: vehicles and pathways for horizontal dissemination in bacteria. *Mob. Genet. Elem.* 2, 211–223. doi: 10.4161/MGE.22967

EFSA and ECDC (2019). The European Union one health 2018 zoonoses report. *EFSA J.* 17:e05926. doi: 10.2903/j.efsa.2019.5926

EFSA and ECDC (2022). The European Union one health 2021 zoonoses report. *EFSA J.* 20:e07666. doi: 10.2903/j.efsa.2022.7666

Feldgarden, M., Brover, V., Haft, D. H., Prasad, A. B., Slotta, D. J., Tolstoy, I., et al. (2019). Validating the AMRFINder tool and resistance gene database by using antimicrobial resistance genotype-phenotype correlations in a collection of isolates. *Antimicrob. Agents Chemother.* 63, e00483–19. doi: 10.1128/AAC.00483-19/SUPPL_FILE/AAC.00483-19-S0004.XLSX

Ferrari, R. G., Rosario, D. K. A., Cunha-Neto, A., Mano, S. B., Figueiredo, E. E. S., and Conte-Juniora, C. A. (2019). Worldwide epidemiology of *Salmonella* serovars in animal-based foods: a meta-analysis. *Appl. Environ. Microbiol.* 85:e00591. doi: 10.1128/AEM.00591-19

Gangiredla, J., Rand, H., Benisatto, D., Payne, J., Strittmatter, C., Sanders, J., et al. (2021). GalaxyTrakr: a distributed analysis tool for public health whole genome sequence data accessible to non-bioinformaticians. *BMC Genomics* 22, 1–11. doi: 10.1186/S12864-021-07405-8/TABLES/2

Gantois, I., Ducatelle, R., Pasmans, F., Haesebrouck, F., Gast, R., Humphrey, T. J., et al. (2009). Mechanisms of egg contamination by *Salmonella Enteritidis*. *FEMS Microbiol. Rev.* 33, 718–738. doi: 10.1111/j.1574-6976.2008.00161.x

Healy, J., and Bruce, B. (2019). "Salmonellosis (Nontyphoidal)" in Chapter 4—CDC yellow book travel health 2019. Available at https://wwwnc.cdc.gov/travel/yellowbook/2020/travel-related-infectious-diseases/salmonellosis-nontyphoidal (Accessed November 9, 2022).

Huang, X., Zhou, X., Jia, B., Li, N., Jia, J., He, M., et al. (2019). Transcriptional sequencing uncovers survival mechanisms of *Salmonella enterica* serovar Enteritidis in antibacterial egg white. *mSphere* 4, e00700–e00718. doi: 10.1128/mSphere.00700-18

Hull, D. M., Harrell, E., Harden, L., and Thakur, S. (2022). Multidrug resistance and virulence genes carried by mobile genomic elements in *Salmonella enterica* isolated from live food animals, processed, and retail meat in North Carolina, 2018–2019. *Int. J. Food Microbiol.* 378:109821. doi: 10.1016/j.ijfoodmicro.2022.109821

Kaas, R. S., Leekitcharoenphon, P., Aarestrup, F. M., and Lund, O. (2014). Solving the problem of comparing whole bacterial genomes across different sequencing platforms. *PLoS One* 9:e104984. doi: 10.1371/JOURNAL.PONE.0104984

Katoh, K., Misawa, K., Kuma, K. I., and Miyata, T. (2002). MAFFT: a novel method for rapid multiple sequence alignment based on fast Fourier transform. *Nucleic Acids Res.* 30, 3059–3066. doi: 10.1093/NAR/GKF436

Leekitcharoenphon, P., Hendriksen, R. S., Le Hello, S., Weill, F. X., Baggesen, D. L., Jun, S. R., et al. (2016). Global genomic epidemiology of *Salmonella enterica* serovar typhimurium DT104. *Appl. Environ. Microbiol.* 82, 2516–2526. doi: 10.1128/AEM.03821-15

Letunic, I., and Bork, P. (2019). Interactive tree of life (iTOL) v4: recent updates and new developments. *Nucleic Acids Res.* 47, W256–W259. doi: 10.1093/NAR/GKZ239

Li, S., He, Y., Mann, D. A., and Deng, X. (2021). Global spread of *Salmonella Enteritidis* via centralized sourcing and international trade of poultry breeding stocks. *Nat. Commun.* 12:5109. doi: 10.1038/s41467-021-25319-7

Lu, S., Killoran, P. B., and Riley, L. W. (2003). Association of *Salmonella enterica* Serovar Enteritidis YafD with resistance to chicken egg albumen. *Infect. Immun.* 71, 6734–6741. doi: 10.1128/IAI.71.12.6734-6741.2003

Moreau, M. R., Wijetunge, D. S. S., Bailey, M. L., Gongati, S. R., Goodfield, L. L., Hewage, E. M. K. K., et al. (2016). Growth in egg yolk enhances *Salmonella Enteritidis* colonization and virulence in a mouse model of human colitis. *PLoS One* 11:e0150258. doi: 10.1371/journal.pone.0150258

Nair, D. V. T., Venkitanarayanan, K., and Johny, A. K. (2018). Antibiotic-resistant *Salmonella* in the food supply and the potential role of antibiotic alternatives for control. *Foods* 7:167. doi: 10.3390/FOODS7100167

Nguyen, L. T., Schmidt, H. A., Von Haeseler, A., and Minh, B. Q. (2015). IQ-TREE: a fast and effective stochastic algorithm for estimating maximum-likelihood phylogenies. *Mol. Biol. Evol.* 32, 268–274. doi: 10.1093/MOLBEV/MSU300

Page, A. J., Cummins, C. A., Hunt, M., Wong, V. K., Reuter, S., Holden, M. T. G., et al. (2015). Roary: rapid large-scale prokaryote pan genome analysis. *Bioinformatics* 31, 3691–3693. doi: 10.1093/BIOINFORMATICS/BTV421

Pontel, L. B., Audero, M. E. P., Espariz, M., Checa, S. K., and Soncini, F. C. (2007). GolS controls the response to gold by the hierarchical induction of *Salmonella*-specific genes that include a CBA efflux-coding operon. *Mol. Microbiol.* 66, 814–825. doi: 10.1111/J.1365-2958.2007.05963.X

Rodrigue, D. C., Tauxe, R. V., and Rowe, B. (1990). International increase in *Salmonella Enteritidis*: a new pandemic? *Epidemiol. Infect.* 105, 21–27. doi: 10.1017/S0950268800047609

Sapkota, A. R., Kinney, E. L., George, A., Hulet, R. M., Cruz-Cano, R., Schwab, K. J., et al. (2014). Lower prevalence of antibiotic-resistant *Salmonella* on large-scale U.S. conventional poultry farms that transitioned to organic practices. *Sci. Total Environ.* 476-477, 387–392. doi: 10.1016/J.SCITOTENV.2013.12.005

Seemann, T. (2014). Prokka: rapid prokaryotic genome annotation. *Bioinformatics* 30, 2068–2069. doi: 10.1093/BIOINFORMATICS/BTU153

Shah, D. H., Zhou, X., Kim, H. Y., Call, D. R., and Guard, J. (2012). Transposon mutagenesis of *Salmonella enterica* serovar Enteritidis identifies genes that contribute to invasiveness in human and chicken cells and survival in egg albumen. *Infect. Immun.* 80, 4203–4215. doi: 10.1128/IAI.00790-12

Song, S., Hwang, S., Lee, S., Ha, N. C., and Lee, K. (2014). Interaction mediated by the putative tip regions of Mdsa and Mdsc in the formation of a *Salmonella*-specific tripartite efflux pump. *PLoS One* 9:e100881. doi: 10.1371/JOURNAL.PONE.0100881

To, T. H., Jung, M., Lycett, S., and Gascuel, O. (2016). Fast dating using least-squares criteria and algorithms. *Syst. Biol.* 65, 82–97. doi: 10.1093/SYSBIO/SYV068

USDA (2019). Cost estimates of foodborne illnesses. Avialable at: https://www.ers.usda.gov/data-products/cost-estimates-of-foodborne-illnesses/cost-estimates-of-foodborne-illnesses/#Pathogen (Accessed November 9, 2022).

van den Berg, R. R., Dissel, S., Rapallini, M. L., van Der Weijden, C. C., Wit, B., and Heymans, R. (2019). Characterization and whole genome sequencing of closely related multidrug-resistant *Salmonella enterica* serovar Heidelberg isolates from imported poultry meat in the Netherlands. *PLoS One* 14:e0219795. doi: 10.1371/journal.pone.0219795

Woehlke, G., and Dimroth, P. (1994). Anaerobic growth of *Salmonella Typhimurium* on l L(+)- and D(−)-tartrate involves an oxaloacetate decarboxylase Na^+ pump. *Arch. Microbiol.* 162, 233–237. doi: 10.1007/BF00301843

Xu, Y., Abdelhamid, A. G., Sabag-Daigle, A., Sovic, M. G., Ahmer, B. M. M., and Yousef, A. E. (2022). The role of egg yolk in modulating the virulence of *Salmonella enterica* serovar Enteritidis. *Front. Cell. Infect. Microbiol.* 12:572. doi: 10.3389/fcimb.2022.903979

Xu, Y., Abdelhamid, A. G., and Yousef, A. E. (2021). Draft genome sequence of *Salmonella enterica* subsp. *enterica* serovar Enteritidis ODA 99-30581-13, a heat-resistant strain isolated from shell eggs. *Microbiol. Resour. Announc.* 10, e01461–20. doi: 10.1128/MRA.01461-20

frontiers | Frontiers in Microbiology

TYPE Original Research
PUBLISHED 22 December 2023
DOI 10.3389/fmicb.2023.1274245

OPEN ACCESS

EDITED BY
Xunde Li,
University of California, Davis, United States

REVIEWED BY
Ben Pascoe,
University of Oxford, United Kingdom
Mónica Oleastro,
National Health Institute Doutor Ricardo Jorge (INSA), Portugal

*CORRESPONDENCE
Seongbeom Cho
✉ chose@snu.ac.kr

RECEIVED 08 August 2023
ACCEPTED 05 December 2023
PUBLISHED 22 December 2023

CITATION
An J-U, Lee S, Guk J-H, Woo J, Song H and Cho S (2023) Circular intermediate-mediated horizontal transfer of the chromosome-encoded *cfr(C)* gene in multi-drug resistant *Campylobacter coli* from swine sources. *Front. Microbiol.* 14:1274245. doi: 10.3389/fmicb.2023.1274245

Circular intermediate-mediated horizontal transfer of the chromosome-encoded *cfr(C)* gene in multi-drug resistant *Campylobacter coli* from swine sources

Jae-Uk An, Soomin Lee, Jae-Ho Guk, Jungha Woo, Hyokeun Song and Seongbeom Cho*

College of Veterinary Medicine and Research Institute for Veterinary Science, Seoul National University, Seoul, Republic of Korea

Campylobacter is a major zoonotic pathogen that causes gastrointestinal and, rarely, immune diseases in humans. The antimicrobial-resistance gene *cfr(C)* carried by *Campylobacter* and is a *cfr*-like gene that targets bacterial 23S rRNA through A2503 methylation. *cfr(C)* confers cross-resistance to five antimicrobial classes ($PhLOPS_A$), including lincosamide, streptogramin A, and pleuromutilin, which are classified as critically important antimicrobials to human by the World Health Organization. To elucidate the genetic variation and horizontal transfer mechanism of *cfr(C)*, we analyzed the genetic background and horizontal transfer unit of *Campylobacter*-derived *cfr(C)* through comparative genomic analysis. We identified nine *cfr(C)*-positive *C. coli* strains of 157 strains isolated from swine sources. Three novel *cfr(C)* gene single nucleotide polymorphism (SNP) sites (19delA, 674C > A, and 890 T > C) were identified from nine *cfr(C)*-positive strains. Among six identified *cfr(C)* SNP variant types (SNP-I to -VI), five types of randomly inserted *cfr(C)*-cassettes on chromosome and one type of plasmid-like element were identified, their gene cassette composition differing depending on the *cfr(C)* variants. Three of six *cfr(C)* cassette types contained aminoglycoside-streptothricin resistance cluster "*aphA3-sat4-aadE*." The *cfr(C)* gene cassette with *pcp* gene (GC-1, GC-4, and GC-5) formed a *pcp*-mediated circular intermediate "*pcp*-hp-*cfr(C)-aphA3*," which has not been previously reported. Other two *cfr(C)* cassette-types with ISChh1 formed circular intermediate "ISChh1-*aphA3-cfr(C)-lnu (G)-pnp-ant1*-hp-ATPase" and "ISChh1-*aphA3-cfr(C)*-hp." In conjugation assay, the *pcp*-mediated circular intermediate was naturally transferred to the plasmid of recipient *C. coli* wild-type strain from swine source, and comparative genomic analysis revealed that *cfr(C)* encoded in *pcp*-mediated circular intermediate was inserted into the plasmid of recipient by homologous recombination with *pcp* and *aphA3*. This study revealed that novel multidrug resistance gene *cfr(C)* carried by *C. coli* from swine sources can be highly genetically diverse and transferable. Moreover, we suggest that the transferability of chromosomal *cfr(C)* may contribute to the global spread of multidrug resistance against clinically important antimicrobials.

KEYWORDS

***Campylobacter coli*, chromosome-encoded, circular intermediate, horizontal transfer, whole genome sequencing**

1 Introduction

Campylobacter species, particularly *C. jejuni* and *C. coli*, are leading zoonotic foodborne pathogen that can cause gastrointestinal infections (such as diarrhea) and immune diseases (such as Guillain-Barré syndrome) in humans (Silva et al., 2011). Unlike in humans, *Campylobacter* causes mostly asymptomatic infections in food-animals, including poultry, cattle, and pigs, and is considered a commensal bacterium (Burnham and Hendrixson, 2018). According to the World Health Organization (WHO), the major route of human campylobacteriosis is via the food-chain of animal products (such as meat and milk) which are contaminated with *Campylobacter*, present in animal feces, during the slaughter process (Jaakkonen et al., 2020).

Since 2013, the US Centers for Disease Control and Prevention has classified drug-resistant *Campylobacter* as a serious antibiotic resistance threat (CDC, 2013). In recent years, *Campylobacter* has become increasingly resistant to clinically important antimicrobials and has developed multiple mechanisms of antimicrobial resistance. These include mutations in target genes, such as 23S rRNA mutations that confer resistance to macrolides and, *gyrA* mutations associated with fluoroquinolone resistance; multidrug efflux pump CmeABC/RE-CmeABC extruding structurally diverse compounds and antimicrobials; and horizontally acquired antimicrobial resistance genes, such as *tet(O)*, *erm(B)*, *fexA*, and *fosXCC* (Aarestrup et al., 2008). Among the two major species of *Campylobacter*, *C. jejuni* and *C. coli*, which are mainly responsible for human infection, *C. coli* is known to be more resistant to antimicrobials (Liu et al., 2019b).

The *cfr* gene, which encodes 23S rRNA methyltransferase, confers resistance to five antimicrobial classes, namely phenicols, lincosamides, oxazolidinones, pleuromutilins, and streptogramin A, known as $PhLOPS_A$ phenotype (Schwarz et al., 2000; Long et al., 2006). WHO classified lincosamides, pleuromutilins, and streptogramin A as "critically important antimicrobials: highly important" and warned that resistance to these antimicrobial agents would make it difficult to treat bacterial infection (WHO, 2019). Since the first report of *cfr* gene in *Staphylococcus sciuri* in 2006, five types of the *cfr* gene family have been reported: *cfr*, *cfr(B)*, *cfr(C)*, *cfr(D)*, and *cfr(E)* (Schwarz et al., 2000; Deshpande et al., 2015; Hansen and Vester, 2015; Candela et al., 2017; Tang et al., 2017; Sassi et al., 2019; Stojković et al., 2019). Tang et al. (2017) first identified plasmid-mediated multi-drug resistance gene *cfr(C)* in *C. coli* isolates of feedlot cattle origin (Tang et al., 2017). Since the first report of *cfr(C)* in *Campylobacter*, three additional studies reported the presence of *cfr(C)* in *Campylobacter* species (Zhao et al., 2019; Liu et al., 2019a; Tang et al., 2020). However, the horizontal transferability of *Campylobacter*-derived *cfr(C)* has been reported in only one study (Tang et al., 2017), and the transfer mechanism of *cfr(C)* is still unclear and requires further research.

An understanding of genetic variation of *cfr(C)* and their transmission mechanisms can help control the propagation of antimicrobial multi-resistance, a serious problem when it is transferred to humans. Thus, in this study we analyzed genetic background and horizontal transfer unit of *cfr(C)* in *C. coli* strains through comparative genomic analysis to elucidate the genetic variation and horizontal transfer mechanism of the *Campylobacter*-derived *cfr(C)* gene from swine sources.

Abbreviations: BLAST, Basic Local Alignment Search Tool; IS, insertion sequence; MIC, minimum inhibitory concentration; NCBI, National Center for Biotechnology Information; Ns, non-synonymous; PCR, polymerase chain reaction; SNP, single nucleotide polymorphism; WGS, whole genome sequencing; WHO, World Health Organization.

2 Materials and methods

2.1 Identification of *cfr(C)*-positive *Campylobacter coli* strains

A total of 157 swine-derived *C. coli* strains were used to screen *cfr(C)* presence. Of these, 130 *C. coli* strains were isolated from six swine farms in South Korea in our previous study (Guk et al., 2021). In addition, 15 *C. coli* strains were collected from 30 swine fecal samples from one slaughterhouse in South Korea in November 2017 and 12 *C. coli* strains from 30 fecal samples from one swine farm in South Korea in April 2018. Confirmation of *cfr(C)* was conducted using polymerase chain reaction (PCR). The primer used and annealing temperature are presented in Supplementary Table 1.

2.2 Antimicrobial susceptibility testing

Minimum inhibitory concentration (MIC) tests were conducted using Sensititre CAMPY2 plates (ThermoFisher Scientific, USA) following the manufacturer's instructions for the following eight antimicrobial agents: azithromycin, ciprofloxacin, erythromycin, gentamicin, tetracycline, florfenicol, nalidixic acid, and clindamycin. The MIC value of each antimicrobial agent was interpreted according to the criteria of the National Antimicrobial Resistance Monitoring System for enteric bacteria.[1] *C. jejuni* ATCC 33560 was used as the quality control strain for the MIC test.

2.3 Whole genome sequencing (WGS)

Total genomic DNA was extracted using NucleoSpin Microbial DNA kit (Macherey-Nagel, Germany) following the manufacturer's instructions. Total genomic DNA was sequenced via a combination of NextSeq® 500 technology (Illumina, Inc., USA) and MinION platforms (Oxford Nanopore Technologies, UK). Raw short-read and long-read data were assembled using hybrid-assembly strategy in Unicycler (v0.5.0) (Wick et al., 2017) and annotated using prokka (v1.14.5) (Seemann, 2014).

2.4 Identification of novel *cfr(C)* variants via single nucleotide polymorphism (SNP) analysis

To identify *cfr(C)* variant types, the nucleotide sequences of *cfr(C)* of nine isolated *C. coli* strains were aligned with that of the reference

1 https://www.cdc.gov/narms/antibiotics-tested.html

strain, *C. coli* Tx40 (National Center for Biotechnology Information [NCBI] accession number: NG_060579). Thereafter, we conducted *cfr(C)* gene SNP-based comparative genomic analysis by comparing the *cfr(C)* sequences of nine strains with that of 28 *C. coli* strains, the WGS of which were deposited in the NCBI database. In addition, SNP-based phylogenetic analysis was performed for *cfr(C)* of nine *cfr(C)*-positive strains together with that of other strains published in NCBI database. Phylogenetic tree was constructed with MEGAX software by using UPGMA method (Kumar et al., 2018). Bootstrap values were calculated with 1,000 replications. The accession numbers of nucleotide sequences are listed in Supplementary Table 2.

2.5 Functional confirmation of *cfr(C)* variants through cloning experiments

To determine the role of *cfr(C)* in conferring florfenicol resistance, a 1,425 bp DNA fragment was amplified from eight *C. coli* strains (CC021, 027, 032, 041, 042, 046, 135, and 159) through PCR. This fragment included the coding sequence of *cfr(C)* (1,140 bp) as well as 63 bp upstream and 163 bp downstream sequences of the gene. For *C. coli* strain CC024, a 1,327 bp DNA fragment was amplified through PCR. This fragment included the coding sequence of *cfr(C)* as well as the 122 bp upstream and 163 bp downstream sequences of the gene. The amplicon was ligated with an *E. coli*/*C. jejuni* shuttle plasmid pUC19 (Yanisch-Perron et al., 1985) to construct plasmid pUC19-*cfr(C)*. The pUC19-*cfr(C)* plasmid was then transformed into *E. coli* DH5α competent cells by heat shock transformation. The *E. coli* transformants were selected from Luria-Bertani agar (Sigma-Aldrich, USA) plates containing 50 mg/L ampicillin and 50 mg/L kanamycin. The confirmation for carrying plasmid pUC19-*cfr(C)* was performed thorough PCR using the *cfr(C)*-specific primers. MIC tests were also conducted for *E. coli* transformants to evaluate the antimicrobial resistance. Used primer and annealing temperature used in the experiments are listed in Supplementary Table 2.

2.6 Analysis of *cfr(C)*-carrying gene cassettes and circular intermediates

The *cfr(C)*-carrying gene cassettes of nine *C. coli* strains were aligned against the corresponding region of reference strain *C. coli* Tx40 ([NCBI] accession number: NG_060579) and *C. coli* SHP40 ([NCBI] accession number: MF037584). Additionally, the inserted positions of *cfr(C)*-carrying gene cassette in nine *C. coli* strains were identified by alignment and comparison with *C. coli* strain ATCC33559. The comparative genomic visualization was performed using "Easyfig (v2.2.3)" (Sullivan et al., 2011). The circular intermediate form of *cfr(C)*-carrying gene cassette was investigated by using inverse PCR and Sanger sequencing. Amplicon sequences were aligned and compared with sequences submitted in the NCBI GenBank database using the Basic Local Alignment Search Tool program (BLAST).[2] The primers and annealing temperature used in the experiments are listed in Supplementary Table 2.

2 https://blast.ncbi.nlm.nih.gov/Blast.cgi

2.7 Conjugation assay

To evaluate the horizontal transferability of *cfr(C)*-carrying gene cassette, we conducted conjugation assay following the previously described methods with slight modification (Davis et al., 2008). The conjugation assay was performed with a gentamicin-resistant wild-type *C. coli* as the recipient and eight *cfr(C)*-positive *C. coli* strains as the donors: CC021, CC027, CC032, CC041, CC042, CC046, CC135, and CC159. Among nine *cfr(C)*-positive strains included in this study, CC024 was excluded from the conjugation assay with the gentamicin-resistant recipient strain, since it carried resistance to gentamicin. To select the transconjugants, Mueller-Hinton agar (Sigma Aldrich) plates containing 1 mg/L gentamicin and 4 mg/L florfenicol were used. The presence of *cfr(C)* gene and circular intermediate form in transconjugants were confirmed using PCR. The antimicrobial resistance was evaluated for transconjugants though MIC tests.

3 Results

3.1 Novel *cfr(C)* SNP variants

Among the 157 swine-derived *C. coli* strains, nine *cfr(C)*-positive strains were identified (Table 1). A total of six SNP variant types were identified in SNP-based comparative genomic analysis: SNP-I (CC021), SNP-II (CC024), SNP-III (CC027 and CC032), SNP-IV (CC041, CC042, and CC046), SNP-V (CC135), and SNP-VI (CC159) (Figure 1 and Supplementary Figure 1). SNP-I carried six SNPs, including a nonsense SNP (19delA, M7fs), which caused frameshift mutation of *cfr(C)* in strain CC021. SNP-II carried two SNPs, 281A > C (E94A) and 952A > G (I318V), and this type was truncated at the 3′ end (1,101 bp). SNP-III carried three SNPs, 281A > C, 532A > C (K178Q), and 952A > G. The SNP-IV type carried three SNPs, including the novel SNP 674C > A (T225K), which was not identified in previously reported strains uploaded in the NCBI database. The SNP-V type carried six SNPs, including the novel SNP 890T > C (sSNP), which was not identified in previously reported strains uploaded in the NCBI database. The SNP-VI type carried seven SNPs, including 533A > G (K178R) and the novel SNP 890T > C.

In the SNP-based phylogenetic tree, the *cfr(C)* nucleotide sequences of the nine strains were genetically similar to those of swine- and human-derived *C. coli* strains isolated from China rather than that of cattle, chicken, and human-derived *C. coli* strains isolated from USA (Supplementary Figure 2). In addition, the *cfr(C)* genes reported from the USA were genetically homogeneous regardless of region and year of isolation, whereas the *cfr(C)* genes reported from China showed high genetic variations.

3.2 Antimicrobial resistance of nine *cfr(C)*-positive *Campylobacter coli* strains and transformants

Two SNP types showed susceptibility to florfenicol: SNP-I (CC021) and SNP-III (CC027 and 032), with MIC values of 2 and 4 mg/L, respectively (Supplementary Table 3). The other types showed resistance to florfenicol (MIC: 8 mg/L). Resistance to clindamycin was identified in three SNP types: SNP-II, -III, and -V. Regardless of the

TABLE 1 Descriptive information of *C. coli* strains used in this study.

	Farm	Stage	MLST (ST)	SNP profile type	FFN	CLI	Gene cassette	Circular intermediate	Conjugation	SNP
CC021	A	Growing	887	SNP-I	S	R	GC-1	CIR-1	Conjugated	19delA*†, 532A > C, 533A > G, 719G > A, 893C > G, 952A > G
CC024	B	Weaning	1,142	SNP-II	R	R	GC-2	-	-	281A > C, 952A > G
CC027	B	Growing	2,699	SNP-III	S	R	GC-3	CIR-2	Not conjugated	281A > C, 532A > C, 952A > G
CC032	B	Finishing	2,699	SNP-III	S	R	GC-3	CIR-2	Not conjugated	281A > C, 532A > C, 952A > G
CC041	C	Growing	830	SNP-IV	R	R	GC-4	CIR-1	Conjugated	674C > A*, 893C > G, 952A > G
CC042	C	Growing	830	SNP-IV	R	R	GC-4	CIR-1	Conjugated	674C > A*, 893C > G, 952A > G
CC046	C	Growing	830	SNP-IV	R	R	GC-4	CIR-1	Conjugated	674C > A*, 893C > G, 952A > G
CC135	D	Diseased	1,096	SNP-V	R	R	GC-5	CIR-1	Conjugated	267C > T, 281A > C, 532A > C, 890 T > C*, 893C > G, 952A > G
CC159	S	Pork	1,556	SNP-VI	R	S	GC-6	CIR-3	Not conjugated	267C > T, 281A > C, 532A > C, 533A > G, 890 T > C*, 893C > G, 952A > G

*Novel SNP sites identified in this study.

†The SNP site in *cfr(C)* leading to premature stop codon.

MLST, Multi-locus sequence typing; SNP, single nucleotide polymorphism; FFN, florfenicol; CLI, clindamycin; S, susceptible; R, resistant; GC, gene cassette type; CIR, circular intermediate type.

10.3389/fmicb.2023.1274245

10.3389/fmicb.2023.1274245

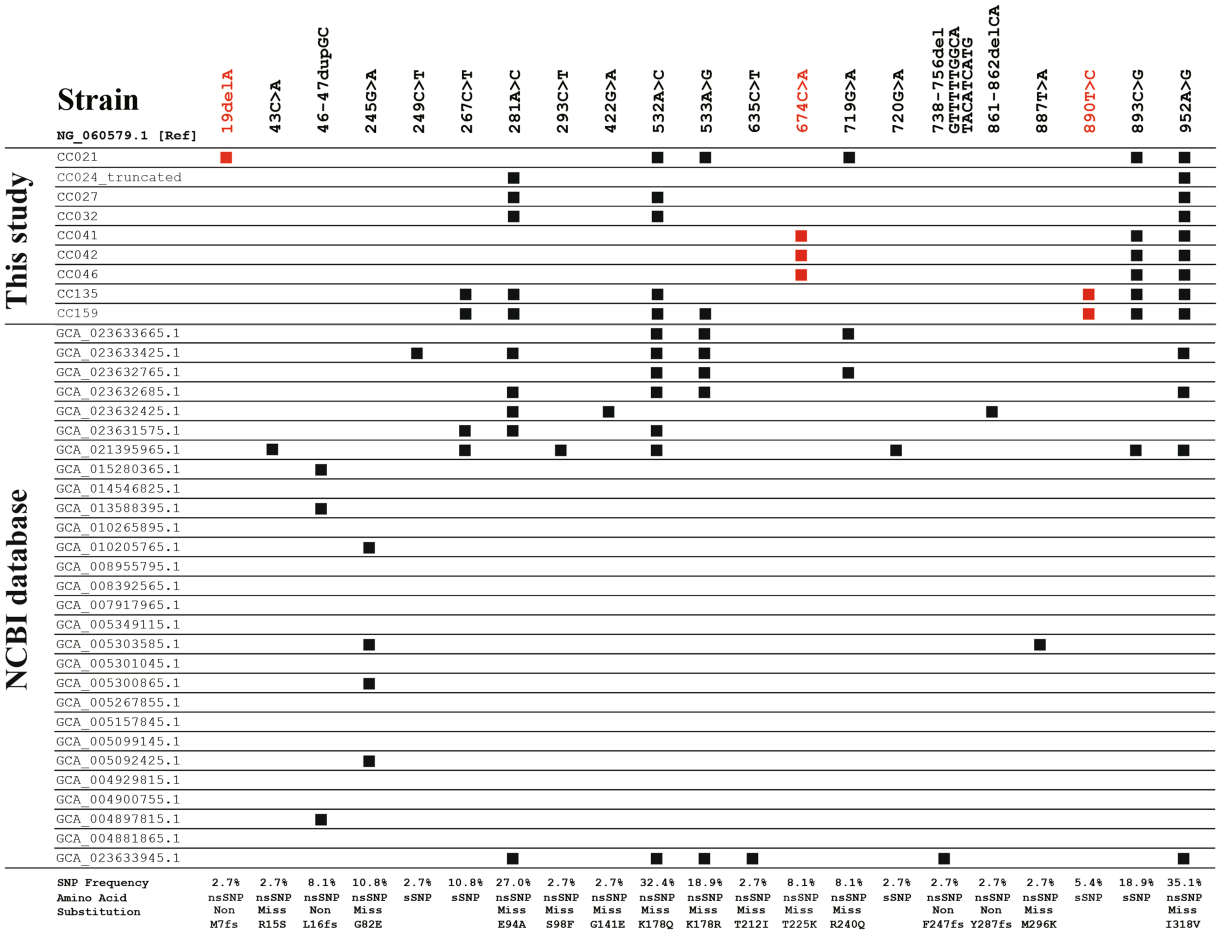

FIGURE 1
Single nucleotide polymorphic (SNP) sites of *cfr(C)* in 37 strains, including nine strains identified in this study and 28 strains obtained from NCBI database. Nucleotide sequence of *cfr(C)* (1,140 bp) of *C. coli* Tx40 strain (NG_060579.1) was used as reference. SNP sites shown in red font represent the novel SNP sites identified in this study. nsSNP, non-synonymous SNP; sSNP, synonymous SNP; Non, non-sense nsSNP; Miss, Miss-sense nsSNP; fs, frameshift mutation.

SNP variants, strains CC024, CC027, CC032 and CC135 exhibited resistance to the macrolide class, namely azithromycin (MIC: ≥64 mg/L) and erythromycin (MIC: ≥64 mg/L). Except for the CC024 strain, all other types showed susceptibility to gentamicin (MIC: ≤4 mg/L). All strains except for CC159 strain showed resistance to the quinolone class, including ciprofloxacin (MIC: ≥1 mg/L) and nalidixic acid (MIC: ≥32 mg/L).

All six SNP types of *cfr(C)* were transformed into *E. coli* DH5α competent cells. The transformant of SNP-I type (CC021) exhibited susceptibility to florfenicol (MIC: 2 mg/L). The other SNP types (SNPs II–VI) exhibited resistance to florfenicol (MICs: 4–8 mg/L). For the clindamycin-resistant phenotype, MICs increased at least two-fold compared to that of *E. coli* DH5α competent cells (increase to ≥32 mg/L from 16 mg/L).

3.3 Gene-cassette carrying *cfr(C)*

A total of six *cfr(C)*-carrying gene cassette types (GC-1–6) were identified, differing based on SNP-types (Figure 2 and Table 1). Except for the gene cassette of strain CC024, all five gene cassettes carrying *cfr(C)* were identified to be encoded on the chromosome. Of the 6 GC types, three types (GC-1, −4, and −5) were flanked by the *pcp* gene in the upstream of *cfr(C)*. Two types (GC-3 and -6) were bracketed by two copies of the IS607 family member ISChh1 upstream and downstream of *cfr(C)*. GC-5 was bracketed by one ISChh1 upstream of *cfr(C)* and downstream of *pcp*. In all six GC types, *aphA3* was encoded downstream of *cfr(C)*. The aminoglycoside-streptothricin resistance cluster "*aphA3-sat4-ΔaadE*" was identified from 3 GC types (GC-1, -2, and -4). The GC-1 type (CC021) was "Δ*pcp*-hp-*cfr(C)-aphA3-sat4-ΔaadE-pcp*," in which the *ppo* gene was deleted compared to corresponding region of the reference *C. coli* SHP40 strain. The GC-4 type (CC041, 042, and 046) was "Δ*pcp*-hp-hp-*cfr(C)-aphA3-sat4-ΔaadE*," with *pcp* deleted upstream of Δ*aadE*. The GC-2 type (CC024) was "hp-Δ*cfr(C)-aphA3-sat4-ΔaadE*-hp," with *pcp* and hp. deleted in the gene cassette compared to the corresponding region of the GC-1 type. The GC-5 type (CC135) was "Δ*pcp*-hp-*cfr(C)-aphA3*-ISChh1." The GC-6 type (CC159) was "ISChh1-*cfr(C)-aphA3*-ISChh1." The gene cassette of the SNP-III type (GC-3) consisted of "ΔISChh1-ATPase-hp-*ant1-pnp (deoD)-lnu (G)-cfr(C)-aphA3*-ISChh1" and contained the insert ATPase-hp-*ant1-pnp-lnu(G)* compared with the corresponding region of GC-6.

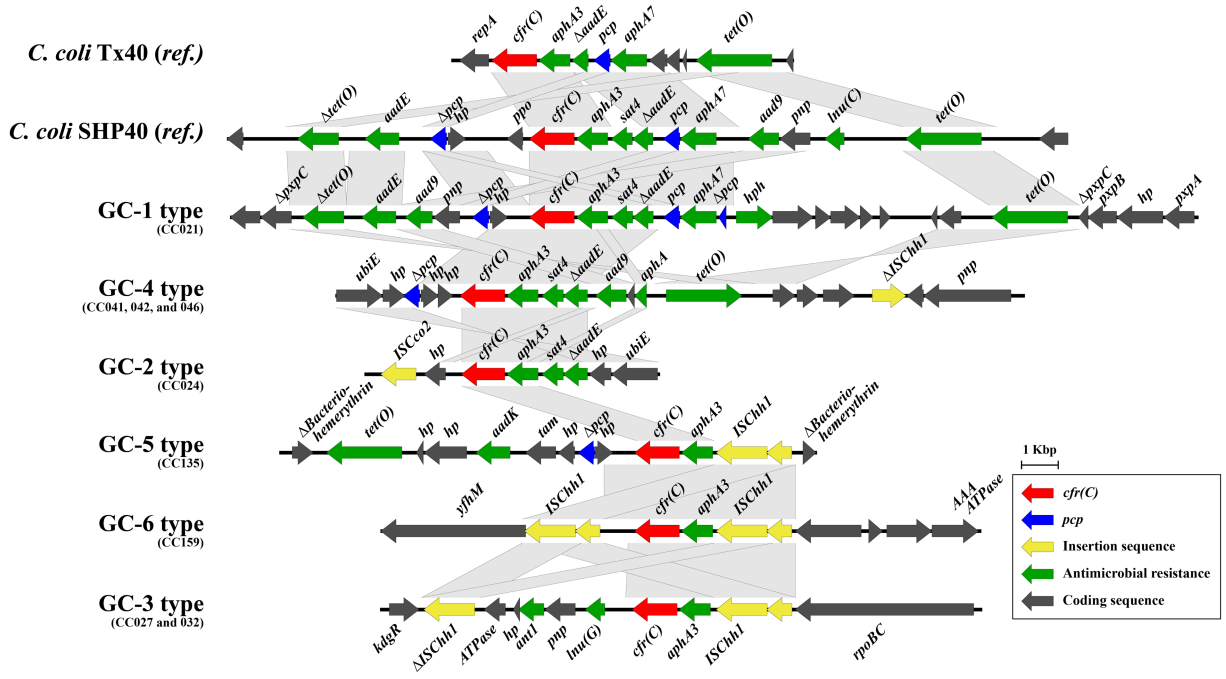

FIGURE 2
Six types of gene cassettes carrying *cfr(C)* identified in comparative genomic analysis of nine strains. The nucleotide sequences of *cfr(C)*-carrying gene cassettes were aligned and compared by using Easyfig (v2.2.3).

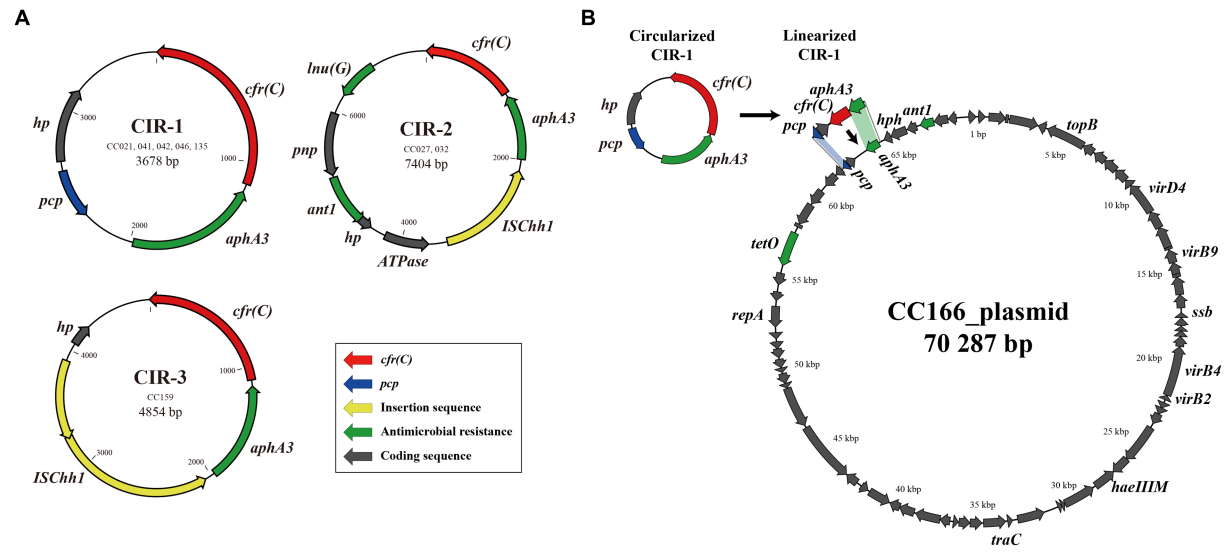

FIGURE 3
cfr(C)-carrying circular intermediates identified by inverse PCR and amplicon sequencing. Three types of circular intermediates were identified from *cfr(C)*-carrying *C. coli*, except for strain CC024. **(A)** Three types of circular intermediates formed by eight *C. coli* strains, **(B)** the genetic environment of recipient strain *C. coli* CC166 plasmid and insertion site of CIR-1.

3.4 Circular intermediate form of *cfr(C)*-carrying gene cassettes and horizontal transferability

Of the six GC types identified in this study, five formed circular intermediates of the *cfr(C)*-cassette. In total, three types of circular intermediates (CIR-1, CIR-2, and CIR-3) were identified (Figure 3A). The CIR-1 type, which was 3,678-bp long and consisted of "*pcp-hp-cfr(C)-aphA3*," was identified from three GC types, GC-1, -4, and -5. The CIR-2 type, which was 7,833-bp long and consisted of "ΔISChh1-*aphA3-cfr(C)-lnu(G)-pnp-ant1*-hp-ATPase," was identified from GC-3. CIR-3, which was 4,854-bp long and consisted of "'ISChh1-*aphA3-cfr(C)*-hp," was identified from GC-6. The circular intermediate form of GC-2 was not identified.

In the conjugation assay, CIR-1 was confirmed to be horizontally transferred to recipient strain. The horizontal transferability of other

10.3389/fmicb.2023.1274245

two types, CIR-2 and CIR-3, was not identified. The transconjugants of CIR-1 exhibited acquired resistance to florfenicol (MIC: 8 mg/L) and clindamycin (MIC: 8 mg/L). In WGS analysis, the "*pcp*-hp-*aphA3*" region encoded on the plasmid of wild-type strain CC166 was replaced into "*pcp*-hp-*cfr(C)-aphA3*" after conjugation with a CIR-1 type strain (Figure 3B). As a result, the size of the plasmid increased from 70,287 to 71,195 bp.

3.5 Favored insertion site of *cfr(C)*-carrying gene cassette

The genomic island of the GC-1 type was composed of Δ*tetO*-*aadE*-*aad9*-*pnp*-Δ*pcp*-hp-*cfr(C)*-*aphA3*-*satA*-Δ*aadE*-Δ*pcp*-*hph*-hp (2)-*traC*-hp (6)-*tetO*, which was inserted into the *pxpC* gene of the *pxpABC* complex at positions 249,516–268,882 bp (19,367 bp), based on the location of the *dnaA* gene that encodes the chromosomal replication protein (Figure 4 and Supplementary Figure 3). GC-4, which was part of a genomic island composed of ΔISChh1-hp (3)-*tetO*-*aphA*-hp-*aad9*-hp-*sat4*-*aphA3*-*cfr(C)*-hp (2)-Δ*pcp*-hp-*ubiE* (14,424 bp), was inserted at positions 1,184,369–1,198,793 bp encoding *lptD*-*pnp*-hp upstream and hp (2)-*sbnD* downstream. For GC-5, the *cfr(C)*-carrying genomic island (11,787 bp), which was composed of ISChh1-*aphA3*-*cfr(C)*-hp (2)-*tam*-*aadK*-hp (2)-*tetO*, was inserted at positions 165,574–177,361 bp on the gene encoding bacteriohemerythrin. As a result of this insertion, both sides of the GC-5 genomic island's insertion site encoded a truncated bacteriohemerythrin gene. The GC-6 genomic island consisted of

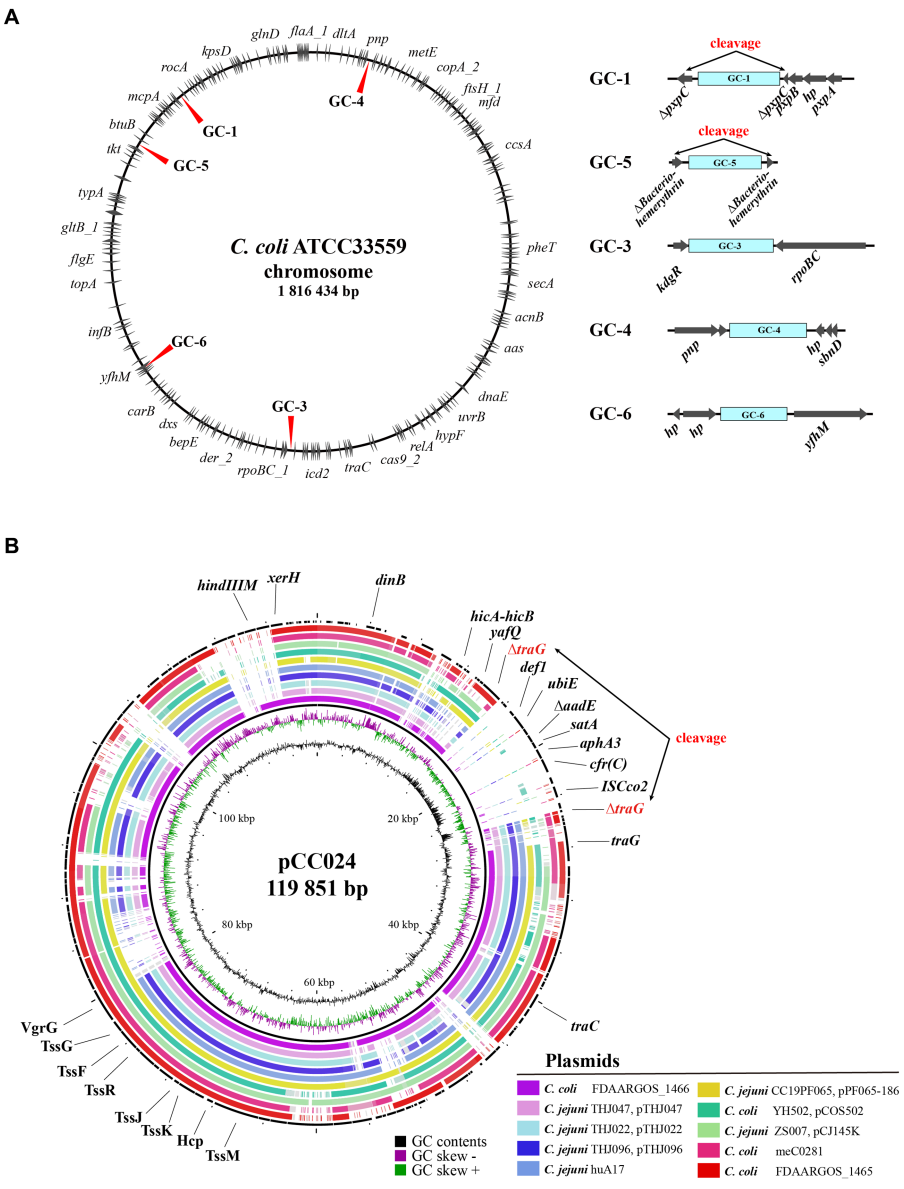

FIGURE 4
Insertion sites of *cfr(C)*-carrying gene cassette in wild type *cfr(C)*-carrying *C. coli*. **(A)** Chromosomal insertion sites of each *cfr(C)*-carrying gene cassette types based on nucleotide sequence of *C. coli* strain ATCC33559. **(B)** Comparative genomic analysis of *cfr(C)*-carrying plasmid-like genetic element of CC024 strain by using BRIG. For comparison, nucleotide sequences of 10 plasmids of *Campylobacter* species with high genetic homology to the plasmid of CC024 were obtained from NCBI database by using BLAST.

ISChh1-*aphA3-cfr(C)*-ISChh1 and was found to be inserted at positions 227,744–234,515 bp, flanked by "*purE-dapB*-AAA ATPase-hp (3)" and "*yfhM-mtgA*-hp" on each side. The GC-3 type was composed of ΔISChh1-ATPase-hp-*ant1-pnp-lnu(G)-cfr(C)-aphA3*-ISChh1, inserted at positions 1,261,026–1,270,356 bp and flanked by "*uxaA-dapA-kdgR*" and "*rpoBC-rplL*" on each side. Lastly, GC-2 of strain CC024 was identified within a circular genetic element with a size of 119,851 bp. The genomic island containing GC-2 was inserted into the *traG* gene.

4 Discussion

The rRNA methyltransferase N, encoded by *cfr* gene, causes m^8-modification of A2503 of 23S rRNA, which is known to confer resistance to two antimicrobial agents, florfenicol and clindamycin (Long et al., 2006). Even though *cfr(C)* is known to induce antimicrobial resistance to critically important antimicrobials to humans, its transfer mechanism is still unclear and requires further research. In this study, nine novel *cfr(C)*-positive *C. coli* strains were isolated from swine sources (swine farms and slaughterhouses). To elucidate the horizontal transfer mechanism of the *Campylobacter*-derived *cfr(C)* gene, we analyzed the genetic background and horizontal transfer unit of *cfr(C)* in *C. coli* strains through comparative genomic analysis.

Compared to the previously reported sequences of *cfr(C)*, two strains (CC021 and CC024) carried incomplete amino acid coding sequences of the *cfr(C)* gene. Insertion or deletion of one or two adenines at the polyadenine site, such as 19delA (amino acid: M7fs) identified in CC021, generates premature stop codons by downstream frameshifting, leading to premature chain termination (Park et al., 2000). Tang et al. (2020) reported loss of resistance to florfenicol and clindamycin of *cfr(C)* due to other nucleotide deletion mutations in the *C. coli* JP10 strain, in which a frameshift mutation occurred due to nucleotide deletion at position 738–756 of *cfr(C)*. The *cfr(C)* amino acid sequence of CC024 (366 amino acids) exhibited 95.51% identity to that of *C. coli* Tx40 (379 amino acids). Notably, the original CC024 strain, as well as its transformant strain, showed resistance to florfenicol. According to a study of *cfr* protein structure and function, the function of the *cfr* protein analog was ensured by a highly conserved amino acid sequence around the C-terminus (G.DIdAACGQL) (Atkinson et al., 2013). In this study, although the amino acid sequence of the *cfr(C)* gene was truncated in the CC024 strain, the conserved C-terminal region of *cfr(C)* was preserved, which may ensure the function of *cfr(C)*.

Remarkably, the transformants of CC027 and CC032 with three missense non-synonymous (ns) SNPs (281A > C, 532A > C, and 952A > G) showed weak resistance to florfenicol (4–8 mg/L). These three missense nsSNPs were also identified in the florfenicol resistant *cfr(C)*-positive strains, CC135 and CC159. The amino acid substitutions (E94A, K178Q, and I318V), due to three SNP sites, have also been identified in the florfenicol and clindamycin-resistant *C. coli* JZ_1_79 and SH96 strains reported by Tang et al. (2020). The *cfr(C)*-encoded rRNA methyltransferase has functional amino acid sites including three substrate entrance sites and eight substrate modulation sites (Atkinson et al., 2013). Considering that the mutation sites of CC027 and CC032 do not overlap with the mutation sites of the previous report, it can be inferred that the three SNPs of these two strains are not associated with the phenotype for florfenicol resistance. Therefore, in relation to decreased resistance to phenicols found in strains CC027 and CC032, further research on the genetic background and expression of *cfr(C)* is needed.

Except for CC159, all eight *cfr(C)*-positive *C. coli* strains showed resistance to clindamycin, although the resistance level was different between strains depending on the carriage of 23S rRNA A2075G substitution: four strains with 23S rRNA A2075G substitutions showed high-level clindamycin resistance, whereas strains without the 23S rRNA A2075G substitution showed low-level resistance. The 23S rRNA A2075G substitution is known to be the most common mechanism underlying high-level resistance to the macrolide and lincosamide classes of antimicrobial agents in *Campylobacter* (Perez-Boto et al., 2010). Considering that the resistance of bacteria to lincosamide is generally mediated by the combination of three mechanisms (ribosomal target methylation or mutation, efflux of antimicrobials, and drug inactivation) (Leclercq, 2002), strains with simultaneous *cfr(C)*-induced A2503 methylation and A2075G substitution could exhibit high resistance to the lincosamide class. Our result suggests that *cfr(C)*-induced A2503 methylation may lead to low-level resistance to clindamycin, which could be enhanced by the acquisition of A2075G substitution.

cfr(C) is encoded on transferable plasmids (Tang et al., 2017;Liu et al., 2019a; Tang et al., 2020) or the chromosome of *cfr(C)*-positive *C. coli* strains (Liu et al., 2019a; Tang et al., 2020). In this study, the *cfr(C)* gene was encoded on the bacterial chromosome in the form of gene cassettes in eight *cfr(C)*-positive *C. coli* strains, except the gene cassette of strain CC024, and a total of six different gene cassettes were identified. Consistent with previous studies, all six *cfr(C)* gene cassettes carried the aminoglycoside resistance gene, *aphA3*, which was encoded upstream of *cfr(C)* in the same direction (Tang et al., 2017; Zhao et al., 2019; Liu et al., 2019a; Tang et al., 2020). Three cassette types, namely GC-1 (CC021), GC-2 (CC041, 042, and 046), and GC-5 (CC024), carried the aminoglycoside-streptothricin resistance gene cluster "*aphA3-sat4-aadE*" in the upstream of the *cfr(C)*-cassette gene. The "*aphA3-sat4-aadE*" cluster was also reported to be encoded in the upstream of the *cfr(C)*-cassette in the *C. coli* SHP40 strain, where the *cfr(C)* gene was first reported on the chromosome (Liu et al., 2019a). In contrast, the aminoglycoside resistance gene cluster "*aphA3-aadE*" without "*sat4*" was encoded in the upstream of the *cfr(C)*-cassette in the plasmids of 2 *C. coli* strains, Tx40 and N61925F (Tang et al., 2017; Zhao et al., 2019). The *aphA3* gene is an aminoglycoside-resistance determinant, encoding aminoglycoside 3′-phosphotransferase, and the *sat4* gene is a streptothricin-resistance determinant, encoding streptothricin N-acetyltransferase (Lysnyansky and Borovok, 2021b). The "*aphA3-sat4-aadE*" cluster is one of the highly transmissible and disseminated clusters, mainly found in the plasmids of gram-positive (*Staphylococcus* and *Enterococcus*) and gram-negative bacteria (*Campylobacter*) (Boerlin et al., 2001; Lysnyansky and Borovok, 2021a; Guirado et al., 2022). The *aphA3-sat4-aadE* cluster is transmitted with various antimicrobial-resistance genes, such as *ermB*, *optrA*, and *tet (O)* (Werner et al., 2001, 2003; Palmieri et al., 2012). Although the *aphA3-sat4-aadE* cluster has been reported to be mediated by mobile genetic elements, such as Tn5405 (Werner et al., 2001), recent studies have also shown that in *Campylobacter* spp., this resistance gene cluster may be mediated by a process of homologous recombination (Qin et al., 2012). Homologous recombination may enable horizontal

transfer and chromosomal integration of gene clusters without mobile genetic elements (de Vries and Wackernagel, 2002). In the case of GC-4, another resistance gene cluster, "*ant1-pnp-lnu(G)*," was encoded in the upstream of the *cfr(C)*-cassette. The lincosamide resistance gene, *lnu (E)*, is encoded in the upstream of the ISEnfa5-flanked *cfr* gene cassette in the *Streptococcus suis* RN4220 strain (Zhao et al., 2014).

The random insertion of a gene cassette into *cfr(C)* has the potential to significantly affect the fitness and survival of *Campylobacter*, as the insertion of the *cfr(C)* gene cluster may interfere with crucial cellular processes of the bacterium. The insertion sites of GC-1 and -5, harboring genomic islands, were different from those of the *potD* gene reported by Tang et al. (2020). GC-1 was inserted into the *pxpC* gene, which encodes 5-oxoprolinase. 5-Oxoproline, a metabolite from the breakdown of glutamine, has been reported to inhibit bacterial growth when it accumulates without proper disposal (Niehaus et al., 2017). GC-5 was inserted into the bacteriohemerythrin-encoding gene. Hemerythrin helps maintain bacterial homeostasis through intracellular oxygen- and redox-sensing functions. Cells cannot rapidly adapt to environmental changes without hemerythrin (Kitanishi, 2022). Our results suggest that the cleavage of these two genes, caused by the insertion of *cfr(C)*-carrying GCs, could have detrimental effects on the survivability of *C. coli* strains. The GC-3, -4, and -6 types were inserted between genes without gene cleavage. The insertion site of GC-3 downstream of the *rpoBC* gene has been previously reported (Tang et al., 2020). However, the other two types of insertion sites, *pnp* to *sbnD* and ATPase-encoding gene to *yfhM*, are novel positions. In contrast, GC-2 (CC024) was inserted into a circular genetic element without a self-replication module, such as the replication initiation protein gene *repA*. This genetic element of CC024 was similar in genetic composition to the previously reported plasmids of *C. jejuni* and *C. coli*. In addition, differences in GC contents between insertion sites and other coding regions indicated that the *cfr(C)*-carrying cluster was not included in ancestral genetic elements. TraG, truncated by GC-2, plays major roles in conjugation, and is associated with the invasion of *C. jejuni* into epithelial cells (Poly et al., 2005). Thus, truncation of the *traG* gene could attenuate the pathogenicity and survivability of *Campylobacter*.

Of the six types of gene cassette, GC-1, -4, and -5 formed circular intermediates and were horizontally transferred to recipient *C. coli* strains. The transferred circular intermediate form was 3,678 bp in length and consisted of the four coding sequences "*pcp-hp-cfr(C)-aphA3*." Although the present study found differences in the length and composition of *cfr(C)*-positive strains, the *pcp* gene-mediated circular intermediate "*pcp-hp-ppo-cfr(C)-aphA3-sat4-aadE*" has also been reported in the *C. coli* SHP40 strain (Liu et al., 2019a). Similar to our study, the *cfr(C)*-cassette was also encoded in the bacterial chromosome of the *C. coli* SHP40 strain. The *pcp* gene encodes an enzyme that is conserved in a variety of organisms, from prokaryotes (archaea and bacteria) to eukaryotes (Barrett et al., 2012). The *pcp* gene is found to be inserted at multiple sites in the bacterial genome, including chromosomes and plasmids, and this multiple insertion of *pcp* could mediate the intermolecular transfer of gene clusters by forming the circular intermediate: the circular intermediates released from chromosome/plasmids could be integrated into other chromosome/plasmids containing a homologous sequence, such as the *pcp* gene (Liu et al., 2019a). These characteristics of the *pcp* gene can facilitate the transmission of *cfr(C)*, which forms a cluster with *pcp*. Similarly, *tetO*-mediated circular intermediates of *ermB*, escaping from original plasmids/chromosome, could be integrated into other bacterial genomes by targeting the multiple inserted *tetO* homologous sequence (Liu et al., 2019b). In particular, the CC041, CC042, and CC046 strains that form GC-4 have been reported as hyper-aerotolerant strains, along with ST830, which is related to clinical isolates, according to our previous study (Guk et al., 2021). Since these strains not only transfer *cfr(C)* to other strains but also have a higher probability for transmission to humans than other *C. coli* strains, hyper-aerotolerant *cfr(C)*-positive *C. coli* potentially carry higher risk than other *cfr(C)*-positive *C. coli* strains.

In GC-3, 4, 5, and 6, *cfr(C)* was flanked by the IS607 family member ISChh1. The IS607 family is one of the major insertion sequences (ISs) that mediate transfer of antimicrobial resistance in *Campylobacter* spp. (Chen et al., 2018). For example, IS607 has been reported to mediate the transfer of the *optrA* gene, which induces resistance to oxazolidinones and phenicols, as well as of *fexA*, a florfenicol–chloramphenicol resistance gene (Tang et al., 2021). The IS607 family encoded in the upstream of the *cfr(C)*-gene cassette was also identified in the plasmids of the JZ_1_79, SH89, and JZ_1_74 strains reported by Tang et al. (2020). Among the three *cfr(C)*-cassette types flanked by IS607, GC-3 and GC-6 were bracketed by two copies of ISChh1 in the same orientation at both sides of the gene cassette and formed the ISChh1-mediated circular intermediates "ISChh1-*aphA3-cfr(C)-lnu(G)-pnp-antl1-hp*-ATPase" and "ISChh1-*aphA3-cfr(C)*-hp," respectively. Even though the circular intermediates of GC-3 and -6, namely CIR-2 and -3, were not horizontally transferred in our study, two copies of IS elements in the same orientation can form a circular intermediate and can be transferred using the mechanism "copy-out-paste-in," since the IS607 family is a highly active IS element (He et al., 2019). Tang et al. (2020) confirmed the existence of IS607 only upstream of the *cfr(C)*-cassette but could not confirm the formation of circular intermediates by the IS607 family. GC-4 and -5, bracketed by the ISChh1 segment and *pcp*, formed a circular intermediate mediated by *pcp* regardless of the position of the ISChh1 segment. These results suggest that two copies of IS607 in the same orientation play an important role in the formation of a circular intermediate form of gene cassettes.

The CIR-1s of five strains (CC021, 041, 042, 046, and 135) were horizontally transferred from the chromosomes into the plasmid of the recipient strain CC166 in the conjugation assay. For all five strains, the *pcp* and *aphA3* genes were present at the insertion sites, suggesting that insertion of CIR-1 may have been mediated by homologous recombination with *pcp* and *aphA3*. The conjugation of gene cassettes targeting homologous gene regions has been reported in several studies. Qin et al. (2012) suggested that the aminoglycoside resistance gene island of *C. coli* strain SX81 may be acquired from the *C. coli* strain RM2228 and mediated by homologous recombination of the *cadF* and *CCO1582* genes (Qin et al., 2012). Taken together with our results, this suggests that the use of *pcp*, which is a commonly encoded gene in *Campylobacter*, as a vector in the horizontal transfer of *cfr(C)*-carrying gene cassettes may be a possible reason for the global success of *cfr(C)* propagation.

This is the first study to elucidate the horizontal transferability of *cfr(C)* and random insertion site of the chromosome-encoded *cfr(C)* cassette in *Campylobacter* spp. The results reveal novel *cfr(C)* variants along with their associated genetic environments in *C. coli*

isolates and indicate the flexibility of *C. coli* in acquiring new antimicrobial resistance genes. The transferability of chromosomal *cfr(C)* to humans may be attributed to the global spread of multidrug resistance against clinically important antimicrobials. Thus, enhanced surveillance is needed to monitor the emergence and spread of *cfr(C)* in *Campylobacter* from swine sources as well as other pathogens.

Data availability statement

The datasets presented in this study can be found in online repositories. The names of the repository/repositories and accession number(s) can be found below: https://www.ncbi.nlm.nih.gov/, PRJNA1000181.

Author contributions

J-UA: Conceptualization, Data curation, Formal analysis, Investigation, Methodology, Software, Validation, Visualization, Writing – original draft, Writing – review & editing. SL: Conceptualization, Data curation, Formal analysis, Investigation, Methodology, Resources, Software, Visualization, Writing – original draft, Writing – review & editing. J-HG: Conceptualization, Formal analysis, Methodology, Writing – original draft. JW: Conceptualization, Formal analysis, Methodology, Writing – original draft. HS: Writing – review & editing. SC: Conceptualization, Funding acquisition, Project administration, Supervision, Validation, Writing – review & editing.

Funding

The author(s) declare financial support was received for the research, authorship, and/or publication of this article. This research was supported by the National Research Foundation of Korea (NRF-2021R1A2C2005907).

Conflict of interest

The authors declare that the research was conducted in the absence of any commercial or financial relationships that could be construed as a potential conflict of interest.

Publisher's note

Supplementary material

The Supplementary material for this article can be found online at: https://www.frontiersin.org/articles/10.3389/fmicb.2023.1274245/full#supplementary-material

References

Aarestrup, F. M., Mcdermott, P. F., and Wegener, H. C. (2008). "Transmission of antibiotic resistance from food animals to humans" in *Campylobacter*. eds. I. Nachamkin, C. M. Szymanski and M. J. Blaser, vol. *3* (Washington, DC: ASM Press), 645–665.

Atkinson, G. C., Hansen, L. H., Tenson, T., Rasmussen, A., Kirpekar, F., and Vester, B. (2013). Distinction between the Cfr methyltransferase conferring antibiotic resistance and the housekeeping RlmN methyltransferase. *Antimicrob. Agents Chemother.* 57, 4019–4026. doi: 10.1128/AAC.00448-13

Barrett, A.J., Woessner, J.F., and Rawlings, N.D. (2012). *Handbook of proteolytic enzymes*. London: Elsevier.

Boerlin, P., Burnens, A. P., Frey, J., Kuhnert, P., and Nicolet, J. (2001). Molecular epidemiology and genetic linkage of macrolide and aminoglycoside resistance in *Staphylococcus intermedius* of canine origin. *Vet. Microbiol.* 79, 155–169. doi: 10.1016/S0378-1135(00)00347-3

Burnham, P. M., and Hendrixson, D. R. (2018). *Campylobacter jejuni*: collective components promoting a successful enteric lifestyle. *Nat. Rev. Microbiol.* 16, 551–565. doi: 10.1038/s41579-018-0037-9

Candela, T., Marvaud, J.-C., Nguyen, T. K., and Lambert, T. (2017). A cfr-like gene cfr (C) conferring linezolid resistance is common in *Clostridium difficile*. *Int. J. Antimicrob. Agents* 50, 496–500. doi: 10.1016/j.ijantimicag.2017.03.013

CDC (2013). Antibiotic resistance threats in the United States, 2013. Available at: https://www.cdc.gov/drugresistance/pdf/ar-threats-2013-508.pdf.

Chen, W., Mandali, S., Hancock, S. P., Kumar, P., Collazo, M., Cascio, D., et al. (2018). Multiple serine transposase dimers assemble the transposon-end synaptic complex during IS607-family transposition. *Elife* 7:e39611. doi: 10.7554/eLife.39611

Davis, L., Young, K., and Dirita, V. (2008). Genetic manipulation of *Campylobacter jejuni*. *Curr. Protoc. Microbiol.* 10, Unit 8A 2 1–8A 2 17. doi: 10.1002/9780471729259.mc08a02s10

de Vries, J., and Wackernagel, W. (2002). Integration of foreign DNA during natural transformation of *Acinetobacter* sp. by homology-facilitated illegitimate recombination. *Proc. Natl. Acad. Sci. U. S. A.* 99, 2094–2099. doi: 10.1073/pnas.042263399

Deshpande, L. M., Ashcraft, D. S., Kahn, H. P., Pankey, G., Jones, R. N., Farrell, D. J., et al. (2015). Detection of a new cfr-like gene, cfr (B), in *Enterococcus faecium* isolates recovered from human specimens in the United States as part of the SENTRY antimicrobial surveillance program. *Antimicrob. Agents Chemother.* 59, 6256–6261. doi: 10.1128/AAC.01473-15

Guirado, P., Miro, E., Iglesias-Torrens, Y., Navarro, F., Campoy, S., Alioto, T. S., et al. (2022). A new variant of the aad E-sat 4-aph A-3 gene cluster found in a conjugative plasmid from a MDR *Campylobacter jejuni* isolate. *Antibiotics* 11:466. doi: 10.3390/antibiotics11040466

Guk, J. H., Song, H., Yi, S., An, J. U., Lee, S., Kim, W. H., et al. (2021). Hyper-Aerotolerant *Campylobacter coli* from swine may pose a potential threat to public health based on its quinolone resistance, virulence potential, and genetic relatedness. *Front. Microbiol.* 12:703993. doi: 10.3389/fmicb.2021.703993

Hansen, L. H., and Vester, B. (2015). A cfr-like gene from *Clostridium difficile* confers multiple antibiotic resistance by the same mechanism as the cfr gene. *Antimicrob. Agents Chemother.* 59, 5841–5843. doi: 10.1128/AAC.01274-15

He, Y. Z., Li, X. P., Miao, Y. Y., Lin, J., Sun, R. Y., Wang, X. P., et al. (2019). The ISApl1 (2) dimer circular intermediate participates in mcr-1 transposition. *Front. Microbiol.* 10:15. doi: 10.3389/fmicb.2019.00015

Jaakkonen, A., Kivisto, R., Aarnio, M., Kalekivi, J., and Hakkinen, M. (2020). Persistent contamination of raw milk by *Campylobacter jejuni* ST-883. *PLoS One* 15:e0231810. doi: 10.1371/journal.pone.0231810

Kitanishi, K. (2022). Bacterial hemerythrin domain-containing oxygen and redox sensors: versatile roles for oxygen and redox signaling. *Front. Mol. Biosci.* 9:967059. doi: 10.3389/fmolb.2022.967059

Kumar, S., Stecher, G., Li, M., Knyaz, C., and Tamura, K. (2018). MEGA X: molecular evolutionary genetics analysis across computing platforms. *Mol. Biol. Evol.* 35, 1547–1549. doi: 10.1093/molbev/msy096

Leclercq, R. (2002). Mechanisms of resistance to macrolides and lincosamides: nature of the resistance elements and their clinical implications. *Clin. Infect. Dis.* 34, 482–492. doi: 10.1086/324626

Liu, D., Li, X., Liu, W., Yao, H., Liu, Z., Fessler, A. T., et al. (2019a). Characterization of multiresistance gene cfr(C) variants in Campylobacter from China. *J. Antimicrob. Chemother.* 74, 2166–2170. doi: 10.1093/jac/dkz197

Liu, D., Liu, W., Lv, Z., Xia, J., Li, X., Hao, Y., et al. (2019b). Emerging erm (B)-mediated macrolide resistance associated with novel multidrug resistance Genomic Islands in Campylobacter. *Antimicrob. Agents Chemother.* 63:e00153-19. doi: 10.1128/AAC.00153-19

Long, K. S., Poehlsgaard, J., Kehrenberg, C., Schwarz, S., and Vester, B. (2006). The Cfr rRNA methyltransferase confers resistance to Phenicols, Lincosamides, Oxazolidinones, Pleuromutilins, and Streptogramin A antibiotics. *Antimicrob. Agents Chemother.* 50, 2500–2505. doi: 10.1128/AAC.00131-06

Lysnyansky, I., and Borovok, I. (2021a). A GC-rich prophage-like genomic region of *Mycoplasma bovirhinis* HAZ141_2 carries a gene cluster encoding resistance to kanamycin and neomycin. *Antimicrob. Agents Chemother.* 65:e01010-20. doi: 10.1128/AAC.01010-20

Lysnyansky, I., and Borovok, I. (2021b). The aad E*-sat 4-aph A-3 gene cluster of *Mycoplasma bovirhinis* HAZ141_2 undergoes genomic rearrangements influencing the primary promoter sequence. *Antibiotics* 10:1335. doi: 10.3390/antibiotics10111335

Niehaus, T. D., Elbadawi-Sidhu, M., De Crecy-Lagard, V., Fiehn, O., and Hanson, A. D. (2017). Discovery of a widespread prokaryotic 5-oxoprolinase that was hiding in plain sight. *J. Biol. Chem.* 292, 16360–16367. doi: 10.1074/jbc.M117.805028

Palmieri, C., Mingoia, M., Massidda, O., Giovanetti, E., and Varaldo, P. E. (2012). *Streptococcus pneumoniae* transposon Tn1545/Tn6003 changes to Tn6002 due to spontaneous excision in circular form of the erm (B)- and aph A3-containing macrolide-aminoglycoside-streptothricin (MAS) element. *Antimicrob. Agents Chemother.* 56, 5994–5997. doi: 10.1128/AAC.01487-12

Park, B. K., Jang, J. S., and Park, K. (2000). Deletion of one adenine base within the polyadenine tract of transforming growth factor-beta receptor type II in human MDA-MB-231 breast cancer cell line. *Int. J. Oncol.* 17, 473–478. doi: 10.3892/ijo.17.3.473

Perez-Boto, D., Lopez-Portoles, J. A., Simon, C., Valdezate, S., and Echeita, M. A. (2010). Study of the molecular mechanisms involved in high-level macrolide resistance of Spanish Campylobacter jejuni and *Campylobacter coli* strains. *J. Antimicrob. Chemother.* 65, 2083–2088. doi: 10.1093/jac/dkq268

Poly, F., Threadgill, D., and Stintzi, A. (2005). Genomic diversity in *Campylobacter jejuni*: identification of *C. jejuni* 81-176-specific genes. *J. Clin. Microbiol.* 43, 2330–2338. doi: 10.1128/JCM.43.5.2330-2338.2005

Qin, S., Wang, Y., Zhang, Q., Chen, X., Shen, Z., Deng, F., et al. (2012). Identification of a novel genomic island conferring resistance to multiple aminoglycoside antibiotics in *Campylobacter coli*. *Antimicrob. Agents Chemother.* 56, 5332–5339. doi: 10.1128/AAC.00809-12

Sassi, M., Guérin, F., Zouari, A., Beyrouthy, R., Auzou, M., Fines-Guyon, M., et al. (2019). Emergence of optr A-mediated linezolid resistance in enterococci from France, 2006–16. *J. Antimicrob. Chemother.* 74, 1469–1472. doi: 10.1093/jac/dkz097

Schwarz, S., Werckenthin, C., and Kehrenberg, C. (2000). Identification of a plasmid-borne chloramphenicol-florfenicol resistance gene in *Staphylococcus sciuri*. *Antimicrob. Agents Chemother.* 44, 2530–2533. doi: 10.1128/AAC.44.9.2530-2533.2000

Seemann, T. (2014). Prokka: rapid prokaryotic genome annotation. *Bioinformatics* 30, 2068–2069. doi: 10.1093/bioinformatics/btu153

Silva, J., Leite, D., Fernandes, M., Mena, C., Gibbs, P. A., and Teixeira, P. (2011). *Campylobacter* spp. as a foodborne pathogen: a review. *Front. Microbiol.* 2:200. doi: 10.3389/fmicb.2011.00200

Stojković, V., Ulate, M. F., Hidalgo-Villeda, F., Aguilar, E., Monge-Cascante, C., Pizarro-Guajardo, M., et al. (2019). cfr (B), cfr (C), and a new cfr-like gene, cfr (E), in *Clostridium difficile* strains recovered across Latin America. *Antimicrob. Agents Chemother.* 64:e01074-19. doi: 10.1128/AAC.01074-19

Sullivan, M. J., Petty, N. K., and Beatson, S. A. (2011). Easyfig: a genome comparison visualizer. *Bioinformatics* 27, 1009–1010. doi: 10.1093/bioinformatics/btr039

Tang, Y., Dai, L., Sahin, O., Wu, Z., Liu, M., and Zhang, Q. (2017). Emergence of a plasmid-borne multidrug resistance gene cfr(C) in foodborne pathogen Campylobacter. *J. Antimicrob. Chemother.* 72, 1581–1588. doi: 10.1093/jac/dkx023

Tang, Y. Z., Lai, Y., Wang, X. Y., Lei, C. W., Li, C., Kong, L. H., et al. (2021). Novel insertion sequence ISChh1-like mediating acquisition of optr a gene in foodborne pathogen *Campylobacter coli* of swine origin. *Vet. Microbiol.* 252:108934. doi: 10.1016/j.vetmic.2020.108934

Tang, Y., Lai, Y., Yang, X., Cao, X., Hu, Y., Wang, X., et al. (2020). Genetic environments and related transposable elements of novel cfr(C) variants in *Campylobacter coli* isolates of swine origin. *Vet. Microbiol.* 247:108792. doi: 10.1016/j.vetmic.2020.108792

Werner, G., Hildebrandt, B., and Witte, W. (2001). Aminoglycoside-streptothricin resistance gene cluster aad E-sat 4-aph A-3 disseminated among multiresistant isolates of *Enterococcus faecium*. *Antimicrob. Agents Chemother.* 45, 3267–3269. doi: 10.1128/AAC.45.11.3267-3269.2001

Werner, G., Hildebrandt, B., and Witte, W. (2003). Linkage of erm (B) and aad E-sat 4-aph A-3 in multiple-resistant *Enterococcus faecium* isolates of different ecological origins. *Microb. Drug Resist.* 9, 9–16. doi: 10.1089/107662903322541847

WHO (2019). *Critically important antimicrobials for human medicine, 6th revision*. Geneva: WHO

Wick, R. R., Judd, L. M., Gorrie, C. L., and Holt, K. E. (2017). Unicycler: resolving bacterial genome assemblies from short and long sequencing reads. *PLoS Comput. Biol.* 13:e1005595. doi: 10.1371/journal.pcbi.1005595

Yanisch-Perron, C., Vieira, J., and Messing, J. (1985). Improved M13 phage cloning vectors and host strains: nucleotide sequences of the M13mp18 and pUC19 vectors. *Gene* 33, 103–119. doi: 10.1016/0378-1119(85)90120-9

Zhao, S., Mukherjee, S., Hsu, C. H., Young, S., Li, C., Tate, H., et al. (2019). Genomic analysis of emerging florfenicol-resistant *Campylobacter coli* isolated from the cecal contents of cattle in the United States. *mSphere* 4:e00367-19. doi: 10.1128/mSphere.00367-19

Zhao, Q., Wendlandt, S., Li, H., Li, J., Wu, C., Shen, J., et al. (2014). Identification of the novel lincosamide resistance gene lnu (E) truncated by ISEnfa5-cfr-ISEnfa5 insertion in *Streptococcus suis*: de novo synthesis and confirmation of functional activity in *Staphylococcus aureus*. *Antimicrob. Agents Chemother.* 58, 1785–1788. doi: 10.1128/AAC.02007-13

Frontiers in Microbiology

Explores the habitable world and the potential of microbial life

The largest and most cited microbiology journal which advances our understanding of the role microbes play in addressing global challenges such as healthcare, food security, and climate change.

Discover the latest Research Topics

See more →

Frontiers

Avenue du Tribunal-Fédéral 34
1005 Lausanne, Switzerland
frontiersin.org

Contact us

+41 (0)21 510 17 00
frontiersin.org/about/contact